The role of metal ions and reactive oxygen species in β-amyloid aggregation and toxicity and their relevance to Alzheimer's disease

Jennifer Helen Mayes

BSc Biochemistry

September 2010

School of Health and Medicine

Lancaster University

Submitted in part fulfilment of the requirements for the degree of

Doctor of Philosophy

ProQuest Number: 11003571

All rights reserved

INFORMATION TO ALL USERS
The quality of this reproduction is dependent upon the quality of the copy submitted.

In the unlikely event that the author did not send a complete manuscript
and there are missing pages, these will be noted. Also, if material had to be removed,
a note will indicate the deletion.

ProQuest 11003571

Published by ProQuest LLC (2018). Copyright of the Dissertation is held by the Author.

All rights reserved.
This work is protected against unauthorized copying under Title 17, United States Code
Microform Edition © ProQuest LLC.

ProQuest LLC.
789 East Eisenhower Parkway
P.O. Box 1346
Ann Arbor, MI 48106 – 1346

Acknowledgements

Firstly, I would like to thank Professor David Allsop for his supervision, his understanding and enthusiasm for this work and Dr Fiona Benson for her support during this study. I would like to thank current members of the Allsop, Benson and Parkin laboratories for all their support, help and input when faced with troublesome experiments. I would also like to thank former Allsop laboratory member Dr Susan Moore for her guidance and enthusiasm during, our sometimes lengthy, discussions. I would like to thank Dr Brian Tabner for his help and knowledge of redox chemistry, and Dr Tom Huckerby for all his assistance. I take great pleasure in thanking The Alzheimer's Society for funding this research and to the friendly lay panel who were so interested in this work. I would also like to thank the Sir John Fisher Foundation whose later funding enabled much of the work in chapter 8.

Finally I would like to thank my friends and family who have offered continuous support, especially my partner, Tom Sunderland, for his endless patience and encouragement.

Abstract

The aggregation and deposition of β-amyloid (Aβ) in the brain has long been implicated in the neurotoxic pathways causing Alzheimer's disease (AD). Recent data suggests that early, soluble oligomers of Aβ are the toxic species. Oxidative stress may be partly responsible for the toxicity of the peptide as hydrogen peroxide (H_2O_2) has been found to be produced during the early stages of aggregation. This study investigates the generation of H_2O_2 by Aβ during the process of aggregation and presents evidence supporting the hypothesis that some form of Aβ oligomer has the capacity for H_2O_2 generation. A technique developed to immobilise Aβ during its aggregation suggested H_2O_2 generation to be an event associated with early Aβ-Aβ interactions, whereas fibrillar Aβ degraded H_2O_2. The development of cross-linking techniques to generate stable oligomeric Aβ found Aβ42 to be the most susceptible to these reactions, correlating with its increased tendency for aggregation. Tyr10 was found to be critical for these reactions, but not for the formation of Aβ fibrils, nor the generation of H_2O_2 by Aβ, indicating that dityrosine dimers are not the sole source of H_2O_2 generation from Aβ. The binding of copper to Aβ, but not iron, was found to be central to the redox reactions enabling generation of H_2O_2, in addition to having complex effects on the aggregation of Aβ. Zinc may also play a regulatory role in mediating Aβ aggregation state and redox potential.

Research of potentially toxic Aβ oligomers is problematic due to the heterogeneous and dynamic nature of Aβ solutions. Development of techniques to cross-link and immobilise Aβ may be useful for studying early oligomeric Aβ, not only in respect of H_2O_2 generation but also in identification of Aβ oligomers responsible for neurotoxicity in AD. This may enable identification of a potential diagnostic marker and also a potential therapeutic target.

Table of Contents

Table of Figures

Abbreviations

Aβ	β-amyloid
ACE	Angiotensin-converting enzyme
AD	Alzheimer's disease
ADAM	A disintegrin and metalloproteinase
AFM	Atomic force microscopy
AICD	APP intracellular domain
ALS	Amyotrophic Lateral Sclerosis
APOE	Apolipoprotein E
APP	Amyloid precursor protein
BACE	β-site APP-cleaving enzyme
BBB	Blood brain barrier
CBD	Copper binding domain
CLN	Colostrinin
CNS	Central nervous system
CP	Cytoplasmic tail
CSF	Cerebrospinal fluid
CTF	C-terminal fragment
DS	Downs syndrome
DTPA	Diethylene triamine pentaacetic acid
ECE	Endothelin-converting enzyme
EDTA	Ethylenediaminetetraacetic acid
fAD	Familial Alzheimer's disease
GFD	Growth factor domain
HFIP	Hexafluoroisopropanol
HNE	Hydroxynonenal
HRP	Horseradish peroxidase
IDE	Insulin-degrading enzyme
KPI	Kunitz-type protease inhibitor

LTP	Long term potentiation
mAb	Monoclonal antibody
MCI	Mild cognitive impairment
MDC	Metalloprotease/disintegrin/cysteine-rich
MMSE	Mini-mental state examination
MND	Motor neuron disease
MT	Microtubule
mRNA	messenger RNA
NFT	Neurofibrillary tangles
NMR	Nuclear magnetic resonance
PB	Phosphate buffer
PBS	Phosphate buffered saline
PBST	Phosphate buffered saline tween
PD	Parkinson's disease
PHF	Paired helical filaments
PICUP	Photo-induced cross-linking of unmodified proteins
PM	Plasma membrane
PVDF	Polyvinylidene fluoride
ROS	Reactive oxygen species
sAD	Sporadic Alzheimer's disease
SDS	Sodium dodecyl sulphate
SOD	Superoxide dismutase
SPM	Scanning Probe Microscope
STM	Scanning tunnelling microscopy
TACE	TNF-α convertase
TFA	Trifluoroacetic acid
TM	Transmembrane
VEGF	Vascular endothelial growth factor

Chapter 1
Introduction

1.1. Alzheimer's disease

Alzheimer's disease (AD) is one of a large group of diseases called amyloidoses. These diseases are characterised by the accumulation of a fibrillar proteinaceous deposit in the affected organ(s). Alzheimer's is among several amyloidoses that target the brain, such as Parkinson's disease (PD), prion disease and motor neuron disease (MND). In each of these diseases, the progressive death of neurons is observed in a different neuronal population, with consequent presentation of neurological symptoms. With AD, neuronal loss causes dementia. In fact, Alzheimer's is the most common form of senile dementia accounting for ~62% of cases (Knapp, 2007).

Although the first described case of "presenile dementia", reported by Alois Alzheimer in 1906, referred to a subject with an early-onset form of the disease, over 97% of cases present after the age of 65 years (Knapp, 2007). It is progressive in nature, showing gradual but irreversible cognitive decline. The earliest manifestation is impairment of memory. However, towards the later stages motor and sensory functions may also be disrupted. The major risk factor for the disease is aging yet it also exhibits great genetic complexity. The majority of cases are sporadic in onset (sporadic AD, sAD). However, 5-10% of cases show autosomal dominant inheritance (familial AD, fAD). By and large fAD corresponds to early-onset AD (under 60 years), and sAD to late-onset (over 60 years) (Blennow et al., 2006; Chauhan and Chauhan, 2006).

1.1.1. Epidemiology

Dementia is a global health problem. With an aging population, due to increasing life expectancy, in both developed and developing countries, its prevalence is set to increase. Over 24 million people worldwide have dementia. With another 4.6 million people developing AD every year, worldwide prevalence figures are predicted to double every 20 years (Ferri et al., 2005). Recent UK research puts the number of dementia sufferers in the UK at over 820 thousand people (1.3% of the population), with more than 15 thousand under the age of 65 (Knapp, 2007; Luengo-Fernandez, 2010). An estimated 37% of these patients are in long-term care institutions, with each patient costing the UK economy over £27000 each year. That is more than the mean national salary. Compared to the care costs of other public health concerns such as cancers and heart disease, research into dementia has been found to be grossly underfunded (Luengo-Fernandez, 2010).

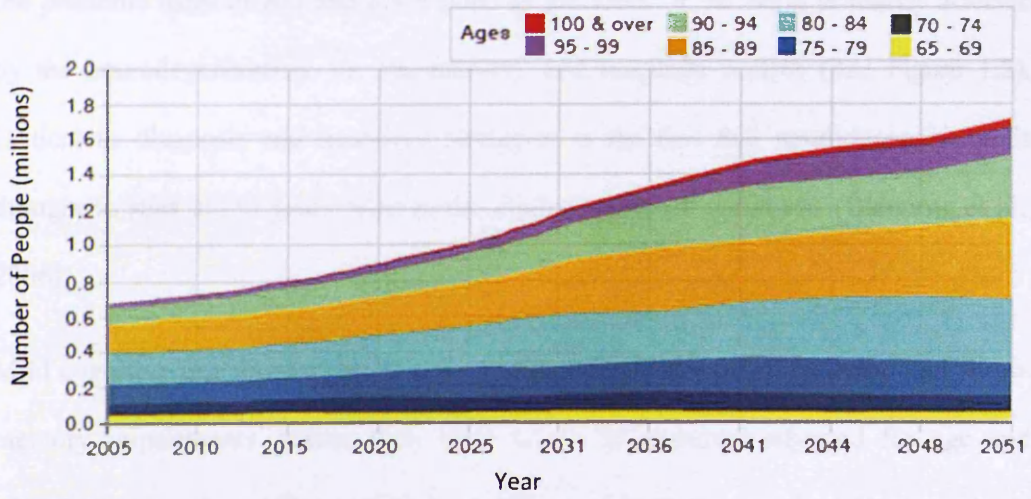

Figure 1.1. Expected rise in prevalence of UK dementia cases
Graph demonstrating the predicted increase in dementia cases until the year 2051, split into age bands (Knapp, 2007).

The cost of care is predicted to escalate, due to increasing life expectancy; prevalence in 60-64 year olds is approximately 1% yet this rises exponentially with age to 24-

33% in individuals aged 85 and older in the western world (Ferri et al., 2005). In the UK, a report funded by the Alzheimer's Society predicts over 1.7 million sufferers by 2051, with the greatest percentage increases occurring in the older categories of 90-94 and 95-99 years, corresponding with the growing percentage of the population reaching these ages (see Figure 1.1.) (Knapp, 2007)

1.1.2. Clinical features

The onset of AD can often be misinterpreted as a part of the normal aging process, as the earliest symptom is often memory loss (Selkoe, 2002). However, being progressive in nature, the clinical manifestations become increasingly profound. The instrumental signs associated with AD are aphasia, apraxia, agnosia and a variety of general cognitive symptoms including impairment of decision making, judgement and orientation (Blennow et al., 2006). These symptoms present with a higher severity in the presenile form of AD and correspond to the areas of the brain primarily affected by the neurodegeneration, i.e. the memory and language centres (See Figure 1.2). Critical to diagnosis and treatment strategies is the fact that neurodegeneration is thought to start 20-30 years prior to the clinical onset of symptoms (Blennow et al., 2006).

Mild cognitive impairment (MCI) is a condition diagnosed when an individual shows memory impairments greater than what would be expected adjusted for age and education, yet other AD associated cognitive impairments are largely not present (Petersen, 2004). It is often thought of as a risk factor for AD. However, it can be symptomatic of other disorders (e.g. vascular dementia) or completely benign and part of normal aging. When symptoms are predominantly memory associated a subtype, amnestic MCI, may be diagnosed. This may be considered a transitional stage

between normal aging and AD, with some reports showing early AD neuropathological changes occurring in amnestic MCI patients. This has lead to speculations of amnestic MCI actually representing early AD. Still, the conversion rate to AD has been estimated at 12% of patients per year (Blennow et al., 2006; Petersen, 2004).

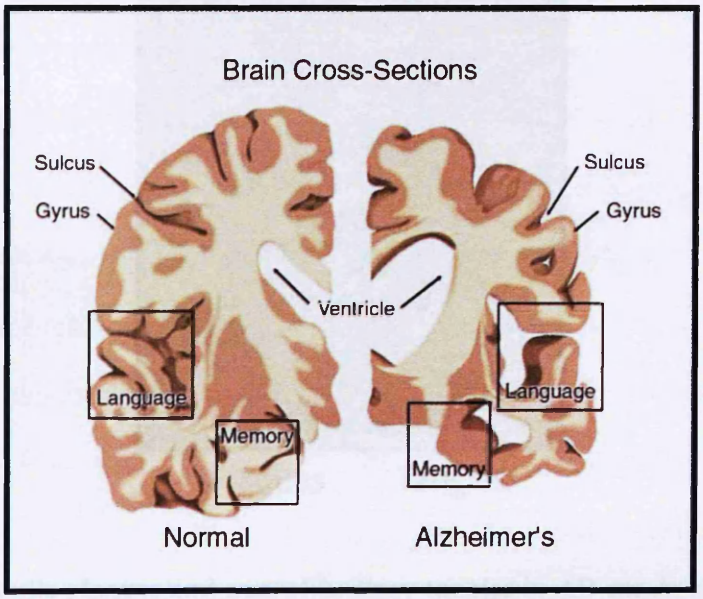

Figure 1.2. AD causes degeneration of memory and language centres.
A diagram comparing the cross-section of a normal brain alongside the gross atrophy observed in a late Alzheimer's brain. The loss of neurons in the memory and language centres is directly responsible for clinical symptoms observed in patients. (Copyright © American Health Assistance Foundation Alzheimer Disease, http://www.ahaf.org/alzdis/about/BrainAlzheimer.htm)

1.1.3. Physiological markers

The finding that characteristic histopathological markers are shared by what was originally thought of as two separate conditions (pre-senile and senile dementia) has lead to them being jointly referred to as AD. Neurodegeneration is accompanied by abnormalities of the synapse with the cholinergic system specifically affected. Neurotransmission by acetylcholine is essential for memory and learning, and is decreased in AD patients. The activity of its degrading enzyme, acetylcholinesterase,

is also reduced. These cholinergic deficits contribute towards symptoms and lead to loss of the affected neurons making the damage irreparable (Chauhan and Chauhan, 2006). Classical AD pathology consists of the presence of extracellular senile plaques and intracellular neurofibrillary tangles (NFTs) (pictured in Figure 1.3), often together with cerebrovascular amyloid deposits.

Figure 1.3. Senile plaques and neurofibrillary tangles in AD cerebral cortex
Senile plaques and neurofibrillary tangles are indicated by arrows. Plaques accumulate extracellularly and are composed of β-amyloid (Aβ). The tangles are composed of hyperphosphorylated tau and accumulate intracellularly (Blennow et al., 2006).

It has been suggested that during the preclinical phase, plaque and tangle load increase to a threshold at which the symptoms start to appear (Blennow et al., 2006). Early onset AD shows a greater plaque and tangle load and also exhibits greater cholinergic deficits, correlating strongly with the severity of dementia, yet, this association is not found in elderly AD patients (Hansen et al., 1988; Wilcock and Esiri, 1982). This has brought into question whether pre-senile and senile dementia should be considered as one disease or whether they represent different regions on a scale of intensified/heightened aging (Mann et al., 1984).

1.1.3.1. Neurofibrillary tangles

Neurofibrillary Tangles (NFTs) are composed of polymerised, hyperphosphorylated tau protein in the form of paired helical filaments (PHFs) (Grundke-Iqbal et al., 1986; Kidd, 1963). Tau is a normal axonal protein which binds microtubules (MT) via its MT binding domains. The largest of the tau isoforms has 4 MT binding domains with exons 2 and 3 spliced in. It functions to aid assembly of MTs and stabilise them. Phosphorylation of tau regulates its activity and is modulated by multiple kinases and phosphatases (Blennow et al., 2006; Iqbal et al., 2005). There are normally 2-3 moles of phosphate per mole of tau. However, in AD this is 3-4 folds higher, seemingly due to aberrant activity of these enzymes. This abnormal phosphorylation renders tau incompetent in its role in MT assembly and it is subsequently sequestered into NFTs. These tangles become ubiquitinated for non-lysosomal degradation. Nonetheless, this appears to be inefficient as they persist in the AD brain (Grundke-Iqbal et al., 1986; Iqbal et al., 2005; Kopke et al., 1993). Tau pathology is generally regarded as a downstream event in the development of AD but may also contribute to neuronal dysfunction and cognitive symptoms. MTs are disrupted and axonal transport becomes impaired, compromising both neuronal and synaptic function. It has been suggested that the presence of these NFTs could effectively "choke" affected neurons by preventing axonal transport (Grundke-Iqbal et al., 1986; Iqbal et al., 2005; Kopke et al., 1993; Oddo et al., 2006).

1.1.3.2. Cerebrovascular deposits

The detection of cerebrovascular amyloid deposits in AD patients occurred early in research (Benedek and McGovern, 1949), yet they were only identified as being largely composed of the same peptide as senile plaque amyloid in Wong et al (1985).

At this time the principal hypothesis was that these cerebrovascular deposits were the origin of the senile plaques (Wong et al., 1985). However, it is now believed that the opposite is the case, with clearance of amyloid proceeding from the brain via the cerebrovasculature. The neurovascular hypothesis states that dysfunctional blood vessels contribute to cognitive symptoms. This may be due to impaired nutrient delivery to neurons with resulting neuronal stress (Farkas and Luiten, 2001; Mayeux, 2003). There is also evidence to suggest that pathogenic mechanisms converge between Aβ and cerebrovascular pathology: abnormalities of the blood vessels also appear to reduce the clearance of Aβ from the brain presumably due to a lack of blood supply to carry the Aβ away. Several links have emerged in this respect:

1. Vascular endothelial growth factor (VEGF) polymorphisms (reportedly associated with sAD) indicate a role for the vascular system in pathogenesis.
2. Cerebrovascular pathology with reduced blood supply reportedly generates a rise in APP expression with subsequent deposition of Aβ (Sadowski et al., 2004a).
3. Down-regulation of a vascular differentiation gene, MEOX2, causes cerebral microvessel loss and consequently a reduction in Aβ efflux (Wu et al., 2005).

Other research maintains that these links are independent of the disease process; coexisting cerebrovascular pathology may only serve to increase the probability of dementia in otherwise asymptomatic patients (Blennow et al., 2006). Potentially cerebrovascular pathology together with vascular disease risk factors (such as coronary heart disease, atherosclerosis, hypercholesterolemia, hypertension, diabetes, obesity and smoking) may accelerate development of AD (Luchsinger and Mayeux, 2004; Mayeux, 2003). Nonetheless, where AD has been identified neuropathologically, concomitant cerebrovascular amyloid pathology is also observed in ~50% of patients (Lim et al., 1999; MRCCFAS, 2001).

1.1.3.3. Amyloid plaques

Senile or amyloid plaques accumulate during normal aging, but to a greater extent in AD, in the cerebral parenchyma and cortical interstitium in a characteristic manner (Gaeta and Hider, 2005; Selkoe, 1991). The central region of these plaques is largely constructed from insoluble, SDS-resistant amyloid fibrils. The peptide component of these was purified from the plaques found in AD brains and identified as β-amyloid (Aβ) (Allsop et al., 1983; Glenner and Wong, 1984). Normally Aβ is a soluble metabolic product found in blood serum and CSF. However, in AD (and Down syndrome (DS) (discussed in 1.3.1.)) it accumulates, becomes insoluble and is sequestered into fibrils and subsequently into plaques. Although the presence of these plaques was held accountable for the neuronal loss exhibited and the resultant development of AD, they are now considered "tombstones", signifying the damage already transpired. Attention has more recently focused on Aβ, the peptide making up these fibrils and its aggregation process, as all biochemical, genetic and neuropathological data suggest that Aβ is central to AD pathogenesis (Selkoe, 2001).

1.2. β-amyloid

Aβ is an amphipatic peptide which is 39-43 residues in length. At ~4.5 kDa, Aβ40 is the major Aβ species produced under normal conditions (Glenner and Wong, 1984; Masters et al., 1985). It is soluble and can be found in CSF at nanomolar concentrations (Vigo-Pelfrey et al., 1993). Aβ42 is a minor species produced and is found heavily enriched in senile plaques. It is generally agreed that it is the accumulation of this species that is more closely related to AD pathogenesis. For

some reason the production of Aβ in the brain becomes pathogenic in AD, possibly due to a multitude of factors that result in increased Aβ42 levels.

As the tertiary structure of monomeric Aβ is critical to its subsequent aggregation, and hence, to AD pathogenesis, much research has set out to determine the structure of Aβ. Scanning tunnelling microscopy (STM) has been successful at examining the structure of Aβ40 monomers at low concentrations where it is thought to be stable. The globular structures observed by Losic et al, are consistent with monomers being 3-4 nm diameter. Using atomic force microscopy (AFM) a typical volume of 5.3 nm^3 was measured, similar to that expected for a monomer. They reported internal morphology of a polypeptide chain folded into 3 or 4 domains as parallel strands 3-4 nm in length, consistent with a single Aβ peptide chain (Losic et al., 2006). Due to the tendency of Aβ42 to aggregate, structural information on the Aβ42 monomer is much harder to ascertain.

Aβ is a metalloprotein showing high affinity for binding Cu(II), Zn(II) and Fe(II) ions (Atwood et al., 2000b; Huang et al., 1999a). The binding site for Cu(II) has been mapped to the region between residues 6-28 at the hydrophilic N-terminus of the peptide and has been shown to have a square planar configuration. Co-ordination is mediated via the electrons of 3 nitrogen atoms contained in the imidazole rings of histidine residues. These are His6, His13 and His14. An oxygen is also needed for coordination which is thought to be donated from the hydroxyl group of Tyr10. However several other candidates are also suggested; the carboxylate of Glu5, an N-terminal aspartate, the amino terminus itself, or perhaps even a water molecule (Karr et al., 2005; Smith et al., 2007a; Streltsov et al., 2008). It has been reported that Cu(I) coordination is via His13 and His14, with Cu(I) central in an almost linear arrangement (Himes et al., 2008; Shearer and Szalai, 2008). Not only does Aβ

contain a metal binding site, but Met35 has metal reducing ability. This means that Aβ can potentially bind and utilise redox active metal ions in reactions forming H_2O_2, such as the reduction of Cu(II) to Cu(I) (Butterfield and Bush, 2004).

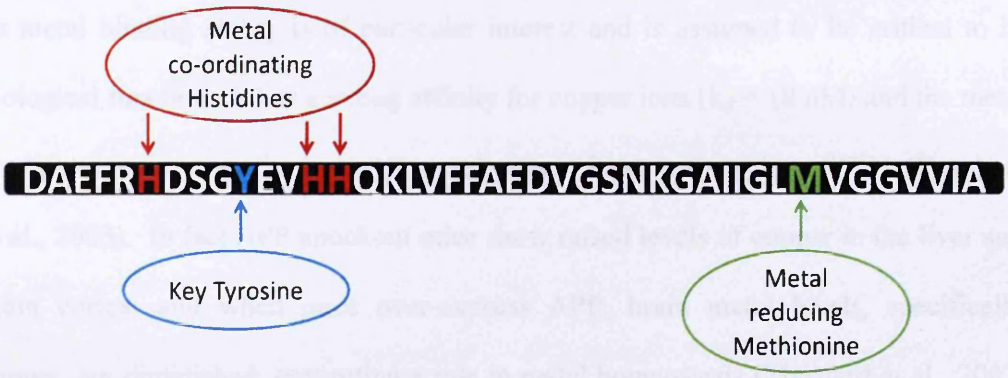

Figure 1.4. Aβ42 sequence
The amino acids involved in metal binding are identified along at the N-terminus with the putative metal reducing site at Met35 at the C-terminus. (Gaeta and Hider, 2005)

1.2.1. Amyloid precursor protein

Aβ is generated from a precursor protein identified as Amyloid Precursor Protein (APP). This protein is a type 1 integral membrane glycoprotein ubiquitously expressed in the human body. Alternative splicing of APP mRNA leads to multiple isoforms of APP being created of different lengths (Selkoe, 2001). The largest isoform, APP770, has both a kunitz-type protease inhibitor (KPI) domain and an OX-2 antigen domain (Blennow et al., 2006). Differential expression of the different APP isoforms has been hypothesised to be one of the factors mediating sAD. In particular, the presence of the KPI domain has been implicated with a shift to KPI containing isoforms being identified in the AD (Matsui et al., 2007). The function of this protein is still unknown. Potential functions have been suggested to include intracellular calcium regulation (Mattson et al., 1993), cell adhesion (Storey et al., 1996), cell growth (Small et al., 1994), vesicle transport along axons (Gunawardena and Goldstein, 2001) and metal ion homeostasis due to a metal binding domain

independent of the Aβ region. Structurally it has a growth factor-like domain next to a large cysteine-rich region containing the metal binding domain in its large N-terminal extracellular tail (see figure 1.5).

Its metal binding ability is of particular interest and is assumed to be critical to its biological function. It has a strong affinity for copper ions ($k_d \approx 10$ nM) and the metal binding domain is similar in structure to copper chaperones such as SOD1 (Barnham et al., 2003). In fact APP knockout mice show raised levels of copper in the liver and brain cortex, and when mice over-express APP, brain metal levels, specifically copper, are diminished, supporting a role in metal homeostasis (Maynard et al., 2002; White et al., 1999). The Aβ domain of APP lies partially embedded in the plasma membrane (PM) with 12-14 residues residing inside the transmembrane (TM) domain of APP. The remaining 28 residues lie outside the membrane (Blennow et al., 2006).

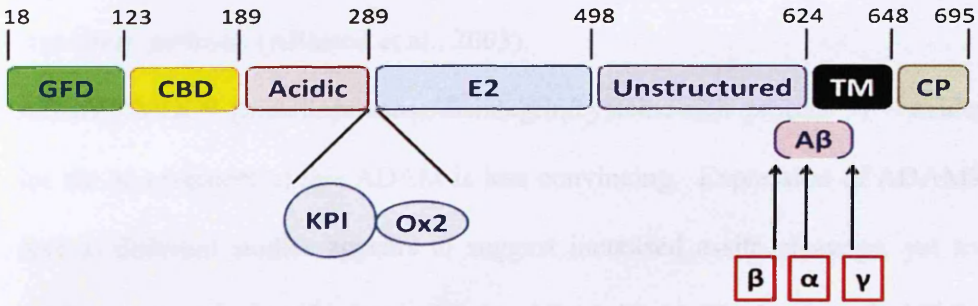

Figure 1.5. The domains of APP.
The domains of the 695 amino acid APP isoform are shown. GFD = growth factor domain, CBD = copper binding domain, Acidic = rich in acidic residues, E2 = glycosylated domain, TM = transmembrane domain, CP = cytoplasmic tail. The KPI and OX2 domains are spliced out of this isoform. The numbers represent the residue boundaries of each domain. The fragment that forms the Aβ peptide is shown, with the cleavage sites for the secretases (β, α and γ) also indicated (adapted from (Kong et al., 2007)).

1.2.2. APP secretases

APP is cleaved at 3 major sites: the α-cleavage site precludes Aβ generation, whilst the β- and γ-cleavage sites permit Aβ generation. Several zinc metalloproteinases have been identified that are able to cleave APP at the α-secretase cleavage site:

1. **ADAM10** (a disintegrin and metalloproteinase) – strong evidence supports this multidomain TM protein in a role in both constitutive and regulated cleavage at the Lys16-Leu17 α-cleavage site (reviewed in (Allinson et al., 2003)). Interestingly, when the peptide corresponding to the AD-associated amino acid substitution Aβ-A21G was tested, it was cleaved at a slower rate to the wt peptide. This substitution corresponds to a naturally occurring AD mutation which also causes cerebral hemorrhages due to amyloid accumulation in the cerebrovasculature (Hendriks et al., 1992).
2. **ADAM17**/TACE (TNF-α convertase) – this potential α-secretase is involved in the shedding of a range of integral membrane proteins in addition to TNF-α. However cleavage of APP at the α-secretase site is reported to be at a far reduced efficiency to the cleavage event generating TNF-α. It has been suggested that the action of ADAM-17 in respect to α-site cleavage of APP may be restricted to the regulatory pathway (Allinson et al., 2003).
3. **ADAM9**/MDC9 (metalloprotease/disintegrin/cysteine-rich protein 9) – evidence for the involvement of this ADAM is less convincing. Expression of ADAM9 in several different studies appears to suggest increased α-site cleavage, yet some evidence suggests this site is modified to His14-Gln15 (Roghani et al., 1999). It has been suggested that this cleavage event may be restricted to certain cell types (Allinson et al., 2003)

There has also been an aspartyl protease, BACE2, identified that is capable of α-cleavage (Thinakaran and Koo, 2008). What appears clear from knockout mice studies is that there is a functional overlap between several α-secretases, acting in concert to cleave APP at the α-site (Allinson et al., 2003; Thinakaran and Koo, 2008).

The major β-secretase has been identified as β-site APP-cleaving enzyme 1 or BACE1. This is an integral membrane aspartyl protease and is found within the *trans*-golgi network and also within endosomes (Vassar et al., 1999). The high levels of neuronal BACE1 suggest APP processing is preferentially channelled through the amyloidogenic pathway (discussed in 1.2.3) (Thinakaran and Koo, 2008). An intramembrane protein complex was identified as the APP cleaving γ-secretase. It is composed of 4 essential components: the proteins nicastrin, PEN-2, APH-1 and presenilin. Together these form the active site which is able to cleave at multiple sites within the TM domain of Aβ (Thinakaran and Koo, 2008; Vassar et al., 1999).

1.2.3. APP processing

The secretases identified in APP cleavage work according to two separate proteolytic pathways determined via whether initial cleavage is performed by α- or β-secretase (see figure 1.6). Cleavage by α-secretase allows the non-amyloidogenic pathway to be followed. This cuts APP within the Aβ domain (at K16-L17 of Aβ) between the β and γ secretase cleavage sites. This generates N-terminal soluble APP fragments (sAPPα) which are released extracellularly. The C-terminal fragment that remains embedded in the membrane (CTF, α-CTF or C83) is then cleaved by the γ-secretase complex within the TM domain, releasing the p3 peptide extracellularly (Blennow et al., 2006; Selkoe, 2001; Smith et al., 2007a).

The cleavage of APP by β-secretase permits the amyloidogenic pathway as it cleaves within the ectodomain of APP, at the N-terminus of the Aβ domain. This releases the N-terminal, soluble sAPPβ fragment. The γ-secretase complex cleaves the remaining CTF (β-CTF or C99) as in the non-amyloidogenic pathway, within the TM domain.

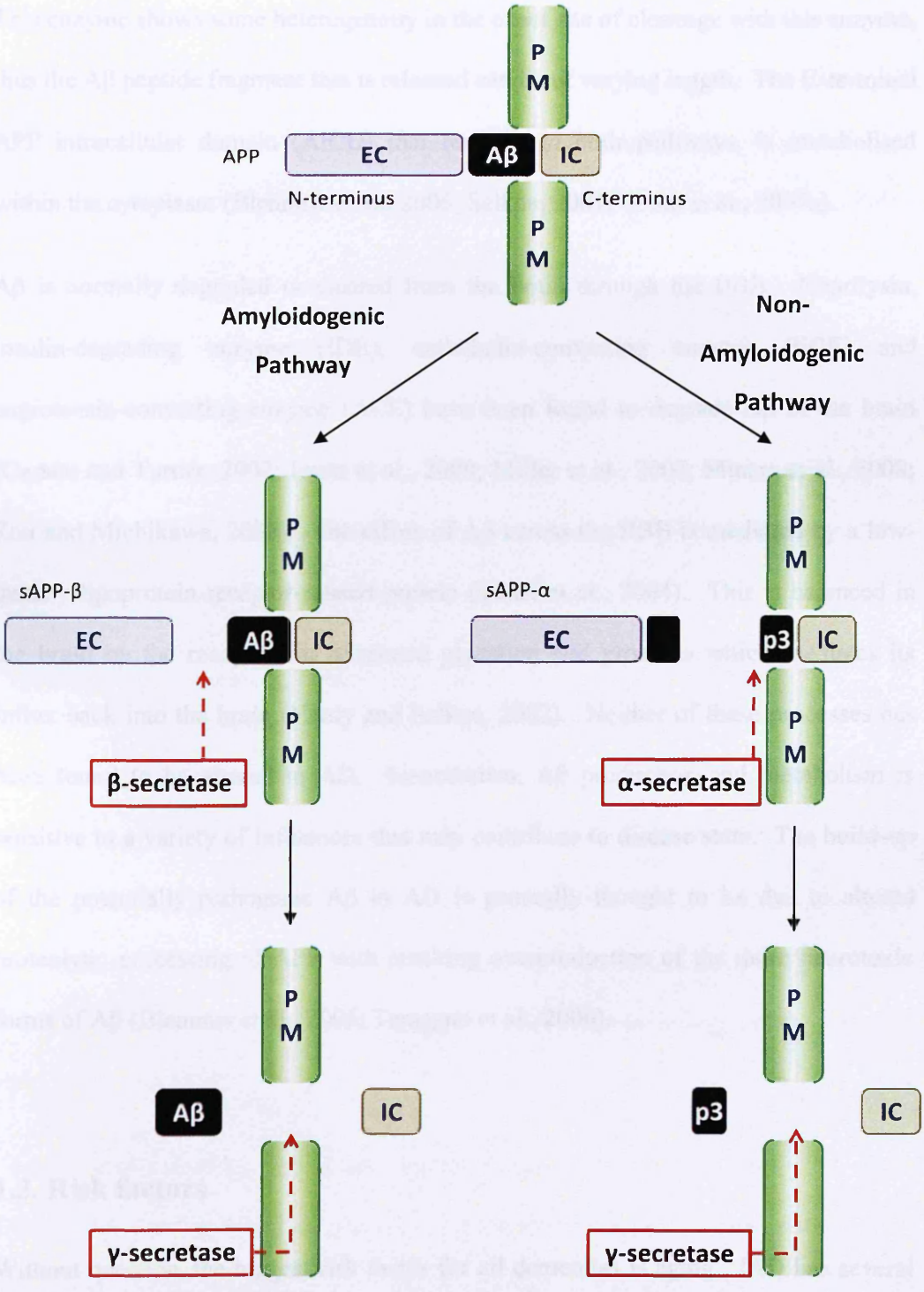

Figure 1.6. The processing pathways of APP
Proteolytic processing of APP is dependent on cleavage by either α or β secretase. This is followed by cleavage by γ-secretase. Amyloidogenic: APP is initially cleaved by β-secretase, the Aβ fragment can be formed and can lead to its aggregation. Non-amyloidogenic: APP is initially cleaved by α-secretase, the Aβ fragment cannot be formed and hence it cannot aggregate. PM = Plasma membrane, EC = extracellular protein/fragment, IC = intracellular protein/fragment (AICD).

This enzyme shows some heterogeneity in the exact site of cleavage with this enzyme, thus the Aβ peptide fragment that is released can be of varying length. The C-terminal APP intracellular domain (AICD) that remains in both pathways, is metabolised within the cytoplasm (Blennow et al., 2006; Selkoe, 2001; Smith et al., 2007a).

Aβ is normally degraded or cleared from the brain through the BBB. Neprilysin, insulin-degrading enzyme (IDE), endothelin-converting enzyme (ECE) and angiotensin-converting enzyme (ACE) have been found to degrade Aβ in the brain (Carson and Turner, 2002; Iwata et al., 2000; Miller et al., 2003; Miners et al., 2008; Zou and Michikawa, 2008). The efflux of Aβ across the BBB is mediated by a low-density lipoprotein receptor-related protein (Tanzi et al., 2004). This is balanced in the brain by the receptor for advanced glycation end products which mediates its influx back into the brain (Hardy and Selkoe, 2002). Neither of these processes has been found to be altered in AD. Nonetheless, Aβ production and metabolism is sensitive to a variety of influences that may contribute to disease state. The build-up of the potentially pathogenic Aβ in AD is generally thought to be due to altered proteolytic processing of APP with resulting overproduction of the more neurotoxic forms of Aβ (Blennow et al., 2006; Tamagno et al., 2006).

1.3. Risk factors

Without question, the biggest risk factor for all dementias is aging. fAD has several genetic predispositions associated with it (discussed in 1.3.1-3). Although sAD has environmental influences a large genetic involvement has been reported. A large twin study has reported 80% hereditability for sAD (Gatz et al., 2006). The Alz gene database (www.alzgene.org) has details on all the published genetic studies of AD.

Verification of genes associated with sAD is problematic due to its heterogeneity. The contribution of any one gene product to the risk of AD is probably very small. Numerous gene products may act in concert acting to increase AD risk together with environmental factors forming a complex interacting network (Blennow et al., 2006).

Where genetic predisposition has not been established, other risk factors have been suggested from epidemiological studies. Many of these factors are linked to a reduced reserve capacity of the brain. This is governed by neuron number, synaptic and dendritic arborisation along with lifestyle associated cognitive strategies and has been linked to early presentation of AD pathological changes (Mortimer et al., 2003). Commonly proposed causes of a low reserve capacity are:

- Small brain size
- Low educational and occupational achievement
- Low mental ability in early life
- Low mental and physical activity in later life

Other studies link head injury to risk of AD. This may also be due to creating reduced reserve capacity although it has also been proposed as a possible initiating pathogenic event, inducing a cascade of events resulting in AD neuropathology (Blennow et al., 2006; Jellinger, 2004).

Genetic factors resulting in fAD are generally associated with mutations in the genes for the APP (Brown, 1991), presenilin 1 and presenilin 2 (part of γ-secretase) (Hutton and Hardy, 1997) providing links to the metabolism of Aβ (discussed in 1.2.5). sAD is more elusive in its etiopathology being highly polygenic and multifactorial (Cummings et al., 1998; Liu et al., 2006).

1.3.1. Mutations in the gene encoding APP

The first genetic mutation identified was in the gene for APP located on chromosome 21 (Goate et al., 1991). Further studies have identified 23 mutations of the APP gene, 19 of which are clearly associated with the disease or other dementias. However APP gene mutations account for less than 1% of AD cases (Lambert and Amouyel, 2007).

The disease causing mutations in the gene for APP cause amino acid substitutions either clustered at the β and γ cleavage sites or involve residues important for Aβ self interactions (residues 21-23) (see figure 1.7) (Blennow et al., 2006; Crews et al., 2010). Consequently, these mutations increase Aβ generation or promote Aβ aggregation. Multiple mutations around the γ-secretase cleavage site specifically cause increased production of the more amyloidogenic Aβ42 compared to Aβ40 (T714I, V715M, V715A, I716V, V717I and V717L) (De Jonghe et al., 2001). Those substitutions clustered around residues 21-23 (A21G (Flemish), E22G (Arctic), E22Q (Dutch), E22K (Italian), D23N (Iowa)) lead to Alzheimer's-like symptoms yet these symptoms can be secondary to inter-cerebral haemorrhage (Bharadwaj et al., 2009; Crews et al., 2010; Dahlgren et al., 2002).

The idea that increased Aβ production causes AD is supported by *in vivo* gene dosage evidence from DS patients. These individuals always develop early onset AD due to an extra chromosome 21 (Trisomy 21). Consequently, these individuals have three copies of the gene for APP resulting in an overproduction of Aβ, accelerated plaque deposition and increased lipid oxidation (Lynch et al., 2000; Odetti et al., 1998). The gene dose effect is also supported by a report of a family with fAD with a duplication of the APP locus with resultant over-expression (Rovelet-Lecrux et al., 2006). This evidence from genetic studies implicates Aβ as being central to the pathogenic pathway leading to AD.

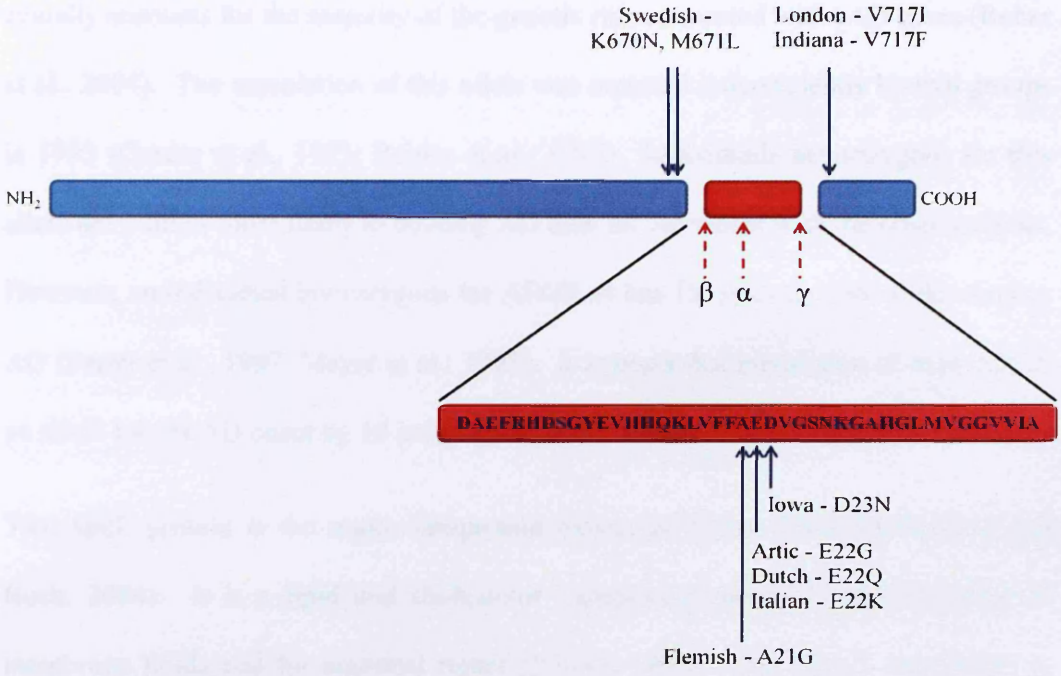

Figure 1.7. Common amino acid substitutions caused by APP gene mutations
Common disease causing mutations in the gene for APP are clustered around the secretase cleavage sites. APP is shown in blue, Aβ in red and the cleavage sites are indicated by red arrows (adapted from (Crews et al., 2010))

1.3.2. Mutations in the genes encoding the presenilins

The majority of fAD cases are explained by mutations in the highly homologous genes for presenilin 1 and presenilin 2 (PSEN1 and PSEN2) located on chromosomes 14 and 1 respectively (Blennow et al., 2006; Levy-Lahad et al., 1995; Sherrington et al., 1995). These gene mutations cause altered APP processing and consequently up-regulation of Aβ generation, especially Aβ42, further supporting the pivotal role of Aβ in the development of AD (Lynch et al., 2000; Odetti et al., 1998).

1.3.3. APOE variants

One of the most common risk factors for sAD is the possession of the apolipoprotein E (APOE) ε4 allele located on chromosome 19. The allele comes in 2 other major forms, APOE ε2 and APOE ε3. It is suggested that carrying the APOE ε4 allele

actually accounts for the majority of the genetic risk connected with sAD cases (Raber et al., 2004). The association of this allele was reported independently by two groups in 1993 (Corder et al., 1993; Poirier et al., 1993). Individuals heterozygous for this allele are 3 times more likely to develop AD than an individual with the other variants. However, an individual homozygous for APOE ε4 has 15 times the risk of developing AD (Farrer et al., 1997; Meyer et al., 1998). It appears that possession of each APOE ε4 allele lowers AD onset by 10 yrs (Corder et al., 1993).

The ApoE protein is the major lipoprotein expressed in the brain (Butterfield and Bush, 2004). It is a lipid and cholesterol transporter needed for the recycling of membrane lipids and for neuronal repair (Poirier, 1994). The ApoE4 transporter is less efficient than the other variants at performing these functions, strengthening links between vascular disease, fat intake and AD. An association is also observed between ApoE4 and oxidative stress. Mouse studies with knock-in human APOE ε4 alleles under the mouse promoter show significantly more oxidative stress when incubated with Aβ42, than the other alleles (Lauderback et al., 2002). Homozygous APOE ε4 individuals have increased lipid oxidation and those with one APOE ε4 allele show heightened catalase and glutathione peroxidise activities, enzymes important for detoxification of ROS (Ramassamy et al., 1999). For these reasons, APOE ε4 allele has been suggested to increase risk of AD as it is less able to cope with Aβ induced oxidative stress. In addition, ApoE has been found to promote Aβ fibrillisation and deposition into plaques and has been proposed to act as a biological chaperone for this process perhaps due to modulation of metal ion content (Holtzman et al., 2000; Moir et al., 1999). ApoE4 has been found to be least effective at acting as a chaperone for solubility of Aβ insulted with metal ion stresses (Moir et al., 1999).

1.4. β-amyloid and Alzheimer's disease

Most researchers would agree that Aβ is central to AD pathogenesis, in particular the longer Aβ42 which is found enriched in plaques. These plaques are not considered pathogenic. However the brain tissue also contains smaller, soluble forms of Aβ, not yet sequestered into plaques. It is these "oligomeric" species that many hold accountable for the neurodegeneration in AD. This soluble pool of Aβ in the AD brain may be a direct determinant of neurodegeneration severity (McLean et al., 1999). It has been observed that these species inhibit hippocampal LTP and disrupt synaptic plasticity. Monomers and fibrils do not exert this effect (Walsh et al., 2002).

The deposition of Aβ is accompanied by major and widespread oxidative stress in the neocortex (Lynch et al., 2000). It is posited that oligomeric Aβ is the source of this oxidative stress, possibly through ROS formation, and is potentially the root of neurodegeneration. The oligomerisation and aggregation of Aβ through various intermediate species (discussed in 1.4.2.) gaining some sort of toxic property during this process is central to thinking on AD pathogenesis and is the basis of the amyloid cascade hypothesis.

1.4.1. Amyloid cascade hypothesis

The amyloid cascade hypothesis was first proposed in 1991 by John Hardy and David Allsop to explain pathogenesis of AD caused by Aβ (Hardy and Allsop, 1991). This hypothesis has been applied to many neurodegenerative diseases to explain the source of amyloid toxicity. Key to this idea is an imbalance in the production and clearance of the amyloidogenic protein: in the familial disease there is often increased production; in the sporadic forms there is presumed to be decreased clearance (possibly due to reduced degradation by neprilysin (Iwata et al., 2000) or IDE (Miller

et al., 2003), reduced perivascular drainage (Weller et al., 1998) or less microglial clearance (Frautschy et al., 1992)). All the factors connected to Aβ aggregation are not understood yet, the process by which soluble Aβ is converted to aggregating Aβ is critical. Anything that alters this process may be considered a trigger and contribute to disease state in sAD (Bharadwaj et al., 2009; Hureau and Faller, 2009).

This hypothesis has proved resilient and although some revisions have been made, it is still central to the beliefs on amyloid toxicity (Hardy and Selkoe, 2002). It is now thought that somewhere during the aggregation of the protein into fibrils the protein gains some form of toxicity, inducing cellular dysfunction and cell death.

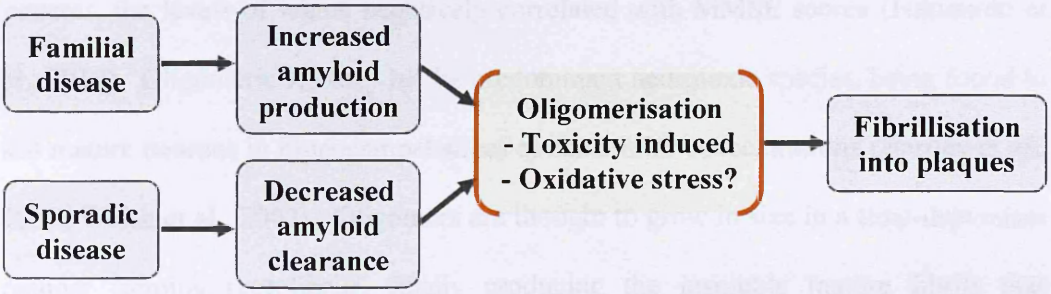

Figure 1.8. Simplified schematic of the amyloid cascade hypothesis.
A consequence of genetic and environmental factors is an imbalance between production of the amyloid and its clearance. In general, the familial disease (governed by genetic influences) is the product of increased generation of the amyloidogenic protein; the sporadic disease (with environmental stimuli) is associated with decreased clearance of it. Soluble oligomeric species exert their toxicity prior to sequestration into insoluble plaques. This results in cellular dysfunction and subsequent cell death of vulnerable cell populations.

1.4.2. Aβ aggregation

The mechanism by which Aβ ultimately leads to neuronal degeneration and dementia appears to critically depend on a conformational change of soluble, monomeric Aβ to a structure with high β-sheet content, permitting subsequent aggregation. The denaturation of the peptide may be the initial event allowing the subsequent mis-folding to occur. Aβ42 is more prone to adopting the β-rich conformation, aggregates

faster and has also been suggested to be able to trigger the mis-folding of the other Aβ species, promoting aggregation (Jarrett et al., 1993).

Monomeric Aβ can be found in AD brains up to 6 times the level of control brains. The increased Aβ concentration drives oligomerisation of Aβ. It is these early, soluble oligomers that seem to be fundamental in the development and early progression of AD as it has been found that the level of soluble Aβ and the degree of cognitive impairment and synaptic loss are strongly correlated (Klein et al., 2001; Lue et al., 1999; McLean et al., 1999). In particular, high-molecular weight soluble Aβ oligomers (40-200kDa) have been found to be elevated in the CSF of Alzheimer's patients, the levels of which negatively correlated with MMSE scores (Fukumoto et al., 2010). Oligomeric Aβ may be the predominant neurotoxic species, being found to kill mature neurons in hippocampal slices at nanomolar concentrations (Hartley et al., 1999; Walsh et al., 2002). Oligomers are thought to grow in size in a time-dependant manner forming protofibrils, finally producing the insoluble mature fibrils that comprise senile plaques (See Figure 1.9) (Walsh et al., 1997). However, the exact sequence of oligomer species that Aβ becomes fibrils through is up for debate.

It is thought the increased hydrophobicity of Aβ42 compared to Aβ40 drives β-sheet formation and fibrillogenesis. In support of this, Aβ40 with a glutamine instead of glutamate at residue 22 (E22Q-Aβ40) is slightly more hydrophobic than wt Aβ40 and fibrillises faster. Consistent with this idea, substitutions that decrease the hydrophobicity of the peptide reduce its rate of polymerisation: A21G-Aβ40 aggregates much slower than wt Aβ40 and F19P-Aβ40 remains totally dissociated (Clements et al., 1996; Walsh et al., 1997). Structural elements in the central hydrophobic core of the peptide may play a key role in controlling aggregation, crucially residues 17-21, together with the C-terminus of the peptide. Amino acid

substitutions created in this region prevent the self associations necessary for aggregation of Aβ, reducing aggregation rate (Walsh et al., 1997).

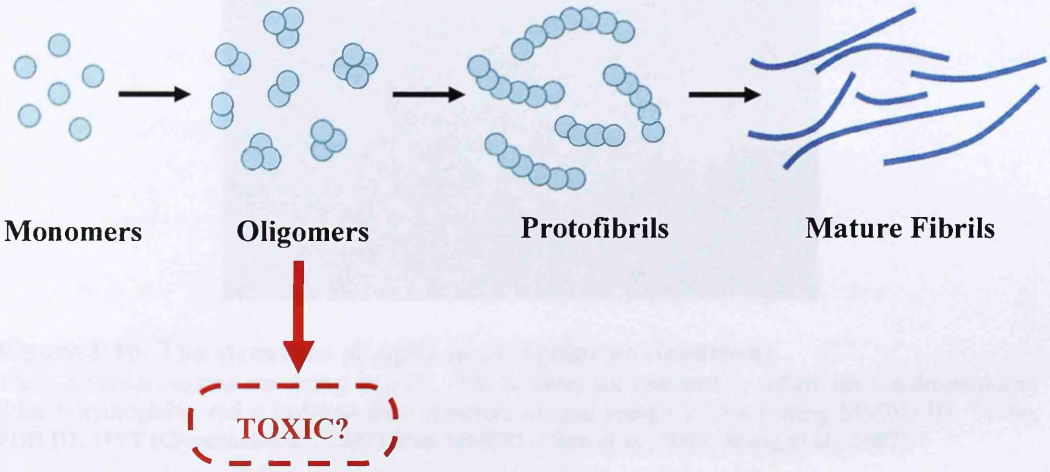

Figure 1.9. The process of Aβ aggregation
Monomeric Aβ is thought to aggregate through a series of small soluble oligomeric species. These are subsequently sequestered into protofibrils and later into mature fibrils. It is early, soluble, oligomeric Aβ that is believed to cause neurotoxicity.

1.4.2.1. Structure of Aβ and its aggregation intermediates

Following cleavage from the parent APP molecule, Aβ presumably adopts a random coil conformation. From here it is hypothesised that the peptide can potentially adopt an α-helical or β-sheet predominated structure, dependant on its environment. The nature of Aβ42 makes its structure invariably difficult to resolve by NMR. Under membrane mimicking conditions (using SDS) Shao and colleagues found the α-helical conformation to be promoted, preventing its aggregation. They observed an extended chain from Asp1-Gly9, followed by 2 α-helical regions between Tyr10-Val24 and Lys28-Ala42, connected by a short looped region (Gly25-Ser26-Asn27) (Shao et al., 1999). The exact locations of these helices are dependent on experimental conditions. Figure 1.10 shows these α-helices in an apolar environment. With the large proportion of the 2nd helix being hydrophobic and considering its proximity to the membrane following cleavage by γ-secretase, it would seem logical to assume this to be the

normal structural impetus. Here, the peptide is thought to be stabilised but does not fully insert into the hydrocarbon interior of the membrane (Shao et al., 1999).

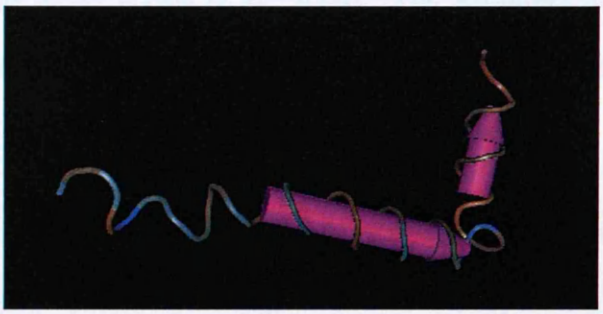

Figure 1.10. The structure of Aβ42 in an apolar environment
The 2 α-helical regions are shown in pink. The residues are coloured to reflect their hydrophobicity (blue = hydrophilic, red = hydrophobic). Structure imaged using Cn3D 4.1 using MMBD ID: 21966, PDB ID: 1IYT (Crescenzi et al., 2002) from MMDB (Chen et al., 2003; Wang et al., 2007).

An earlier study of Aβ40 reported a similar α-helical structure, with the loop region potentially lying at the water/lipid boundary (Coles et al., 1998). They observed that deprotonation of E22 and D23 destabilised the helix which may be the forerunner for aggregation. In support of this, the shortest fragment of Aβ sequence that retains fibril forming ability is Aβ14-23 and Aβ lacking this sequence is unable to form fibrils (Tjernberg et al., 1999). In addition, residues 21-23 are substituted in some AD causing mutations. Whether aggregation proceeds from α-helix to β-sheet or from random coil to β-sheet is unclear. In either case, an altered microenvironment, such as high Aβ concentration, decreases in pH or metal association, the specific side chain interactions are replaced by hydrogen bonding between the amino and carbonyl groups of the main chain; a β-sheet conformation is adopted and oligomerisation proceeds instigating Aβ toxicity (Barrow and Zagorski, 1991; Burdick et al., 1992; Fraser et al., 1991; Huang et al., 2004; Liu et al., 2006; Shao et al., 1999).

Initial oligomerisation presumably involves the formation of Aβ dimers which have been found to be stable structures and are often observed prior to aging of Aβ

solutions. These have been described as being 6-7nm by 3nm and show a characteristic internal structure, with 3-4nm strands of the peptide orientated at 90° to the long axis of the dimer (Losic et al., 2006). The Aβ dimer must have intrinsic stability as following rigorous deseeding of Aβ preparations structures described as dimeric have been reported to persist (Walsh et al., 1997).

The structure of the neurotoxic, soluble oligomers is elusive due to indications that the aggregates are highly polymorphic together with the dynamic, heterogeneity of aggregation solutions. Losic and colleagues have reported them to be 3-4nm in width consisting of end-to-end association of the monomer units. As with the orientation of monomers in the dimer, the polypeptide chain is at 90° to the axis of the oligomer, otherwise known as a cross-β conformation (as shown in figure 1.11). This would suggest that it is the linear association of Aβ subunits that creates oligomers (Losic et al., 2006). Indeed, Walsh and colleagues have observed only three stable species, being Aβ dimers, protofibrils and mature fibrils. This was the case when they tested both Aβ40 and Aβ42. Initially samples were dominated by dimers. These decreased in a time-dependant manner with a concomitant increase in protofibril levels (Walsh et al., 1997). This evidence does not mean these are the only Aβ species or the most important Aβ species in neuronal degeneration seen in AD. However, it is consistent with the hypothesis that Aβ oligomerises through a series of short-lived intermediates forming protofibrils. These then act as centres for growth of mature fibrils. This seems to be the accepted hypothesis in the majority of reports, yet secondary and tertiary structures of oligomers have been reported to differ between preparation techniques. There may be oligomer forming events independent from the fibrillisation pathway or several mechanisms of aggregation; oligomers formed through different mechanisms may be structurally different (Klug et al., 2003; Losic et al., 2006).

Protofibrils are usually described as curved fibrils less than 200 nm in length formed from linear β-sheet packing of Aβ molecules (see figure 1.11). Residues 18-40 form two β-strands whilst residues 1-17 remain relatively unstructured. An intermolecular salt bridge between D23 and K28 stabilises the linear structural arrangement of the molecular subunits (Luhrs et al., 2005). Mature fibrils are observed as being 6-8nm wide and are formed from association of these protofibrils (Balbach et al., 2002; Malinchik et al., 1998). Luhrs and colleagues report a mature fibril to contain 4 protofibrils coiled around each other, with a twist of 0.45° per molecule (Luhrs et al., 2005). There also is some evidence that smaller Aβ peptides can also form anti-parallel β-strands (Hou and Zagorski, 2004).

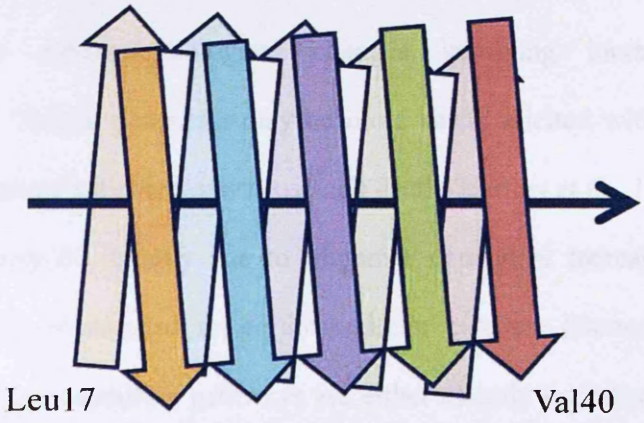

Figure 1.11. The cross-β conformation of Aβ
Diagram shows the core β-structure of residues 17-40. Each Aβ molecule is coloured differently to show how inter-β-strand interactions occur. The direction of the fibril axis is indicated by an arrow (adapted from (Luhrs et al., 2005).

1.4.3. Oligomeric β-amyloid induced neurotoxicity

The links between Aβ and the neurodegeneration observed in AD are robust, with the general consensus agreeing that the oligomeric species are critical. Less clear is which oligomer species are important in the pathogenesis of AD. Numerous groups have reported the observation of a wide range of polymers prior to the formation of protofibrils, several of which have been implicated as being the oligomeric culprit.

These include the dityrosine dimer (Barnham et al., 2004; Smith et al., 2007a), tetramer (Ono et al., 2009) up to hexamers (Butterfield and Bush, 2004), 12-mers that are able to bind receptors inducing toxicity (Lambert et al., 1998), and a 56kDa Aβ species (Aβ*56) that induces memory deficits in transgenic mice (Lesne et al., 2006). Identification of the toxic species is inherently troublesome due to the heterogenic and changing nature of Aβ solutions. It may be that one or several of these oligomeric species are inherently toxic to neuronal cells. On the other hand, the actual process of oligomerisation from monomer/dimer to protofibril may be the root of its toxicity.

Oligomeric Aβ is believed to affect normal neuronal functioning *in vivo* altering the efficacy of hippocampal synapses at physiological concentrations. Aβ affected neurons show electrophysiological changes involving increased membrane depolarisation. Action potentials may be more easily elicited with the potential to cause chronic stress and eventually cause cell death (Hartley et al., 1999; Walsh et al., 2002). This may be directly due to oligomer dependent increases in membrane permeability and subsequent raised intracellular calcium (Demuro et al., 2005). Furthermore, many signalling pathways are either directly or indirectly regulated by calcium levels or membrane depolarisation, including those pathways that lead to autophagy and cell death (Abramov et al., 2004).

It has been reported that oligomers can actually form discrete pores in membranes. This has been called the "channel hypothesis" of amyloid pathogenesis. Many disease-associated amyloid proteins have been reported to form these pores, inserting irreversibly as discrete channels into the membrane increasing bilayer conductance (Arispe et al., 1993; Hirakura et al., 2000; Kagan et al., 2004; Lashuel et al., 2002; Mirzabekov et al., 1996). Other research has found that permeabilisation of membranes by oligomeric Aβ insertion does not require pore formation (Kayed et al.,

2004). Generation of ROS by Aβ within the membrane would oxidatively damage the phospholipid hydrocarbon tails, thus increasing membrane permeability. Brain membrane phospholipids are largely composed of polyunsaturated fatty acids which are particularly sensitive to oxidation. This process generates aldehydes, indicative of oxidative stress and clearly increased in AD brains (Praticò, 2008).

The interaction of metal ions with Aβ is central to potential oxidative toxic mechanisms of the peptide. Redox active metal ions, such as copper and iron, are found to interact with Aβ, promote auto-aggregation of the peptide and provide the biochemical means for ROS generation. Zinc ions are also found to promote aggregation of Aβ although the ion does not permit redox chemistry (Huang et al., 2004; Liu et al., 2006). The binding of zinc to Aβ has been suggested to be in competition with copper ions, protecting against ROS formation by the petide-copper ion complex (Cuajungco et al., 2000; Smith et al., 2007a). These ideas are investigated in Chapter 7.

It is widely thought that oligomers are the toxic entity. Indeed, it has been reported that Aβ42 owes its greater toxicity to its tendency to form stable early oligomers whereas Aβ40 tends to remains monomeric (Chen and Glabe, 2006). Oligomers may be a transient phase in the fibrillisation process rather than a stable subset of structures (Oddo et al., 2006). It is also possible that only some oligomers are stable, potentially formed independent of the fibrillisation pathway; oligomers may be a particular stage of the aggregation process, or separate structures formed away from the fibrillisation process. With the number of reported structural conformations of Aβ, it would seem naive to preclude the possibility of a complex inter-changing of low-order species, some of which are "off" the fibrillisation pathway and dependent on all manner of micro-environmental factors. Nevertheless, the aggregation of Aβ42 *in vitro* has been

found to involve the formation of several distinct transient species, some of which have been found in the AD brain. These may then slowly rearrange into protofibrils and mature fibrils (Bitan et al., 2003a; Bitan et al., 2003b).

1.4.4. Aβ and the oxidative changes in AD

Oxidative damage is a major feature in AD pathophysiology exhibited by the damage to lipid membranes along with various other cellular components. This alters the properties of the membranes affecting fluidity, ion transport, enzymatic activity, protein cross-linking, and can result in cell death (Chauhan and Chauhan, 2006). Evidence for oxidative stress in AD neurons comes from the observation of lipid peroxidation products (HNE) along with DNA oxidation products (8-HO-guanidine) and protein oxidation products (producing free carbonyls, carbonyl modified neurofilament protein, glycation and glycoxidation products) (Smith et al., 1996). Protein nitration is also observed along with DNA adducts to both mitochondrial and nuclear DNA accompanied by antioxidant activity disruptions (Smith et al., 2007a). Autopsy specimens of the frontal lobe from AD brains exhibit these modifications together with reductions in oxidation sensitive enzymatic activity (i.e. creatine kinase and glutamine synthase). These alterations may contribute to symptoms exhibited by affecting susceptible neurons (Aksenova et al., 1999; Lynch et al., 2000). There is evidence that following initial elevation of these markers they then decrease as the disease progresses to advanced AD. This may be due to the fact neurons that have evaded apoptotic death have responded to the insults by increasing cellular defences (Perry et al., 2002). However, by this time the neurodegenerative damage exerted may be extensive and irreparable.

The Aβ-induced oxidative stress model is an attractive hypothesis for the oxidative adducts observed in AD. However, it remains unclear whether the generation of Aβ is the cause or effect; Aβ induces oxidative stress yet generation of Aβ is increased as a result of oxidative stress (Chauhan and Chauhan, 2006). Once at a sufficient concentration to induce oxidative damage, Aβ is thought to actually induce its own production creating a positive feedback cycle (Atwood et al., 2003; Gaeta and Hider, 2005). In fact, many pro-oxidising agents increase Aβ generation via an increase in BACE-1 expression and activity pointing towards an antioxidant role for Aβ (Paola et al., 2000; Tamagno et al., 2006; Tamagno et al., 2005).

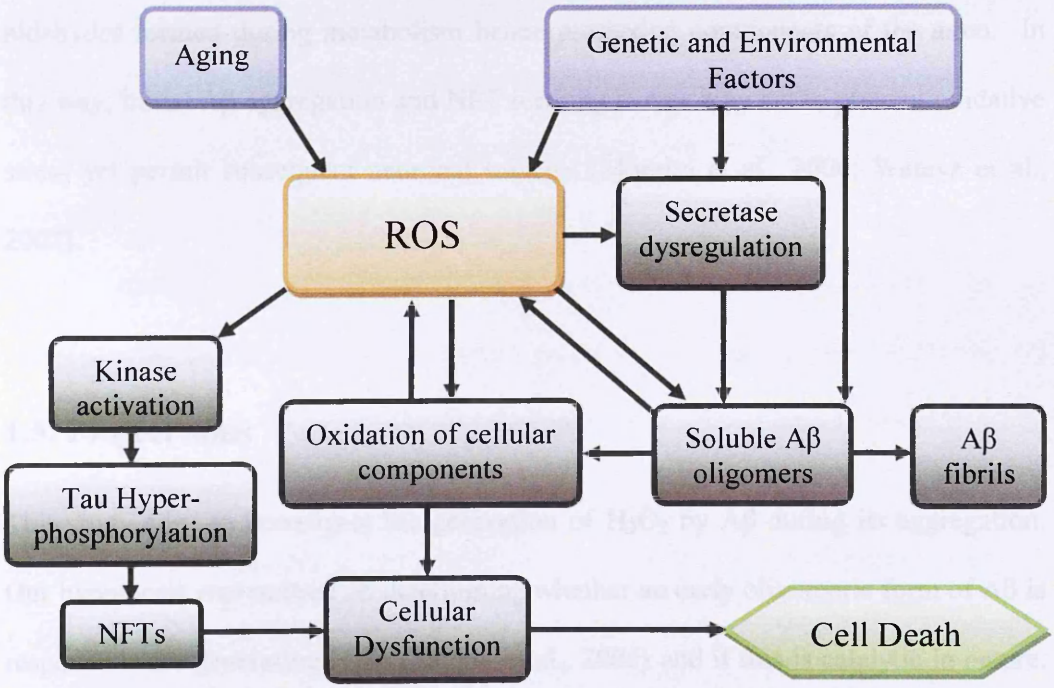

Figure 1.12. Schematic of how cell death may be brought on by oxidative mechanisms

ROS generation may be central to the mechanism by which neuronal death is caused. Aging causes general increases in ROS, whereas genetic and environmental factors increase soluble oligomer load. These influences bring about AD plaques and tangles and result cellular dysfunction and cell death.

Aβ is able to scavenge free radicals and chelate metal ions, both neuroprotective properties (Moreira et al., 2006) yet both may result in altered Aβ properties including

its aggregation state. This effect may be complex and critically regulated. Low concentrations of Aβ may be anti-oxidative, with production of Aβ kept at base levels. However as it detoxifies ROS it becomes itself oxidatively modified and aggregates, identifying senile plaques as compensatory responses to oxidative stress. Over a specific threshold and promoted by increased Aβ42:Aβ40 the Aβ is no longer an antioxidant, but a pro-oxidant, binding redox metals, generating H_2O_2 and critically up-regulating its own production creating a self propagating feedback loop (Chauhan and Chauhan, 2006).

It is suggested that tau and neurofilament protein may act similarly to scavenge toxic aldehydes formed during metabolism hence protecting components of the axon. In this way, initial Aβ aggregation and NFT forming events may act to prevent oxidative stress yet permit subsequent neuronal toxicity (Moreira et al., 2006; Wataya et al., 2002).

1.5. Project aims

This study aims to investigate the generation of H_2O_2 by Aβ during its aggregation. Our hypothesis was centred on determining whether an early oligomeric form of Aβ is responsible for generating H_2O_2 (Tabner et al., 2005) and if this is catalytic in nature. To test this several lines of investigation were followed:

1. The Aβ to be used in this study needed to be of optimum quality. The tendency of Aβ to aggregate has the consequence of forming pre-aggregated Aβ (called "seeds") even within lyophilized peptide stocks. To investigate the early stages of aggregation the peptide needed to be deseeded as far as possible, ideally to a point at which only monomeric Aβ remained.

2. H_2O_2 generation was assessed during the aggregation process from Aβ40 and Aβ42 and from different Aβ amino acid substituted peptides, to draw conclusions on the aggregation associated events that are involved with Aβ mediated H_2O_2 generation.
3. The aggregation of Aβ is dynamic and heterogeneous in nature therefore we could not attribute H_2O_2 generation to any specific sub-species. For this reason we attempted to make stably cross-linked oligomers to test specifically for their H_2O_2 generating abilities but to also characterize some of their other properties.
4. A technique was developed to attempt to capture and immobilize Aβ species to determine if Aβ prevented from further aggregation could retain its ability to generate H_2O_2. We aimed to test different time points during the aggregation of Aβ to assess their H_2O_2 generating capacity, but also the ability of Aβ to degrade H_2O_2.
5. The effect of a range of redox active metals implicated in Aβ-toxicity on the generation of H_2O_2 during the aggregation of Aβ was investigated. From this we hoped to deduce the metal ions important for H_2O_2 generation and their effects on aggregation of Aβ.
6. Inhibition of aggregation was investigated for its effect on H_2O_2 generation by Aβ, using a group of short peptide inhibitors being developed. These are specifically designed to target the early Aβ-Aβ associations that initiate aggregation, therefore may inhibit the formation of H_2O_2 by oligomeric Aβ.

The intention of these objectives was to help to identify and characterise the processes involved in the early generation of H_2O_2 during the aggregation of Aβ (Tabner et al., 2005). This has lead to conclusions on the role of Aβ-mediated oxidative pathways in the development of AD.

Chapter 2
Materials and Methods

2.1. Materials

2.1.1. General reagents

All general reagents were purchased from Sigma-Aldrich with the following exceptions. Ammonium hydroxide (NH_4OH), diethylene triamine pentaacetic acid (DTPA), monoclonal 6E10 and biotinylated 6E10 (AbCam), Streptavidin Europium, Enhancer solution and DELFIA Europium-labelled Streptavidin (Perkin Elmer, Buckinghamshire), glacial acetic acid and acetone (AnalaR), ethanol (Fisher Scientific), glycine (Melford), 30% acrylamide/bis 37.5:1 (NBS Biologicals, Cambridgeshire), Instant Blue (AMS Biotechnology Ltd, Oxon), Mark 12 unstained protein standards (Invtrogen), multicoloured protein markers (NEN Life sciences), 10-acetyl-3,7-dihydroxyphenoxazine (ADHP) (Cambridge Bioscience), OR inhibitors (Cambridge Peptides), Mica sheets (Agar Scientific Ltd, Essex). MilliQ water (Millipore) was used to make up all buffers.

2.1.2. Peptides

Recombinant Aβ was purchased from rPeptide, Georgia. Synthetic Aβ peptides and short custom peptides were purchased from American Peptide Company (APC), California. Aβ42-1 (reverse Aβ42) was purchased from California Peptide Research Inc. Aβ42 Met35Nle was from Cambridge Bioscience, Cambridge. All were >95% purity.

2.2. Methods

2.2.1. Peptide preparation

The development of the preparation protocol of deseeding Aβ is explained in chapter 3. The optimal method found for deseeding Aβ was found in this chapter to be using TFA. Nevertheless, its use had been problematic until late in the research. For this reason many experiments were carried out using non-TFA treated Aβ, although all key experiments were repeated using TFA-treated Aβ.

All Aβ peptides were kept frozen at -20°C until prepared for use. Throughout its preparation the peptide was kept on ice to prevent any aggregation. Each vial of lyophilised Aβ was initially dissolved in 0.01% NH_4OH, pH 10.6, to 0.5 mg/ml. The vials were then vortexed for 6 secs every 10 mins for 1 hr and then sonicated for 4 x 30 secs or until completely dissolved. For non-TFA treated samples the solution was then aliquoted into appropriate sized portions for the experiment pending and the solvent evaporated off by benchtop speedvac. All peptides were subsequently treated with 1,1,1,3,3,3-hexafluoroisopropanol (HFIP) by adding the solvent to the peptide at 0.5mg/ml, vortexed and sonicated for 4 x 30 secs, and the HFIP removed by evaporation in the speedvac. The peptide was then HFIP treated once again just before solubilisation into buffer for use.

Where Aβ has been TFA treated, during the NH_4OH treatment the vial was split into 3-5 working portions into glass vials and the solvent evaporated using a benchtop speedvac. TFA with 4.5% thioanisol was then added to the vials one at a time to a concentration of 1 mg/ml, vortexed and sonicated for 30 secs, and then placed under a stream of nitrogen (N_2) gas until all the liquid had evaporated. Unless otherwise

stated, HFIP was then added to 0.5 mg/ml, vortexed and sonicated for 4 x 30 secs and the HFIP removed by evaporation in the speedvac.

In all cases 10 mM phosphate buffer (PB), pH 7.4, was then added to the peptide to the required concentration, vortexed and sonicated for 4 x 30 secs or until dissolved and ready for aggregation sampling. With each batch, especially when TFA used, the pH was checked (to be at pH 7.4) using pH test strips. This method for preparation was used in all experiments except where stated otherwise.

Where test substances were added, such as metal ions, ethylenediaminetetraacetic acid (EDTA), ascorbic acid and OR aggregation inhibitors, these were made up at the appropriate concentration in 10 mM PB and then used to solubilise the peptide, vortexed and sonicated as above.

2.2.2. Determination of Aβ concentration

Caution was taken when trying to ascertain Aβ concentration. Copper based concentration assays were avoided due to the copper binding properties of Aβ. Concentration was determined by UV absorbance. Aβ solutions were prepared and 50 µl added to a UVette (a UV transparent cuvette). This was then placed in a desktop UV spec and the absorbance read at λ270 nm with the extinction coefficient of 1480. The extinction coefficient is based on the existence of one tyrosine residue in the primary Aβ sequence. Chemical treatments and aggregation may modify this residue as it is susceptible to oxidation and implicated in the Aβ-Aβ interactions required for aggregation. For these reasons, this technique was not used to compare results where different treatments have been applied or where aggregation is believed to have proceeded.

2.2.3. Thioflavin T

Thioflavin T was dissolved in MilliQ water to a stock concentration of 1 mM. This stock solution was kept wrapped in foil to prevent exposure to light. 100 mM glycine was prepared also in MilliQ water, and 2.5 M sodium hydroxide (NaOH) added to pH 8.5. The 100 mM glycine-NaOH buffer was then used to make up a working solution of 15 μM thioflavin T in 50 mM glycine-NaOH buffer. This was kept at 4°C in the dark, and used for up to a week. For use, the 15μM thioflavin T was allowed to come to room temperature for 30 mins and then used to prime the Synergy 2 multilabel plate reader. At each time point 3 x 5 μl 100 μM Aβ or 10 μl <100 μM Aβ was aliquoted in triplicate into a Nunc 96 well black microtitre plate. The samples were then injected with 50 μl 15 μM thioflavin T, mixed and read 10 times over 2 mins with the platereader at Ex λ450nm and Em λ482nm (LeVine, 1993). Average fluorescence was calculated over the course of the 2 mins together with standards deviations and plotted as relative fluorescence units (RFU).

2.2.4. Oligomeric immunoassay

Aβ samples were diluted 1:125 in assay buffer, 0.5% γ-globulin, 0.05% Tween 20, 50 mM tris-HCl, 150 mM NaCl, pH 7.6, vortexed and frozen at -80°C until use. Clear 96 well Maxisorb microtitre plates were coated with 100 μl, 1 μg/ml monoclonal antibody (mAb) 6E10 in 10 mM phosphate buffered saline (PBS), covered with a plate seal and left at 4°C overnight. Plates were then blocked with 150 μl assay buffer with 1% gelatine from fish skin added to a final concentration of 0.022%. This was then incubated for 1 hr at 37°C and then washed with 4 x 300 μl PBS Tween (PBST) using a platewasher. Excess liquid was tapped out of the plate and 100 μl of the peptide samples aliquoted into the wells in quadruplicate. The plate was then

incubated for 1 hr at 37°C and subsequently washed with 4 x 300 µl PBST. Excess liquid was once again tapped out of the plate and 100 µl biotinylated mAb 6E10 in assay buffer was added to the wells at a concentration of 1 µg/ml. Following a further incubation for 1 hr at 37°C and 4 x 300µl PBST wash, 100µl 1:500 dilution of Europium-labelled streptavidin in 0.05% γ-globulin, 0.5% bovine serum albumin (BSA), 20µM DTPA, 10 mM tris, 150 mM NaCl, pH 7.4, was added to each well. This was then shaken for 10 mins on a Victor 2 plate reader, covered in foil and placed on a rocking table for a further 50 mins. Enhancer solution was allowed to come to room temperature, and after washing with 4 x 300 µl PBST, 100 µl of Enhancer was added to each well. Plates were shaken again for 10 mins and then read using the Victor 2 microplate reader using the time-resolved DELFIA system. Averages and standard deviations were plotted in relative fluorescence units (RFU).

2.2.5. Amplex red

A stock solution of 10 mM ADHP (Amplex red) in dimethyl sulphoxide (DMSO) was aliquoted into 50 µl portions. Each aliquot had 10 secs of $N_{2(g)}$ introduced into it and then frozen in $N_{2(l)}$ and stored at -80°C. 1 KU/ml stock solution of horseradish peroxidase (HRP) in 10 mM PB, pH 7.4, was prepared and aliquoted into 15 µl portions. 10 secs of $N_{2(g)}$ was introduced into the aliquots and then they were frozen in $N_{2(l)}$ and stored at -80°C. The HRP was then diluted to 10 U/ml and split into 100 µl aliquots which can then be used to make up the Amplex red working solution. 5 mls Amplex red working solution was made for each experiment using 50 µl 10 mM Amplex red stock solution and 100 µl 10 U/ml HRP in 10 mM PB. The resultant working solution was 100 µM Amplex red, 200 mM/ml HRP. For fluorescence measurements, 15 µl of the test solution or H_2O_2 concentration (for concentration

curve) was pipetted in triplicate into the wells of a Nunc 384 well black plate. 15 µl Amplex red working solution was then added to each well and the plate shaken and fluorescence read on the Victor 2 microplate reader at Ex λ563nm and Em λ587nm (Zhou et al., 1997). Averages and standard deviations were converted to concentration of H_2O_2 and plotted.

2.2.6. Atomic force microscopy

2µl 25 µM Aβ in 10 mM PB was diluted by either 1:10 or 1:100 in MilliQ water was pipetted onto a piece of cleaved mica. This was allowed to dry and then imaged using a Digital instruments multimode Scanning Probe Microscope (SPM) using tapping mode with an AppNano ACT, aluminium (reflex) coated probe with spring constant of 40 N/m (nanoScience Instruments Inc). At least 3 x 10 µm image scans of each sample were performed followed by 5, 2 and 1 µm scans.

2.2.7. Sodium dodecyl sulphate polyacrylamide gel electrophoresis (SDS-PAGE)

Tris-glycine buffered SDS-PAGE gels were made using Biorad Mini gel kit, using glass plates separated by 0.75 mm spacers. Gels were made using a two layered system with a resolving gel for protein separation and then a stacking gel. The percentage gel required was obtained by altering the amount of acrylamide in the resolving gel recipe. Table 1.1 shows the recipe for 2 x 16.5% gels.

The resolving gel was pipetted between the cleaned glass plates to ~15 mm below the top of the glass. 2 drops of butanol were then pipetted onto the top of the resolving gel and the gel given time to polymerise. The butanol was then washed out from between the plates with MilliQ water, the stacking gel poured on top and a comb

inserted to create wells. Gels were given further time for polymerisation, then either used or wrapped in saran wrap and kept at 4°C until their use, within 24 hrs.

Solution	16.5% Resolving gel (mls)	Stacking gel (mls)
MilliQ water	1.8	5.6
1.5M Tris-HCl, pH 8.8	2.5	-
0.5M Tris-HCl, pH 6.8	-	2.5
30% Acrylamide/Bis mix	5.5	1.7
10% SDS	0.1	0.1
10% Ammonium persulphate (APS)	0.1	0.1
TEMED	0.01	0.01

Figure 2.1. Recipes for resolving and stacking gel to make 16.5% SDS tris-glycine gels.
Ingredients added in the order shown.

Samples for gel electrophoresis had equi-volume SDS Sample buffer (0.125 M Tris-HCl, pH 6.8, 2% SDS, 10% glycerol, 0.01% bromophenol blue, 0.1 M dithiothreitol (DTT)) added to them, and then heated to 98°C for 3 mins. Samples along with either Mark 12 unstained protein markers or multicoloured protein markers were loaded into the wells of the gel and then electrophoresed at a constant voltage of 180 V, for 60 mins, in Tris-glycine running buffer (25 mM tris, 0.192 M glycine, 1% SDS).

2.2.8. Instant Blue

Following electrophoresis of gels they were put into Instant Blue protein stain overnight on a rocking table. The stain was then removed and replaced with MilliQ water to destain.

2.2.9. Aβ detection by western blot

Blotting was performed using a semi-dry blotting system. For each blot to be performed 1 piece of 0.45 μm Immobilon-p polyvinylidene fluoride (PVDF) paper was soaked for 30 secs in methanol. The nitrocellulose and 6 pieces of blotting paper were then soaked in semi-dry blotting buffer for at least 30 mins. Once the gel has finished running, 3 x pre-soaked blotting papers were layered in the blotting tank, following by the nitrocellulose, then the gel, and lastly 3 more pre-soaked blotting papers. The stack was then rolled to eliminate air bubbles and the lid to the tank put on with extra weight applied to the top. The blots were run at constant amps of 0.06 amps per blot for 2 hrs.

Once run, the blots were either put straight into block (2% dried milk powder, 10 mM PBST) for 1 hr, or dried to be stained later. If the blot was dried, the blot went into 100% methanol for 30 secs, MilliQ water for 2 mins, then 10 mM PBS for 1 min, prior to going into the blocking solution. Subsequently the blots were incubated with 1:10000 dilution of mAb 6E10 in blocking solution for 90 mins, washed with PBST for 4 x 5 mins, then incubated with 1:10000 dilution of polyclonal anti-mouse-HRP in block for 90 mins. Finally, the blots were washed with PBST for 4 x 5 minutes and left in PBST for developing the blot by ECL Kit to visualise the bands.

2.2.10. Photo-induced cross-linking of unmodified proteins (PICUP)

18 μl 25 μM Aβ or control peptide samples were used for PICUP reactions which were performed completely in the dark. To the peptide sample, 1 μl 20 mM APS was added, followed by 1 μl 1 mM tris(2,2'-bipyridyl) dichlororuthenium(II). This mixture was mixed briefly and placed in the cross-linking apparatus. This utilised the timed shutter from a camera to permit source of light to pass to the sample for a

controlled length of time, during which the light dependent reaction could take place. The samples were exposed to light for the required length of time (between 0-1 secs). Finally 10 µl 10% β-mercaptoethanol in 10 mM PB was added to each sample to quench the cross-linking reaction (Bitan et al., 2003a). 30 µl SDS gel loading buffer was then added to each sample ready for gel electrophoresis.

2.2.11. Formation of SDS-stable oligomers

Non-PICUP cross-linking of Aβ was investigated using H_2O_2 and HRP, and, H_2O_2 with $CuCl_2$. 30 µl reaction mixtures were made up of 25 µM Aβ with 100 µM, 10 µM or 1 µM H_2O_2 and either HRP (100, 10 or 1 U/ml) or $CuCl_2$ (1.33, 0.133 or 0.013 mM). The reaction mixtures were mixed and incubated at 37°C for 1 hr or 24 hrs. Samples had 30 µl SDS gel loading buffer added to them following the incubation time to quench the reaction and prepare them for gel electrophoresis. When being made for immobilisation experiments, reaction mixtures were kept at the same concentrations but volumes were increased according to the immobilisation procedure requirements. SDS gel loading buffer was not added following the cross-linking incubation but instead mAb 6E10 was added as set out in immobilisation protocol.

2.2.12. Development of immobilisation of Aβ to assess H_2O_2 generation

This protocol was developed over the course of experiments and is still being finalised. In early experiments 25 or 50 µM Aβ was aggregated over a range of time periods in 10 mM PB, pH 7.4 at 37°C. Samples of the Aβ solution were taken for thioflavin T, immunoassay and Amplex red in addition to 50-100 µl sample which was then incubated at 37°C for 60 mins on a surface pre-coated with mAb 6E10 (test surfaces included a range of microtitre plates, nitrocellulose membrane, dynabeads

and 0.6 ml Greiner PCR tubes). The surface was then washed 3 times with 10 mM PB and then 10 mM PB added to the immobilised Aβ and incubated for 24 or 48 hrs at 37°C. The buffer was then assessed for its H_2O_2 concentration by Amplex red.

The most recent protocol does not use a surface for the immobilisation of Aβ samples but instead uses ultracentrifugation of the 6E10-bound Aβ. Recovery of the antibody was tested using a range of biotinylated 6E10 dilutions made in 10 mM PB. These were then centrifuged for 1 or 2 hrs at 16,110 x g and also for 1 hr in the airfuge at approx. 136,000 x g. 3 x 100 µl samples were taken before and after centrifuge steps and coated onto a clear 96 well Maxisorb microtitre plate. The level of antibody present in the sample was then detected using streptavidin-Europium detection used for the oligomeric immunoassay.

When testing Aβ samples 25 or 50 µM Aβ42 was aggregated in 10 mM PB at 37°C for various lengths of time to test different aggregation time points. Samples were taken for thioflavin T, immunoassay and Amplex red fluorescence determination. To the remaining Aβ solution, the mAb 6E10 was then added to a final concentration of 1-4 µg/ml and incubated for 2 hrs at 37°C to allow antibody binding. This was then placed in the airfuge and spun at approx 136,000 x g for 90-180 mins. Thioflavin T and immunoassay samples were taken from the supernatant and from control PB samples. Following immobilisation on mAb 6E10, ultra-centrifugation and supernatant removal, each tube had either 100 µl 10 mM PB added or 1 µM H_2O_2 and were gently mixed. Thioflavin T samples were taken to gauge recovery of Aβ. The immobilised Aβ samples were then incubated at 37°C for 48 hrs and then placed in the airfuge for a further 90-180 mins. The supernatant from each sample was then tested for its H_2O_2 concentration using the Amplex red assay.

Where cross-linked samples were tested, the HRP/H_2O_2 cross-linking procedure was followed, except using scaled up volumes of each reagent to have a reaction mixture of total volume 180 µl. 75 µM of each Aβ peptide was prepared in 10 mM PB and split into 2 samples, 1 to be cross-linked, the other as a non-cross-linked control. To the cross-linked sample HRP and H_2O_2 was added to the Aβ to final concentrations of 100 U/ml, 100 µM and 25 µM respectively in 10 mM PB. To the non cross-linked samples 10 mM PB was added to the peptide to bring it to 25 µM. All samples were incubated at 37°C for 1 hr at which point samples were taken for thioflavin T and Amplex red fluorescence determination. 6E10 was then added at 10 µg/ml and incubated for a further 2 hrs at 37°C and then placed in the airfuge for 2 hrs at approx 136,000 x g. Supernatants were removed and tested for their fluorescence in the thioflavin T and Amplex red assays. 100 µl 10mM PB was added to each immobilised sample and gently mixed. These were then incubated at 37°C for 24 hrs, placed in the airfuge for 2 hrs at approx. 136,000 x g. The supernatants were removed and tested for their H_2O_2 concentration using the Amplex red fluorescence assay.

2.2.13. Statistical Analyses

For the large majority of the data produced multiple comparisons were required. For these, ANOVAs were performed followed by planned pairwise comparisons of means using Tukey HSD. The ANOVA reports a p value (Prob > F) which reports whether or not at least one pair of means is statistically different. However, it does not report which groups differ from each other. The Tukey HSD is essentially a t-test that corrects for experiment-wide error rate when there are multiple comparisons. Pearson's correlation coefficients have also been used when appropriate.

Chapter 3
Deseeding of β-amyloid

3.1. Introduction

Increasing evidence implicates the early soluble oligomers of Aβ to be the primary toxic species causing AD (Chromy et al., 2003; Kayed et al., 2003; Kim et al., 2003; Walsh et al., 1999). For this reason, studies of the early aggregation and toxicity of β-amyloid are critically dependant on the starting material of the peptide being tested. Yet, the inherent predisposition of Aβ for time-dependent aggregation in aqueous solution plagues its investigation (Teplow, 1998). This fact has led to manufacturers of synthetic and recombinant Aβ using a range of solvents and processes to prevent its aggregation during production, some more successful than others. As a consequence there is much variability in the peptide state received from different companies. This can be compounded with lot-to-lot variability from the same company (May et al., 1992). Most, if not all, commercially available peptides contain some proportion of pre-aggregated material that "seeds" the aggregation process, especially where Aβ42 is concerned. There are many published "deseeding" techniques using a range of solvents designed to disaggregate the peptide to create a monomeric starting material, such as using DMSO, HFIP (Dahlgren et al., 2002; Walsh et al., 1999), NaOH and NH_4OH (for high pH) (Fezoui et al., 2000), TFA (Arimon et al., 2005; Jao et al., 1997; Zagorski et al., 1999), in combination with sonication and filtering (Huang et al., 1997). Each claims to be the optimal method to produce seed-free Aβ.

For our investigations into H_2O_2 generation, a process believed to occur at the very early stages of aggregation (Tabner et al., 2005), it was vital for us to have a

consistent and highly deseeded starting material. For this reason, detailed investigation into where to source our peptide, its production method, solvent use and pre-experiment deseeding techniques were performed. For this we primarily utilised 3 techniques to ascertain the level of pre-aggregated material in the samples: thioflavin T, oligomeric immunoassay and AFM.

3.1.1. Thioflavin T

Thioflavin T is a fluorescent dye commonly used to monitor aggregation of amyloidogenic proteins. Aggregation is accompanied by an increase in the β-sheet content of the protein. When thioflavin T binds to β-sheet, its structure changes, shifting its excitation and emission wavelengths from Exλ385nm Emλ445nm to Exλ450nm and Emλ482nm. This means that it can be used as a measure of the aggregation state of the peptide (LeVine, 1993, 1999).

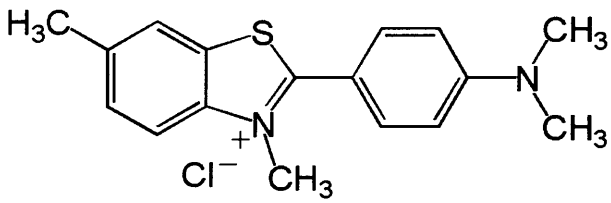

Figure 3.1. The structure of thioflavin T

3.1.2. Oligomeric immunoassay

The monoclonal antibody 6E10 binds specifically to the first 17 residues of the Aβ peptide. Each Aβ subunit can only bind one of these antibodies therefore, when the same antibody is used for capture and detection, only aggregated Aβ should be detected. Although this can give no information on the size of the aggregates, a negative signal can signify a monomeric preparation of Aβ as no detection antibody can bind to a captured monomer. Also notable is that once Aβ has aggregated fully to

mature fibrils, the immunoassay signal, although still raised in comparison to control samples, is reduced compared to maximum fluorescence. This is presumably due to detection antibody binding sites being obscured due to the quaternary structure of the fibrils, or, due to them being washed off the capture antibody because of their size.

3.1.3. Atomic force microscopy

AFM has some major advantages over other methods of imaging Aβ aggregates. Samples do not need to be conductive or semi-conductive as needed with STM. Sample preparation is very simple in comparison to Electron Microscopy, EM, and by using intermittent contact mode, or tapping mode, the soft biological samples can be imaged in a more natural state. It works via a cantilever tapping across the surface of the sample with a laser focused on the back of the tip reflecting off the tip and into a photodetector. This measures the position of the beam, and the computer program can interpret this data. Because the beam is tapping over the surface, this form of AFM can image, not only the topography of the surface, but also the interaction of the tip with the sample. This is called the phase and effectively gives a measure of the "elasticity" of the sample on the surface.

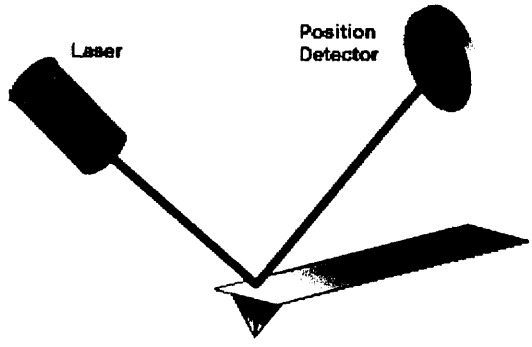

Figure 3.2. AFM cantilever and laser reflecting off it into the photodetector.

3.2. Results

3.2.1. Selection of recombinant peptide

Preliminary studies had identified that in general recombinantly made Aβ contained less seeds than synthetically made, although all key experiments were also performed with a synthetically produced Aβ to corroborate results. In addition, rPeptide had been identified as the most consistent producer of recombinant Aβ. They provided a choice of 4 solvents for the peptide to be prepared in: HFIP, NaOH and the acids HCl and TFA (referred to as rAβ42-HFIP, rAβ42-NaOH, rAβ42-HCl and rAβ42-TFA respectively). We initially compared these 4 pre-treatments for their Aβ42 seed content and subsequent aggregation properties by thioflavin T and oligomeric immunoassay (figure 3.3).

Where the peptide had been prepared in the acids, rAβ42-HCl and rAβ42-TFA, no significant increases in thioflavin T fluorescence were observed upon incubation at 100 μM, in 10 mM PBS at 37°C over 72 hrs. The high thioflavin T fluorescence throughout the 72 hr incubation suggests that the samples were already highly aggregated. Similarly, the immunoassay results indicated these peptides were highly aggregated at T=0. In fact Pearon's correlation coefficients were significantly negatively correlated (HCl: $r = -0.601$, TFA: $r = -0.802$, $p \leq 0.002$, $n = 24$) implying the samples contained a high proportion of mature fibrils upon wetting the peptide.

The rAβ42-NaOH sample at 100 μM started at approximately half the starting thioflavin T fluorescence of the HCl and TFA treated samples and this fluorescence showed significant increases over the course of the 72 hrs ($r = +0.800$, $p \leq 0.000$, $n = 18$). The immunoassay started at a higher fluorescence than the HCl and TFA treated samples, but, as with the TFA treated sample, this decreased over time ($r = -0.89$, $p \leq$

0.000, n = 24). Although this sample appeared to start in a less aggregated state than the HCl and TFA treated samples, it was still largely aggregated upon wetting.

The rAβ42-HFIP sample started lowest in its thioflavin T fluorescence and this increased steadily over the 72 hr period ($r = +0.864$, $p \leq 0.000$). In addition, the immunoassay showed increasing fluorescence over the first 24 hrs, at which it plateaued then started to drop. This indicated that this was the best peptide for further study. However, the immunoassay clearly showed that this peptide contained aggregates upon wetting and therefore still required deseeding for investigation into the early aggregation process.

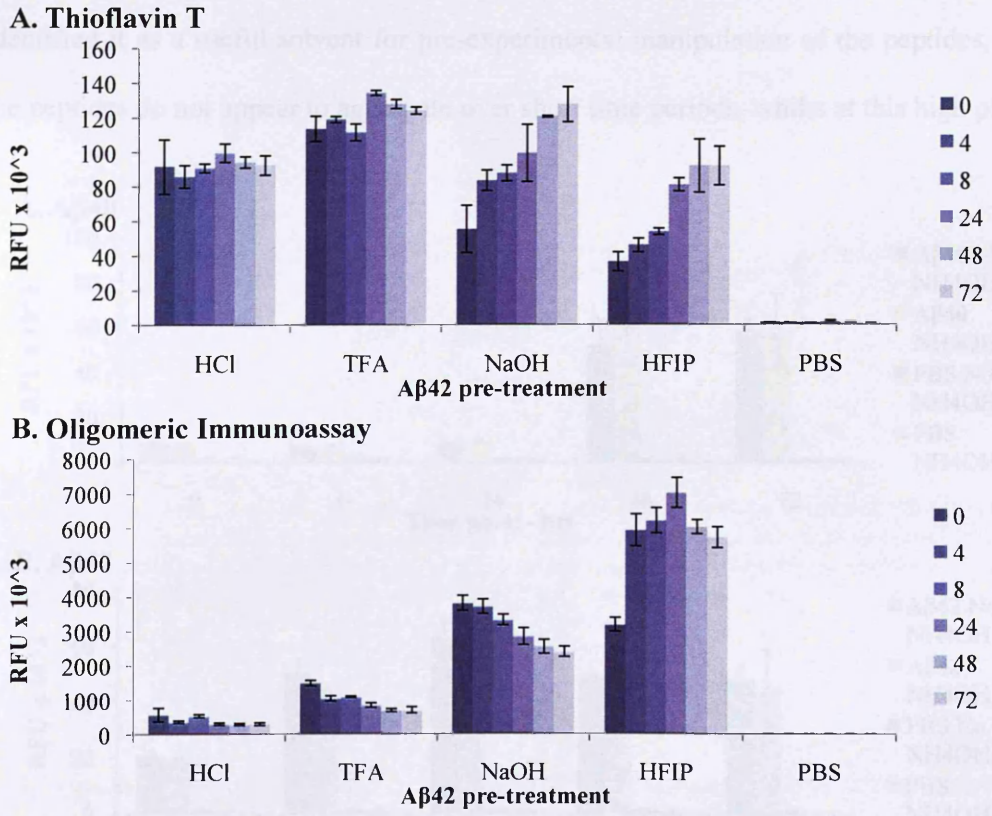

Figure 3.3. Aggregation of Aβ42 measured by thioflavin T and oligomeric immunoassay

Recombinant Aβ42 prepared by the manufacturer with HCl, TFA, NaOH or HFIP, were dissolved in 0.001% NH_4OH, pH 10.04 and buffered to pH 7.4 by addition of 5 x PBS to a final concentration of 100 μM Aβ42 in 10 mM PBS. Samples were aggregated at 37°C over 72 hrs with samples being taken for thioflavin T (A) and oligomeric immunoassay (B) at given time intervals. Results are means ± S.D. (Thioflavin T: n=3, Immunoassay: n=4)

3.2.2. The effect of buffering out NH_4OH on aggregation

Using NH_4OH or NaOH at a pH greater than 10 is thought to prevent aggregation and also assist in initial solubilisation of the Aβ (Guilloreau et al., 2007; Streltsov et al., 2008). The peptide should not aggregate prior to buffering the solution down to pH 7.4. This was tested using NH_4OH (see figure 3.4). The treatment made no difference to either the starting thioflavin T fluorescence or the aggregation properties of both 100 μM Aβ40 and Aβ42. The immunoassay indicated that Aβ40 was near monomeric upon solubilisation (data not shown) but Aβ42 required effective deseeding. Although this process did not aid any deseeding of Aβ42, it did show that NH_4OH treatment did not have a detrimental effect on the peptide and its aggregation. This identified it as a useful solvent for pre-experimental manipulation of the peptides, as the peptides do not appear to aggregate over short time periods, whilst at this high pH.

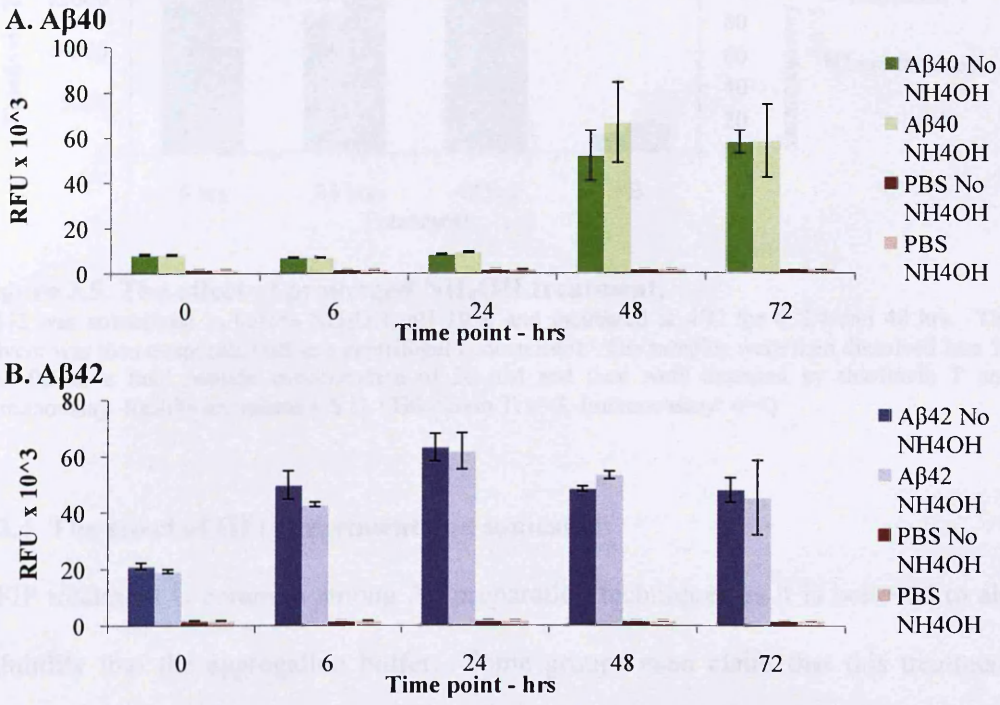

Figure 3.4. The effect of buffering out NH_4OH on aggregation of Aβ40 and Aβ42
100 μM Aβ40 and Aβ42 prepared by either dissolving straight into 10 mM PBS, or, solubilising into 0.01% NH_4OH, pH 10.6, first and then buffering this out to a final concentration of 10 mM PBS, pH 7.4. Thioflavin T fluorescence was then assessed over 72 hrs (A = Aβ40, B = Aβ42). Results are means ± S.D. (n=3)

3.2.3. The effect of NH_4OH as a deseeding treatment

In 3.2.2. the Aβ was only in the NH_4OH for enough time to solubilise the peptide and then buffered out. We also tested if incubating the peptide in NH_4OH for longer time periods followed by removal of the solvent was able to deseed Aβ42. This was unsuccessful as both immunoassay and thioflavin T data showed no decrease in fluorescence with increased incubation time (see figure 3.5). In fact, there appeared to be a small increase in the fluorescence of 50 μM Aβ42 over time, indicating the NH_4OH may not fully prevent the propensity of Aβ42 to aggregate. For these reasons NH_4OH treatment was not used to deseed Aβ42 and was only used for short time periods to split vials of Aβ with prolonged exposure avoided.

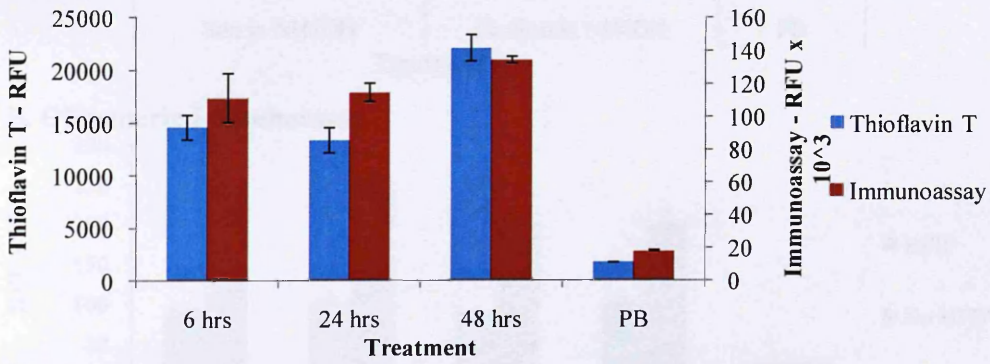

Figure 3.5. The effect of prolonged NH_4OH treatment.
Aβ42 was solubilised in 0.01% NH_4OH, pH 10.6, and incubated at 4°C for 6, 24 and 48 hrs. The solvent was then evaporated off in a centrifugal concentrator. The samples were then dissolved into 10 mM PB to a final peptide concentration of 50 μM and then were assessed by thioflavin T and immunoassay. Results are means ± S.D. (Thioflavin T: n=3, Immunoassay: n=4)

3.2.4. The effect of HFIP treatment and sonication

HFIP treatment is common among Aβ preparation techniques as it is believed to aid solubility into the aggregation buffer. Some groups even claim that this treatment removes all Aβ42 seeds from the sample creating a monomeric solution (Shelat et al., 2008). Sonication, likewise, is believed to be needed to not only lift the peptide into solution, but also aid deseeding of the peptide (Evans et al., 1995; Huang et al., 1997).

We found HFIP treatment to be useful for reducing the initial fluorescence from the recombinant Aβ42 solubilised at 25 μM in 10 mM PB, in both thioflavin T and the immunoassay (see figure 3.6.). However, it was clear from the immunoassay results, that even with the HFIP treatment the fluorescence was above the fluorescence from PB, indicating a fully deseeded peptide had not been obtained.

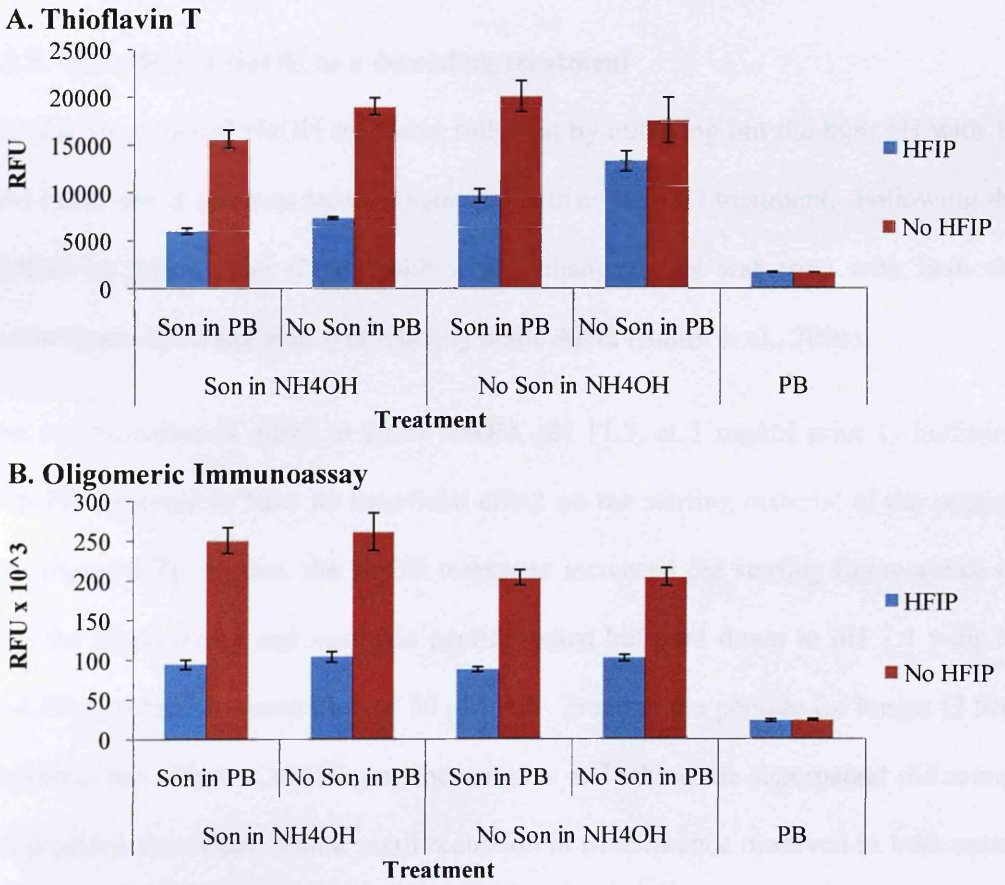

Figure 3.6. The effect of HFIP and sonication on deseeding.
Aβ42 was split in 0.01% NH_4OH, pH 10.6, incubated at 4°C for 30 mins. Samples were then prepared with and without sonication in the NH_4OH, with and without HFIP treatment and with and without sonication in the 10 mM PB. Aβ42 was prepared at 25 μM in the 10 mM PB and assessed by thioflavin T (A) and Immunoassay (B). Results are means ± S.D. (Thioflavin T: n=3, Immunoassay: n=4)

Sonication was performed at both the NH_4OH and solubilisation into the PB steps. Where HFIP treatment was not performed, sonication appeared to have limited effectiveness. However, where the HFIP treatment was performed both sonications

appeared to be useful in reducing thioflavin T fluorescence yet only the sonication in PB showed a small decrease in the oligomeric immunoassay fluorescence. This identified both HFIP treatment and sonication as useful deseeding techniques. Nevertheless further deseeding of Aβ42 would be preferable for investigation of early Aβ oligomerisation.

3.2.5. The effect of NaOH as a deseeding treatment

We also investigated NaOH treatment followed by buffering out the high pH with 10 mM PB to see if this was more advantageous than NH_4OH treatment. Following the method in Smith et al (2006) with a few changes, this was tried with both the recombinant Aβ42 and also synthetically made Aβ42 (Smith et al., 2006).

The solubilisation of Aβ42 in 2mM NaOH, pH 11.3, at 1 mg/ml prior to buffering with PB appeared to have no beneficial effect on the starting material of the peptide (see Figure 3.7). In fact, the NaOH treatment increased the starting fluorescence of both the recombinant and synthetic peptide when buffered down to pH 7.4 with 10 mM PB to a final concentration of 50 μM Aβ. Treating the peptide for longer (2 hrs) amplified this effect. Centrifuging the samples and taking the supernatant did rescue the peptides somewhat, with a small reduction in fluorescence observed in both cases. However, it was clear that NaOH treatment did not improve the starting material of the peptide from the double HFIP treated samples. In fact, when these samples were allowed to aggregate over 24 hrs, the NaOH treatment had detrimental effects on their aggregation properties. The NaOH treated recombinant peptide showed reduced aggregation related fluorescence and the synthetic NaOH Aβ42 did not appear to show any aggregation related fluorescence increases (data not shown).

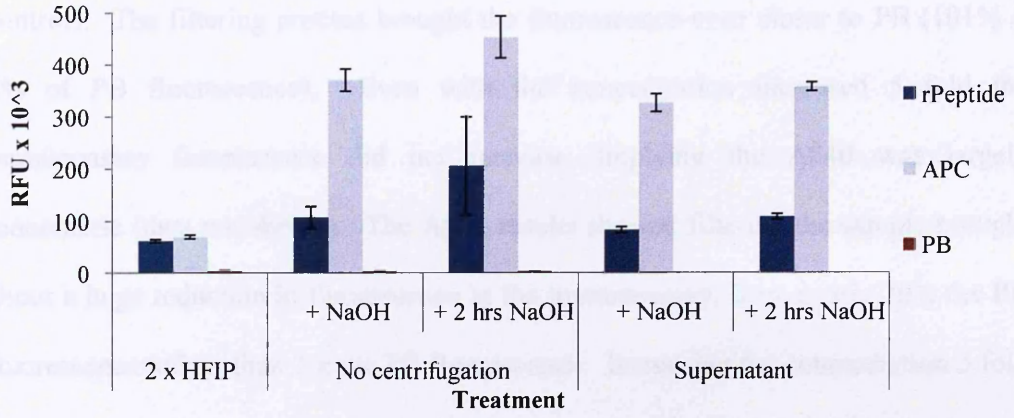

Figure 3.7. The effect of NaOH on deseeding.
Recombinant and synthetic Aβ42 was split in 0.01% NH_4OH, pH 10.6, followed by 2 x HFIP treatments. To appropriate tubes, 2mM NaOH, pH 11.3 was added to the Aβ42 at 1 mg/ml, vortexed and sonicated with or without 2 hour incubation at 4°C, with or without centrifugation for 10 mins at 16,110 x g. The NaOH treated samples and supernatants were then buffered out with 10 mM PB to a final Aβ42 concentration of 50 μM and oligomeric content assessed by immunoassay. Results are means ± S.D. (n=4)

3.2.7. Filtering

Filtering appears to be a logical strategy for removing the larger seeds of Aβ from the solution. This technique is employed by several research groups (Balcells et al., 2008; Evans et al., 1995; Huang et al., 1997). We initially investigated the deseeding ability of 10kDa and 30kDa molecular weight cut off filters (Vivaspin) as, in theory, they should filter out anything larger than dimers and hexamers respectively.

Filtering was performed following HFIP treatment of the peptides, at 50 μM Aβ in 10 mM PB. As Aβ40 appears to contain less seeds than Aβ42 upon solubilisation, it was hypothesised that the filters would remove a larger proportion of the peptide from the Aβ42 than the Aβ40 sample. This was not the case as the filters removed a similar and substantial quantity of peptide from both samples (see Figure 3.8.A) alluding to the idea that the "stickiness" of Aβ was going to cause a large loss of protein on the filter. The immunoassay results from 50 μM Aβ40 were as expected, with the sample prior to filtering giving a fluorescence only marginally raised compared to PB

controls. The filtering process brought the fluorescence even closer to PB (101% ± 5% of PB fluorescence). Even with the concentration increased 5 fold the immunoassay fluorescence did not increase, implying the Aβ40 was largely monomeric (data not shown). The Aβ42 results showed filtering the sample brought about a huge reduction in fluorescence in the immunoassay, from nearly 20 x the PB fluorescence to less than 2 x the PB fluorescence. Increasing the concentration 5 fold caused a minor increase in the fluorescence (data not shown) indicating a large proportion of the oligomeric content had been removed by the filtering process, although it was not as close to monomeric as the filtered Aβ40 sample.

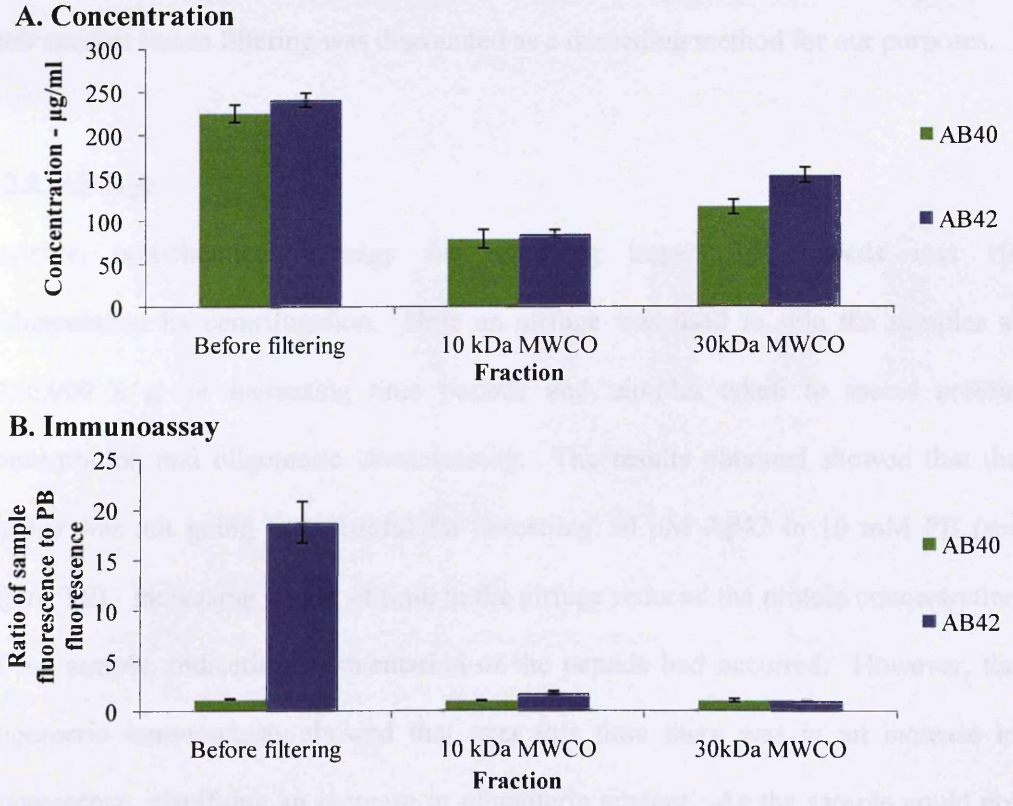

Figure 3.8. Filtering Aβ40 and Aβ42 in 10mM PB

HFIP treated Aβ40 and Aβ42 was solubilised into 10 mM PB to a concentration of 50 µM, and samples vortexed and sonicated. These were then assessed for protein concentration by UV absorption at 270nm (extinction coefficient = 1490) and samples taken for immunoassay. The rest of the Aβ was put through either a 10 or 30 kDa MWCO filter by centrifugation for 30 mins at 4000g at 4°C. The filtrate was then also assessed for its protein concentration (A) and by immunoassay (B). Results are means ± S.D. (Concentration: n=3, Immunoassay: n=4)

Filtering the peptides with these filters did aid the deseeding of Aβ42 yet with the cost of a huge loss of protein content on the filter. This large loss of peptide was considered an unacceptable cost. Furthermore, subsequent investigations with filters identified an incompatibility with the Amplex red assay (which would be used for assessing H_2O_2 generation by Aβ), as the filters are coated with glycerol. When PB was assessed by Amplex red before and after filtering through these filters the fluorescence generated was substantially increased in the filtered sample. We believe this was due to a small amount of this glycerol, a known incompatible substance in the Amplex red, washing off the filter into the sample producing a false positive result for H_2O_2 generation. Subsequent experiments to remove this glycerol were limited in their success hence filtering was discounted as a deseeding method for our purposes.

3.2.8. Airfuge

Another, non-chemical strategy for removing larger Aβ42 seeds was via sedimentation by centrifugation. Here an airfuge was used to spin the samples at ~136,000 x g for increasing time periods and samples taken to assess protein concentration and oligomeric immunoassay. The results obtained showed that the airfuge was not going to be useful for deseeding 50 μM Aβ42 in 10 mM PB (see figure 3.9). Increasing length of time in the airfuge reduced the protein concentration of the sample, indicating sedimentation of the peptide had occurred. However, the oligomeric immunoassay showed that over this time there was in an increase in fluorescence, signifying an increase in oligomeric content. As the sample could not be chilled in the airfuge, this increase may be due to the normal aggregation that would happen over this time period at this temperature. However, aggregation of Aβ42 at this concentration and temperature indicated that the aggregation observed

was much more than would be expected within this time period. The centrifugal forces may be concentrating the peptide towards the bottom of the sample, driving a small amount of aggregation of the peptide, rather than simply sedimenting larger aggregates. Nevertheless, the process did not aid deseeding of Aβ42 and therefore all centrifugal steps were avoided once the peptide was solubilised into PB.

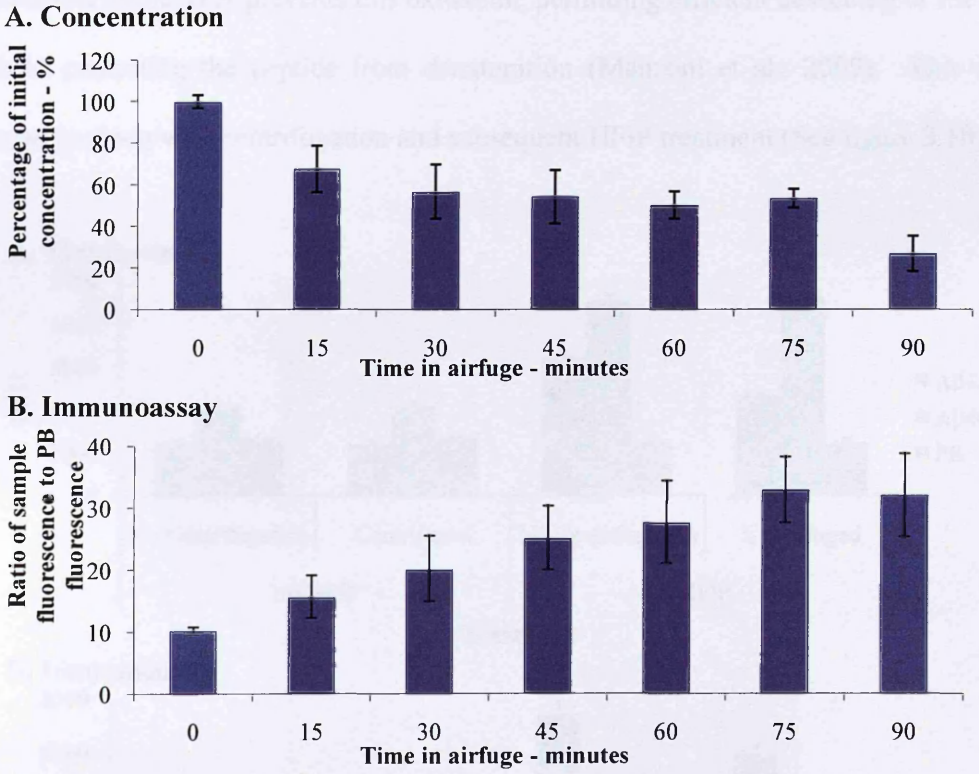

Figure 3.9. The effect of centrifugal sedimentation of the sample
HFIP treated Aβ42 was solubilised at 50 μM in 10 mM PB, vortexed and sonicated, and the initial protein concentration and immunoassay samples taken. The Aβ42 was then spun in the airfuge for up to 90 minutes at 87,000 rpm (approx. 136,000 x g), with samples taken for immunoassay and assessing protein concentration every 15 mins. Protein concentration expressed as a percentage of the initial protein concentration (A). Immunoassay expressed by the ratio of the sample fluorescence to PB fluorescence (B). Results are means ± S.D. (Concentration: n=3, Immunoassay: n=4)

3.2.9. TFA treatment of Aβ42

The treatment of Aβ with TFA has been considered a deseeding technique by several groups as its low pH promotes the random coil conformation of Aβ encouraging disaggregation (Arimon et al., 2005; Jao et al., 1997; Zagorski et al., 1999).

Treatment of the peptide with neat TFA (Jao et al., 1997) was infrequently successful, quite often appearing to completely denature the peptide, rendering it aggregation incompetent. We believe this to be at least partially due to oxidation of the methionine residue (Met35) which has been shown to reduce fibrillisation rate (Butterfield and Bush, 2004). Manzoni et al reported that the addition of 4.5% thioanisol to the TFA prevents this oxidation, permitting efficient deseeding of the Aβ whilst protecting the peptide from denaturation (Manzoni et al., 2009). This was tested in along with centrifugation and subsequent HFIP treatment (See figure 3.10).

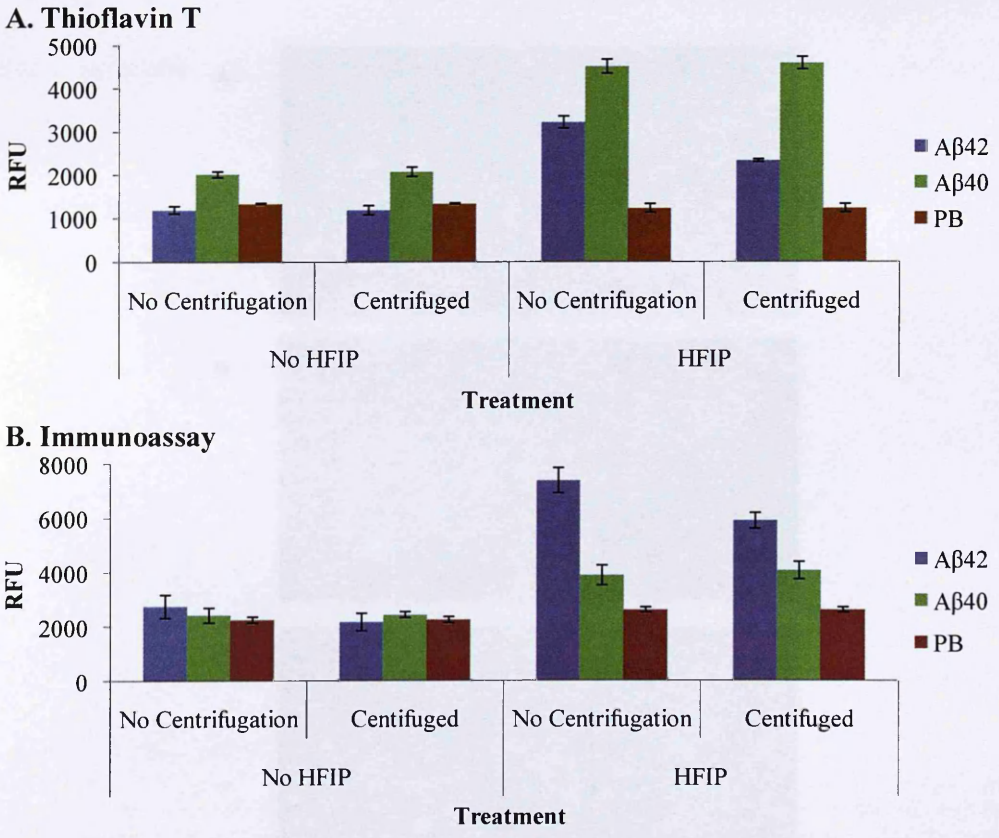

Figure 3.10. The effect of TFA treatment on Aβ

NH_4OH treated Aβ40 and Aβ42 were subsequently treated with TFA, 4.5% thioanisol, vortexed and sonicated for 30 secs. Half the samples were then centrifuged for 15 minutes at 16110 x g and then all samples dried under $N_{2(g)}$. One centrifuged and one non-centrifuged tube from each set of samples were then HFIP treated 2 times as described earlier. All samples were then solubilised in 10 mM PB, pH 7.4, to a final concentration of 25 μM, vortexed and sonicated for 4 x 30 secs. Samples were then analysed for thioflavin T (A) and Oligomeric immunoassay (B) starting fluorescence. Results are means ± S.D. (Thioflavin T: n=3, Immunoassay: n=4)

The thioflavin T and oligomeric immunoassay data supported this claim bringing the fluorescence of 25 μM Aβ42 in both assays right back to PB levels, indicating an almost monomeric solution in the oligomeric immunoassay. This was observed in both the centrifuged and non-centrifuged samples showing the centrifugation did not provide any additional deseeding to the samples. In the Aβ40 samples the TFA treatment retained more thioflavin T fluorescence than the Aβ42 indicating the β-sheet content was affected less than the Aβ42, yet it also appeared to be monomeric from the immunoassay. Deseeding of the Aβ42 sample was confirmed by AFM, where images were observed to be the same as PB controls (see figure 3.11).

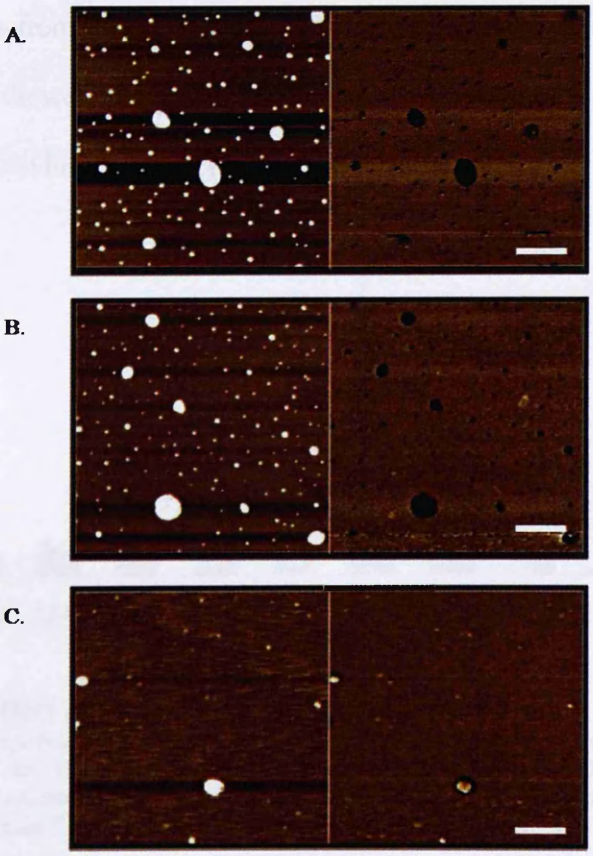

Figure 3.11. AFM of TFA deseeded Aβ42
TFA deseeded Aβ42 was solubilised at 25 μM into 10 mM PB, pH 7.4, vortexed and sonicated, then diluted 10 fold into MilliQ water. 2 μl was then dotted onto cleaved mica and imaged using a Digital Instruments SPM in tapping mode. Left-hand image is height, right-hand image is phase contrast. Images are Aβ42 (A and C) and PB control (B). Bar represents 2μm in A and B, and 200 nm in C.

Subsequent treatment of the samples with HFIP provided no additional deseeding and actually increased the fluorescence observed from all samples in both assays. Thus we can conclude that although HFIP aids deseeding of more aggregated samples, it somewhat permits early aggregation, perhaps promoting certain oligomeric species. Unfortunately, due to the preparation requirements of using TFA, one HFIP treatment had to be incorporated into the final deseeding strategy to permit transfer from the glass vials used for the TFA to the 0.6 ml PCR tubes used for solubilising the peptide.

Of importance here is the ability of the TFA treated peptides to subsequently aggregate. The addition of 4.5% thioanisol during the TFA deseeding appeared to protect the peptides from TFA-mediated oxidation of Met35; subsequent sampling at later time points showed increased thioflavin T and immunoassay fluorescence, indicating aggregation had occurred (this can be seen in Chapter 4).

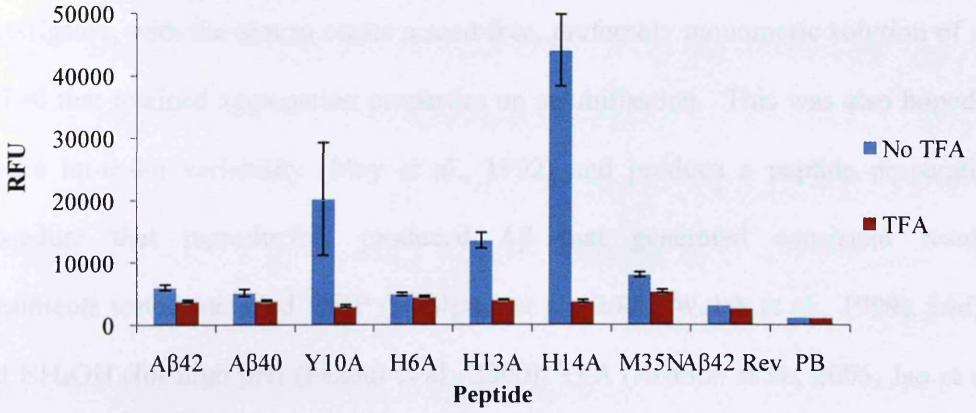

Figure 3.12. The effect of TFA treatment on Aβ peptides
NH_4OH treated Aβ peptides were subsequently treated with TFA, 4.5% thioanisol, vortexed and sonicated for 30 secs. Non TFA treated and TFA treated samples were then solubilised in 10 mM PB, pH 7.4, to a final concentration of 25 μM, vortexed and sonicated for 4 x 30 seconds. Samples were then analysed for thioflavin T fluorescence. Results are means ± S.D. (n=3)

This technique was also tested in a range of Aβ peptides to see if it was appropriate to treat all the peptides in the same manner to provide a similar starting point for comparison of their properties (Aβ40, Aβ42 and Aβ42 substituted peptides Y10A,

H6A, H13A, H14A and M35N) (See figure 3.12). It was also tested on the synthetically produced peptide (data not shown). The thioflavin T data showed a clear reduction in the thioflavin T fluorescence in all the Aβ samples tested.

3.3. Discussion

The inherent predisposition of Aβ for aggregation means that it invariably contains a large proportion of pre-aggregated "seeds" that promote further aggregation and severely hamper the investigation of the early aggregation of the Aβ peptide. As Aβ42 has a greater tendency for aggregation it is afflicted by this issue more so than Aβ40. Yet, perhaps for this very reason, evidence implicates Aβ42 as being responsible for neurotoxicity in AD. To be able to investigate early aggregation and the properties of early oligomers, published methods for deseeding Aβ were investigated, with the aim to create a seed-free, preferably monomeric solution of Aβ at T=0 that retained aggregation properties on solubilisation. This was also hoped to reduce lot-to-lot variability (May et al., 1992) and produce a peptide preparation procedure that reproducibly produced Aβ that generated consistent results. Treatments tested included HFIP (Dahlgren et al., 2002; Walsh et al., 1999), NaOH and NH_4OH (for high pH) (Fezoui et al., 2000), TFA (Arimon et al., 2005; Jao et al., 1997; Zagorski et al., 1999), sonication and filtering (Huang et al., 1997). DMSO was discounted as a potential deseeding treatment as it interferes with the Amplex red reagent used for determination of H_2O_2 generation by Aβ.

Initial experiments were designed to select the best supplier preparation of Aβ. It had been found that many suppliers of Aβ could not guarantee the aggregation state of the peptide. Sometimes it was far less aggregated than others when it would arrive almost

completely aggregated. Previous unpublished work in our laboratory by Dr. Susan Moore (Lancaster University) had identified a supplier of recombinant Aβ that had proved to be far more consistent than others in the quality of peptide delivered (rPeptide). rPeptide provided 4 solvent options for the lyophilisation of Aβ: HCl, TFA, HFIP and NaOH. Without any subsequent treatment, the Aβ42 sample lyophilised in HFIP (Aβ42-HFIP) was the only peptide to show aggregation associated fluorescence increases in the thioflavin T and oligomeric immunoassay and so was selected for further study. However, it still showed a large proportion of pre-aggregated material; it needed further treatment for the study of early oligomeric species. The other treatments however, did provide us with our first insight into their usefulness as a subsequent deseeding technique.

The acid treatments Aβ42-HCl and Aβ42-TFA in particular showed no aggregation associated fluorescence changes. The drying of the peptide at acid pH, should promote protonation of E22 and D23 and consequently the α-helical Aβ structure (Coles et al., 1998). However the subsequent solubilisation at neutral pH showed large β-sheet associated fluorescence in the thioflavin T. This was suggested to be due to any remaining solvent forcing the peptide through its pI of 5.5 (Fezoui et al., 2000). This could have had potentially irreversible consequences on the aggregation state of the peptides. For this reason subsequent testing of deseeding techniques was done with consideration of this possibility.

On the other hand, the use of NaOH as the lyophilisation solvent should avoid the pI upon solubilisation. However it did not appear to promote an aggregate free starting material. In fact, experiments with NH_4OH to keep the Aβ away from its pI at pHs greater than 10, showed that it could prevent further aggregation of the Aβ but did not act to deseed the peptide. In fact, incubation of the peptide at 4°C for 48 hrs in 0.01%

NH_4OH permitted aggregation associated increases in fluorescence in both thioflavin T and immunoassay; time dependent aggregation proceeded yet at a far reduced rate. Unlike observations by Fezoui and colleagues using NaOH, we found no advantage to the aggregation state of the peptide (Fezoui et al., 2000), yet we found no disadvantage for using it for short periods which would enable easier handling of the peptide. NaOH treatment was also tested, following a later method by Smith et al (Smith et al., 2006). Yet this also confirmed earlier observations that the high pH did not aid the deseeding process. In fact the immunoassay showed clear increases in fluorescence in both recombinant and synthetic Aβ42 when NaOH was incubated with the Aβ for 2 hrs at 4°C compared to non-incubated samples showing a time-dependent effect of NaOH on aggregation state.

HFIP treatment was the only solvent treatment that had reproducibly reduced fluorescence measured at T=0 in both thioflavin T and oligomeric immunoassay. Together with sonication during NH_4OH, HFIP and PB solubilisation steps, this comprised the basis for the deseeding of Aβ for the majority of the length of this research. Other techniques investigated including filtering and ultracentrifugation, were hoped to be useful as no chemical modification of the Aβ would be induced. However, these proved unsuccessful for several reasons. Filtering resulted in costly loses of Aβ due to both the removal of a large proportion of higher order aggregates and lower order Aβ "sticking" to the filter, along with the incompatibility with the Amplex red reagent. Ultracentrifugation, was intended to sediment larger aggregated Aβ such as protofibrils. Increasing time in the airfuge reduced the concentration of Aβ in the supernatant yet this was in conjunction with increases in immunoassay fluorescence; Aβ was not deseeded.

The deseeding of Aβ with TFA had always proven to be problematic, despite evidence that this strong acid promoted the random coil conformation of Aβ, promoting its disaggregation (Arimon et al., 2005; Jao et al., 1997; Zagorski et al., 1999). Treatment of Aβ with 100% TFA often rendered it unable to aggregate, possibly due to the oxidation of Met35 by TFA (shown to reduce fibrillisation rate) (Butterfield and Bush, 2004). TFA has been shown to induce peptide oxidation (Shen et al., 1994). Unfortunately late in this research, we became aware of research by Manzoni et al that used 4.5% thioanisol added to the TFA. The use of thioanisol as an antioxidant during peptide exposure to TFA reportedly protects the peptide from Met35 oxidation whilst the TFA promotes deseeding of Aβ (Manzoni et al., 2009). When this was tested effective deseeding of Aβ42 was achieved, together with other Aβ42 amino acid substituted peptides, some of which were highly aggregated upon arrival. Great care had to be taken during deseeding by this process due to the reactivity of TFA, requiring careful handling and consideration of its incompatibilities with certain laboratory equipment. This meant a further HFIP treatment had to be performed to transfer the samples to the tubes used for aggregating Aβ. This also ensured all traces of the TFA had been removed by the stream of nitrogen gas, which could lower the pH of the PB used to solubilise the peptide. A small reduction in the pH used for aggregation of the peptide may alter its aggregation properties. Reducing the pH low enough allows protonation of E22 and D23, stabilising the α-helical structure, thus slowing aggregation (Coles et al., 1998). However, the treatment of Aβ with TFA had now become a viable deseeding method that would hopefully aid the investigation of the early aggregation properties of Aβ.

Unfortunately, this method of deseeding was only brought to our attention late in the project. For this reason, much of the following work was performed on Aβ40 and

Aβ42 that had received no TFA deseeding, but had been HFIP treated twice with sonication as this had produced the best preparation of peptide at this time. Key experiments were repeated with the peptides being deseeded using the TFA method.

3.4. Conclusions

- The optimal deseeding conditions for Aβ peptides were found to be treating the peptide with TFA containing 4.5% thioanisol, in a glass vial, vortexing and sonicating on ice, followed by evaporation under a stream of nitrogen.
- This may be attributable to the low pH of the TFA promoting the α-helical Aβ structure, yet the thioanisol protecting the Met35 from oxidation.
- High pH could prevent aggregation for short time periods, yet it does not act to deseed the peptide
- Sonication always appeared to be beneficial in deseeding Aβ
- Prior to the use of TFA to deseed Aβ, HFIP treatment was the best deseeding method available. This was the protocol used throughout much of this research. However, key experiments were repeated with TFA deseeded Aβ

Chapter 4
Hydrogen peroxide generation by β-amyloid

4.1. Introduction

In 1956 Harman first proposed that aging is the result of cumulative damage to cells directly caused by free radical mediated damage and oxidative stress (Harman, 1956). Since aging is the greatest risk factor for AD this has generated the hypothesis that oxidative stress may be a major factor in Aβ production and deposition. AD brains exhibit many signs of extensive oxidative stress with the products of oxidation reactions being detected in the CSF and plasma of patients. Many aspects of AD may contribute to this oxidative stress, including soluble and fibrillar Aβ, brain metals, NFT, glial activation, abnormalities of the mitochondria and aging (Chauhan and Chauhan, 2006).

Oxidative stress is caused when the production of ROS overcomes the cellular defence mechanisms to detoxify it (Lynch et al., 2000). ROS are reactive molecules that contribute to a damaging oxidative environment. These include H_2O_2, peroxynitrite, and free radicals. Free radicals are particularly harmful as their unpaired electrons make them very unstable and highly reactive as they try to pair up their electrons. Free radicals generated in the body are toxic and have to be neutralised or removed. If not, they will react with many different types of molecules in an attempt to gain an electron. Nevertheless, once an electron is obtained the donor molecule finds itself with an unpaired electron thus becomes a free radical. Therefore it is vital that the body has mechanisms of detoxifying these radicals (Chauhan and Chauhan, 2006).

The high reactivity of free radicals means that they can only exert effects locally, being only able to diffuse over short, nanometre distances. H_2O_2 on the other hand is a freely permeable oxidising agent. Although not as toxic as free radicals, it is still cytotoxic and pro-apoptotic, yet its effects can extend beyond its site of generation and are perhaps more likely to be responsible for the global increases in oxidative damage observed in AD (Lynch et al., 2000). The Fenton reaction can utilise this H_2O_2 to later generate the more harmful hydroxyl radical with the aid of redox-active metals. Multivalent redox active metals are fundamental to the concept of redox chemistry as they enable electron transfer to occur. The ability of redox active metals to occupy different valence states permits redox cycling, a property utilised by many biological enzymes. However, if unregulated, ROS can be produced in an inappropriate and excessive manner causing damage (Smith et al., 2007a). The degree of ROS-mediated damage in neurons indicates a state of oxidative stress. In response to oxidative stress a living system can dynamically regulate its defences to respond to insults. A cell that fails to sufficiently defend against oxidative imbalance will inevitably enter into apoptotic cell death (Moreira et al., 2006).

It is critical that oxidative balance is rigorously controlled in the brain. Although only comprising 2% of body mass it consumes 20% of the body's oxygen uptake due to its high metabolic rate (Smith et al., 2007a). Hence an environment is created in which there is a heightened potential for oxidative stress. To combat this environment the brain is abundant in antioxidant enzymes to a far greater extent than any other organ. However, considering the potential for oxidative injury this is still at a relatively low level. Combined with the accumulation of metals that is observed with aging, the environment is ideal for redox and Fenton chemistry, generating ROS (Smith et al., 2007a). Neuronal cells are highly concentrated with unsaturated fatty acids, prime

targets for oxidative damage, and their low mitotic index means cells that succumb to apoptotic signals cannot be regenerated (Lynch et al., 2000). Neurodegeneration follows leading to the clinical features of AD. In fact, oxidative stress is considered to be one of the earliest features of brain pathology in AD, occurring prior to signs of neurodegeneration and senile plaque formation, long before symptom presentation (Nunomura et al., 2010). It has been hypothesized that these features are compensatory responses to ensure neurons do not yield to oxidative insults. If the source of the oxidative stress is directly from oligomeric Aβ (as discussed in 1.4.3), then perhaps, the plaques form a mechanism of sequestering away this toxic species.

The early stages of the Aβ aggregation process have been implicated in neuronal oxidative stress by various indirect mechanisms. These include hypotheses such as adverse metal binding (Huang et al., 2004), pore formation (Lashuel et al., 2002), membrane permeabilisation (Kayed et al., 2004), ion leakage (Walsh et al., 2002) and loss of antioxidant activity (Smith et al., 2007a). Evidence that Aβ may actually be directly responsible for this oxidative stress via the generation of H_2O_2 and free radicals was first reported by Huang and colleagues (Huang et al., 1999a) yet it was much earlier that H_2O_2 was suggested to mediate the toxicity of Aβ (Behl et al., 1994). Research in our laboratory has observed this generation of H_2O_2, not only from Aβ but also from aggregating proteins implicated in other neurodegenerative diseases, such as α-synuclein (Parkinson's disease), ABri (British dementia), and fragments of the prion protein (prion disease) (Tabner et al., 2001; Tabner et al., 2002; Turnbull et al., 2003a, b; Turnbull et al., 2001a). As a consequence of this evidence we have speculated that this H_2O_2 generation may be a common toxic mechanism exhibited by these peptides, causing neuronal cell death (Allsop et al., 2008; Tabner et al., 2002).

The mechanism by which these peptides generate H_2O_2 is thought to involve the redox cycling of metal ions (Huang et al., 1999a) with subsequent Fenton chemistry generating free radicals. Aβ was originally thought to be able to generate these radicals without the presence of metals. However, it was later shown that only trace metals were needed to permit the reaction and these were already present in the buffers used (Butterfield, 2002; Dikalov et al., 2004; Guilloreau et al., 2007; Turnbull et al., 2001b). In this chapter, the generation of H_2O_2 was investigated with no added metal ions, and so was reliant on those at trace levels within the buffer (Chapter 7 addresses the metal ion dependency of this reaction). Furthermore, experiments were carried out to ascertain how H_2O_2 is generated by Aβ; is there a particular type of early oligomer that structurally forms an enzymatic active site for its generation? Or do our observations support another manner of H_2O_2 formation by Aβ, either as a by-product of early aggregation or in fact a characteristic of Aβ monomers.

4.2. Results

4.2.1 H_2O_2 generation by Aβ42

The principle method utilised to measure H_2O_2 generation from Aβ solutions was Amplex red. This has been used to investigate H_2O_2 generation by amyloidogenic peptides previously by our research group (Allsop et al., 2008; Masad et al., 2007) and also by others (Deraeve et al., 2006). The published assay required an excessive and costly quantity of sample to be used for the determination of H_2O_2 concentration. We needed to reduce this quantity but maintain accuracy and the linear relationship between H_2O_2 concentration and fluorescence at sub-micromolar concentrations. This was achieved by using reduced volumes of the Amplex red working solution and the

sample in a 384 well microtitre plate (see figure 4.1). We also confirmed that the assay detected low concentrations of H_2O_2 generated by an enzymatic system. Here L-amino acid oxidase (L-AAO) was incubated with varying amounts of an L-amino acid substrate (L-AA, leucine in this case). D-AAO was used as a control. As can be seen in figure 4.2, the H_2O_2 generated by this enzymatic system could be detected at very low concentrations.

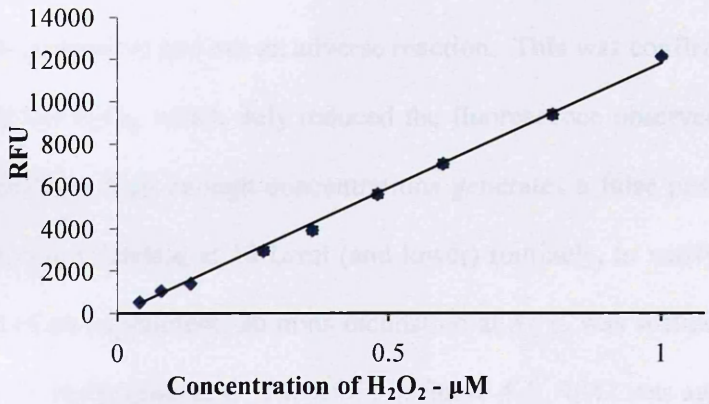

Figure 4.1. H_2O_2 concentration curve
A series of H_2O_2 concentrations were made in 10 mM PB. 15 µl of the H_2O_2 concentration was plated into a black 384 well plate in triplicate, followed by 15 µl Amplex red working solution. The fluorescence was read on the Victor 2 microplate reader at Ex λ563 nm and Em λ587 nm. Results are means ± S.D (n=3)

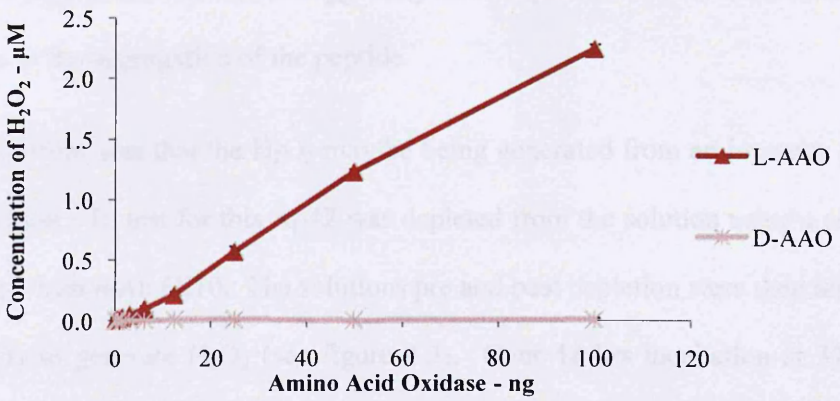

Figure 4.2. H_2O_2 generation by L-AAO
A series of L and D-AAO concentrations were made in 10 mM PB. L-Leucine was added to each and incubated at 37°C for 20 mins. 15 µl of the reaction mixtures was plated into a black 384 well plate in triplicate, followed by 15 µl Amplex red working solution. The fluorescence was read on the Victor 2 microplate reader at Ex λ563nm and Em λ587nm. Results are means ± S.D (n=3).

We then verified H_2O_2 production from aggregating solutions of Aβ42 with no added metal ions or reducing agent (see figure 4.3). The aggregation of Aβ42 at 37°C was measured using the thioflavin T and oligomeric immunoassay. Both confirmed aggregation associated increases in fluorescence over the 48 hr period. During this time over 600 nM H_2O_2 was generated from this solution. As several compounds have been shown to generate false positive results in the Amplex red assay, it was important to verify that the positive signal generated in the Amplex red assay was from H_2O_2 generation and not an adverse reaction. This was confirmed using catalase to degrade the H_2O_2, which duly reduced the fluorescence observed. Of note is that catalase itself, at high enough concentrations generates a false positive signal in the assay. We used catalase at 10 U/ml (and lower) routinely, to verify H_2O_2 generation at the end of an experiment: 30 mins incubation at 37°C was sufficient for catalase to eliminate the H_2O_2 generated. However, in figure 4.4, Aβ42 was aggregated with and without 10 U/ml catalase present throughout the 48 hr incubation period. The presence of catalase in the solution significantly reduced the amount of H_2O_2 detected (One way ANOVA, $p \leq 0.000$). Both the thioflavin T and oligomeric immunoassay showed no significant differences suggesting that the presence of the catalase made no difference to the aggregation of the peptide.

Another concern was that the H_2O_2 may be being generated from an impurity present in the solution. To test for this Aβ42 was depleted from the solution using a series of incubations with mAb 6E10. The solutions pre and post depletion were then tested for their ability to generate H_2O_2 (see figure 4.3). Over 48 hrs incubation at 37°C the solution before depletion of Aβ42 generated nearly 1 μM H_2O_2. Yet, following one incubation with 6E10 this had been reduced to less than 100 nM. After 3 incubations

with 6E10 no H_2O_2 was made, presumably due to all of the Aβ42 being selectively removed from the solution. This supported Aβ as the likely source of the H_2O_2.

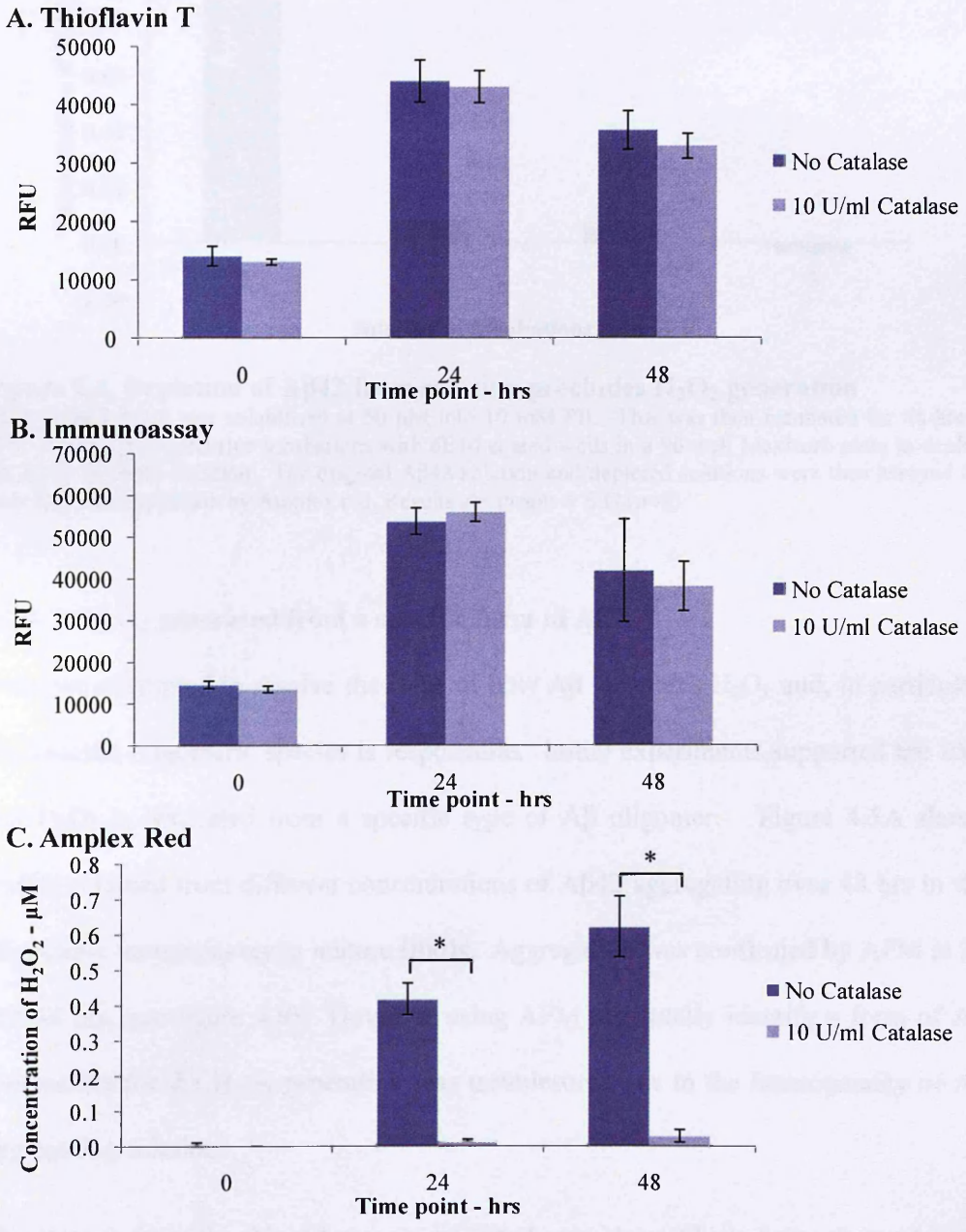

Figure 4.3. The effect of catalase on aggregation and H_2O_2 generation
HFIP treated Aβ42 was solubilised at 25 µM into 10 mM PB, pH 7.4, with and without the presence of 10 U/ml catalase. These were incubated at 37°C and samples taken at various time intervals for thioflavin T (A) and Immunoassay (B) to assess aggregation state and Amplex red (C) to measure H_2O_2 concentration. Results are means ± S.D (Thioflavin T and Amplex Red: n=3, Immunoassay: n=4, * indicates ANOVA $p \leq 0.000$).

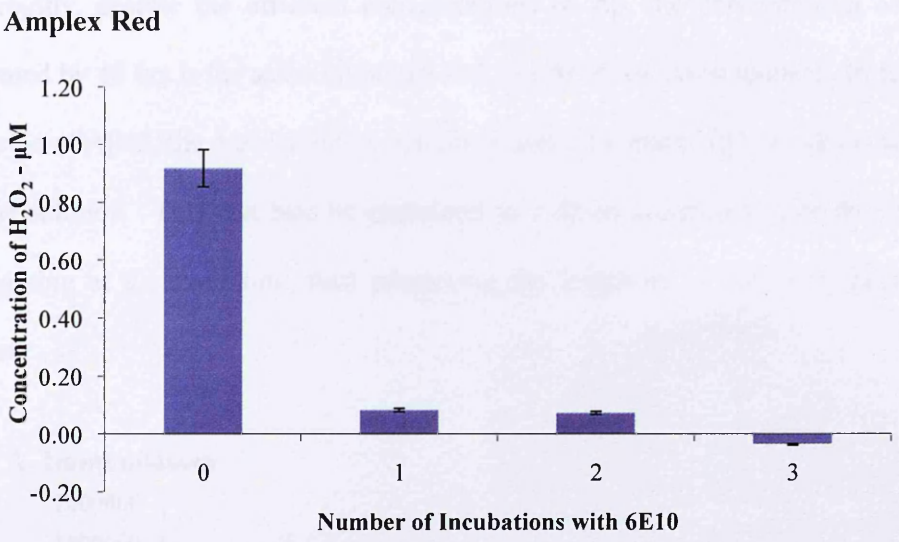

Figure 4.4. Depletion of Aβ42 from solution precludes H_2O_2 generation
HFIP treated Aβ42 was solubilised at 50 µM into 10 mM PB. This was then incubated for 48 hrs at 37°C following consecutive incubations with 6E10 coated wells in a 96 well Maxisorb plate to deplete the Aβ42 from the solution. The original Aβ42 solution and depleted solutions were then assayed for their H_2O_2 concentration by Amplex red. Results are means ± S.D (n=3)

4.2.2. Is H_2O_2 generated from a specific form of Aβ?

Next, we attempted to resolve the issue of how Aβ generates H_2O_2 and, in particular, if a specific oligomeric species is responsible. Initial experiments supported the idea that H_2O_2 is generated from a specific type of Aβ oligomer. Figure 4.5A shows results obtained from different concentrations of Aβ42 aggregating over 48 hrs in the oligomeric immunoassay to mature fibrils. Aggregation was confirmed by AFM at 24 and 48 hrs (see figure 4.6). However using AFM to actually identify a form of Aβ responsible for the H_2O_2 generation was troublesome due to the heterogeneity of Aβ aggregating solutions.

The images from the 25 µM sample of Aβ clearly show fibrils being formed from smaller, undetermined Aβ species at 24 hrs, which were fully sequestered into mature, super-coiled fibrils at 48 hrs. These events coincided with the slowing down of H_2O_2 generation supporting evidence that mature fibrils are inert in this respect.

Importantly, despite the different concentrations of Aβ, the concentration of H_2O_2 generated by 48 hrs is the same (although at 5 μM Aβ it has taken longer). In fact, per molecule of Aβ42, the 5 μM solution actually made 10 x more H_2O_2 in 48 hrs than the 50 μM solution. This can best be explained as a direct consequence of the solution aggregating at a slower rate, thus preserving the longevity of the H_2O_2 generating species.

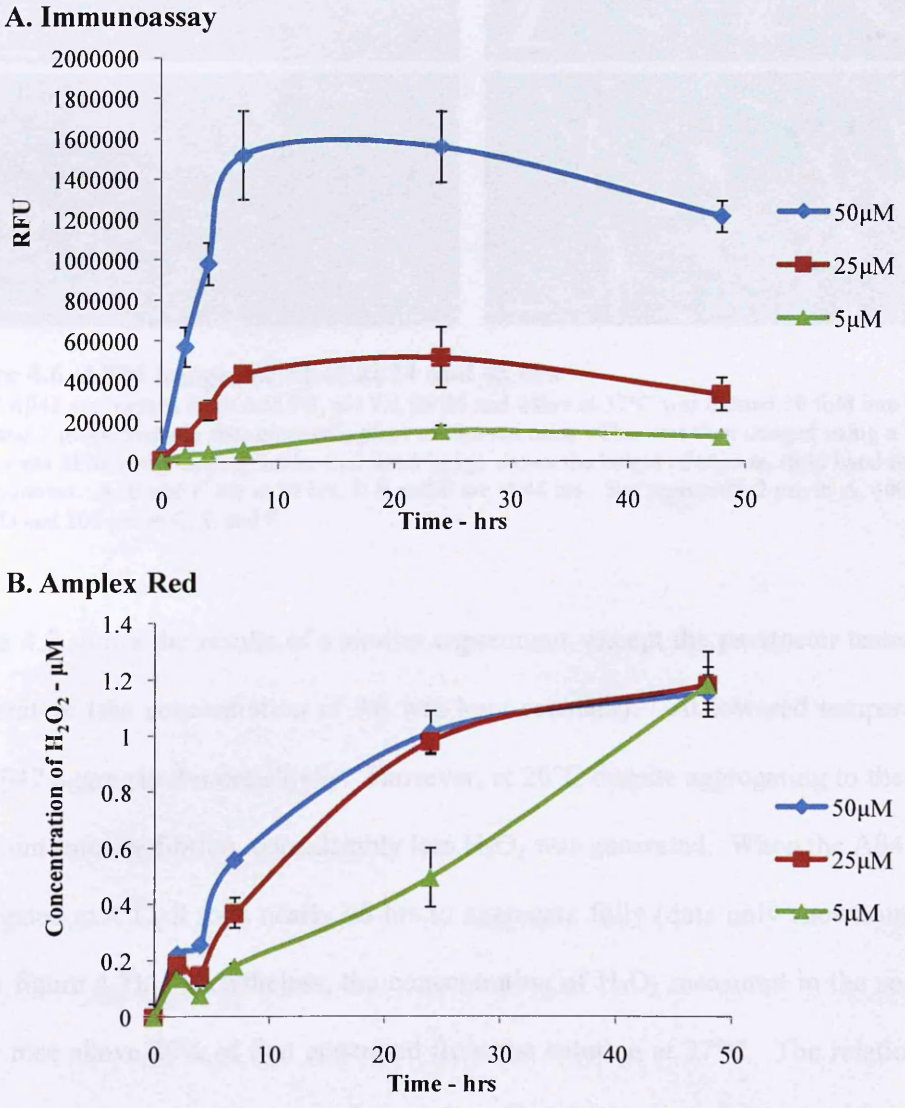

Figure 4.5. The effect of concentration on aggregation and H_2O_2 generation
5, 25 and 50 μM HFIP treated Aβ42 was aggregated in 10 mM PB, pH 7.4 at 37°C and samples taken for immunoassay (A) and Amplex red (B) analysis at various time points over 48 hrs. Results are means ± S.D. (Immunoassay: n=4, Amplex red: n=3)

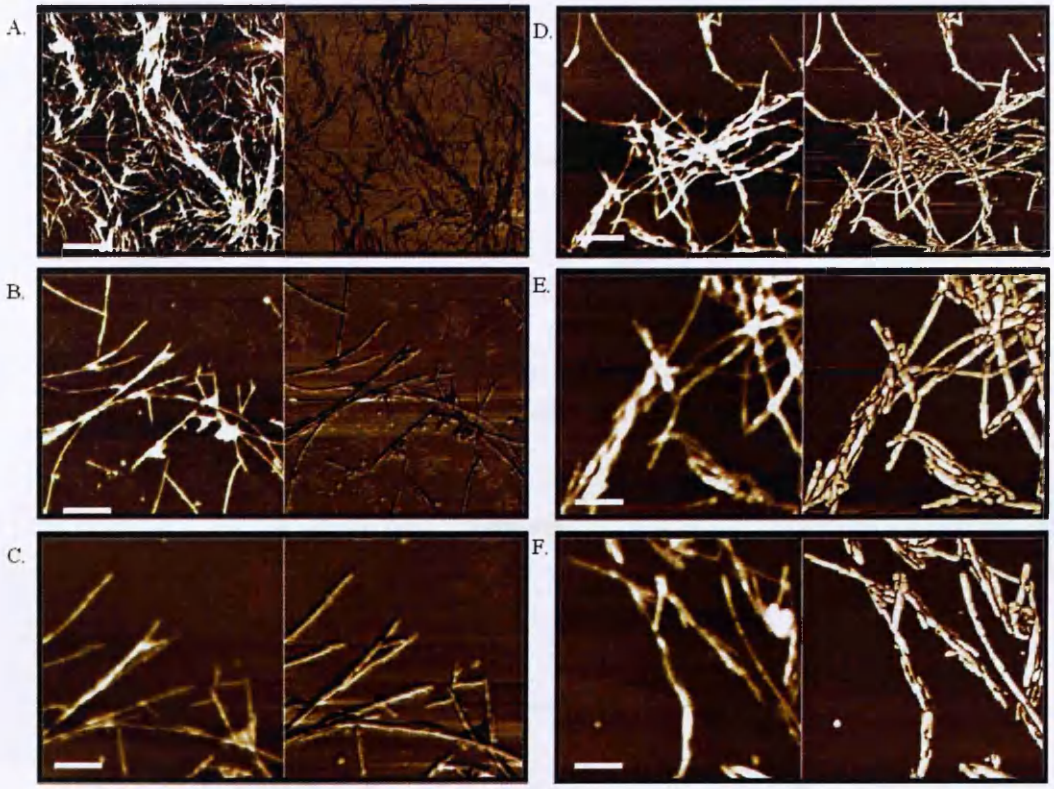

Figure 4.6. AFM images of Aβ42 at 24 and 48 hrs
25 μM Aβ42 aggregated in 10 mM PB, pH 7.4 for 24 and 48hrs at 37°C was diluted 10 fold into MilliQ water and 2 μl spotted into the centre of a piece of cleaved mica. This was then imaged using a Digital Instruments SPM using tapping mode. Left hand image shows the height of objects, right hand image is phase contrast. A, B and C are at 24 hrs, D E and F are at 48 hrs. Bar represents 2 μm in A, 400 nm in B and D and 200 nm in C, E and F.

Figure 4.7 shows the results of a similar experiment, except the parameter tested was temperature (the concentration of Aβ was kept constant). At lowered temperatures the Aβ42 aggregated more slowly. However, at 20°C despite aggregating to the same end point (mature fibrils), considerably less H_2O_2 was generated. When the Aβ42 was aggregated at 4°C, it took nearly 96 hrs to aggregate fully (data only shown until 48 hrs in figure 4.7). Nevertheless, the concentration of H_2O_2 measured in the solution never rose above 20% of that generated from the solution at 37°C. The relationship between temperature and enzymatic activity offers further support to the idea that a particular oligomeric species of Aβ generates H_2O_2 through a catalytic mechanism.

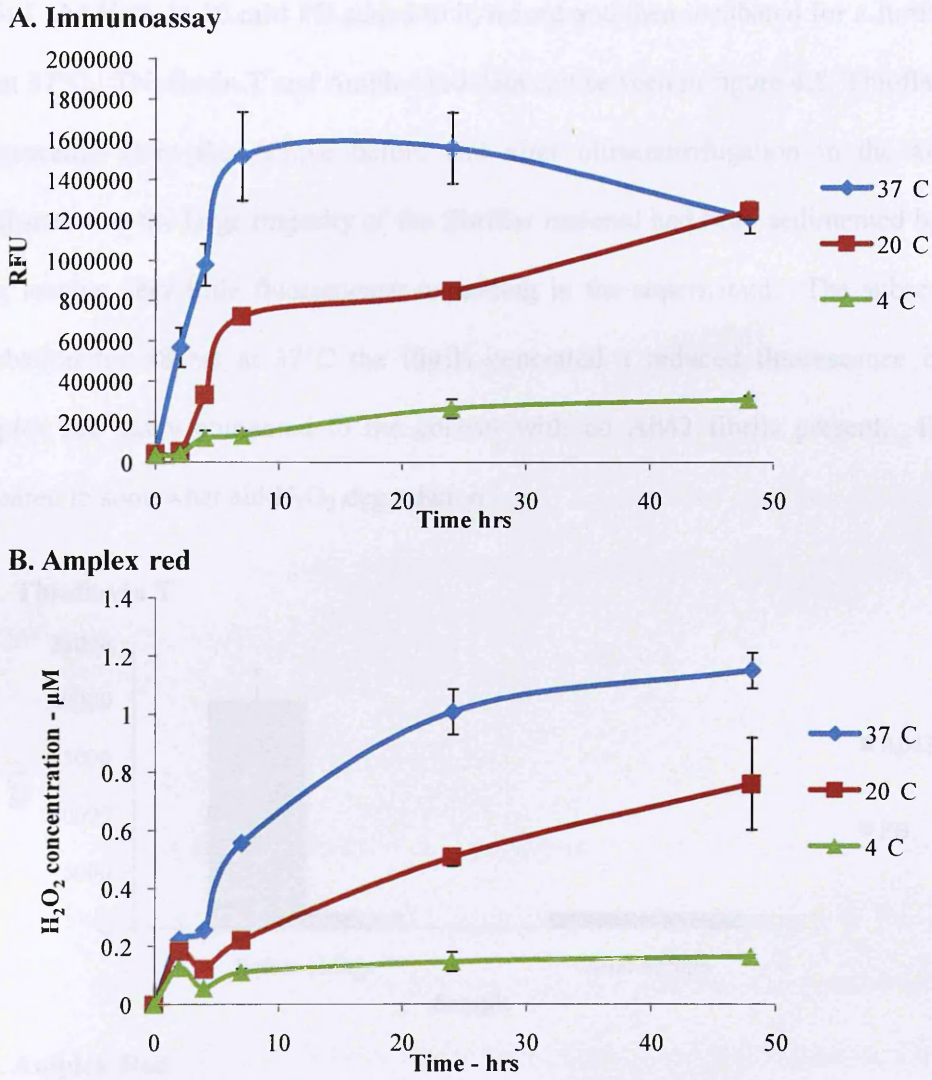

Figure 4.7. The effect of temperature on aggregation and H_2O_2 generation
50 µM HFIP treated Aβ42 was aggregated in 10 mM PB, pH 7.4 at 37, 20 and 4°C and samples taken for immunoassay (A) and Amplex red (B) analysis at various time points over 48 hrs. Results are means ± S.D. (Immunoassay: n=4, Amplex red: n=3)

4.2.2.1. Do Aβ fibrils degrade H_2O_2?

The generation of H_2O_2 appears to be relatively rapid in the early stages of aggregation, and then slows as mature fibrils are formed. This raised the question of whether these fibrils were inert in H_2O_2 generation, or whether fibrils play a role in degradation of the H_2O_2. To test this 25 µM Aβ42 was aggregated for 48 hrs in 10 mM PB at 37°C to form mature fibrils such as those seen in figure 4.6. Following this, the solution was put in the airfuge to pellet the fibrillar material. The pellet had

fresh 1 μM H_2O_2 in 10 mM PB added to it, mixed and then incubated for a further 48 hrs at 37°C. Thioflavin T and Amplex red data can be seen in figure 4.8. Thioflavin T fluorescence from the sample before and after ultracentrifugation in the airfuge confirmed that the large majority of the fibrillar material had been sedimented by this step, leaving very little fluorescence remaining in the supernatant. The subsequent incubation for 48 hrs at 37°C the fibrils generated a reduced fluorescence in the Amplex red assay compared to the control with no Aβ42 fibrils present. Fibrils appeared to somewhat aid H_2O_2 degradation.

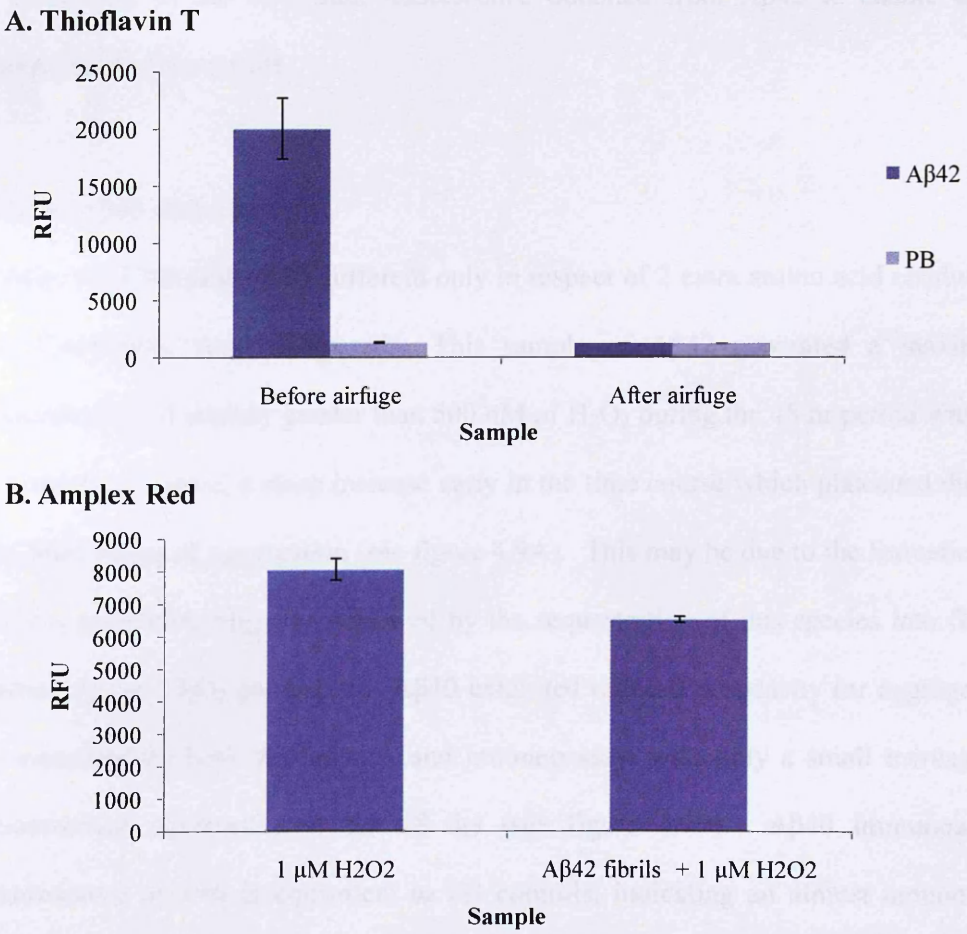

Figure 4.8. Aβ42 fibrils degrade H_2O_2
25 μM Aβ42 in 10 mM PB was incubated at 37°C for 48 hrs to form fibrils. The solution was then placed in the airfuge for 3 hrs at 87,000 rpm (~136,000 x g), at which point the buffer was removed and sampled for thioflavin T fluorescence (A). To the pellet and control 1 μM H_2O_2 in 10 mM PB was added, gently mixed and transferred to 0.6 ml Greiner PCR tubes, which were then incubated at 37°C for a further 48 hrs. The solutions were then tested using the Amplex red assay for H_2O_2 (B). Results are means ± S.D (n=3)

4.2.3. H_2O_2 generation and aggregation from Aβ peptides

To investigate the dependence of both H_2O_2 formation and aggregation of Aβ on particular residues implicated in its metal binding and aggregation, a range of different Aβ peptides were tested. These included Aβ40 and Aβ42 substituted peptides Y10A, H6A, H13A, H14A, M35N and also the reverse peptide Aβ42-1. These Aβ peptides were TFA treated to promote deseeding of the samples, then aggregated at 25 μM, in 10 mM PB over 48 hrs at 37°C and tested in the thioflavin T assay, oligomeric immunoassay and Amplex red assay over 48 hrs. Aggregation was then expressed as a percentage of the maximum fluorescence obtained from Aβ42 to enable direct comparison of the results.

4.2.3.1. Aβ40 and Aβ42

Firstly, wt Aβ40 and Aβ42, different only in respect of 2 extra amino acid residues at the C-terminus, were compared. This sample of Aβ42 generated a maximum concentration of slightly greater than 500 nM of H_2O_2 during the 48 hr period with, as previously observed, a steep increase early in the time course which plateaued during the latter stages of aggregation (see figure 4.9A). This may be due to the formation of a H_2O_2 generating oligomer followed by the sequestration of this species into fibrils halting further H_2O_2 generation. Aβ40 exhibited reduced propensity for aggregation as measured by both thioflavin T and immunoassay, with only a small increase in fluorescence observed over the 48 hrs (see figure 4.9B). Aβ40 immunoassay fluorescence at T=0 is equivalent to PB controls, indicating an almost monomeric solution was obtained. Although small, the increase in fluorescence observed in the oligomeric immunoassay signified the solution contained aggregates. Despite the reduced aggregation of Aβ40, over the 48 hrs Aβ40 appeared to generate almost as

much H_2O_2 as Aβ42 (nearly 400 nM). However, over the following 24 hrs this H_2O_2 generation ceased and actually decreased suggesting opposing processes may be at play, one generating H_2O_2, the other removing it from solution.

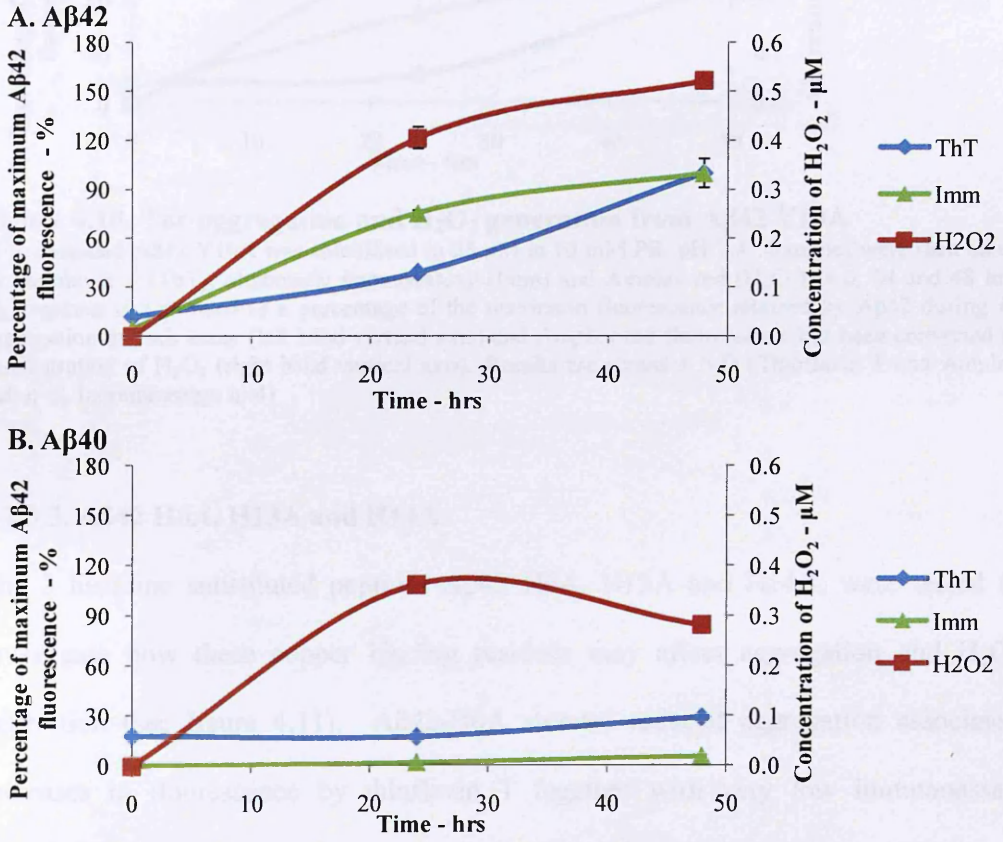

Figure 4.9. The aggregation and H_2O_2 generation from Aβ42 and Aβ40
TFA deseeded Aβ40 and Aβ42 were solubilised to 25 µM in 10 mM PB, pH 7.4. Samples were then taken for thioflavin T (ThT), oligomeric immunoassay (Imm) and Amplex red (H_2O_2) at 0, 24 and 48 hrs. Aggregation is expressed as a percentage of the maximum fluorescence attained by Aβ42 during its aggregation in each assay (left hand vertical axis) and Amplex red fluorescence has been converted to concentration of H_2O_2 (right hand vertical axis). Results are means ± S.D (Thioflavin T and Amplex red: n=3, Immunoassay: n=4)

4.2.3.2. Aβ42-Y10A

The substituted Aβ42 Y10A, despite its inability to form di-tyrosine dimers, aggregated over the 48 hr period albeit at a reduced rate compared to Aβ42 (see figure 4.10). It also generated H_2O_2, again, at a reduced rate, reaching just 300 nM corresponding with the early stages of its aggregation, and then it plateaued.

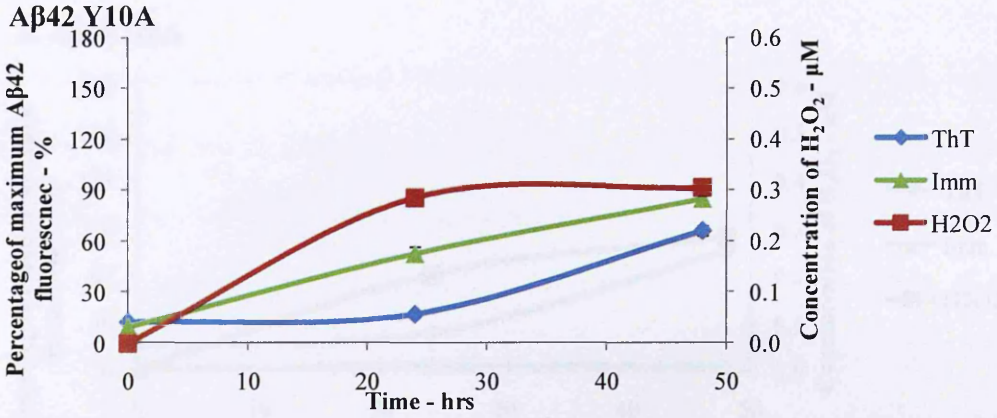

Figure 4.10. The aggregation and H_2O_2 generation from Aβ42 Y10A
TFA deseeded Aβ42 Y10A was solubilised to 25 µM in 10 mM PB, pH 7.4. Samples were then taken for thioflavin T (ThT), oligomeric immunoassay (Imm) and Amplex red (H_2O_2) at 0, 24 and 48 hrs. Aggregation is expressed as a percentage of the maximum fluorescence attained by Aβ42 during its aggregation in each assay (left hand vertical axis) and Amplex red fluorescence has been converted to concentration of H_2O_2 (right hand vertical axis). Results are means ± S.D (Thioflavin T and Amplex red: n=3, Immunoassay: n=4)

4.2.3.3. Aβ42 H6A, H13A and H14A

The 3 histidine substituted peptides Aβ42 H6A, H13A and H14A, were tested to investigate how these copper binding residues may affect aggregation and H_2O_2 generation (see figure 4.11). Aβ42-H6A showed reduced aggregation associated increases in fluorescence by thioflavin T together with very low immunoassay fluorescence, yet this was more likely due to a loss of affinity for the antibody. A small positive signal was detected so some binding did occur yet His6 lies within the binding epitope for 6E10 and may be involved in Aβ-6E10 binding. Concurrently, generation of H_2O_2 by this peptide was ~50% of Aβ42 by 48 hrs. In comparison, H13A and H14A Aβ42 exhibited greater aggregation associated increases in fluorescence in respect of the thioflavin T assay, where they surpassed that of Aβ42. The oligomeric immunoassay showed slightly reduced aggregation associated fluorescence for both peptides. The concentration of H_2O_2 generated by these peptides was again reduced compared to wt Aβ42, at ~400 nM.

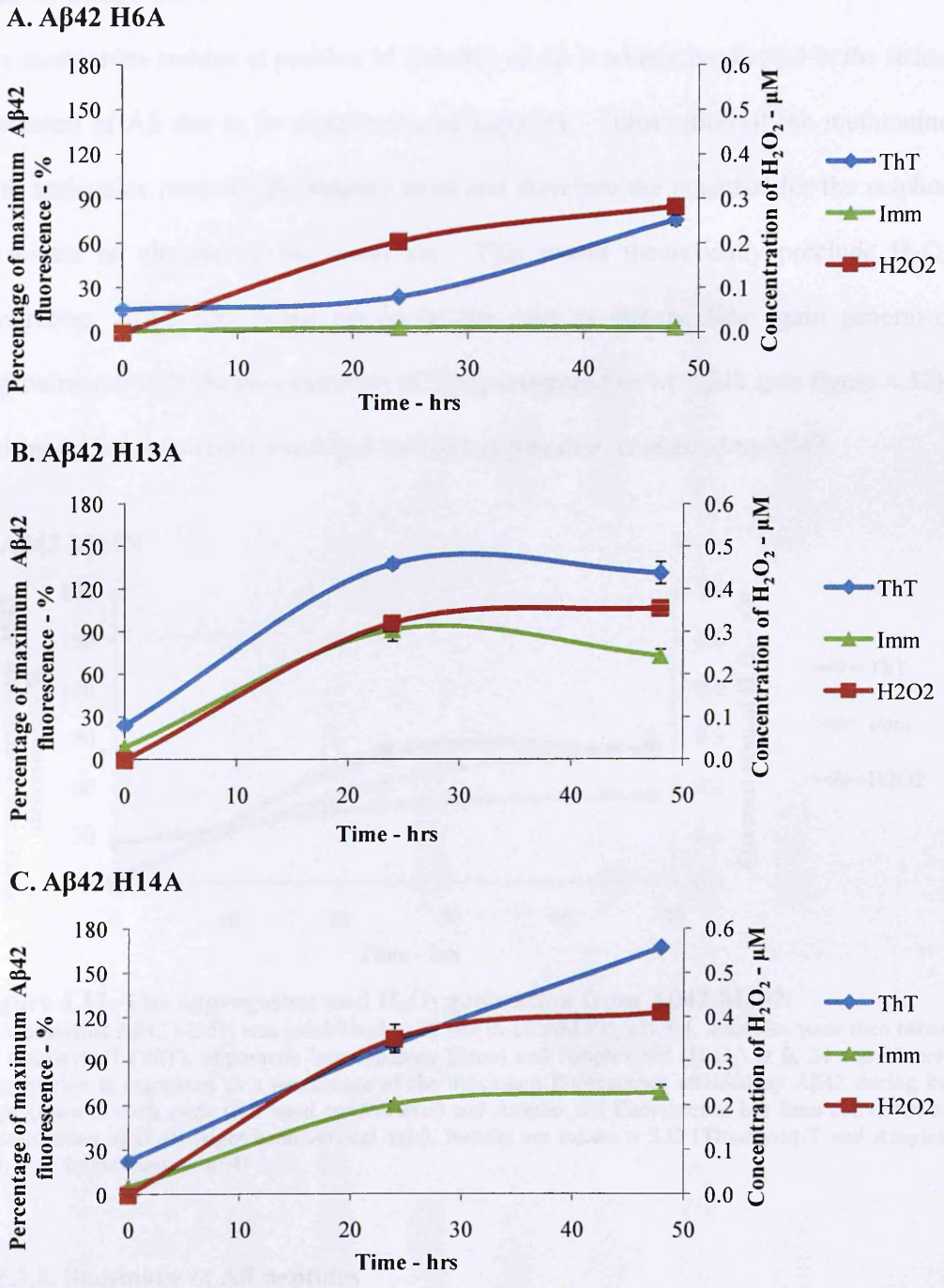

Figure 4.11. The aggregation and H_2O_2 generation from Aβ42 H6A, H13A and H14A

TFA deseeded Aβ42 H6A, H13A and H14A was solubilised to 25 µM in 10mM PB, pH 7.4. Samples were taken for thioflavin T (ThT), oligomeric immunoassay (Imm) and Amplex red (H_2O_2) at 0, 24 and 48 hrs. Aggregation is expressed as a percentage of the maximum fluorescence attained by Aβ42 during its aggregation in each assay (left hand vertical axis) and Amplex red fluorescence has been converted to concentration of H_2O_2 (right hand vertical axis). Results are means ± S.D (Thioflavin T and Amplex red: n=3, Immunoassay: n=4)

4.2.3.4. Aβ42 M35N

The methionine residue at positive 35 (Met35) of Aβ is widely implicated in the redox chemistry of Aβ due to its metal reducing capacity. Substitution of the methionine with norleucine removes the sulphur atom and therefore the potential for the sulphur to donate an electron to the metal ion. This would theoretically preclude H_2O_2 generation. This was found not to be the case as this peptide again generated approximately half the concentration of H_2O_2 compared to wt Aβ42 (see figure 4.12). This peptide concurrently exhibited reduced aggregation compared to Aβ42.

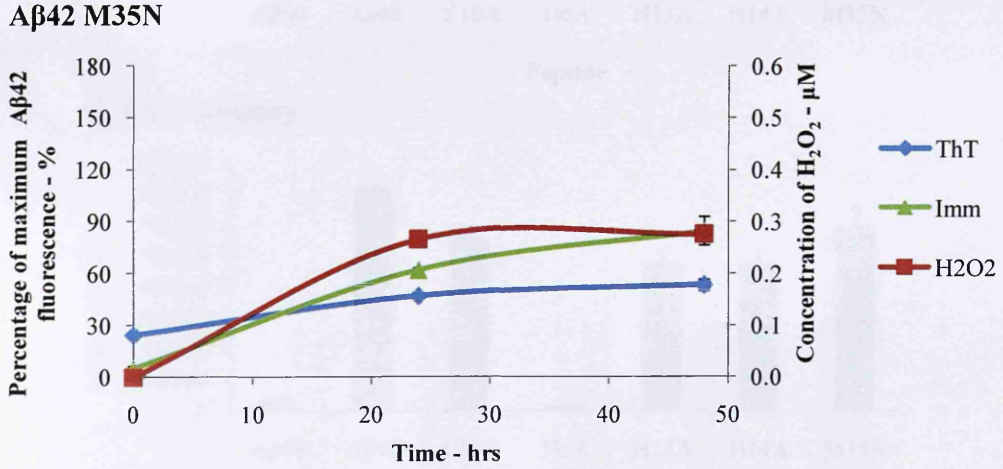

Figure 4.12. The aggregation and H_2O_2 generation from Aβ42 M35N
TFA deseeded Aβ42 M35N was solubilised to 25 µM in 10 mM PB, pH 7.4. Samples were then taken for thioflavin T (ThT), oligomeric immunoassay (Imm) and Amplex red (H_2O_2) at 0, 24 and 48 hrs. Aggregation is expressed as a percentage of the maximum fluorescence attained by Aβ42 during its aggregation in each assay (left hand vertical axis) and Amplex red fluorescence has been converted to concentration of H_2O_2 (right hand vertical axis). Results are means ± S.D (Thioflavin T and Amplex red: n=3, Immunoassay: n=4)

4.2.3.5. Summary of Aβ peptides

Comparing the increase in aggregation associated fluorescence from the peptides at 48 hrs and the H_2O_2 generation from each peptide over this time clearly shows that the amount of aggregation does not directly correlate with the concentration of H_2O_2 generated (see figure 4.13). All the peptides exhibited reduced generation of H_2O_2

compared to wt Aβ42. H13A and H14A demonstrated increased aggregation associated fluorescence in the thioflavin T assay, whilst H6A, M35N and Y10A displayed reduced thioflavin T fluorescence.

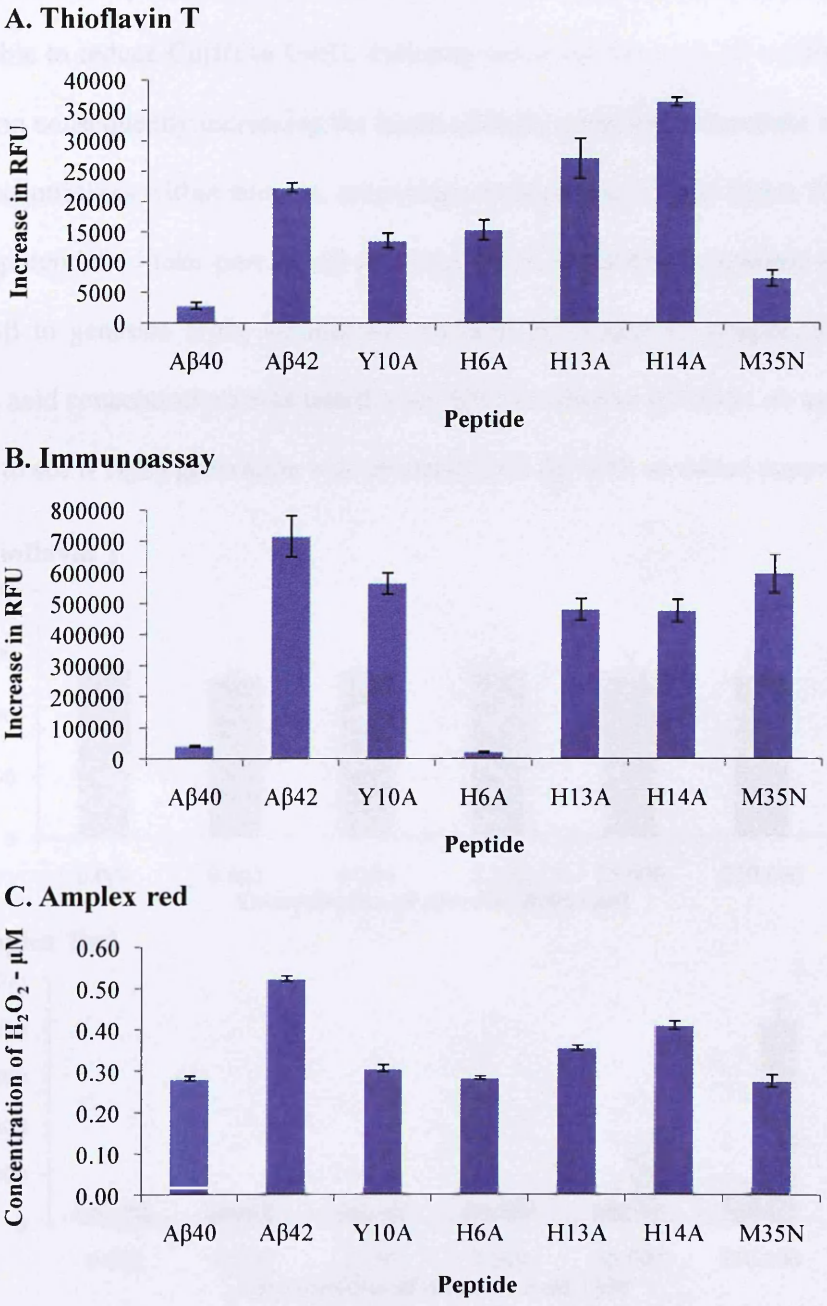

Figure 4.13. Aggregation and H_2O_2 generation from Aβ peptides by 48 hrs
TFA deseeded Aβ peptides were aggregated at 37°C for 48 hrs at 25 µM in 10mM PB, pH 7.4. Aggregation was assessed by thioflavin T fluorescence (A), Immunoassay fluorescence (B) and H_2O_2 generation by Amplex red fluorescence (C). Results are means ± S.D (Thioflavin T and Amplex red: n=3, Immunoassay: n=4)

4.2.4. The effect of ascorbic acid on H_2O_2 generation

Ascorbic acid (Vitamin C) is utilised in conjunction with copper ions by several research groups to investigate ROS generation by Aβ (Dikalov et al., 2004; Guilloreau et al., 2007; Murray et al., 2005; Nadal et al., 2008). This is because it is an electron donor, able to reduce Cu(II) to Cu(I), initiating redox cycling and Aβ mediated H_2O_2 generation consequently increasing the levels of H_2O_2 measured. Ascobate is found at high concentrations within neurons, on average estimated at 10 mM (Rice, 2000), so it has the potential to take part in Aβ-mediated ROS generating reactions. As I have found Aβ to generate H_2O_2 without the addition of exogenous copper, a range of ascorbic acid concentrations was tested with Aβ42 to observe its effect on aggregation but also to see if H_2O_2 generation was elevated from Aβ with no added copper.

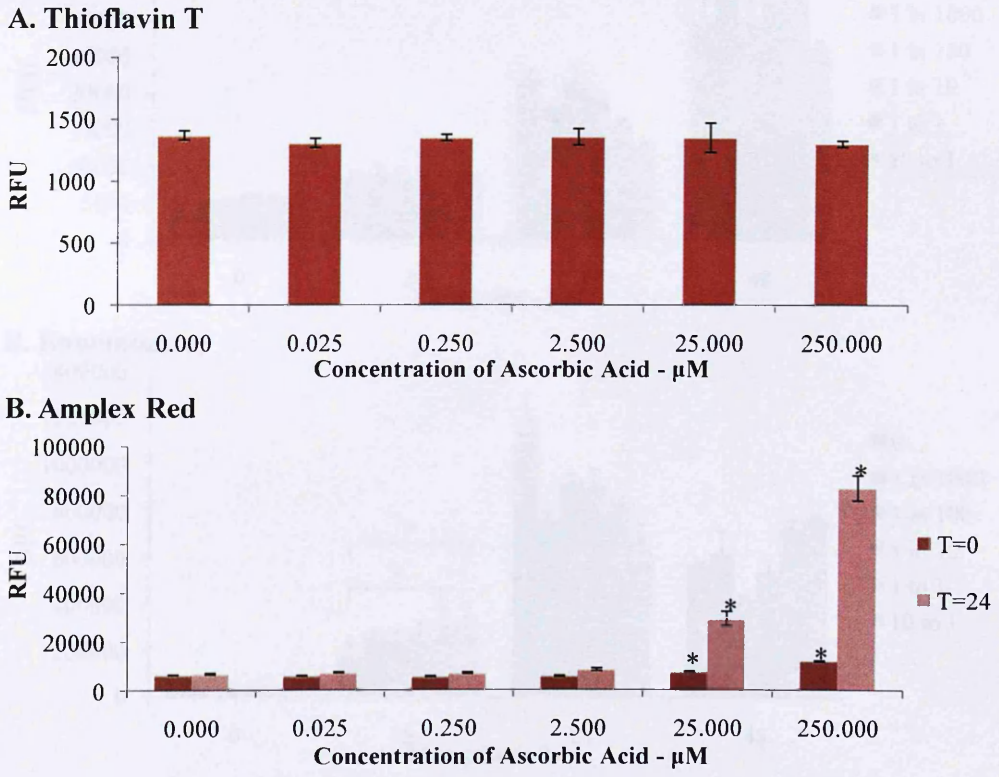

Figure 4.14. Ascorbic acid concentration dependent effects in thioflavin T and Amplex red

A concentration range from 0.025 to 250 µM ascorbic acid was made in 10 mM PB and tested in the thioflavin T assay (A) and Amplex red assay (B). The samples were then incubated for 24 hrs at 37°C and tested again in the Amplex red. Results are means ± S.D (n=3), * indicates Tukey HSD $p \leq 0.000$.

Controls with no Aβ were initially tested for in the thioflavin T and Amplex red assays (see figure 4.14). No concentration dependent effect was observed in the thioflavin T assay. However in the Amplex red assay, at 25 and 250 μM ascorbic acid significantly increased fluorescence was detected (Tukey HSD test, $p \leq 0.000$, n=3). The samples were then incubated at 37°C for 24 hrs and tested again in the Amplex red assay which showed further increases in fluorescence at these concentrations. This indicated that the presence of these higher levels of ascorbic acid generated H_2O_2. The generation of such a strong positive signal is indicative of ascorbic acid acting as a pro-oxidant, reacting with the free Cu(II) ions in the buffer solution.

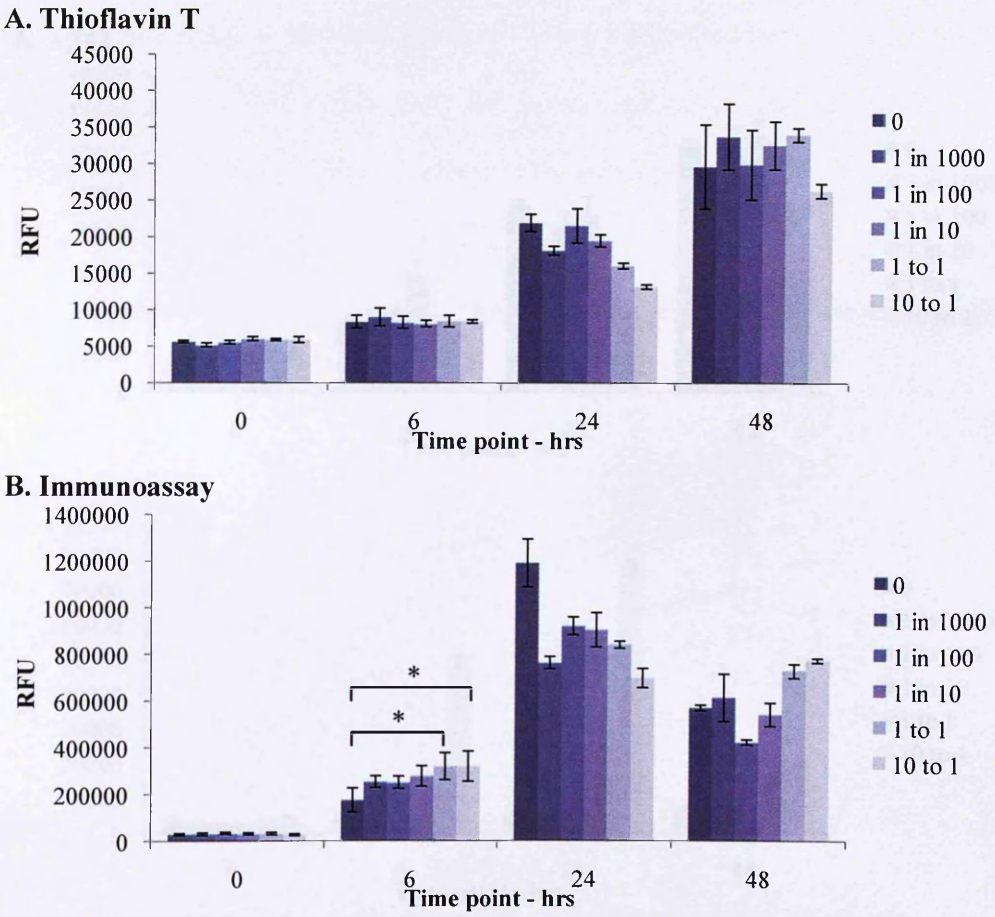

Figure 4.15. The effect of ascorbic acid on the aggregation of Aβ42
25 μM Aβ42 was solubilised into a range of ascorbic acid concentrations in 10 mM PB and incubated at 37°C. Samples were taken and tested for thioflavin T fluorescence (A) and in the oligomeric immunoassay (B) at various time points over 48 hrs. Results are means ± S.D (Thioflavin T: n=3, Immunoassay: n=4), Tukey HSD * indicates p = 0.005.

These concentrations of ascorbic acid were incubated with Aβ42 and aggregation of the peptide at 37°C monitored over 48 hrs by thioflavin T and immunoassay (see figure 4.15). At 6 hrs the thioflavin T assay showed no significant difference in the fluorescence measured from the samples. However, the immunoassay detected small, significant increases in fluorescence at 25 and 250 μM ascorbic acid (Tukey HSD p = 0.005); increasing ascorbic acid concentration appeared to promote oligomer formation. At 24 hrs aggregation both thioflavin T and immunoassay showed a concentration dependant effect but with decreased fluorescence measured with increasing ascorbic acid. By 48 hrs no concentration dependant effect were identified.

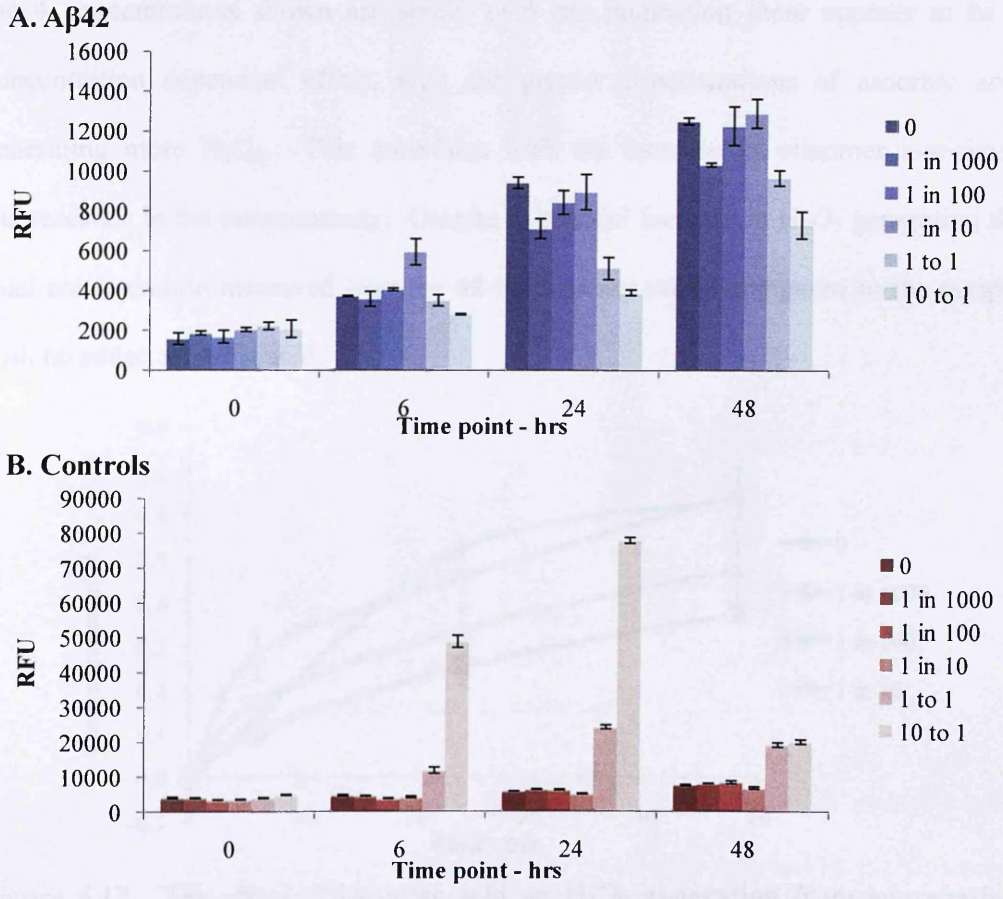

Figure 4.16. The effect of ascorbic acid on Amplex red fluorescence from aggregating Aβ42 and PB controls

25 μM Aβ42 was solubilised into a range of ascorbic acid concentrations in 10 mM PB and incubated at 37°C. Samples were taken and tested for Amplex red fluorescence at various time points over 48 hrs. Legend refers to the ratio of Aβ to ascorbic acid in the sample. Results are means ± S.D (n=3)

Amplex red fluorescence was monitored over the 48 hrs in both the Aβ samples and controls (see figure 4.16). The increases in fluorescence observed in controls containing 25 and 250 μM ascorbic acid (1:1 and 10:1) at 24 hrs mirror those previously observed. However, at 48 hrs the level of fluorescence from these controls dropped. The high levels of H_2O_2 generated by these controls meant the level of H_2O_2 generated from the corresponding Aβ42 samples could not be calculated, yet it can be considered to be less than that of the ascorbic acid alone.

H_2O_2 generation by Aβ42 was calculated over the time course for the lower concentrations of ascorbic acid (see figure 4.17). Although the differences between the 4 concentrations shown are small, at 6 hrs incubation there appears to be a concentration dependant effect, with the greater concentrations of ascorbic acid generating more H_2O_2. This correlates with the increase in oligomer associated fluorescence in the immunoassay. Despite this initial increase in H_2O_2 generation the final concentration measured over the 48 hrs was not raised compared to the sample with no added ascorbic acid.

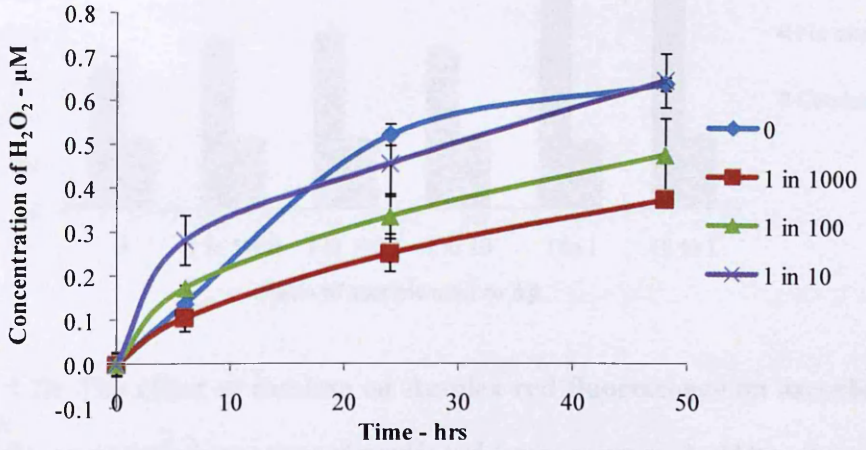

Figure 4.17. The effect of ascorbic acid on H_2O_2 generation from aggregating Aβ42

25 μM Aβ42 was solubilised into a range of ascorbic acid concentrations in 10 mM PB and incubated at 37°C. Samples were taken and tested of Amplex red fluorescence at various time points over 48 hrs. Appropriate PB control fluorescence values have been subtracted and fluorescence converted to concentration of H_2O_2. Results are means ± S.D (n=3)

To check that the signals in the Amplex red, especially those from the controls with the highest ascorbic acid concentrations, were from H_2O_2 generation, samples were diluted 4:1 v/v with 50 U/ml catalase or with 10 mM PB (see figure 4.18). These were incubated at 37°C for 30 mins and then Amplex red fluorescence measured. This brought all fluorescence readings down to below PB control levels indicating H_2O_2 was responsible for all the positive fluorescence readings from the experiment.

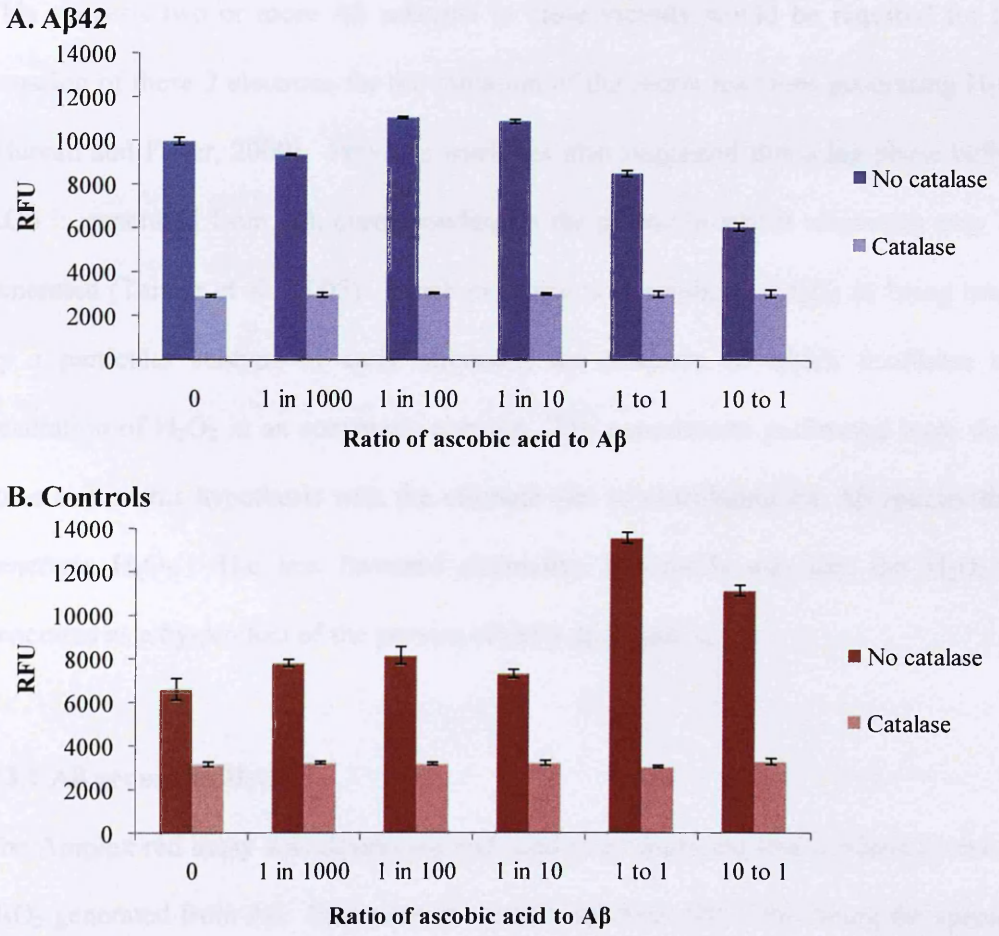

Figure 4.18. The effect of catalase on Amplex red fluorescence on ascorbic acid samples

25 μM Aβ42 was solubilised into a range of ascorbic acid concentrations in 10 mM PB and incubated at 37°C for 48 hrs. Catalase in 10 mM PB was then added to the samples to a final concentration of 10 U/ml catalase and 20 μM Aβ42. These were then incubated for 30 mins at 37°C and then sampled, together with controls with no added catalase, for their fluorescence in the Amplex red assay. Results are means ± S.D (n=3)

4.3. Discussion

One of the earliest features of AD brain pathology is the detection of markers of oxidative damage. Huang and colleagues first reported the possibility that Aβ may be directly responsible for this oxidative damage via the generation of H_2O_2 (Huang et al., 1999a). Monomeric Aβ appears an unlikely candidate for the generation of H_2O_2 as the reduction of 2 Cu(II) ions is now the favoured mechanism of H_2O_2 generation. This suggests two or more Aβ subunits in close vicinity would be required for the donation of these 2 electrons for the initiation of the redox reactions generating H_2O_2 (Hureau and Faller, 2009). Previous work has also suggested that a lag phase before ROS is generated from Aβ, corresponding to the period in which oligomers may be generated (Tabner et al., 2005). Much evidence now implicates H_2O_2 as being made by a particular subtype of early oligomer, the structure of which facilitates the generation of H_2O_2 in an enzymatic manner. The experiments performed were done so as to test this hypothesis with the ultimate aim of elucidating the Aβ species that generates H_2O_2. The less favoured alternative hypothesis was that the H_2O_2 is generated as a by-product of the process of early aggregation.

4.3.1 Aβ generates H_2O_2

The Amplex red assay was developed and used to measure the low concentrations of H_2O_2 generated from Aβ. Experiments were focused on Aβ42, this being the species that exhibits greater toxicity and also generates more H_2O_2 than Aβ40. Control experiments were initially performed to confirm that the positive Amplex red signal generated by Aβ was from H_2O_2 (by the addition of catalase) and that the Aβ was the source of the H_2O_2 (by depletion of Aβ).

H_2O_2 was found to be made from Aβ42, the signal for which was eliminated by the addition of catalase. Of interest, when Aβ42 was aggregated for 48 hrs with and without the presence of 10 U/ml catalase, although H_2O_2 was eliminated, the thioflavin T and immunoassay fluorescence data suggested that the presence of catalase made no difference to the aggregation of the peptide. This appears to contradict reports that Aβ the self-oxidation of key residues drives aggregation of the peptide; whether it be through oxidation of Tyr10 to form dityrosine dimers (Barnham et al., 2004; Smith et al., 2007a), or of Met35 (Bitan et al., 2003b). On the other hand, it is possible that Aβ oxidation proceeds preferentially to H_2O_2 degradation by catalase, or that sufficient oxidation occurs despite the presence of the catalase. Another explanation may be the presence of some pre-aggregated Aβ42 upon wetting, seeding its aggregation (β-sheet folded Aβ triggers the mis-folding of more Aβ (Jarrett et al., 1993)), thus oxidation may not be required to initiate it.

The depletion of Aβ42 from solution by successive incubations with the mAb 6E10, found that removing the Aβ42 from the solution rendered the solution increasingly less capable of generating H_2O_2. This indicated that the likely source of the H_2O_2 was the Aβ and not a contaminant dissolved in the buffer. The requirement of oxygen as a substrate for H_2O_2 generation by Aβ was tested. However efforts to reduce the supply of oxygen for H_2O_2 generation by the creation of a nitrogen atmosphere for the Aβ to aggregate were unsuccessful (data not shown).

4.3.2. H_2O_2 may be generated by a specific form of Aβ

The heterogeneous and dynamic nature of Aβ aggregating solutions plagues attempts to attribute any specific characteristic, including toxicity of Aβ, to any discrete species (Bharadwaj et al., 2009). Evidence suggests that a specific form of pre-fibrillar Aβ is

responsible for the neuronal toxicity observed in AD, yet identification of this species is yet to be achieved due to the properties of this problematic peptide. Investigation of whether the generation of H_2O_2 is an enzymatic property of a specific type of early Aβ species due to the redox cycling of metal ions, required significant consideration of these problems. If a key pathogenic event in the development of AD is the generation of H_2O_2 by Aβ then targeting this process may be a valid approach for developing disease-course altering therapeutics. However, the way in which the Aβ generates H_2O_2 may also be of importance when considering other AD drug development strategies. For example, inhibition of aggregation: if H_2O_2 generation is made by a specific early oligomer, and an inhibitor only inhibits aggregation after the formation of this oligomer, then the outcome may be an increase in the levels of the H_2O_2 generating oligomer, thus exacerbating the toxicity.

Initial experiments testing how concentration and temperature affected Aβ aggregation and its generation of H_2O_2 suggested H_2O_2 was in fact made by a specific early form of Aβ. The effect of lowering the concentration slowed the aggregation of the peptide. However, the concentration of H_2O_2 generated was not determined by the concentration of Aβ present. If the generation of H_2O_2 was made as a by-product of aggregation, it may be expected that tenfold less peptide present would generate substantially less H_2O_2. This was not the case. In actuality, slowing the aggregation by reducing Aβ concentration increased the H_2O_2 generation per molecule of Aβ present. This clearly supports the idea that the lifespan of a specific form of Aβ in solution is a determinant of the level of H_2O_2 generated. It was subsequently hypothesised that slowing aggregation of Aβ42 using temperature may also prolong the longevity of the H_2O_2 generating Aβ species. This too could generate more H_2O_2, but also, the lower temperature may protect the H_2O_2 from naturally degrading in

solution. In complete contrast, lowering temperature greatly reduced the generation of H_2O_2 by Aβ42. Despite contradicting the hypothesised effect, the best explanation for these results still supports the generation of H_2O_2 being due to a specific form of Aβ; if H_2O_2 was made as a by-product, equal concentrations of Aβ aggregating from the same starting point, to mature fibrils, should generate similar quantities of H_2O_2. This was not the result observed. Furthermore, temperature is linked to the enzymatic activity of proteins. Reducing temperature may decrease H_2O_2 generation due to the reduction of enzymatic activity of the specific H_2O_2 generating form of Aβ despite the potential for the lowered temperature to increase the longevity of this Aβ species. This evidence appears to support the hypothesis that H_2O_2 generation is dependent on the presence and longevity of particular H_2O_2 generating oligomeric species.

Calculation of the rate of H_2O_2 generation at different stages of Aβ aggregation would be more appropriate to compare the ability of Aβ species to generate H_2O_2, rather than absolute H_2O_2 concentrations. However, as relatively few measurements could be performed during Aβ aggregation, often due to sampling time constraints and the large consumption of samples for Amplex red testing, rates could not be reasonably calculated. In future experiments, a greater number of samples should be taken to allow rates of H_2O_2 generation to be compared at different stages of aggregation and between different Aβ peptides. Without calculation of rates, the H_2O_2 made by Aβ42 appears to be largely generated during the early stages but then slows as Aβ is sequestered into fibrillar material.

There is evidence that Aβ may generate ROS at one stage of aggregation but actually scavenge it at another (Hureau and Faller, 2009; Naylor et al., 2008). Unlike other Aβ aggregation species, fibrils can be sedimented by centrifugation and so could be easily tested to see if they play a role in the degradation of H_2O_2. When 1 μM H_2O_2 was

added to the Aβ42 fibrils and incubated for 48 hrs there was ~20% decrease in the H_2O_2 detected compared to control samples implying that fibrils aid the decomposition of H_2O_2. This may be due to a specific characteristic of the fibrils, or they merely provide an easy substrate for oxidation by H_2O_2. However, this does mean that where heterogeneous solutions of Aβ42 are concerned, the concentration of H_2O_2 measured may actually be the net effect of 2 opposing actions: those generating H_2O_2 and those degrading it. Aβ aggregation intermediates may also degrade H_2O_2. However, these could not be tested in this respect as the airfuge is ineffective for sedimentation of earlier Aβ species. Additionally we found the airfuge may actually induce some aggregation whilst investigating it as a potential deseeding technique (figure 3.9). However, oxidation of early Aβ by H_2O_2 (albeit at a far increased concentration) has been observed whilst investigating cross-linking of the peptide (see chapter 5).

4.3.3. The aggregation and H_2O_2 generation from Aβ peptides

4.3.3.1. Wild type Aβ

Aβ40 lacks 2 hydrophobic residues at the C-terminus of the peptide, Ile41 and Ala42. These 2 amino acids are responsible for the increased aggregation and toxicity observed by Aβ42 compared to Aβ40. The reduced aggregation of Aβ40 could be clearly seen in the thioflavin T and immunoassay results. H_2O_2 was also reduced in comparison to Aβ42, being generated over the first 24 hrs but followed by a decrease in H_2O_2 detected at 48 hrs. As Aβ40 is very much monomeric upon wetting, it may be that this represents the formation of the H_2O_2 generating species, which consequently becomes oxidised permitting its fibrillisation. This also suggests that the H_2O_2 generating Aβ species is formed very early during the aggregation process. Maybe

with Aβ42 this species is more stable, persisting in solution despite the tendency for fibrillisation. This may support the idea that some oligomers are formed "off" the fibrillisation pathway. There certainly appear to be two processes at play with Aβ40, one generating H_2O_2, the other removing it from solution, maybe by competing species in the heterogeneous aggregating solution. This effect has been observed repeatedly during this work and has been suggested by other researchers (Hureau and Faller, 2009; Naylor et al., 2008). Once the immobilisation technique is finalised (described in chapter 6), it would be of interest to test Aβ40 for both H_2O_2 generation and degradation, as it was often observed that Aβ40 appears to quench H_2O_2 generated during an experiment, more so than any other Aβ peptide. This supports evidence on the redox properties of Aβ that supports a role as both pro- and antioxidant, dependent on the microenvironment. Concentration and oxidation state may be major factors in controlling a gain in toxicity (Smith et al., 2007a).

4.3.3.2. Aβ42-Y10A

Aβ42-Y10A, despite its inability to form dityrosine dimers, was aggregation and H_2O_2 generation competent, albeit both at a reduced rate to wt Aβ42, generating ~300 nM H_2O_2 compared to 500 nM by Aβ42. This supports other research that suggests Aβ42-Y10A generates H_2O_2 at half the rate of the wt Aβ42 (Barnham et al., 2004). This does eliminate dityrosine dimers as both a pre-requisite for aggregation and as the sole H_2O_2 generating Aβ species. On the other hand, the reduced aggregation and production of H_2O_2 by Aβ42 Y10A does indicate this residue as playing a prominent role in Aβ aggregation and its redox chemistry of Aβ generating H_2O_2. It may be that di-tyrosine dimers are a stabilising influence on oligomer generation. This would help explain both decreased aggregation and H_2O_2 generation. If the tyrosine plays a role

in copper co-ordination by the peptide (Smith et al., 2007a), then perhaps this substitution reduces the binding of copper to the peptide, thus decreasing the metal-catalysed generation of H_2O_2. Soluble dityrosine dimers may be a key species in Aβ-mediated toxicity, as these stable, covalently bonded species are found in the brains of AD patients. Other research has found Aβ-Y10A to form oligomeric species. However, where the wt peptide was toxic to cell cultures, Aβ-Y10A was not (Barnham et al., 2004). This implicates the role that this tyrosine residue has in forming dityrosine bonded Aβ, promoting early aggregation interactions as being relevant to the neurotoxicity of Aβ in AD. Whether this is related to oxidative mechanisms is yet to be determined. Interestingly though, one of the 3 amino acids different in rat Aβ is Tyr10 (a phenylalanine in rat Aβ). This peptide has reduced aggregation potential, neurotoxicity to cell cultures and also reduced AD oxidative neuropathology compared to human Aβ (Huang et al., 1999b).

4.3.3.3. Histidine substituted Aβ42

The histidine substituted Aβ42s showed 2 different effects; H6A-Aβ42 showed decreased aggregation yet H13A and H14A-Aβ42 showed increased aggregation compared to wt Aβ42 in the thioflavin T assay yet reduced in the oligomeric immunoassay. The assays measure different aspects of the aggregation process; the thioflavin T assay appears to measure fibrillar content preferentially whereas the oligomeric immunoassay is more sensitive to the early oligomeric changes. This would imply that these 2 mutants are more fibrillogenic than the native Aβ42, with early oligomeric species being sequestered rapidly into fibrils. All three showed H_2O_2 generation albeit significantly reduced in comparison to wt Aβ42 (Tukey HSD $p \leq 0.001$ at 24 and 48 hrs) with H6A-Aβ42 reduced more so than H13A and H14A-

Aβ42. Consequently, not one of these histidine residues is critical for the coordination of trace levels of redox active metals to permit H_2O_2 generation by the peptide. It may be that the substitution of just one of these histidines reduces the affinity of copper for binding Aβ. This may have dual effects to decrease the level of H_2O_2 generated: reducing the redox potential of Aβ oligomers and increasing sequestration of Aβ into fibrils decreasing oligomer longevity. If the copper binding site in H_2O_2 generating oligomers is a hybrid between 2 (or more) Aβ molecules then not all the histidines in one molecule would be essential. If this was the case then it may be predicted that, due to their proximity His13 and His14 may be almost interchangeable for copper coordination, whereas His6 may of greater importance. These results support this with H6A Aβ42 exhibiting reduced aggregation and H_2O_2 generation compared to both H13A and H14A, which are more equivalent to each other. A triple histidine mutant would be interesting to investigate to confirm that loss of this metal binding site ablates H_2O_2 generation.

4.3.3.4. Aβ42-M35N

This Aβ substituted peptide also showed reduced aggregation and H_2O_2 generation compared to wt Aβ42. Met35 is widely implicated in the redox properties of Aβ. This amino acid, a thio ether, is thought to be critical to Aβ redox chemistry as its side chain is highly susceptible to oxidation, due to its sulphur atom having the potential to donate electrons for the reduction of metal ions (Vogt, 1995). There is evidence that with Aβ40, substitution of Met35 with norleucine, removing the sulphur atom, causes it to become non-oxidative and non-neurotoxic (Varadarajan et al., 1999). However, in our experiments M35N Aβ42 retained some of the H_2O_2 generating capability of the wt Aβ42. This suggests that although Met35 maybe the primary source for metal

reduction, another source of electrons must also capable of initiating the metal catalysed redox reactions (maybe Tyr10). Additionally, its reduced propensity for aggregation indicates that Met35 has a role in mitigating the aggregation of Aβ42. Aβ with Met35 pre-oxidised has been found to aggregate slower (Butterfield and Bush, 2004). This may be linked to decreased ability to reduce copper which hypothetically initiates redox cycling, thus linking aggregation and redox processes. It may be that the reduced H_2O_2 generated by M35N Aβ42 caused less oxidation of Aβ residues, such as Tyr10, to take place. The formation of dityrosine dimers from oxidised Tyr10 of Aβ may help drive early aggregation perhaps stabilising early interactions.

The biochemistry behind how the Met35 in Aβ may be capable of facilitating redox reactions by Aβ/metal complexes, where other methionine containing proteins do not, has been suggested to be due to Aβs structural properties. The C-terminus of Aβ42 is helical in nature, with each residue interacting with the amino acid 4 units away. This brings Met35 to within van der Waals distance of the backbone carbonyl of Iso31 (Shao et al., 1999). This isoleucine may be able to prime the lone pair of electrons of the sulphur atom of Met35 for oxidation making it easier for electron abstraction. This is supported experimentally using Iso31Pro which reportedly disrupts the helical structure of the C-terminus rendering the peptide non-oxidative and non-toxic, due to the loss of electron priming (Butterfield and Bush, 2004; Kanski et al., 2002b). Following electron priming, Met35 then has to come within ~14Å of the metal ion for transfer of the electron to take place (Page et al., 1999). As Met35 is at the C-terminus and the metal ion bound towards the N-terminus, folding of the peptide would need to facilitate this interaction, the alternative being via binding of two or more peptide molecules as when the peptide oligomerises. In this case the metal-bound N-terminus may become stacked against the Met35 in the C-terminus of the

adjacent Aβ unit (Smith et al., 2007a). This may permit copper-mediated radicalisation of Met35 provoking the formation of a stable carbon centred radical on the peptide backbone, with ensuing aberrant oxidative chemistry (Rauk et al., 2000).

Oligomerisation may be the process that permits the interaction of Met35 of Aβ with the bound metal ion. Consequently, it would seem reasonable to expect that some forms of oligomeric species may be much more efficient in this respect than others. The lack of the methionine residue with this norleucine substituted peptide means that another source of electrons is available for the reduction of Cu(II) to initiate redox cycling yet this source does not appear to be as efficient as Met35.

4.3.4. Ascorbic Acid

Ascorbic acid is an antioxidant used by several research groups when investigating Aβ redox capabilities and the generation of ROS. This is due to its ability to reduce Cu(II) to Cu(I) initiating the redox reactions of the Aβ/copper complex. Ascorbic acid is usually considered an antioxidant due to its ability to donate electrons, capable of detoxifying oxidising agents such as H_2O_2. The effect of ascorbic acid is not fully concentration dependant; *in vitro* it is observed that at high enough concentrations ascorbic acid becomes a pro-oxidant, able to initiate Fenton chemistry which uses free metal ions to convert H_2O_2 to hydroxyl radicals.

A range of ascorbic acid concentrations were tested for their effects on Aβ42 aggregation and H_2O_2 generation. The controls for these reactions indicated that the 2 highest concentrations of ascorbic acid showed time dependant generation of H_2O_2 which was eliminated by the addition of catalase. This suggests that the ascorbic acid at these concentrations is able to reduce the endogenous Cu(II) in the buffer solution to generate H_2O_2. By 48 hrs the level of H_2O_2 detected in these 2 controls decreased

significantly (Tukey HSD, $p \leq 0.000$). This may be due to the level of H_2O_2 generated causing the ascorbic acid to become itself oxidised to dehydroascorbate, depleting the H_2O_2 from the solution but also decreasing the concentration of ascorbic acid so it no longer generates H_2O_2. Interestingly, these high levels of fluorescence are not present in the Aβ42 containing counterparts. In fact, fluorescence measured from these samples is reduced in comparison to the lower concentrations of ascorbic acid, implying the Aβ may be removing the H_2O_2 generated by the ascorbic acid from the solution. However, a more likely explanation is that the Cu(II) ions are no longer free in solution but instead bound to Aβ: at high ascorbic acid levels this data supports evidence that ascorbic acid plus free copper generates more H_2O_2 than ascorbic acid plus Aβ-Cu(II) (Guilloreau et al., 2007; Nadal et al., 2008). Ascorbic acid can be considered a better electron donor than Aβ so these results may be expected. Taking this viewpoint, it is possible to consider Aβ binding copper as an anti-oxidant mechanism. However, even though ascorbate levels in the brain can be high, free copper is kept at a minimum to prevent detrimental redox reactions. Consequently, the fact that ascorbic acid and free copper generates more H_2O_2 has little biological relevance. Also, with no copper added to Aβ, incubation with these higher levels of ascorbic acid generates less H_2O_2 than Aβ alone. This suggests that where Cu(II) levels are minimal and most likely Aβ-bound, greater generation of H_2O_2 results from Aβ reduction of Cu(II) than when high levels of ascorbic acid were present.

The presence of lower levels of ascorbic acid appeared to cause a small increase early oligomerisation of Aβ42 (immunoassay at 6 hrs). H_2O_2 generation from the Aβ42 samples at 6 hrs was somewhat correlated with this, providing support that an oligomeric species of Aβ is responsible for H_2O_2 generation. These effects in this first 6 hrs may be directly due to increased reduction of Cu(II) to Cu(I) by the presence of

ascorbic acid. The early increase in H_2O_2 generation with ascorbic acid may have caused increased oligomerisation of Aβ due to oxidative modification of Aβ (maybe in a similar manner to the cross-linked Aβ generated in chapter 5). Despite this, by 48 hrs, the addition of ascorbic acid, even at the highest concentration did not increase H_2O_2 generation by the Aβ42 compared to that with no added ascorbic acid. This appears to contradict other evidence that a reductant such as ascorbic acid elevates H_2O_2 generation (Barnham et al., 2004; Dikalov et al., 2004; Guilloreau et al., 2007; Murray et al., 2005; Nadal et al., 2008). Importantly though, is that in this experiment no copper was added to the samples relying on the copper naturally occurring in the buffer solutions. This was done as metal ions are found to have varying effects on the aggregation and H_2O_2 generation at different concentrations (investigated in chapter 7). It may be that adding copper and ascorbic acid elevates the H_2O_2 generated by Aβ for longer which may reflect age-dependent metal accumulation.

4.3.5. Is Aβ generated ROS directly responsible for neuronal cell death?

A theory that carries a lot of support is that membrane insertion of Aβ may direct oxidative stress at membrane lipids increasing membrane permeability. It has been suggested that a transient sulphuramyl free radical, formed by the reaction of Met35 with the metal ion, could abstract a proton from nearby unsaturated bonds in phospholipid acyl chains. This would create a carbon centred radical on the lipid that readily reacts with molecular oxygen forming the peroxyl free radical. Subsequently a cascade of reactions could be initiated, amplifying the original Aβ peptide free radical (Butterfield and Bush, 2004). The products of lipid peroxidation, such as HNE, would be formed from the systematic breakdown of membrane lipids by free radical attack altering membrane permeability. Following the abstraction of a proton the methionine

becomes positively charged. This SH^+ group is an acid with a pK_A of -5 meaning any close by base, such as water, would except this proton instantaneously. Met35 is reformed and capable of reaction with the metal ion all over again creating a catalytic cycle (Butterfield and Bush, 2004; Smith et al., 2007a; Varadarajan et al., 2001). Supporting this hypothesis is evidence that reports lipid oxidation is increased with Cu-Aβ compared to free copper. Furthermore, it has been reported that catalase could not protect against the Cu-Aβ induced oxidation, illustrating the danger of free-radicals generated within the membrane (Murray et al., 2005).

For lipid peroxidation to take place it would seem fundamental for Met35 to be within the bilayer. Even if Aβ does not insert fully into the membrane as some hypothesise, the C-terminus of Aβ has a putative TM domain placing Met35 within the lipid bilayer (Smith et al., 2007a). Gly37Asp substitution on Aβ was hypothesised to alter the position of Met35 placing it outside of the lipid membrane. This substituted peptide showed no oxidative stress or neurotoxicity, consistent with Met35 being required within the bilayer (Kanski et al., 2002a).

As evidence suggests the small soluble aggregates of Aβ are the toxic species, the idea that these species may be able to insert into the membrane, placing them for reaction with lipids, has gained standing. On the other hand it may be that this H_2O_2 generation is of little consequence to the toxicity of the peptide and the early species of Aβ42 exert their toxicity via another mechanism. However, evidence that oxidative stress is an early event in the pathogenesis of AD and that early Aβ species generate ROS which causes oxidative stress cannot be ignored as a possible key pathogenic event in the development of AD.

4.4. Conclusions

- Increasing evidence suggests that small soluble oligomeric Aβ is responsible for neurotoxicity in AD
- Aβ generates H_2O_2 during the early stages of its aggregation possibly implicating an early oligomeric species as being responsible for its formation
- Aβ42 has been found to generate more H_2O_2 than Aβ40, corresponding to the increased toxicity attributed to Aβ42
- Aβ42 substituted peptides implicated in metal binding (H6A, H13A, H14A and possibly Y10A), redox cycling (M35N) and dimerisation (Y10A) generated less H_2O_2 than wt Aβ42
- These peptides retained some ability to generate H_2O_2, therefore none of these residues was absolutely critical for this process
- The histidine substituted Aβ42 may have somewhat reduced affinity for metal binding therefore the metal ion is reduced by Met35 at a decreased rate
- Substitution of Met35 showed that another residue, possibly Tyr10 is also able to donate an electron to the metal ion, although at a reduced rate
- Substitution of Tyr10 demonstrated that dityrosine dimers are not a pre-requisite for fibrillisation of Aβ, or the sole source of H_2O_2. However it appears that the formation of the Aβ species that generates H_2O_2 was reduced
- Aβ plus ascorbic acid with no added metals showed low levels of this anti-oxidant to elevate early H_2O_2 generation by Aβ but also appeared to promote Aβ oligomerisation in a concentration dependant manner.
- There is evidence that H_2O_2 generation by Aβ may be targeted *in vivo* at lipid membranes and that this may be accountable, at least in part, for the oxidative stress observed in the AD brain and potentially the pathogenesis of AD

Chapter 5
Cross-linking of β-amyloid

5.1. Introduction

Strong evidence suggests that a form of oligomeric Aβ is responsible for neurotoxicity in AD. The generation of H_2O_2 by Aβ occurs during the early stages of Aβ aggregation possibly implicating oligomeric Aβ in H_2O_2 formation and providing a potential source of oligomer mediated toxicity. However the transient and dynamic nature of Aβ in solution plagues identification of the species responsible. Here, several methods of cross-linking have been tested in an attempt to create fixed yet natural oligomeric Aβ. The Aβ species created may then be tested for their ability to generate H_2O_2. The cross-linking methods tested were photo-induced cross-linking of unmodified proteins (PICUP) and 2 methods inducing oxidation of Aβ using copper or HRP with H_2O_2. The results of these experiments were visualised by SDS-PAGE.

5.1.1. Photo-induced cross-linking of unmodified proteins (PICUP)

PICUP was originally designed to aid elucidation of protein-protein interactions in large, multi-protein, complexes (Fancy and Kodadek, 1999). This method utilises the photolysation of Ru(II)bpy by a persulphate generating Ru(III), and a sulphate radical (see Figure 5.1.). Ru(III) is a powerful oxidant, able to abstract an electron from tyrosine's aromatic ring, forming an electrophilic tyrosine intermediate. This can form cross-linked proteins by two mechanisms dependant on the residue targeted. If another tyrosine is nearby, a di-tyrosine cross-link would be formed through arene coupling. Alternatively, a nucleophilic lysine or cysteine is attacked by the tyrosine radical, with the final protein complex being linked from tyrosine to cysteine/lysine.

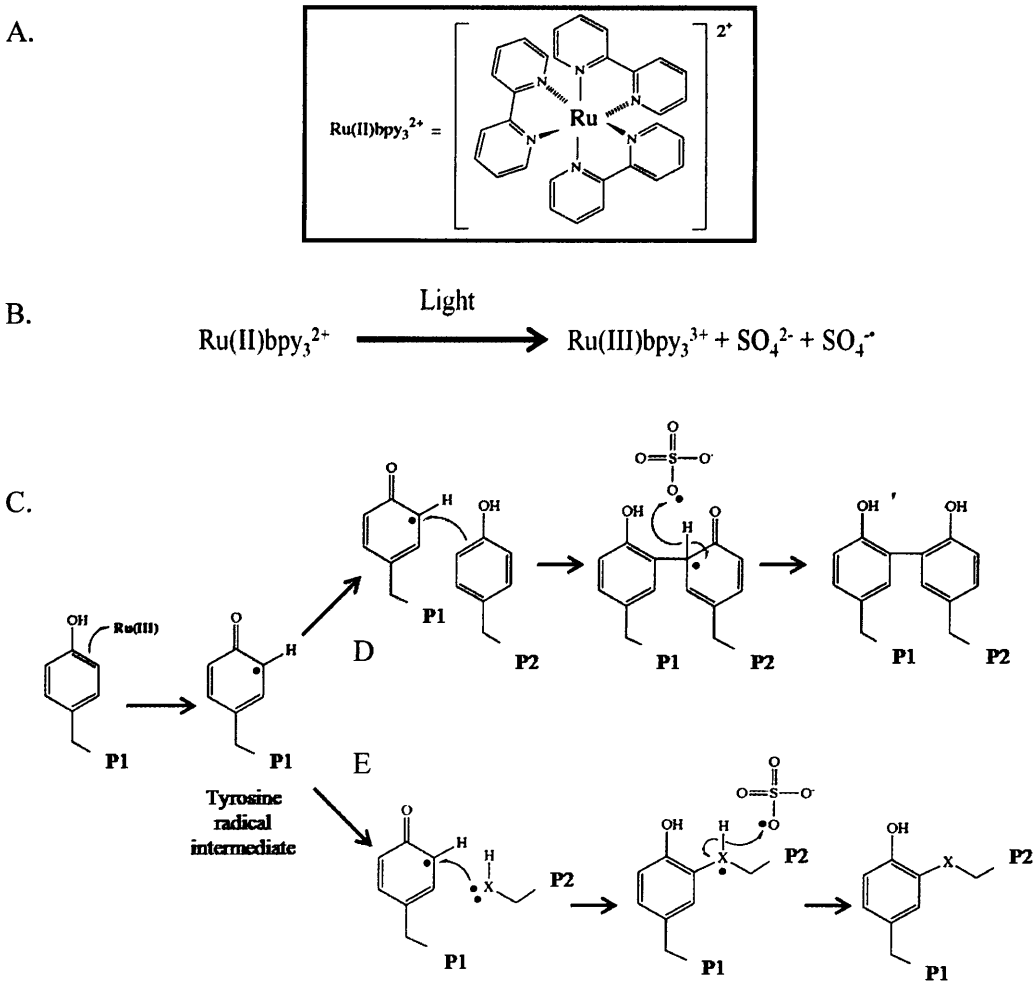

Figure 5.1. Proposed mechanism of PICUP
The structure of Ru(II)bpy is shown in A. Exposure to light causes oxidation of Ru(II)bpy by a persulphate forming Ru(III) (B). This then oxidises tyrosine residues forming a tyrosine radical intermediate within a peptide chain, P1 (C). This radical can then undergo reaction with another tyrosine residue (D) in a second protein chain, P2, or, react with a nucleophilic residue (E) in a second protein chain, P2. Adapted from Fancy and Kodadek (Fancy and Kodadek, 1999).

Aβ contains one tyrosine residue (Y10) providing the substrate for Ru(III) to abstract an electron from. This can then react with a second Aβ Y10 or with nucleophilic residues in the Aβ sequence, such as the two lysine residues (K16 and K28). This technique has been developed by Teplow and colleagues to investigate early Aβ aggregation (Bitan et al., 2001). By analysing the range of cross-linking oligomers generated by PICUP, they obtained evidence suggesting that Aβ40 and Aβ42 aggregate via different pathways. This theory is based on the premise that Aβ

subunits that are closer to each other, such as in an oligomer, are more likely to be cross-linked than peptide chains that are further away. This leads to the idea that the spectrum of bands observed upon gel electrophoresis is made up of both natural and unnatural oligomers. However, PICUP of Aβ is critically dependant on the availability of key residues. Oligomerisation of the peptide may obscure, or require Tyr10, limiting Aβ cross-linking rather than promoting it. Indeed, dityrosine cross-linked Aβ has been implicated as playing a central role in Aβ-mediated toxicity and is a common oxidative stress-related protein modification (Smith et al., 2007a). It is therefore likely, that a proportion of PICUP generated cross-linked Aβ are the same as naturally formed oligomers.

5.1.2. Cross-linking of Aβ via oxidation

The transient nature of the oligomeric species confines analysis by PICUP to relying on a "snapshot" of the oligomer population at a given point in the aggregation process. The PICUP technique also contains an inherent issue when trying to use it for assessing oligomeric properties; only a proportion of the oligomers formed may be considered "natural". This makes investigation of their characteristics problematic. To bypass these issues cross-linking via oxidation of Aβ attempts to turn the problem on its head, promoting oligomerisation of the peptide and consequently increasing natural oligomer concentration, which can subsequently be tested for their H_2O_2 generation. Such oxidative mechanisms have long been implicated in Aβ aggregation as well as its mechanism of toxicity. Two methods have been investigated here both utilising H_2O_2 as the oxidising agent. The first uses Cu(II) as a catalyst, as its ability to utilise two oxidation states permits redox cycling. This has been shown to generate SDS stable Aβ including dityrosine dimers (Atwood et al., 2004). The second

employs the enzyme horseradish peroxidase (HRP) to catalyse the oxidation of Aβ by the H_2O_2 which has also been shown to form Aβ dimers (Galeazzi et al., 1999).

The AD brain is in a highly oxidative state, having increased brain metals and a reduced capacity to detoxify oxidation events with aging. In addition, evidence from our laboratory and others indicate Aβ is itself able to generate H_2O_2 (Huang et al., 1999a; Tabner et al., 2005; Tabner et al., 2002). This infers that utilising HRP and Cu(II) to form early SDS-stable oligomers may generate natural oligomers preferentially. The initial oxidation events could occur on the residues most liable to attack rather than Tyr10 solely (as with PICUP).

5.1.3. The purpose of cross-linking

The heterogeneous and dynamic nature of solutions of Aβ makes characterisation of the oligomeric species highly problematic. Evidence suggests that these oligomeric species are responsible for neuronal toxicity in AD yet identification of the particular oligomer culpable remains a contentious issue. Potential offenders include the dityrosine dimer (Barnham et al., 2004; Smith et al., 2007a), tetramers (Ono et al., 2009) up to hexamers (Butterfield and Bush, 2004), 12-mers that are able to bind receptors inducing toxicity (Lambert et al., 1998), and a 56 kDa Aβ species (Aβ*56) that induces memory deficits in transgenic mice (Lesne et al., 2006).

Generation of cross-linked Aβ serves to "fix" oligomers and prevent further aggregation. This would enable the Aβ species generated to be tested, primarily for their ability to generate H_2O_2, an event that may be linked to the toxicity of Aβ oligomers.

5.2. Results

5.2.1. PICUP of Aβ40

All of our evidence suggested that, even without TFA treatment, HFIP-treated rAβ40-HFIP was largely monomeric upon wetting. This made it an obvious starting point for developing cross-linking techniques for identifying toxic oligomers. The more toxic Aβ42 inevitably contains a portion of pre-aggregated material, which complicates interpretation of results. As can be seen in figure 5.2, with non cross-linked Aβ40 (no light exposure) only the monomeric species is observed at all three time-points despite aggregation being observed over this time period. Following cross-linking of the Aβ40 samples SDS-stable oligomers were observed up to a tetramer in size (see figure 5.2. at 0 hrs aggregation, 1/30 sec light exposure). The distribution of these oligomers for all aggregation time points follows the pattern outlined by Teplow and colleagues for random association of monomeric species (Bitan et al., 2001). This assumes that the probability of a monomer cross-linking with another monomer is twice as likely as a monomer cross-linking to a cross-linked dimer, and so on and so forth. As light exposure increases, the more monomers get consumed into dimers, and dimers into trimers and tetramers. With this in mind, the presence of natural, low order oligomers in pre-aggregated solutions should generate more, higher order PICUP cross-linked Aβ40 species. Conversely, the opposite was observed to be the case, with the pre-aggregated Aβ40 generating fewer trimers and tetramers than freshly wetted Aβ40.

It was observed that despite increased cross-linking, the level of monomer present did not appear to decrease accordingly. This may be partially due to cross-linked species having more antibody binding sites, misrepresenting the level of cross-linked Aβ.

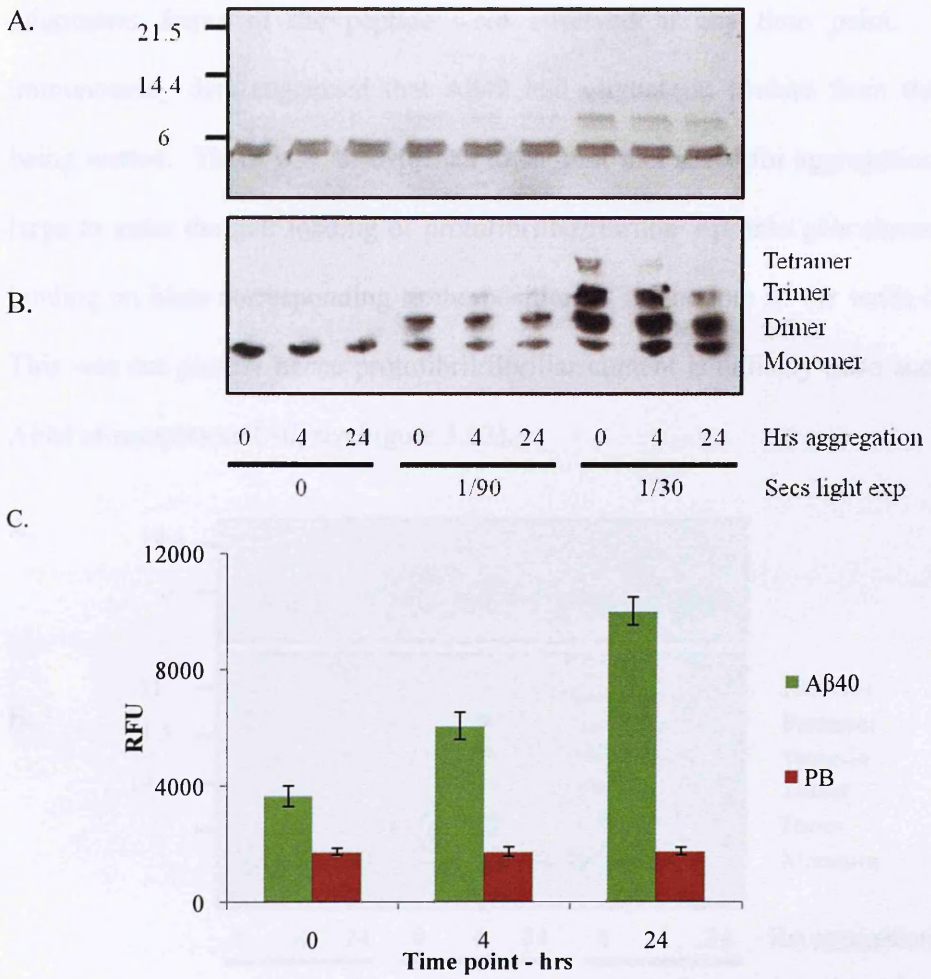

Figure 5.2. PICUP of Aβ40

25 μM TFA treated Aβ40 was aggregated in 10 mM PB at 37°C over 24 hrs with samples taken for cross-linking and immunoassay at 0, 4 and 24 hrs. These samples were then submitted to PICUP cross-linking with light exposures of 0, 1/90 or 1/30 seconds. Samples of PICUP cross-linked Aβ40 containing final concentration of 15 μM Aβ40, 0.67 mM APS, 33.3 μM Ru(II)bpy and 3.3% β-mercaptoethanol were diluted 1:1 with SDS gel loading buffer. 15 μl (for Instant blue staining) and 5 μl (for western blot) of these samples were then run on 16.5% SDS Tris-Glycine gels and stained both Instant Blue (A) and by western blot probed with mAb 6E10 (B). Immunoassay results are shown in C (means ± S.D, n=4)

5.2.2. PICUP of Aβ42

This method was subsequently tested on Aβ42 (see figure 5.3). When the samples were not exposed to light, preventing any cross-linking from occurring, a single band was observed representing the monomeric form of the peptide. The size of this band was considerably reduced when the Aβ42 had been pre-aggregated for 24 hrs, yet no

oligomeric forms of the peptide were observed at any time point. However, immunoassay data suggested that Aβ42 had oligomeric content from the point of being wetted. There was no evidence to suggest that seeds for aggregation were too large to enter the gel: loading of protofibrillar/fibrillar Aβ onto gels shows antibody binding on blots corresponding to the position of the bottom of the wells on the gel. This was not present hence protofibril/fibrillar content is unlikely (also supported by AFM of samples at T=0, see Figure 3.13).

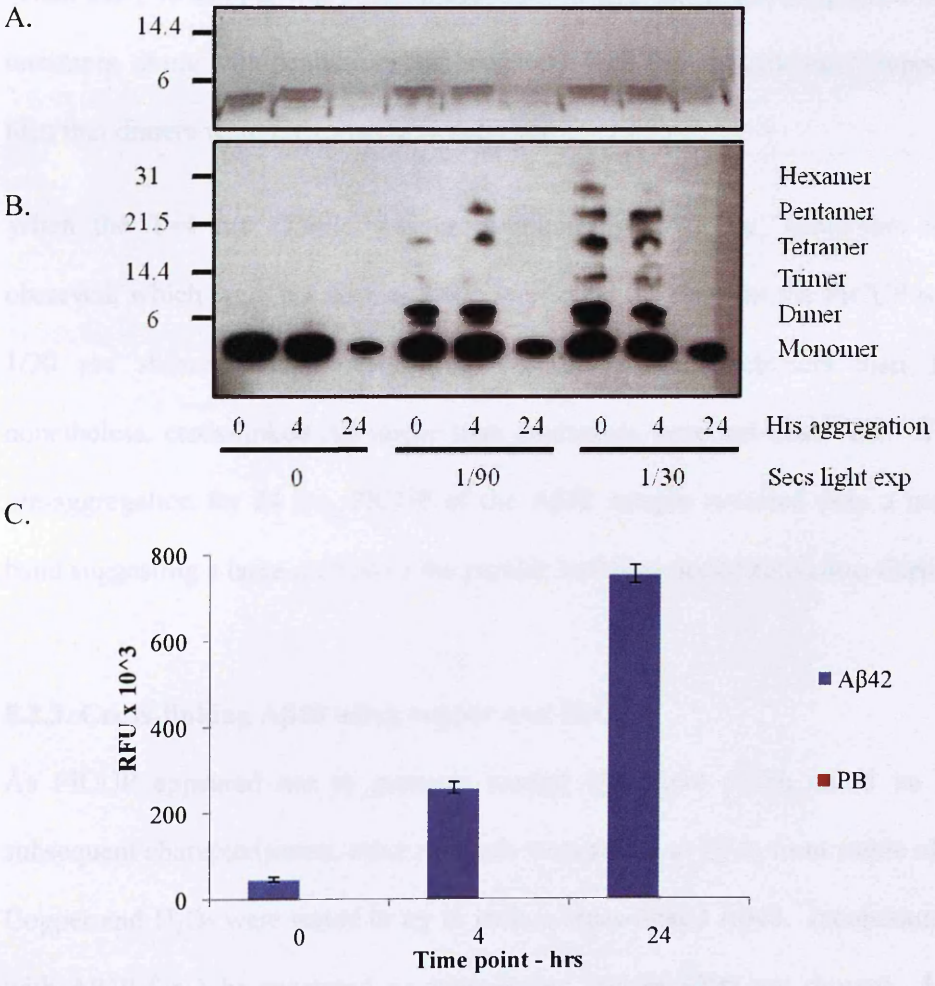

Figure 5.3. PICUP of Aβ42

25 μM TFA treated Aβ42 was aggregated in 10 mM PB at 37°C over 24 hrs with samples taken for cross-linking and immunoassay at 0, 4 and 24 hrs. These samples were then submitted to PICUP cross-linking for 0, 1/90 or 1/30 seconds. Samples of PICUP cross-linked Aβ42 containing final concentration of 15 μM Aβ42, 0.67 mM APS, 33.3 μM Ru(II)bpy and 3.3% β-mercaptoethanol were diluted 1:1 with SDS gel loading buffer. 15 μl (for Instant blue staining) and 5 μl (for western blot) of these samples were then run on 16.5% SDS Tris-Glycine gels and stained both Instant Blue (A) and by western blot probed with mAb 6E10 (B). Immunoassay results are shown in C (means ± S.D, n=4)

Cross-linking of the Aβ42 samples, interestingly, did not follow the typical band distribution observed with Aβ40. Firstly, for freshly wetted Aβ42, when exposed to light for 1/90 sec few trimers were observed, yet a larger band of tetramers appeared. If the sample was purely monomeric, trimers would be twice more likely to be generated than tetramers suggesting that pre-PICUP, the sample contains dimers which are subsequently cross-linked to tetramers. This may go some way to explaining the oligomeric content observed in the oligomeric immunoassay at T=0. When the T=0 sample was cross-linked for 1/30 sec, again there appeared to be more tetramers, along with pentamers and hexamers, than trimers generated, supporting the idea that dimers were pre-existing in solution.

When the T=4 hrs sample was cross-linked for 1/90 sec, pentamers were also observed, which were not seen at T=0. Increasing the time for the PICUP reaction to 1/30 sec showed darker staining for tetramers and pentamers than 1/90 sec, nonetheless, cross-linked Aβ larger than pentamers were not observed. Following pre-aggregation for 24 hrs, PICUP of the Aβ42 sample revealed only a monomeric band suggesting a large portion of the peptide had been sequestered into fibrils.

5.2.3. Cross-linking Aβ40 using copper and H_2O_2

As PICUP appeared not to generate natural oligomers which could be used for subsequent characterisation, other methods were tested to try to form stable oligomers. Copper and H_2O_2 were tested to try to induce cross-linked Aβ40. Incubation of these with Aβ40 for 1 hr generated no cross-linked species (data not shown). However, when incubated for 24 hrs SDS-stable oligomers up to tetramers were generated at the highest concentrations of H_2O_2 (see figure 5.4). The level of copper ions present appeared to have only a small effect on the cross-linked Aβ40 made, albeit its

presence was needed. Later investigations with copper showed it to have its greatest effect on Aβ aggregation at sub-equimolar concentrations (see chapter 7). However, testing of lower copper concentrations did not form any cross-linked species.

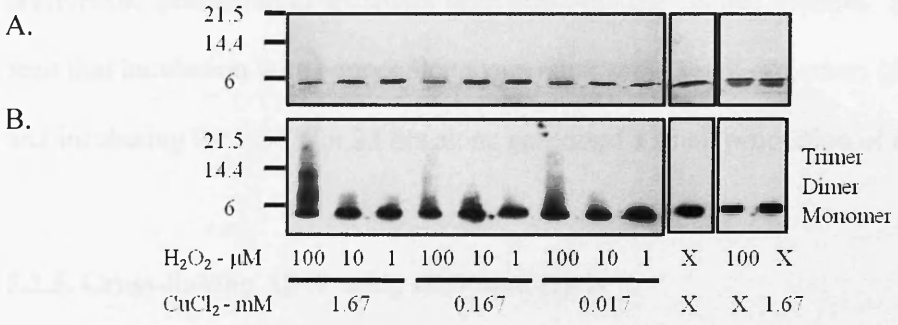

Figure 5.4. Cross-linking Aβ40 with copper and H_2O_2 for 24 hrs.
25 µM Aβ40 in 10 mM PB, pH 7.4, was incubated for 24 hrs at 37°C with various concentrations of H_2O_2 and copper (II) chloride. Samples were then diluted 1:1 with SDS gel loading buffer. 15 µl (for Instant blue staining) and 5 µl (for western blot) of these samples were then run on 16.5% SDS Tris-Glycine gels and stained both Instant Blue (A) and by western blot probed with mAb 6E10 (B).

5.2.4. Cross-linking Aβ42 using copper and H_2O_2

When Aβ42 was incubated with copper and H_2O_2, cross-linking of Aβ42 again required 24 hrs (shown in figure 5.5).

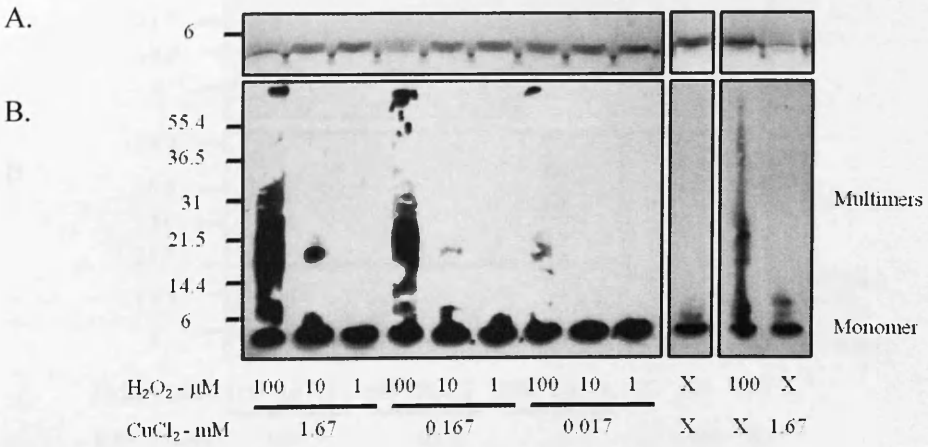

Figure 5.5. Cross-linking Aβ42 with copper and H_2O_2 for 24 hrs.
25 µM Aβ42 in 10 mM PB, pH 7.4, was incubated for 24 hrs at 37°C with various concentrations of H_2O_2 and copper (II) chloride. Samples were then diluted 1:1 with SDS gel loading buffer. 15 µl (for Instant blue staining) and 5 µl (for western blot) of these samples were then run on 16.5% SDS Tris-Glycine gels and stained both Instant Blue (A) and by western blot probed with mAb 6E10 (B).

Here, few distinct oligomeric bands were observed, but rather, at the highest H_2O_2 concentrations, a large smear ranging from dimer to approximately heptamer. At lower H_2O_2/copper concentrations a band of ~18 kDa in size was produced, implying preferential generation of tetramers from cross-linking via this method. It can also be seen that incubation with copper alone generated some small oligomers (dimer/trimer) and incubating the Aβ42 for 24 hrs alone generated a small proportion of dimers.

5.2.5. Cross-linking Aβ40 using HRP and H_2O_2

HRP is commonly used to catalyse the oxidation of a substrate by H_2O_2. This appeared to be a far more efficient mechanism of oxidising the Aβ40 than using copper (II) chloride as observed (see figure 5.6). Incubation of the Aβ40 with HRP and H_2O_2 for only 1 hour at 37°C generated not only dimers to tetramers, but also multimers, albeit at low levels (with 100U/ml HRP and 100μM H_2O_2 present).

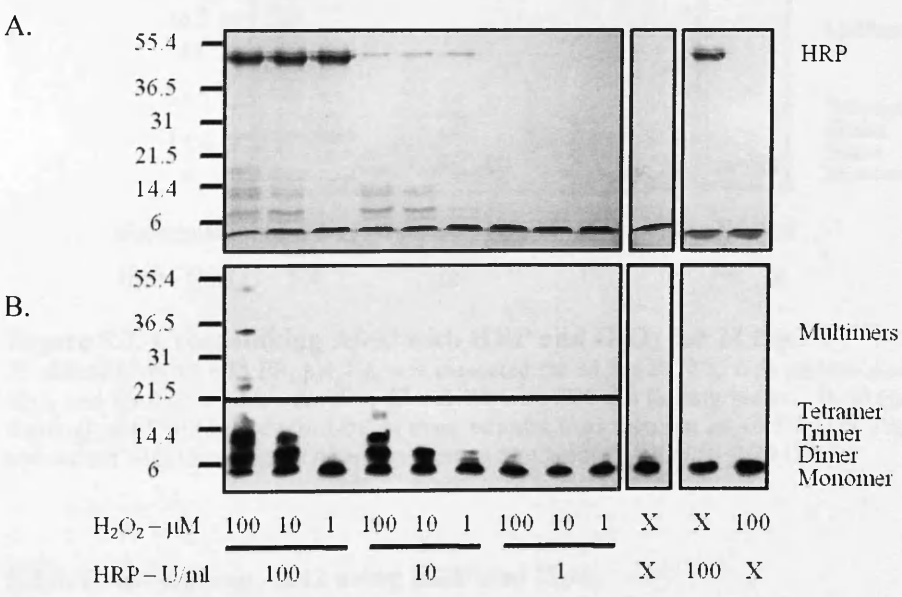

Figure 5.6. Cross-linking Aβ40 with HRP and H_2O_2 for 1 hr.
25 μM Aβ40 in 10 mM PB, pH 7.4, was incubated for 1hr at 37°C with various concentrations of H_2O_2 and HRP. Samples were diluted 1:1 with SDS gel loading buffer. 15 μl (for Instant blue staining) and 5 μl (for western blot) of these samples were then run on 16.5% SDS Tris-Glycine gels and stained both Instant Blue (A) and by western blot probed with mAb 6E10 (B. Overexposed, C. Normal exposure).

Bands at ~8-mer and 10-mer Aβ40 appeared to be specifically generated by the reaction of HRP and H_2O_2. This suggests that these oligomers are not just being made from random association of monomers as with PICUP of Aβ40, as this would predict a 7-mer band being larger than an 8-mer band, and yet a 7-mer band is not present.

Extending the incubation period to 24 hrs generated a strong band at ~45kDa when 100 μM H_2O_2 and 100 U/ml HRP were used (see figure 5.7). This corresponds to a dodecamer (10-mer). A spectrum of other low-order, SDS-stable species were also observed. Both HRP and H_2O_2 were required for these species to be formed and over the concentrations tested both reagents exhibited a concentration dependant effect.

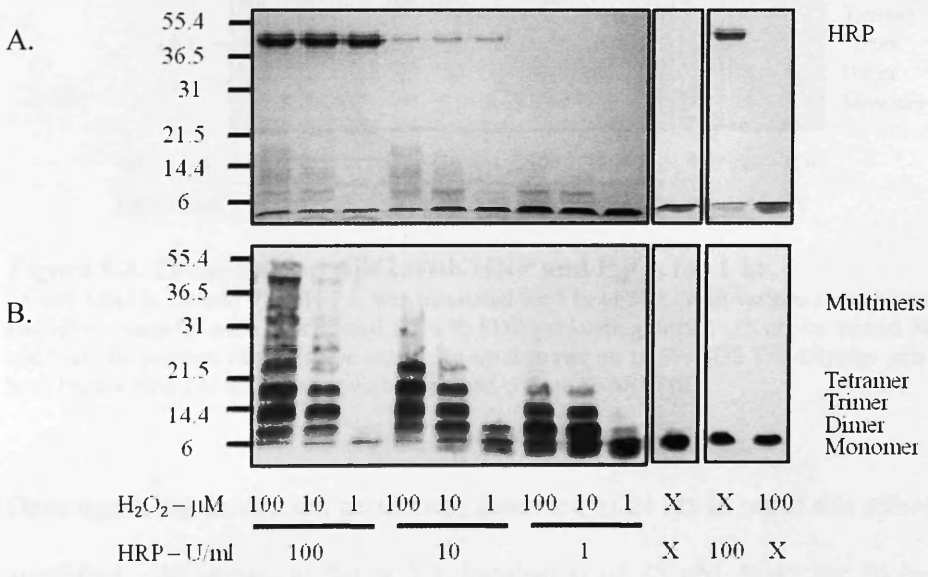

Figure 5.7. Cross-linking Aβ40 with HRP and H_2O_2 for 24 hrs.
25 μM Aβ40 in 10 mM PB, pH 7.4, was incubated for 24 hrs at 37°C with various concentrations of H_2O_2 and HRP. Samples were then diluted 1:1 with SDS gel loading buffer. 15 μl (for Instant blue staining) and 5 μl (for western blot) of these samples were then run on 16.5% SDS Tris-Glycine gels and stained both Instant Blue (A) and by western blot probed with mAb 6E10 (B).

5.2.6. Cross-linking Aβ42 using HRP and H_2O_2

The cross-linking of Aβ42 using HRP generated notably more cross-linked species than when performed on Aβ40. When incubated for only 1 hr at 37°C strong bands were observed particularly at the dimer, tetramer and pentamer level (see figure 5.8).

In addition, at the highest concentration of HRP and H_2O_2, a relatively strong band was visible at ~45 kDa, presumably representing a 10-mer, together with a lighter band at 56 kDa.

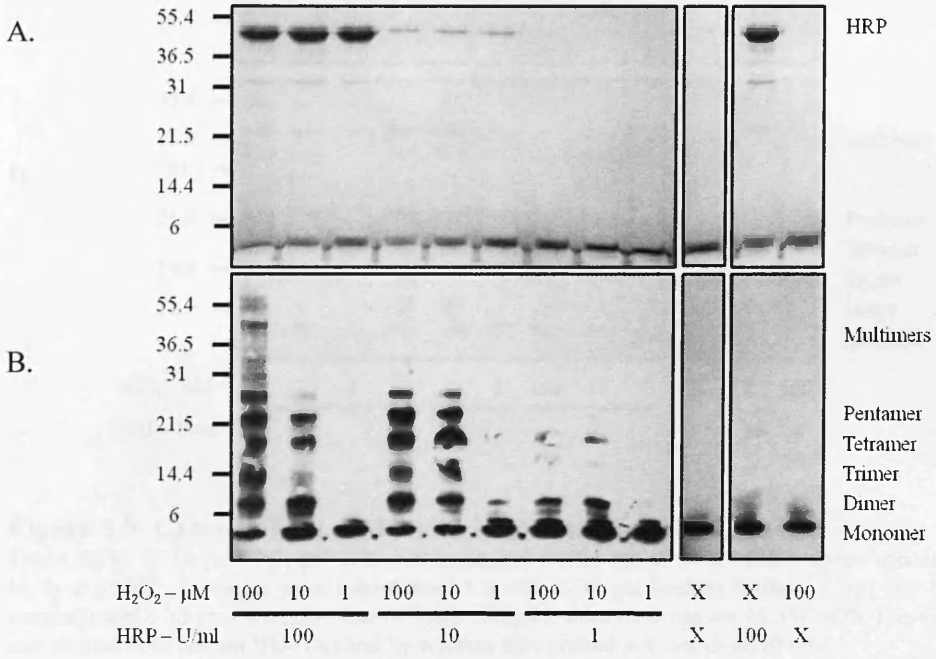

Figure 5.8. Cross-linking Aβ42 with HRP and H_2O_2 for 1 hr.
25 μM Aβ42 in 10 mM PB, pH 7.4, was incubated for 1 hr at 37°C with various concentrations of H_2O_2 and HRP. Samples were then diluted 1:1 with SDS gel loading buffer. 15 μl (for Instant blue staining) and 5 μl (for western blot) of these samples were then run on 16.5% SDS Tris-Glycine gels and stained both Instant Blue (A) and by western blot probed with mAb 6E10 (B).

Once again, the incubation period was extended to 24 hrs to see if this effect could be amplified. As shown in figure 5.3, incubation of 25 μM Aβ42 for 24 hrs at 37°C allowed aggregation to progress to the point at which the majority of the Aβ has been consumed into fibrils with only a small proportion of monomer remaining visible on the western blot. At the highest HRP concentration, this effect was again observed (see figure 5.9), although over exposure of the blot did present a 45 kDa band remaining at the highest H_2O_2 concentration (data not shown). Despite the propensity of Aβ42 to form fibrils, at the lower concentrations of HRP, bands up to hexamer were still observed, with a pattern similar to that observed when incubated for 1 hr.

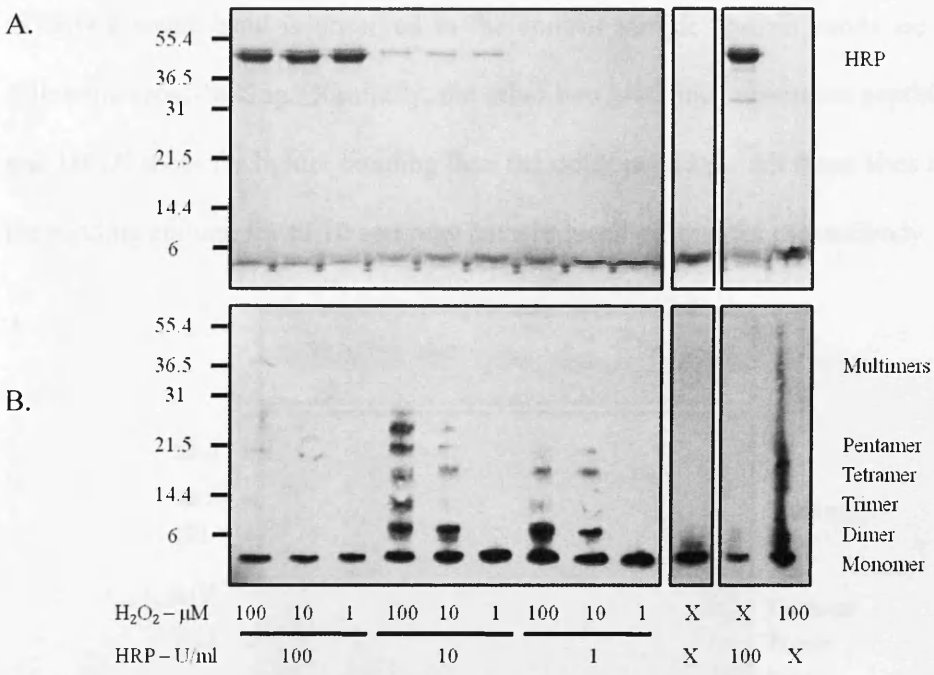

Figure 5.9. Cross-linking Aβ42 with HRP and H_2O_2 for 24 hours.
25μM Aβ42 in 10 mM PB, pH 7.4, was incubated for 24 hrs at 37°C with various concentrations of H_2O_2 and HRP. Samples were then diluted 1:1 with SDS gel loading buffer. 15 μl (for Instant blue staining) and 5 μl (for western blot) of these samples were then run on 16.5% SDS Tris-Glycine gels and stained both Instant Blue (A) and by western blot probed with mAb 6E10 (B).

5.2.7. Cross-linking Aβ mutant proteins using HRP and H_2O_2

Having observed the generation of SDS-stable cross-linking of both Aβ40 and Aβ42 using HRP and H_2O_2, functional Aβ42 mutants implicated in Aβ metal binding (H6A, H13A and H14A), redox chemistry (M35N), and dimerisation (Y10A) were subsequently investigated. These were anticipated to give some insight into the residues and processes involved in the formation of these oligomers.

Aβ40 and Aβ42 presented with a similar banding pattern as observed previously, with Aβ42 showing a greater proportion of larger molecular weight protein bands (see figure 5.10). In comparison the Y10A-Aβ42 shows one band at what appears to be monomer in size, clearly implicating this tyrosine as being critical for the cross-linking reaction. H6A-Aβ42 has greatly reduced binding affinity for the mAb 6E10,

as only a small band is observed in the control sample and no bands are observed following cross-linking. Similarly, the other two histidine substituted peptides, H13A and H14A show far lighter banding than the other peptides. All these sites are within the binding epitope for 6E10 and may have reduced affinity for the antibody.

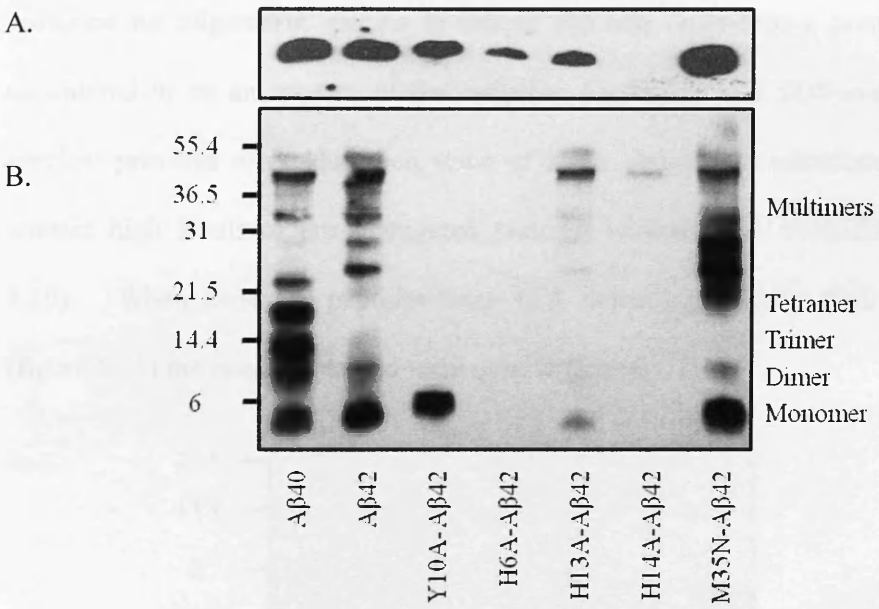

Figure 5.10. Cross-linking of Aβ peptides with HRP and H_2O_2 for 1 hr.
Freshly wetted 30 μM Aβ in 10 mM PB, pH 7.4, was incubated for 1 hr at 37°C with 100 μM H_2O_2 and 100 U/ml HRP. Samples were then diluted 1:1 with SDS gel loading buffer. 5 μl of these samples were then run on 16.5% SDS Tris-Glycine gels and stained by western blot probed with mAb 6E10. A = Non cross-linked samples, B = cross-linked samples.

H13A presents a small amount of monomer, yet the majority of the peptide appears to be between pentamer and 12-er in size, with particular staining at the 45 kDa species (10-mer). The H14A substituted peptide interestingly, presents only one band, also at this size. This is particularly interesting as the control blot showed no bands for H14A even following over-exposure. This was initially thought to be due to reduced binding affinity for the antibody. However TFA deseeding showed this not to be the case (see figure 5.11); H14A was too aggregated to enter the gel matrix. Yet, following cross-linking with HRP and H_2O_2, this 45 kDa band was observed. Together with this 45

kDa band, the final peptide tested, M35N, showed particularly strong staining for bands between pentamer and heptamer species.

This initial investigation of cross-linking these substituted Aβ peptides was performed on non-TFA deseeded peptides with only HFIP treatment. Even though control blots indicated no oligomeric species in any of the non cross-linked samples, this was considered to be an artefact of the reducing conditions and SDS-instability of the species; previous work identified some of these amino acid substituted peptides to contain high levels of pre-aggregated material without TFA deseeding (see figure 3.10). When these Aβ peptides were TFA deseeding prior to their cross-linking (figure 5.11) the results obtained were quite different.

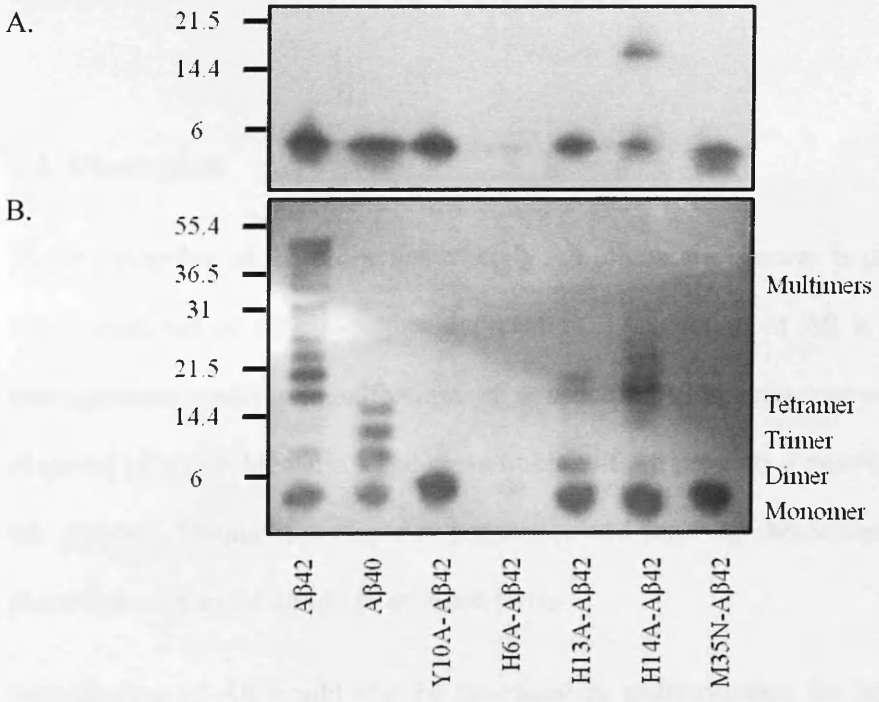

Figure 5.11. Cross-linking of TFA deseeded Aβ peptides with HRP and H_2O_2 for 1 hr.

Freshly wetted 30 μM TFA treated Aβ in 10 mM PB, pH 7.4, was incubated for 1 hr at 37°C with 100μM H_2O_2 and 100 U/ml HRP. Samples were then diluted 1:1 with SDS gel loading buffer. 15 μl (for Instant blue staining) and 5 μl (for western blot) of these samples were then run on 16.5% SDS Tris-Glycine gels and stained both Instant Blue and by western blot probed with mAb 6E10 Non-cross-linked samples (A) cross-linked (B).

The TFA deseeded Aβs generated far fewer of the larger multimers, across all peptides. Aβ42 appeared to retain its tendency for generation of higher cross-linked species, with the 45 kDa species remaining a preferred species. Aβ40 on the other hand loses this band and shows cross-linked oligomers up to tetramer in size. Y10A remained monomeric, unaffected by the cross-linking process and H6A lacks reactivity for the mAb 6E10 as only a very faint band was ever observed with this peptide. TFA deseeded H13A only presented cross-linked species at dimer and light bands at tetramer/pentamer in size. This was emulated by H14A, except this peptide had a band at tetramer in size in the TFA-deseed control suggesting the deseeding process was not as effective on the H14A substituted peptide. The TFA deseeded M35N also generated only a light band at tetramer in size following cross-linking.

5.3. Discussion

The investigation of the properties of early Aβ oligomeric species is plagued by the innate tendency of Aβ for further aggregation. A solution of Aβ is dynamic and heterogeneous making identification of a specific Aβ species responsible for an observed effect problematic. The cross-linking of Aβ presents a possible solution to this problem, "fixing" the oligomer population and enabling characterisation of their properties such as the ability to generate H_2O_2.

Cross-linking of Aβ would also be beneficial in circumventing the issues of SDS-stability of Aβ species which further hinders identification of the toxic Aβ species. It has long been observed that many oligomeric species appear to be SDS-labile. Aβ40 has been found to migrate as a single band, representing the monomeric form, and Aβ42 up to five bands, regardless of the aggregation state of the peptides (Walsh et

al., 1997). This indicates that Aβ40 aggregates are all disaggregated by SDS, whereas Aβ42 may have several SDS-stable species, but these may be formed from the dissociation of fibrils or protofibrils, or from SDS promoting Aβ self association.

Under the reducing conditions used here, with no cross-linking performed, both Aβ40 and Aβ42 migrated as a single monomeric band, at all time points tested during its aggregation. This is presumably due to a combination of factors: the dynamic and transient nature of the intermediates, together with SDS-instability. Following 24 hrs aggregation the band representing the monomer becomes considerably smaller in Aβ42 but not the Aβ40 sample, indicating the Aβ42 has been sequestered into larger, fibrillar aggregates and that Aβ42 has a greater inclination for this. The fact that pre-aggregation of the sample generated no visible oligomers supports the hypothesised mechanisms observed for Aβ aggregation: Aβ is sequestered into fibrillar species via a series of transient and highly dynamic oligomeric intermediates.

5.3.1. PICUP cross-linking

The first technique investigated to achieve cross-linked, stable, Aβ was PICUP. This technique is based on the idea that self-associating Aβ molecules (oligomers) are closer together, and more likely to become cross-linked than those not self-associating.

When this technique was used to compare cross-linking of Aβ40 pre-aggregated for different lengths of time, no evidence for the presence of oligomeric Aβ40 was observed. The banding observed followed the pattern set out in Bitan et al, for the random association of monomers (Bitan et al., 2001). This suggests that the Aβ40 present at these time points is not self-associating in small, low-order oligomers. If self-association is occurring only a very small population of Aβ40 is partaking at any

one time. In fact, instead of an increase in cross-linked Aβ40 banding as aggregation proceeded, the reverse was observed. This does not mean that small Aβ40 oligomers do not exist, but supports low order oligomeric Aβ40 being a short-lived entity, directly sequestered into fibrils. The alternative would be Aβ40 forming fibrils without oligomeric intermediates. This would infer early aggregation commencing via linear association of monomers, with subsequent monomers joining the end of the growing chain. This hypothesis is less favoured as evidence implicating other oligomeric Aβ playing a role in the mechanism of toxicity is strong (Chromy et al., 2003; Kayed et al., 2003; Kim et al., 2003; Lambert et al., 1998). However, there is evidence that Aβ40 and Aβ42 may aggregate via different pathways (Bitan et al., 2003a) . Perhaps the longevity of these species in the brain is critical to why Aβ42 is considered more toxic than Aβ40.

PICUP cross-linking of Aβ42 suggested that low order, self-interacting Aβ42 were present prior to cross-linking, in particular dimers. This was the case at 0 and 4 hrs aggregation time. This supports evidence that the Aβ dimer may be an important intermediate species during the aggregation of Aβ42 as it appears to be somewhat conserved during the process of aggregation. Dityrosine dimers have been implicated as playing a critical role in AD pathogenesis and in H_2O_2 generation by the peptide (Barnham et al., 2004; Smith et al., 2007a). In addition, when the samples were cross-linked for 1/90 sec pentamers were observed at 4 hrs which were not seen at 0 hrs. This suggests an increase in stable, low-order Aβ42 species had occurred over the 4 hr aggregation time, which PICUP had then cross-linked.

When the Aβ42 was aggregated for 24 hrs prior to the PICUP cross-linking reaction the only band observed was for the monomer at any cross-linking reaction time. The sequestration of Aβ42 into fibrils by 24 hrs would result in the concentration of low-

order Aβ42 being notably reduced in the solution. The likelihood of these becoming cross-linked by the PICUP reagents would be severely compromised and only monomeric Aβ42 is observed.

The fact remains that, despite dimers appearing to be a significant intermediate during the aggregation of Aβ42 initiated by its self-association, they were not observed when PICUP cross-linking reaction was not permitted due to the lack of light exposure. This means that these dimers may not be the dityrosine dimers that have been implicated in AD pathogenesis (Barnham et al., 2004; Smith et al., 2007a). Dityrosine cross-linked Aβ42 would be SDS-stable, like the PICUP cross-linked Aβ42. Either the dityrosine Aβ42 dimer is at such a low concentration to not be detected by western blot or the dimer-self interactions may be other, weaker interactions, perhaps in dynamic equilibrium with other low-order self-interactions, with dimer the more favourable. It may, in fact be a combination of the two.

The differences between the PICUP cross-linking observed here with Aβ40 and Aβ42, do not necessarily suggest different aggregation pathways, despite the differences between the banding observed. It certainly appears that Aβ42 has a far greater tendency to form the low-order self interactions that may initiate the aggregation process, or at least these interactions are less transient in nature than those of Aβ40 (described in figure 5.12). The increased hydrophobicity of Aβ42 compared to Aβ40 may provide Aβ42 with a greater tendency to self-associate into oligomers and a reduced propensity to disaggregate back to monomers (hence the difficulties with deseeding the peptide). Oligomeric self-interactions are transient in nature for both Aβ40 and Aβ42, but those for Aβ42 appear to be longer-lived, in particular dimers. This supports evidence by Walsh and colleagues who detected only 3 stable Aβ species: dimers, protofibrils and mature fibrils (Walsh et al., 1997).

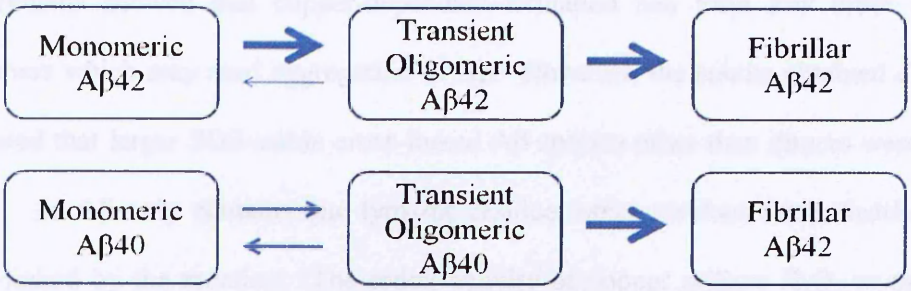

Figure 5.12. The tendency for aggregation of Aβ40 and Aβ42
The formation of early oligomeric Aβ is in dynamic equilibrium with monomers and other Aβ species. The tendency of one Aβ species for forming another is represented by the thickness of the arrow.

Although cross-linked Aβ was generated by PICUP, the species visualised as bands on the gel, comprised a mixture of natural oligomers, cross-linked to become SDS-stable due to their proximity, and unnatural oligomers, those formed by chance. This technique was thoroughly investigated by S. Ma and D. Hou (Lancaster University) to attempt to optimise the cross-linking of natural oligomers and reduce that of unnatural oligomers. However, this was largely unsuccessful and although interesting to use for investigation of Aβ aggregation, these cross-linked species were considered inappropriate for isolation and characterisation.

5.3.2. Copper and H_2O_2 cross-linking

It has been observed that Aβ binds copper, altering the rate of Aβ aggregation (investigated further in chapter 7) (Atwood et al., 1998). The interaction of copper with Tyr10 and histidines of Aβ has also been reported to be linked to the formation of dityrosine cross-links and the initiation of the aggregation process, with this considerably enhanced by the addition of H_2O_2 (Atwood et al., 2004). Due to this evidence, this was initially investigated as a potential way to make dityrosine cross-linked Aβ, so as to specifically characterise its properties.

Experiments showed that copper-dependant oxidation can form low order Aβ40 oligomers which may seed aggregation of Aβ. However, the results obtained clearly indicated that larger SDS-stable cross-linked Aβ species other than dimers were also made. As Aβ only contains one tyrosine residue, other residues were clearly also cross-linked by the reaction. The redox activity of copper utilises H_2O_2 to oxidise susceptible residues in Aβ such as Tyr10 but perhaps also other nucleophilic residues such as Lys16 of Lys28. The oxidised residues then react with another nucleophilic residue forming cross-linked Aβ, in much the same manner as with PICUP. The difference being that copper binds Aβ *in vivo*, in the oxidative atmosphere of the brain, therefore the hope is that this process produces natural oligomers, rather than the mixture of natural and unnatural oligomers generated by PICUP.

Both Aβ40 and Aβ42 required 24 hrs to generate cross-linked Aβ using copper and H_2O_2 yet formation of cross-linked Aβ42 was far more prolific generating a range of multimeric species. Comparison of these results, suggests that the Aβ40 and Aβ42 behave quite differently when subjected to oxidative stress. This difference may be due to several reasons, none of which exclusive of each other:

1. Aβ42 is more susceptible to oxidative stress. The nucleophilic residues are oxidised easier, thus cross-links are enhanced between Aβ molecules.
2. Aβ42 binds copper with different strength compared to Aβ40. This causes the copper to be more effective in oxidising residues in the Aβ primary sequence
3. Aβ42 has a greater propensity for aggregation. Its greater hydrophobic interactions mean Aβ42 molecules are in closer proximity to one another promoting cross-linking.

Regardless, the fact that the levels of oligomer generation by this cross-linking technique correlates with the aggregation speed of the peptides, supports the belief that the species being formed may be natural to the aggregation process. Interestingly though, with Aβ40, where cross-linking was successful, the cross-linking banding pattern appears to follow the banding pattern expected for the random association of monomers set out for PICUP cross-linking. This is in contrast to Aβ42, where a tetramer appears to be the preferred cross-linked species. This may be significant as recently Teplow and colleagues generated synthetic oligomers up to tetramers and found tetramers to be the most toxic to neuronal cell cultures (Ono et al., 2009). In addition, it appears that under these conditions Aβ42 but not Aβ40 can form SDS-stable dimers with the addition of copper alone, perhaps due to Aβ-copper binding stabilising the dimers. These differences between the peptides again, may be due to any or all or the reasons outlined above, yet they reiterate the existence of clear variation between the way Aβ40 and Aβ42 react in an oxidative environment.

5.3.3. HRP and H_2O_2 cross-linking

HRP was a far more efficient method for creating SDS-stable cross-linked Aβ with both Aβ40 and Aβ42 exhibiting cross-linking following only 1 hr incubation but also following 24 hrs incubation, with Aβ42 more so than Aβ40. In addition this banding did not follow the banding pattern for the random association of monomers. In particular, bands at ~45 kDa and 56 kDa appear darker than smaller bands. This implies that the cross-links formed are made because of a natural tendency for the formation of these bonds rather than the random association of monomers during the incubation time. Natural Aβ oligomers may have been generated and stabilised by the cross-linking which may be manipulated to enable the investigation of such oligomers.

Interestingly, when Aβ42 was incubated for 24 hrs at the highest HRP concentration, only a small monomer band remains, just as if Aβ42 had been allowed to aggregate normally and had been consumed into fibrils. This supports the cross-linked Aβ42 species made by HRP and H_2O_2 as being natural intermediates in the aggregation process. The reaction has perhaps prolonged the longevity of these species, effectively increasing their concentration in solution at any given time. Of note, this effect was not seen when copper was used to cross-link Aβ42 for 24 hrs. However, as seen in chapter 7, high concentrations of copper such as those used in these experiments inhibit the aggregation of Aβ, therefore under these conditions the cross-linked oligomers probably do not progress to fibrils.

In contrast, the lower concentrations of HRP tested continued to show some cross-linked species, similar to those observed with 1 hr incubation. As the supply of H_2O_2 for oxidative events would be the limiting factor in generating these cross-links it may be that, with Aβ42, the reaction may have largely gone to completion by 1 hr. If the reaction acts to prolong the longevity of the oligomeric species, the stability instilled in them by the cross-linking may somewhat prevent their sequestration into fibrils. This suggests that the hydrophobicity of Aβ which drives initial self-interactions may cause the formation of highly transient oligomeric species. Yet, in the highly oxidative environment of the brain or due to interaction with metals, in particular copper, these transient species may be stabilised into longer lived, cross-linked species, such as those observed here. This may go some way towards explaining the increased toxicity of Aβ42 as Aβ42 has greater susceptibility to these events.

If the cross-linking events observed with Aβ42 incubated with HRP and H_2O_2 are representative of the key oligomeric species made during aggregation, it is possible to track the possible order of early oligomerisation through the bands observed.

Although in dynamic equilibrium with other species, initially dimers may be formed, followed by tetramers. Dimers and tetramers persist in solution, with pentamers and hexamers forming, presumably due to the addition of a tetramer to either a monomer or dimer respectively. These pentamers/hexamers have been identified previously as the possible toxic Aβ species (so called paranuclei) (Bitan et al., 2003b). This is followed by the appearance of 45 kDa and 56 kDa cross-linked species, perhaps made by the cross-linking of these pentamers and hexamers. The 56 kDa species is of particular interest as it has been reported by Ashe and colleagues as being critical to Alzheimer's development, being present in the brains of transgenic mice (Tg2576) prior to the manifestation of the disease (Lesne et al., 2006).

A selection of amino acid substituted Aβs were tested for their generation of cross-linked species. The key result here was that Y10A-Aβ42 was incapable of forming any cross-linked species indicating that this tyrosine residue is central to the HRP/H_2O_2 cross-linking reaction; the oxidation of this tyrosine is the critical event that permits the cross-link to be formed as it has been shown to be for the formation of di-tyrosine dimers (Barnham et al., 2004; Smith et al., 2007a). However, this tyrosine is not required for thioflavin T fluorescence increases associated with Aβ fibrillisation (figure 4.10) suggesting this may be an oligomer specific event.

The other substituted peptides generated some interesting results largely due to the difference observed with and without TFA-deseeding of the peptides. In chapter 3 it was seen that these substituted peptides were highly aggregated until TFA deseeding was performed. When cross-linking was performed without TFA deseeding prior to use, H13A, H14A and M35N-Aβ42 all presented a band at the 45 kDa position. These were not present in controls with no cross-linking or in the TFA-deseeded cross-linked samples. This suggests that multimers were present in the Aβ solutions

with no TFA-deseeding which subsequent cross-linking stabilised so they were visualised on the blot. Following TFA-deseeding the loss of these higher multimeric bands, in particular the 45 kDa band, show that these substituted peptides have a reduced propensity to form this 45 kDa cross-linked species compared to wt Aβ42. This highlights the need for effective deseeding prior to the use of Aβ peptides for results to be suitably comparable. The presence of varying proportions of pre-aggregated material in the non-TFA treated samples falsely overestimated the propensity of the Aβ42 amino acid substituted peptides for formation of cross-linked oligomers via this method. However, the presence of this 45 kDa band in non-TFA treated Aβ samples, which are effectively partially aggregated, shows that they do have some tendency to form this cross-linked Aβ species. In addition, the reduction in cross-linking of these samples compared to wt Aβ42 suggests that His13A, His14A and Met35 influence the cross-linking of Aβ via oxidation by HRP and H_2O_2, although not critically like Tyr10, possibly due to altered Aβ metal binding properties.

Aβ42 was the only peptide to retain its tendency to form these cross-linked multimers following its deseeding with TFA. This may be connected to the increased toxicity of this peptide compared to the toxicity observed with the other peptides (Barnham et al., 2004; Smith et al., 2010; Varadarajan et al., 1999). The increased HRP/H_2O_2 mediated cross-linking that occurs with Aβ42 compared to the other Aβ peptides, indicates that Aβ42 is more susceptible to oxidative attack that generates cross-linked oligomers. This may be a decisive event in the formation of toxic oligomers.

5.4. Conclusions

- Three potential methods of cross-linking have been investigated in an attempt to create stable oligomeric Aβ species that could be tested for their ability to generate H_2O_2
- PICUP appeared to mainly generate randomly cross-linked Aβ randomly rather than "fixing" the natural oligomeric species formed during aggregation
- With copper and H_2O_2 Aβ42 became cross-linked with preference for tetramers
- With HRP and H_2O_2 Aβ peptides showed some tendency to form larger multimers at ~45 and 56 kDa
- Aβ42 showed the greatest propensity of all the peptides tested to form cross-linked oligomers
- Aβ42-Y10A showed no cross-linked species indicating this tyrosine to be critical in the formation of covalent Aβ-Aβ bonds via this method.
- The susceptibility of the Aβ peptides tested to the oxidative modifications driving the covalent cross-linking may be directly linked to their ability to form of toxic oligomers.
- The ability to generate these cross-linked Aβ species will hopefully permit their capacity for H_2O_2 generation to be tested
- Further testing and characterization of these low-order oligomers, might allow identification of the particular species responsible for neurotoxicity

Chapter 6
Development of a technique to immobilise Aβ

6.1. Introduction

The experiments described within this chapter aimed to develop a technique to primarily enable quantification of H_2O_2 generation from Aβ at different stages of its aggregation. Much of the evidence thus far supported indications that H_2O_2 was generated in a catalytic manner by a particular type of small oligomeric species. Nonetheless, the ever-changing quaternary structure of Aβ in solution makes elucidation of the Aβ species responsible for H_2O_2 generation seemingly unachievable. However, the idea arose that if a solution of Aβ was prevented from aggregating whilst these H_2O_2 generating species were present, it should still generate H_2O_2. With this in mind, the method of immobilising Aβ on the mAb 6E10 was developed (depicted in figure 6.1). This antibody binds Aβ with strong affinity and has been shown to prevent Aβ from further aggregation (Taylor et al., 2003). Using it to capture Aβ at various stages of its aggregation was hoped to provide a "snapshot" of oligomeric species present at any given moment.

This idea was developed through many stages to try to optimise the protocol. The initial results described show some of that developmental process. The method has not been fully finalised. However, the best method to date has been used to look at the ability of Aβ42 at different stages of aggregation to generate and also degrade H_2O_2. Additionally, this method has been utilised to test Aβ42 substituted peptides and also the HRP/H_2O_2 cross-linked Aβ generated in chapter 5.

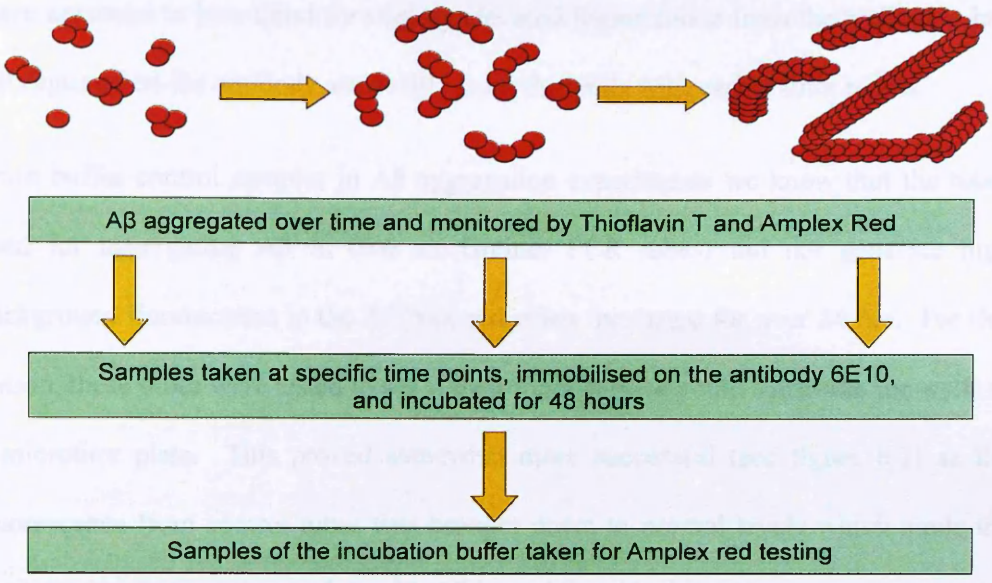

Figure 6.1. Schematic of the method rational for immobilisation of Aβ for determination of H_2O_2 generation

6.2. Results

6.2.1. Initial development of immobilisation of Aβ

The first attempt at immobilisation of Aβ utilised Iwaki Maxisorb 96 well microtitre plates coated with mAb 6E10. Aβ was aggregated for different times and then incubated on the 6E10 to capture it. Once captured it was washed with 10 mM PB x 3 then incubated in more PB for 24 or 48 hrs. The PB was then removed from the wells and its H_2O_2 concentration determined by Amplex red. This technique proved unsuccessful as the plates themselves were designed for maximum antibody binding and not for the long incubation times we needed. Consequently, the treatment on the surface of the wells generated hugely inflated background fluorescence readings in the Amplex red assay. This created problems when trying to decipher a small positive signal above the large background fluorescence due to the size of the errors. Other plates were tested but all carried the same problem. However, throughout this testing,

there appeared to be a trend for slightly elevated fluorescence from the wells that had Aβ captured on the antibody, especially from the wells with earlier time points.

From buffer control samples in Aβ aggregation experiments we knew that the tubes used for aggregating Aβ in (0.6 ml Greiner PCR tubes) did not generate high background fluorescence in the Amplex red when incubated for over 24 hrs. For this reason, these tubes were tested to see if their inner surface could substitute for wells of a microtitre plate. This proved somewhat more successful (see figure 6.2) as the fluorescence from control tubes was brought down to normal levels which made the positive signals from those tubes with Aβ immobilised inside clearer.

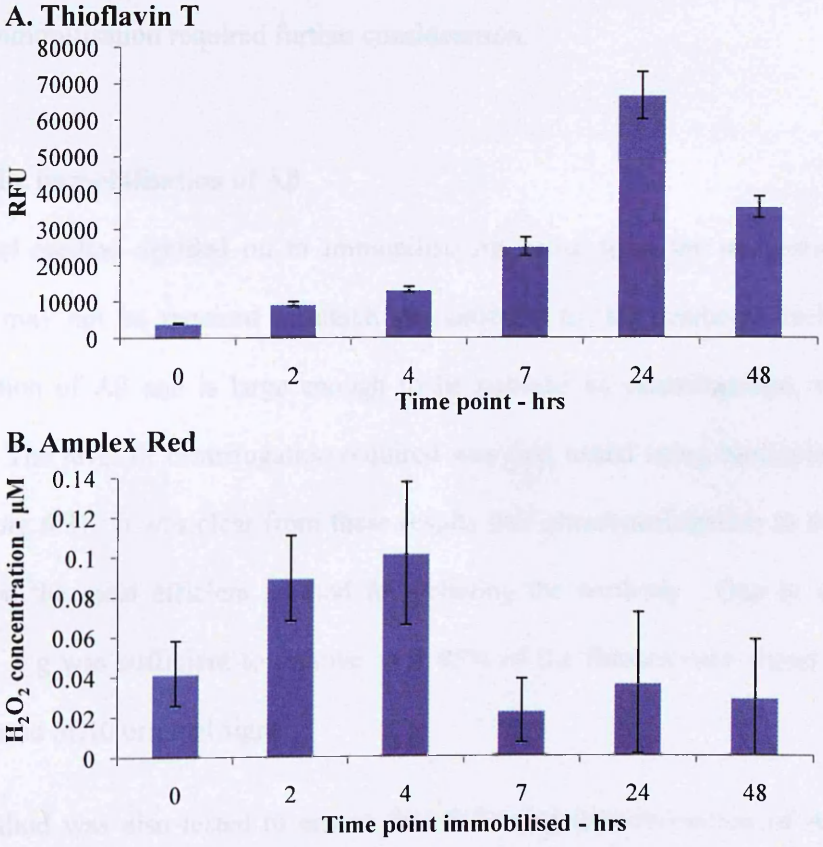

Figure 6.2. H_2O_2 generation from immobilised Aβ42
25 µM Aβ42 was aggregated over 48 hrs in 10 mM PB, pH 7.4 at 37°C. At various time points during the aggregation process samples of the Aβ42 solution was taken and incubated in 0.6 ml tubes, pre-coated with 6E10 to capture a "snapshot" of the oligomeric species present. The tubes were then washed with 3 x 10 mM PB then incubated for 48 hrs in PB. This buffer was then assessed for its H_2O_2 concentration by Amplex red. A = Thioflavin T fluorescence, B = H_2O_2 generated from immobilised Aβ42 from each of the time points. Results are means ± S.D (n=3)

Not only were positive fluorescence signals observed but the earlier time points of 2 and 4 hrs Aβ42 incubation appeared to generate more H_2O_2 than the other time points. This data supported our hypothesis that early Aβ species prevented from further aggregation retained the ability to generate H_2O_2. However, the concentration of H_2O_2 generated was very low (~100 nM) and the errors associated with the experimental procedure considered too large. The quantity of Aβ captured by the antibody needed optimisation. We tried maximising the surface area to volume ratio using dynabeads: small magnetic beads that could be coated with 6E10 inside the tubes. This was successful to a degree with 0.5 μM H_2O_2 generated from Aβ42 aged for 1 hr, yet was excessively costly for the samples we wanted to test so development of Aβ immobilisation required further consideration.

6.2.2. The immobilisation of Aβ

The final method decided on to immobilise Aβ came from the suggestion that a surface may not be required to attach the antibody to: the antibody itself inhibits aggregation of Aβ and is large enough to be pelleted by centrifugation, when Aβ-bound. The level of centrifugation required was first tested using biotinylated-6E10 (see figure 6.3). It was clear from these results that ultracentrifugation in the airfuge would be the most efficient method for pelleting the antibody. One hr at approx 136,000 x g was sufficient to remove over 95% of the fluorescence signal from the biotinylated 6E10 original signal.

The method was also tested to ensure that following immobilisation of Aβ on the antibody, the Aβ was also centrifuged down into a pellet. Aβ42 was pre-aggregated for 3 hrs, immobilised for 2 hrs then centrifuged in the airfuge for 3 hrs to ensure maximum recovery of Aβ in the pellet. Thioflavin T results indicated this was

successful (see figure 6.4) with fluorescence in the supernatant approaching PB levels and almost complete recovery of the fluorescence signal in the resuspended pellet.

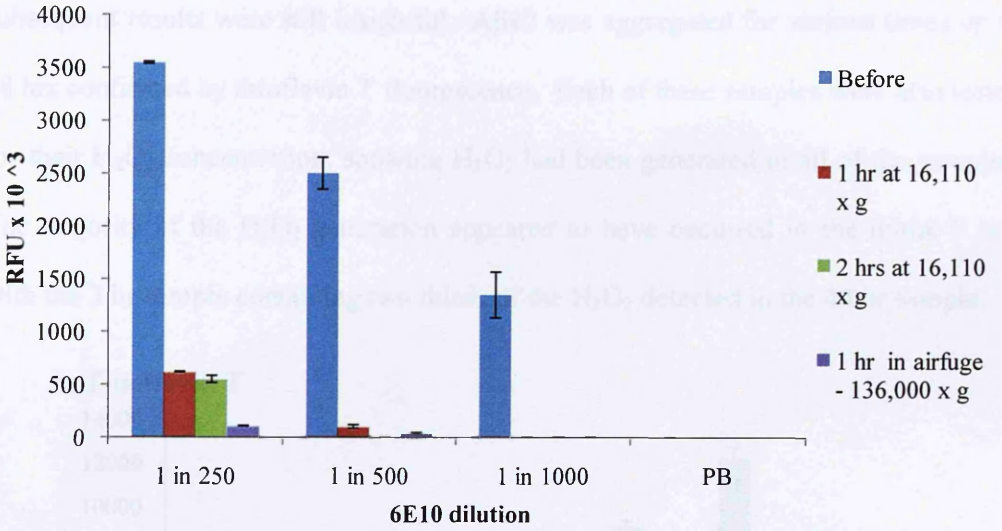

Figure 6.3. The centrifugation of biotinylated 6E10
A range of biotinylated 6E10 dilutions were made in 10 mM PB. These were then centrifuged for 1 or 2 hrs at 16,110 x g and also for 1 hr in the airfuge at approx. 136,000 x g. 3 x 100 µl samples were taken before and after centrifuge steps and coated onto a clear 96 well Maxisorb microtitre plate. The level of antibody present in the sample was then detected using streptavidin-Europium detection used for the oligomeric immunoassay. Results are means ± S.D (n=4)

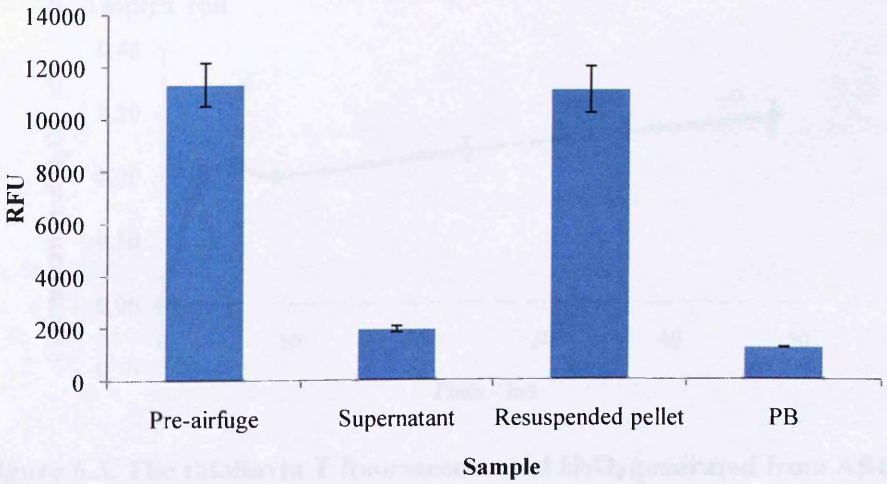

Figure 6.4. The ultracentrifugation of immobilised Aβ42
50 µM Aβ42 was aggregated in 10 mM PB at 37°C for 3 hrs. The mAb 6E10 was then added to the solution to a final concentration of 1 µg/ml and incubated for 2 hrs to allow antibody binding, then placed in the airfuge and spun at approx 136,000 x g for 3 hrs. Samples were taken for thioflavin T fluorescence determination prior to adding the antibody, from the supernatant and resuspended pellet and control PB samples. Results are means ± S.D (n=3)

Following the 3 hrs centrifugation the sample holder felt warm. To avoid any sample heating the time for centrifugation was reduced to 90 mins. However, this impeded recovery of the immobilised Aβ42 substantially (figure 6.5A). Despite this, the subsequent results were still insightful. Aβ42 was aggregated for various times up to 48 hrs confirmed by thioflavin T fluorescence. Each of these samples were also tested for their H_2O_2 concentration, showing H_2O_2 had been generated in all of the samples. The majority of the H_2O_2 generation appeared to have occurred in the initial 3 hrs, with the 3 hr sample containing two thirds of the H_2O_2 detected in the 48 hr sample.

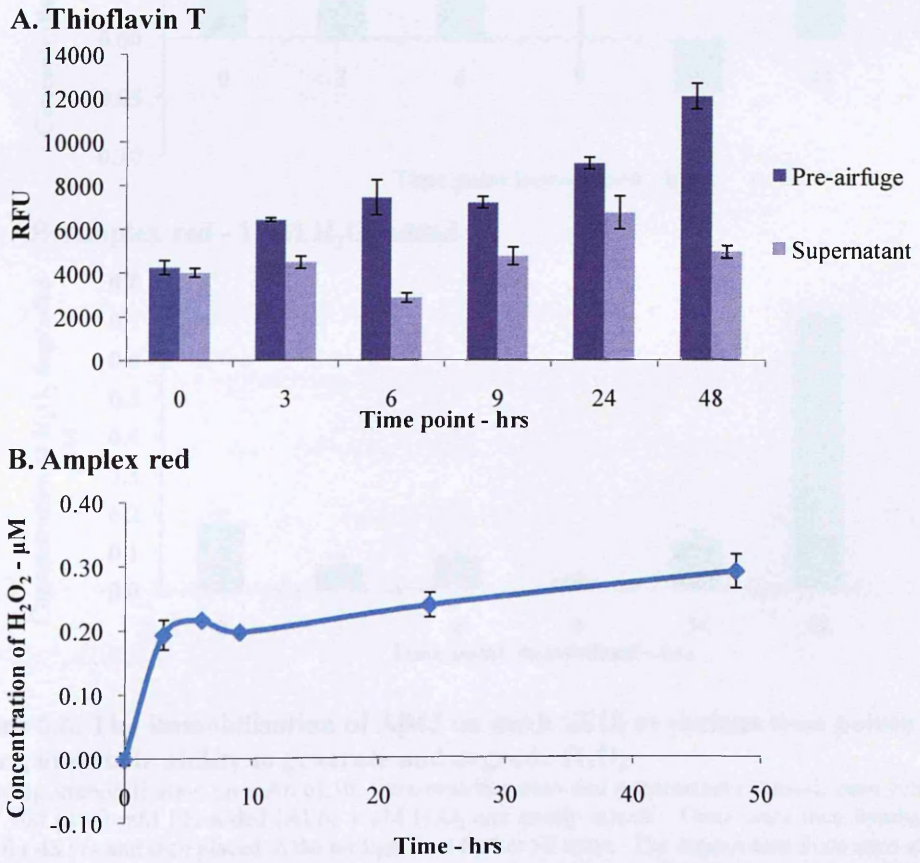

Figure 6.5. The thioflavin T fluorescence and H_2O_2 generated from Aβ42 samples at various time points over 48 hrs, prior to immobilisation of on mAb 6E10

300 µl of 25 µM Aβ42 in 10 mM PB was incubated at 37°C for the appropriate length of time, set off in reverse order so they would all be ready for immobilisation at the same time. 100 µl was removed from each tube and tested for its fluorescence in both the thioflavin T assay (A) and Amplex red (B). 2 µl mAb 6E10 was then added to the remaining 200 µl of each sample and incubated for 2 hrs at 37°C to allow antibody binding. Samples were then placed in the airfuge and spun for 90 mins at ~136,000 x g. The supernatant was removed and thioflavin T fluorescence determined (A). Results are means ± S.D (n=3)

Following immobilisation of the peptide and centrifugation in the airfuge this H_2O_2 was removed in the supernatant. Fresh 10 mM PB was added to one set of samples, and to another set of samples 1 μM H_2O_2 was added. These were then incubated for 24 hrs at 37°C. The results obtained from this can be seen in figure 6.6.

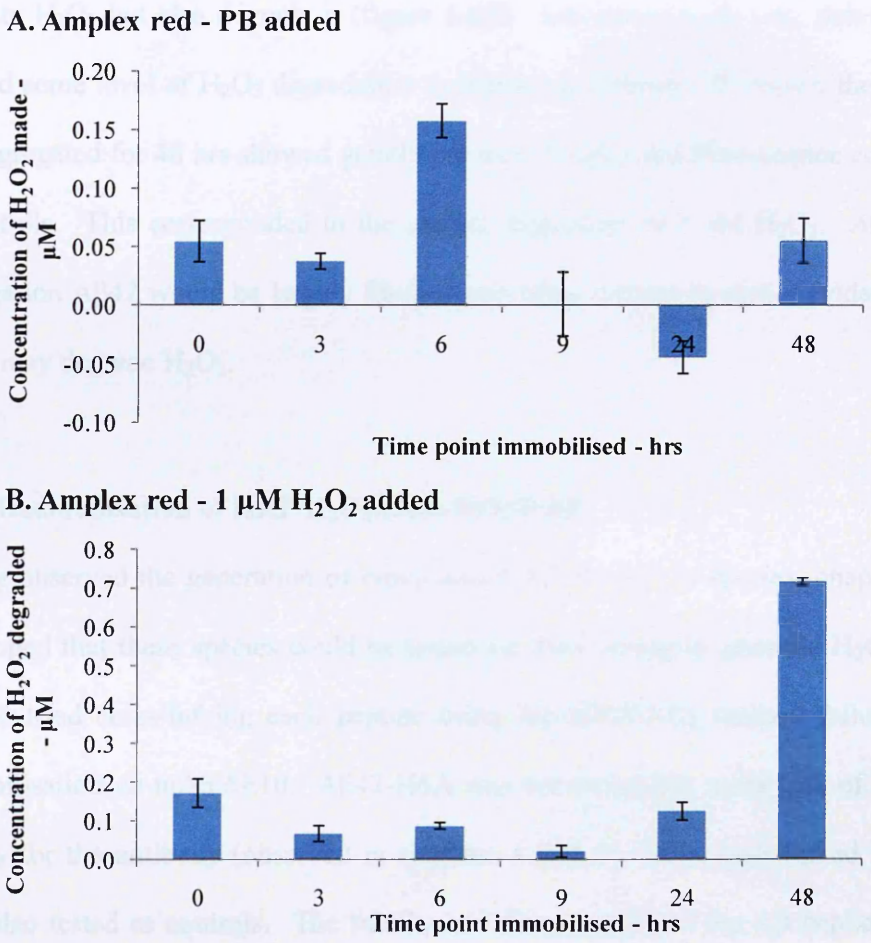

Figure 6.6. The immobilisation of Aβ42 on mAb 6E10 at various time points over 48 hrs, and their ability to generate and degrade H_2O_2

Following immobilisation on mAb 6E10, ultra-centrifugation and supernatant removal, each tube had either 100 μl 10 mM PB added (A) or 1 μM H_2O_2 and gently mixed. These were then incubated at 37°C for 48 hrs and then placed in the airfuge for a further 90 mins. The supernatant from each sample was then tested for its H_2O_2 concentration using the Amplex red assay. Results are means ± S.D (n=3)

Generation of H_2O_2 into the fresh PB was low, probably a direct consequence of the lack of recovery of the immobilised peptide following centrifugation. The greatest Amplex red signal was observed from the sample incubated for 6 hrs and

corresponded to ~150 nM of H_2O_2. Although this method requires further development, the errors associated with the data had been substantially reduced from earlier methods.

H_2O_2 was added to the Aβ42 samples to investigate the idea that Aβ may not only generate H_2O_2 but also degrade it (figure 6.6B). Interestingly, all time points tested showed some level of H_2O_2 degradation compared to controls. However, the sample pre-aggregated for 48 hrs showed greatly reduced Amplex red fluorescence compared to controls. This corresponded to the sample degrading ~0.7 μM H_2O_2. At 48 hrs aggregation Aβ42 would be largely fibrillar providing support to earlier evidence that fibrils may degrade H_2O_2.

6.2.3. Immobilisation of HRP/H_2O_2 cross-linked Aβ

Having observed the generation of cross-linked Aβ oligomeric species (chapter 5) it was hoped that these species could be tested for their ability to generate H_2O_2. For this we tried cross-linking each peptide using the HRP/H_2O_2 method followed by immobilisation on mAb 6E10. Aβ42-H6A was not tested due to its lack of binding affinity for the antibody (observed in chapters 4 and 5). Non cross-linked samples were also tested as controls. The thioflavin T fluorescence of the Aβ peptides with and without cross-linking showed an increase in fluorescence when all the peptides were cross-linked (figure 6.7). This indicated that the cross-linking had been successful. However, of interest was the observation that Aβ42-Y10A showed an increase in thioflavin T fluorescence, considering that no stable cross-linked multimers were observed on western blots from this peptide.

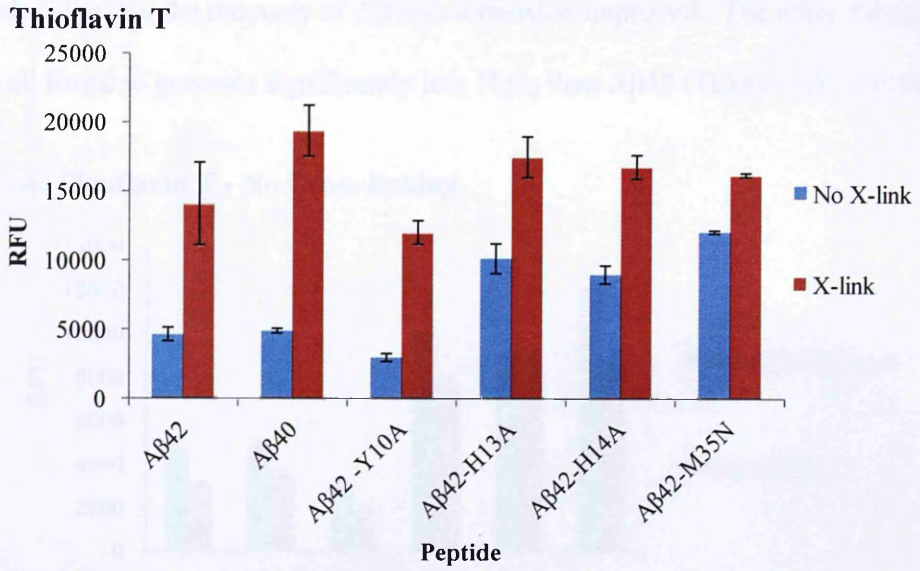

Figure 6.7. Thioflavin T of cross-linked and non cross-linked Aβ peptides
75 μM of each Aβ peptide was prepared in 10 mM PB and split into 2 samples, 1 to be cross-linked, the other as a non-cross-linked control. To the cross-linked sample HRP and H_2O_2 was added to the Aβ to final concentrations of 100 U/ml, 100 μM and 25 μM respectively in 10 mM PB. To the non cross-linked samples 10 mM PB was added to the peptide to bring it to 25 μM. All samples were incubated at 37°C for 1 hr at which point samples were taken for thioflavin T fluorescence determination. Graph compares fluorescence obtained from cross-linked (X-link) and non cross-linked (no X-link) before immobilisation. Results are means ± S.D (n=3)

Following incubation of the Aβ peptides in either cross-linking or non-cross-linking conditions for 1 hr at 37°C the peptides were immobilised by addition of the antibody for 2 hrs and then centrifuged in the airfuge for 2 hrs. Thioflavin T fluorescence was measured prior to immobilisation and then from the supernatant following centrifugation. This again suffered from poor retrieval of peptide following centrifugation, although the extra 30 minutes did appear to recover a greater amount of non cross-linked Aβ42 than in the previous experiment (see figure 6.8). After 24 hrs incubation at 37°C in fresh 10 mM PB, the H_2O_2 generated from the immobilised, non cross-linked samples, was measured (see figure 6.9). The amount of H_2O_2 generated from the Aβ42 sample was greatly improved from the previous experiment, with over 400 nM H_2O_2 being generated over 24 hrs. This supports the thioflavin T

data showing that the recovery of Aβ was somewhat improved. The other Aβ peptides were all found to generate significantly less H_2O_2 than Aβ42 (Tukey HSD, $p \leq 0.000$).

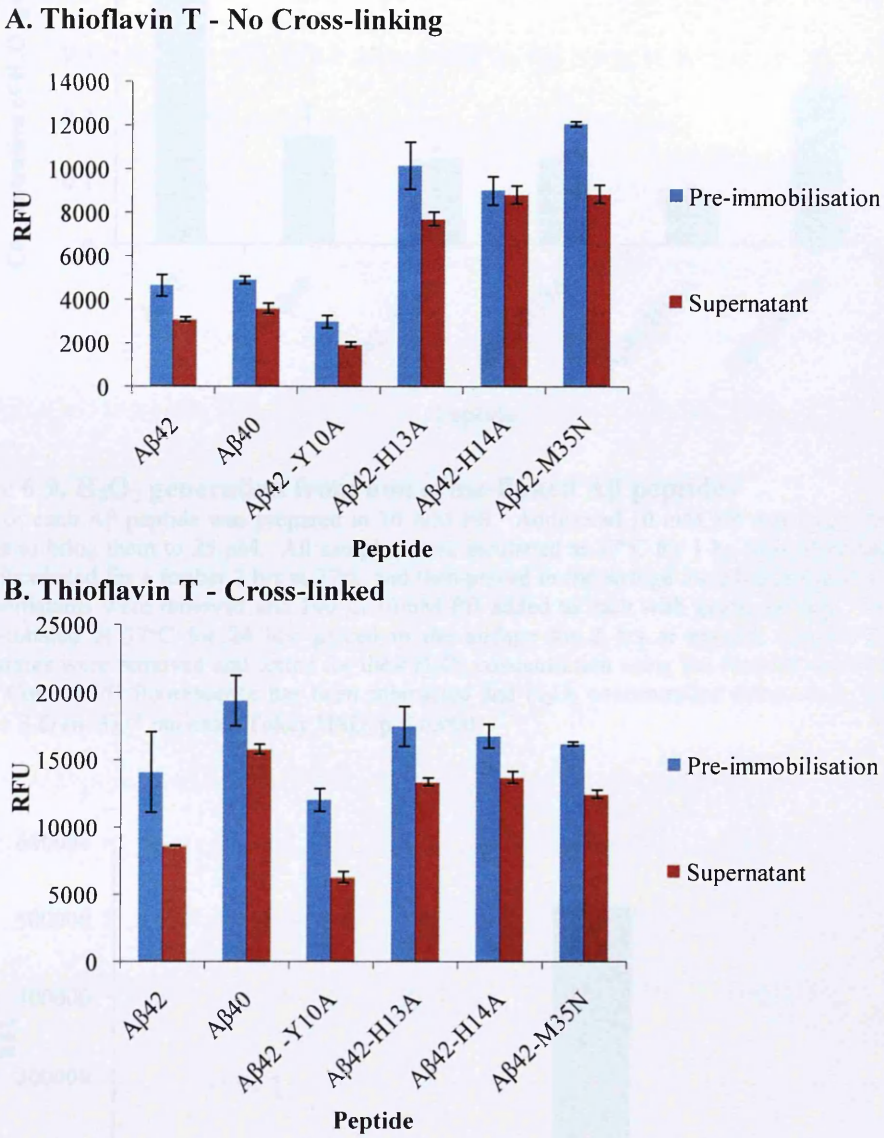

Figure 6.8. Thioflavin T of cross-linked and non cross-linked Aβ peptides before and after ultracentrifugation

75 μM of each Aβ peptide was prepared in 10 mM PB and split into 2 samples, 1 to be cross-linked, the other as a non-cross-linked control. To the cross-linked sample HRP and H_2O_2 was added to the Aβ to final concentrations of 100 U/ml, 100 μM and 25 μM respectively in 10 mM PB. To the non cross-linked samples 10 mM PB was added to the peptide to bring it to 25 μM. All samples were incubated at 37°C for 1 hr, then 6E10 added at 10 μg/ml and incubated for a further 2 hrs at 37°C and then placed in the airfuge for 2 hrs at approx 136,000 x g. Samples were taken for thioflavin T fluorescence determination prior to addition of the 6E10 and from the supernatant following ultracentrifugation. A = Non cross-linked samples, B = Cross-linked samples. Results are means ± S.D (n=3)

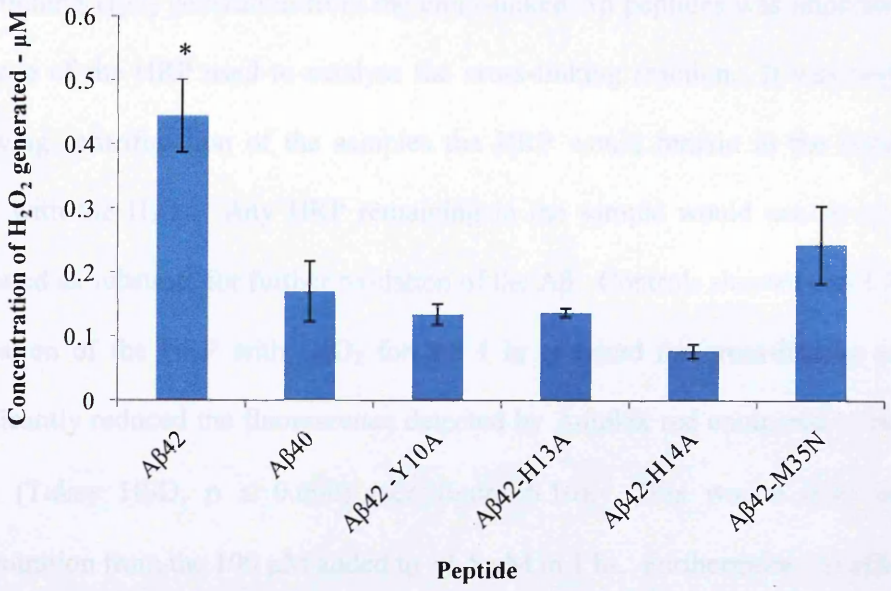

Figure 6.9. H_2O_2 generation from non cross-linked Aβ peptides

75 µM of each Aβ peptide was prepared in 10 mM PB. Additional 10 mM PB was then added to the peptides to bring them to 25 µM. All samples were incubated at 37°C for 1 hr, then 6E10 added at 10 µg/ml, incubated for a further 2 hrs at 37°C and then placed in the airfuge for 2 hrs at approx 136,000 x g. Supernatants were removed and 100 µl 10mM PB added to each with gentle mixing. These were then incubated at 37°C for 24 hrs, placed in the airfuge for 2 hrs at approx. 136,000 x g. The supernatants were removed and tested for their H_2O_2 concentration using the Amplex red fluorescence assay. Control PB fluorescence has been subtracted and H_2O_2 concentration determined. Results are means ± S.D (n=3), * indicates Tukey HSD, $p \leq 0.000$.

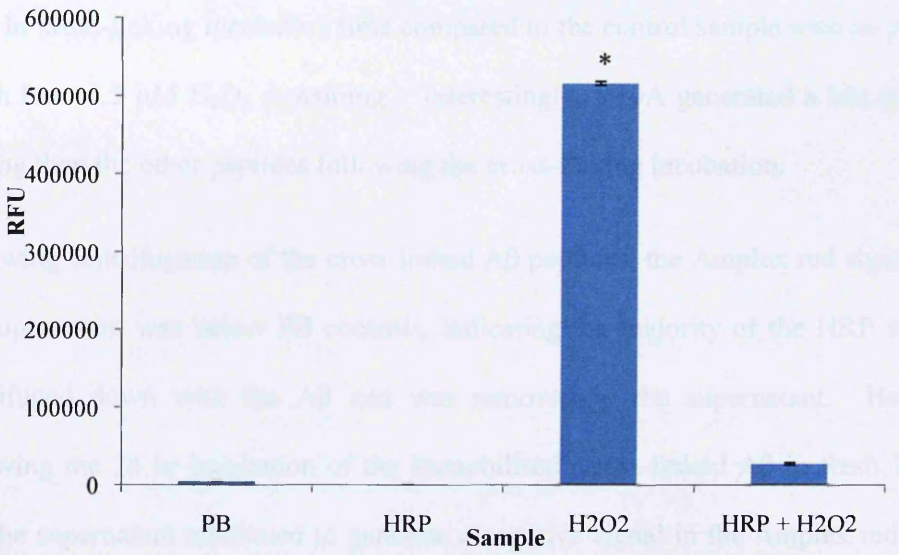

Figure 6.10. Amplex red fluorescence from control samples before immobilisation

Control samples were prepared to contain 10 mM PB, 100 U/ml HRP, 100 µM H_2O_2 and both HRP and H_2O_2, all in 10 mM PB. These were incubated at 37°C for 1 hr and then tested for their fluorescence in the Amplex red assay. Results are means ± S.D (n=3), * indicates Tukey HSD, $p \leq 0.000$.

Determining H_2O_2 generation from the cross-linked Aβ peptides was impeded by the presence of the HRP used to catalyse the cross-linking reaction. It was hoped that following centrifugation of the samples the HRP would remain in the supernatant along with the H_2O_2. Any HRP remaining in the sample would use up any H_2O_2 generated as substrate for further oxidation of the Aβ. Controls showed that following incubation of the HRP with H_2O_2 for the 1 hr required for cross-linking to occur significantly reduced the fluorescence detected by Amplex red compared to the H_2O_2 alone (Tukey HSD, $p \leq 0.000$) (see figure 6.10). This was a drop in H_2O_2 concentration from the 100 μM added to ~1.5 μM in 1 hr. Furthermore, the HRP in 10 mM PB after the 1 hr incubation had ~30% of the fluorescence from PB alone.

The presence of HRP in the Aβ samples was also be seen in the Amplex red data from the pre-immobilised samples but also from the supernatants following centrifugation of the samples (see figure 6.11). This showed all the Aβ samples to have negative H_2O_2 readings following cross-linking having used up all of the 100 μM H_2O_2 during the 1 hr cross-linking incubation time compared to the control sample with no peptide, which has ~1.5 μM H_2O_2 remaining. Interestingly, Y10A generated a less negative reading than the other peptides following the cross-linking incubation.

Following centrifugation of the cross-linked Aβ peptides, the Amplex red signal from the supernatant was below PB controls, indicating the majority of the HRP was not centrifuged down with the Aβ and was removed in the supernatant. However, following the 24 hr incubation of the immobilised, cross-linked Aβ in fresh 10 mM PB, the supernatant continued to generate a negative signal in the Amplex red assay. This indicated that some HRP had remained in the sample. In fact, the signal becomes more negative in both the peptide samples and controls. Unfortunately, this means that attempts to determine whether cross-linked Aβ was able to generate H_2O_2 were

unsuccessful. If any had produced any H_2O_2, it would have been mopped up by the presence of the small amount of HRP.

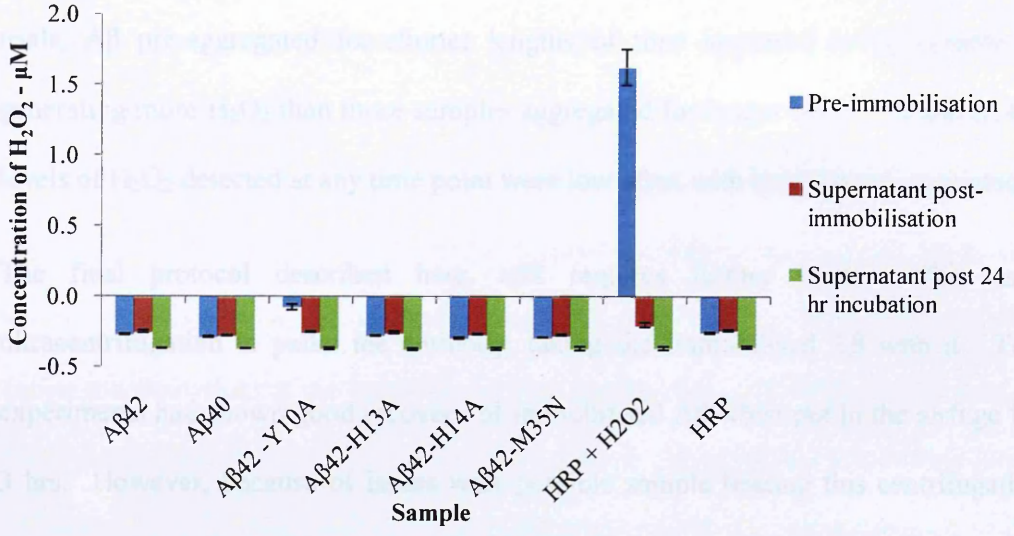

Figure 6.11. H_2O_2 generation from cross-linked and immobilised Aβ peptides
75 µM of each Aβ peptide was prepared in 10 mM PB. HRP and H_2O_2 were added to the Aβ to final concentrations of 100 U/ml, 100 µM and 25 µM respectively in 10 mM PB. All samples were incubated at 37°C for 1 hr, then 6E10 added at 10 µg/ml, incubated for a further 2 hrs at 37°C and then placed in the airfuge for 2 hrs at approx 136,000 x g. Supernatants were removed and 100 µl 10mM PB added to each with gentle mixing. These were then incubated at 37°C for 24 hrs, placed in the airfuge for 2 hrs at approx. 136,000 x g. Samples were taken prior to adding 6E10 and from the supernatants following both centrifuge steps and tested for their H_2O_2 concentration using the Amplex red fluorescence assay. Control PB fluorescence has been subtracted and H_2O_2 concentration determined. Results are means ± S.D (n=3)

6.3. Discussion

To investigate the ability of different stages of Aβ aggregation for H_2O_2 generation the idea of immobilising Aβ was developed. This was based on the hypothesis that if a specific form of Aβ was responsible for the generation of H_2O_2, then a solution of Aβ containing this species would still generate H_2O_2 if prevented from aggregating. Capturing Aβ at different times during its aggregation using the mAb 6E10 was attempted in several manners and the development of this technique is still in

progress. The largest obstacle has been optimising the amount of Aβ captured by the antibody and various surfaces were tested to optimise Aβ immobilisation: microtitre plates, PCR tubes, nitrocellulose membrane and dynabeads. Consistently during these trials, Aβ pre-aggregated for shorter lengths of time appeared to be capable of generating more H_2O_2 than those samples aggregated for longer times. However, the levels of H_2O_2 detected at any time point were low often with large errors associated.

The final protocol described here, still requires further work. This used ultracentrifugation to pellet the antibody, taking the immobilised Aβ with it. Test experiments had shown good recovery of immobilised Aβ when put in the airfuge for 3 hrs. However, because of issues with possible sample heating this centrifugation time was reduced to 90 mins for the immobilisation of different aggregation time points of Aβ yet this was detrimental to sample recovery. Recovery was improved by increasing the time to 2 hrs (see figure 6.5A T=0 compared to figure 6.8A Aβ42) nonetheless, this aspect requires improvement. A chilled centrifuge was considered. However, placing the airfuge in the cold room may still allow the sample holder to warm somewhat overtime and condensation within the air pipes should be avoided. A chilled centrifuge was tried overnight at ~16,000 x g but Aβ recovery was poor. Increasing the concentration of 6E10 may be useful or perhaps using a polyclonal antibody for Aβ instead of 6E10. This would allow more cross-linking of the antibodies with the Aβ, making larger complexes that should sediment easier.

When Aβ aggregated for different lengths of time were immobilised by this method, the recovery of peptide was low. In addition, without a reliable method of calculating the concentration of Aβ in solution, that isn't affected by the aggregation state of the peptide (which would obviously be an issue here) no quantification of recovery rate can be calculated. Although thioflavin T fluorescence was measured, this serves only

as a guide as it is dependent on both concentration and aggregation state of the peptide. It was hoped that the high recovery rate observed in the test conditions would be replicated, in which case samples at each time point could have been directly compared. However, as it stands, the results obtained for H_2O_2 generation by each time point immobilised may reflect the amount of Aβ recovered after ultracentrifugation rather than differences in the type of Aβ present and its H_2O_2 generating ability. However unsuccessful this experiment was in some ways, it is very close to becoming a useful technique. The error bars are far reduced from the earlier manifestations of the protocol and the fact that H_2O_2 generation is still detected supports the hypothesis that a specific form of early Aβ species is responsible for its formation. Much improvement is obviously required but if a technique such as this could help in identifying the oligomer/oligomer population that generates the H_2O_2, it may provide a specific target for potential therapeutics. It could also determine whether potential aggregation inhibitors also reduce these earlier potentially toxic species. In addition, much aggregation inhibitors/potential therapeutics cannot be assessed for their effect on H_2O_2 generation by Aβ due to adverse reactions between them and the reagents used. This technique enables this as, theoretically, the test agent is washed off with only the Aβ species remaining.

All Aβ42 time points tested also showed some ability in aiding H_2O_2 degradation compared to controls. This indicates that throughout the aggregation process there are Aβ species present that are susceptible to oxidation by low levels of H_2O_2. This indicates that the H_2O_2 concentration measured from solutions of Aβ is the net quantity of that being generated and degraded, possibly with different Aβ species being responsible for the opposing actions. In fact, if oxidation of Aβ is an oligomeric stabilising event, as proposed in chapter 5, the reduction of H_2O_2 by the immobilised

Aβ may have been due to such events. Aβ42 aggregated for 48 hrs showed the largest difference, with over 70% of the H_2O_2 added degraded. At this time point it can be assumed that the large majority of the Aβ42 has been sequestered into fibrils, indicating that fibrils may be particularly susceptible to oxidative damage from the H_2O_2, promoting its degradation within the solution. There are many ways in which elevated H_2O_2 may induce oxidative modification of Aβ. Carbonyl adducts, histidine loss and dityrosine cross-links, appear to cause a raised resistance of Aβ to proteases (Lynch et al., 2000). Several other oxidative modifications of tyrosine are possible; DOPA, dopamine and dopamine quinine adducts have been extracted from AD plaques (Ali et al., 2004). Other modifications to Aβ found within senile plaques include Met35 oxidation (discussed in 4.3.3.4) and 2-oxo-histidine (Atwood et al., 2000a). This may point towards mature fibril and plaque formation being a protective mechanism against oxidative stress, being a "sink" for oxidative modification.

Although immobilisation of Aβ has shown H_2O_2 generation from Aβ prevented from further aggregation, the Aβ species immobilised remain heterogeneous. This means that the species responsible for the H_2O_2 generation still cannot be identified. It was put forward that maybe one, or several of the cross-linked species generated in chapter 5 may actually be responsible. For this reason Aβ peptides were cross-linked with HRP and H_2O_2 as described in chapter 5 and immobilised to try to determine H_2O_2 generation from these species. Interestingly, thioflavin T results from these samples showed increased fluorescence from all of the cross-linked samples compared to their non cross-linked counterparts, including Aβ42-Y10A. This peptide showed no cross-linked species on SDS-gels yet this thioflavin T data suggests otherwise. It is therefore posited that cross-links are made by the oxidation of Aβ42-Y10A by HRP

and H_2O_2. However, without the tyrosine residue partaking in the cross-link, they are unstable in the reducing conditions of the SDS-gel.

Recovery of the immobilised Aβ was marginally improved compared to the Aβ time course experiment due to increasing the time for centrifugation (figures 6.5 and 6.6). In support of this, results with the non cross-linked samples showed Aβ42 to generate approximately 3 times the highest level of H_2O_2 obtained when Aβ42 had been immobilised at different aggregation time points. Although there may have been different rates of peptide recovery of the substituted peptides, it is interesting to note that H_2O_2 generation was detected in all the samples, yet all reduced in comparison to wt Aβ42, supporting earlier observations that none of the substituted residues tested are pre-requisites for H_2O_2 generation.

Unfortunately, the presence of the HRP used to generate the cross-links consequently eliminated the ability to determine the H_2O_2 generation from the cross-linked oligomers. Although the majority of it remained in the supernatant following ultracentrifugation of the samples, enough remained to remove any H_2O_2 potentially made by the Aβ. In fact the presence of the HRP brings fluorescence below control levels. As HRP is one of the components of the Amplex red working solution, this was first thought to be possibly due to altering the reaction dynamics. However, the fact that the negative signal further decreases following the 24 hr incubation indicates the HRP remaining continues to use up all the residual oxidising power from the buffer. The issues with HRP here may be able to be overcome if recovery of Aβ could be improved sufficiently to permit the addition of an immobilised-Aβ washing step into the protocol. This would hopefully remove any residual HRP thus allowing H_2O_2 generation from the cross-linked peptides to be determined.

Another possibility that has been investigated is the use of cerium chloride to visualise H_2O_2 generation from the cross-linked species separated by gel electrophoresis (Seitz et al., 1991). This was investigated using L-AAO supplied with an L-AA in the wash solution, and found to generate H_2O_2 from within the gel matrix forming a band on the gel. This was developed to improve its sensitivity for H_2O_2 as I have found Aβ to generate only a very small level of H_2O_2. However, the experiments for this are yet to be completed with Aβ and will require careful consideration of whether non-reducing conditions should be employed and also whether a sufficient quantity of Aβ can be loaded onto a gel to get a signal from.

Although this experiment was unsuccessful at its objective, the fact that Aβ42-Y10A appeared to be less susceptible to oxidative attack by H_2O_2 is of interest. In other words, Tyr10 is the prime target for oxidative modification of Aβ42 (supporting other research (Atwood et al., 2000a)). And, as has been observed, this modification is critical for the generation of SDS-stable cross-linked Aβ multimers. The oxidative nature of neuronal cells supports the idea that oxidation of this residue may be a key step in the initiation of aggregation of the peptide in the brain.

6.4. Conclusions

- A protocol was developed to enable immobilization of Aβ aggregates for determination of their ability to generate H_2O_2
- Testing of Aβ samples taken during its aggregation consistently showed Aβ immobilized earlier in its aggregation generated more H_2O_2 than later time points

- The time point corresponding to mature Aβ fibrils showed increased H_2O_2 degradation compared to other time points
- The observation of H_2O_2 degradation as well as generation indicates that the measured concentration of H_2O_2 from a solution of Aβ can be considered the net concentration, perhaps with different Aβ species responsible for its generation and degradation
- When immobilized, Aβ42 generates more H_2O_2 than Aβ40 and the other Aβ42 amino acid substituted peptides (Y10A, H13A, H14A and M35N)
- Aβ42-Y10A forms cross-links using HRP/H_2O_2 detectable by thioflavin T fluorescence increases yet these are not SDS-stable
- H_2O_2 generation could not be determined from cross-linked Aβ samples due to a small amount of HRP remaining in the sample. Improving peptide recovery may enable this testing as washing of the immobilized Aβ may be possible
- Tyr10 was identified as possibly the prime target for oxidative modification of Aβ42, which may be key for stabilization of early oligomeric Aβ
- This method still requires further work especially in respect of peptide recovery

Chapter 7
The effect of metal ions on H_2O_2 generation by β-amyloid

7.1. Introduction

Metal ions are a key contributor to pathogenesis of AD, having clear involvement in promoting Aβ aggregation and ROS generation, both of which are central pathological events in disease development. The brain has complex systems to regulate metal ion metabolism; although vital to enzymatic and structural protein functions, their potential for redox reactions needs to be tightly controlled to prevent oxidative damage to cellular components (Hureau and Faller, 2009).

7.1.1. Metal ions in AD

The biometals copper (Cu), iron (Fe) and zinc (Zn) have been widely implicated in the pathogenesis of AD. The brain shows an age-dependant concentration of Cu, Fe and Zn in the neocortex (Huang et al., 2004) and strong signals for these metals are observed in a typical senile plaque (see figure 7.1) (Liu et al., 2006). Both Aβ and its precursor APP are metalloproteins, hence dyshomeostasis of metal interactions may be linked to AD. The presence of metals promotes Aβ aggregation and conversely, metal chelators are able to dissolve Aβ deposits and attenuate amyloid burden in APP transgenic mouse models of AD. Even trace amounts of these metals can initiate auto-aggregation of Aβ and lead to its neurotoxicity (Huang et al., 2004; Liu et al., 2006). This evidence supports the idea that the dysregulation of cerebral biometals and the subsequent redox reactions of these metal ions, leading to oxidative stress, may play a prominent role in AD development (Huang et al., 2004; Liu et al., 2006).

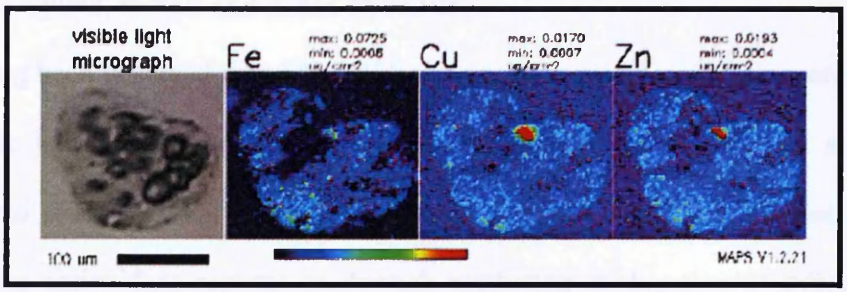

Figure 7.1. The elemental profile of a typical senile plaque
Senile plaques were identified from cryo-sectioned AD brain tissue then stained and analysed for their elemental content. The increased concentration of these metal ions can be seen localised within the plaque. (Liu et al., 2006)

APP is also implicated in copper homeostasis and is believed to modulate copper-induced toxicity and oxidative stress in neuronal cultures. This is supported by evidence that APP knockout mice exhibit increased brain copper levels (White et al., 1999) presumably due to the loss of a copper chelation capacity of APP (one possible biological role). In line with this, overexpression of the APP Swedish mutation in mice reduces brain copper levels prior to amyloid plaque formation (Maynard et al., 2002). In these mice, iron and zinc are also dysregulated (Smith et al., 2007a).

Further evidence for the role of metal ions in AD pathogenesis is the fact that the AD brain shows a fourfold decrease in the level of gene expression for metal regulatory proteins (Colangelo et al., 2002). Consequently, the AD brain has reduced capability to deal with the oxidative insults inflicted by increased redox active metal ion activity. In fact, cerebral biometal metabolism may be tightly linked to the processing of APP as the 5'untranslated region (5'UTR) of APP mRNA has been found to hold a functional iron-response element (IRE). Fe and Zn ions can promote APP expression via this IRE in a dose-dependent manner whilst copper can mediate its expression via the promoter region, supporting its role as a redox active metalloprotein (Liu et al., 2006; Rogers et al., 2002).

7.1.2. β-amyloid, metals and redox chemistry

It has long been observed that Aβ peptides can initiate synaptosomal lipoperoxidation and raise levels of H_2O_2 inducing neuronal oxidative stress (Behl et al., 1994; Butterfield et al., 1994). This may be through causing an indirect increase in ROS, decreasing antioxidant activity or through mediating dysfunction of mitochondria (Chauhan and Chauhan, 2006). The idea that the source of this oxidation could actually be the peptide itself was not considered at the time. However, in 1999, Huang et al reported characteristics of Aβ that lent itself to oxidative abilities; Aβ was found to be redox active, able to generate H_2O_2 directly, in a cell free manner via reduction of multivalent metal ions (Huang et al., 1999a).

It is believed that the high affinity interactions between redox active metal ions and Aβ through its histidine residues provide a structural environment capable of facilitating these redox reactions. Aβ has been found to reduce Cu(II), and, albeit to a lesser extent, Fe(III). The ensuing reactions generate H_2O_2 and hydroxyl radicals (Liu et al., 2006). Both of these are potent ROS capable of damaging cellular components and may be directly related to the widespread oxidative damage observed in the AD brain (Smith et al., 1996). It is proposed that following redox reactions between Aβ and the metal ion, the reduced metal ion participates in a Fenton reaction with H_2O_2 to make the hydroxyl radical. The Haber-Weiss reaction can form more hydroxyl radicals from superoxide and H_2O_2, catalysed by the metal ion. The reaction scheme outlined below has been proposed, where $M^{(n+1)+}$ is the oxidised metal ion, and M^{n+} represents the reduced ion (Huang et al., 1999a; Liu et al., 2006).

1. $(A\beta)_2 + M^{(n+1)+} \rightarrow A\beta{:}A\beta^{+\cdot} + M^{n+}$
2. $M^{n+} + O_2 \rightarrow M^{(n+1)+} + O_2^-$
3. $O_2^- + O_2^- + 2H^+ \rightarrow H_2O_2 + O_2$

} Redox reactions making H_2O_2

4. $M^{n+} + H_2O_2 \rightarrow M^{(n+1)+} + OH^{\bullet} + OH^{-}$ Fenton Reaction

5. $O_2^{-} + H_2O_2 \rightarrow OH^{\bullet} + OH^{-} + O_2$ Haber-Weiss Reaction

Metal ion homeostasis is altered in AD, accumulating to 3-5 fold normal concentrations. This is thought to create an environment primed for these Aβ-mediated redox reactions (Lovell et al., 1998). Cu(I) is far more reactive than Fe(II) when taking part in hydroxyl radical formation in the Fenton reaction, corresponding with the belief that copper is more important in these reactions in AD. The radicalised Aβ that is produced may react with oxygen, reforming the non-radicalised Aβ, the conformational changes induced possibly promoting its oligomerisation (Huang et al., 1999b). Vital to these reactions is thought to be the oxidation of the sulphur atom of Met35-Aβ as it acts as a source of electrons providing the electrochemical property needed for these reactions (Varadarajan et al., 1999). Oxidised Met35-Aβ has been isolated from AD amyloid plaques and is copper bound (Butterfield and Bush, 2004; Smith et al., 2007a). In addition, the generation of H_2O_2 by Aβ-metal complexes is theoretically catalytic in nature, and the subsequent Fenton chemistry generates highly reactive hydroxyl radicals thus making it a potent source of ROS (Butterfield et al., 2001; Huang et al., 1999a; Tabner et al., 2002).

Different Aβ species have varying levels of these redox properties correlating with their aggregation potential, neurotoxicity to cell cultures and AD oxidative neuropathology such that Aβ42 (human) > Aβ40 (human) > Aβ40 (rat/mouse) (Huang et al., 1999b; Liu et al., 2006). The H_2O_2 generated by Aβ is thought to mediate cytotoxicity as addition of catalase detoxifies the H_2O_2 and reduces cell death *in vitro* (Huang et al., 1999b). If the H_2O_2 generated by Aβ is not efficiently degraded or detoxified, it is feasible that these interactions are responsible for the oxidative stress

induced neuronal lesions and, the ensuing loss of neurons and intellectual faculties (Deraeve et al., 2006). Yet there is conflicting evidence on the aggregation state-dependency of these reactions. Some have found them to be independent of aggregation state. However, as the presence of copper induces Aβ auto-aggregation, and the process of oligomerisation is dynamic by nature, the exact state of Aβ is nothing but ambiguous. In fact, many believe that the physiochemical properties of Aβ are thought to determine whether the peptide acts as a pro- or anti-oxidant indicating, at an absolute minimum, a partial dependency on its conformation and consequently its aggregation state (Atwood et al., 2003; Gaeta and Hider, 2005).

7.1.3. Aβ and copper

Copper is the metal ion largely implicated in metal-Aβ mediated toxicity due to its redox capabilities and binding affinity for Aβ. In neuronal cells copper is normally kept bound to key regulatory proteins to prevent its redox activity and production of damaging ROS. Extracellular concentrations of copper are normally maintained at 0.2-1.7 μM. Following presynaptic excitation it is released into the synaptic cleft where it reaches up to a concentration of 15 μM. The concentration of copper found within senile plaques however, is ~400 μM (Lovell et al., 1998; Smith et al., 2007a). This is a grossly inflated local level and is presumably sequestered there bound to Aβ, facilitating ROS generation (discussed further in 1.5.2).

Aβ itself has been found to bind Cu(II) at sub μM concentrations and does so with an unusually strong affinity indicating a role for this binding *in vivo* (Atwood et al., 1998; Atwood et al., 2000b). Even synthetically made Aβ contains significant concentrations of Cu (and Fe) (Turnbull et al., 2001a; Turnbull et al., 2001b). Despite this, it is also believed that the manner in which Aβ binds copper ions allows

the ion to move into and out of the fibril architecture (Karr et al., 2005). It has been shown that Cu(II) induces Aβ aggregation, with this effect being greater with Aβ42 and under mildly acidic conditions (such as the mild acidosis observed in AD brains) (Atwood et al., 1998). In addition, Cu(II) bound Aβ has altered PM interactive properties which modify its binding and its functional abilities (Karr et al., 2005). Copper has two oxidation states, of either Cu(I) or Cu(II) permitting electron transfer reactions producing ROS, given an electron donor/acceptor to react with. Aβ42, as well as being tightly linked to AD pathogenesis, has the greatest affinity for metal ions. It has been found that theoretically Aβ42 can bind up to 2.5 Cu(II) ions per peptide unit (Atwood et al., 2000b). It has been suggested that the amount of H_2O_2 produced by the peptide may be directly correlated to the number of Cu(II) ions bound to the peptide and that this production is catalytic in nature (Deraeve et al., 2006).

7.1.4. Aβ and iron

Iron is also found localised in plaques, albeit at a much lower concentration of around 1 μM although this could be a secondary effect due to copper as copper can mediate cellular iron uptake (Lovell et al., 1998). Although iron is redox active and promotes aggregation Aβ, it is unclear whether it takes part in the electron transfer reactions with Aβ as Aβ is not believed to interact directly with iron *in vivo* as they do not co-purify. It is thought that the altered iron homeostasis seen in AD may be due to secondary effects such as altered activities of oxidatively damaged enzymes or simply due to copper-mediated cellular iron uptake (Smith et al., 2007a).

7.1.5. Aβ and zinc

Zinc irons are released into the synapse during signal transmission to a concentration of 200-300 μM, but like copper ions, their concentration is increased in senile plaques to as high as 1 mM (Assaf and Chung, 1984; Lovell et al., 1998). However, only mature cored senile plaques test positive for zinc reactivity (Lee et al., 1999), implying that the sequestration into plaques is a later event in the amyloid pathology of AD. Zinc is found at increased levels in the CSF of AD patients (Hershey et al., 1983). The role of zinc in the pathogenesis of AD is unclear due to some conflicting data. Affinity calculations of the interaction of zinc with Aβ indicate they may interact under physiological conditions (Bush et al., 1994). Zinc has been found to promote aggregation and plaque formation, with the metal precipitating Aβ at alkaline pHs. However, Aβ40 and Aβ42 are equally affected (Atwood et al., 1998). Further data suggests that zinc might be more neuroprotective rather than neurotoxic as it appears to attenuate the toxicity of Aβ to neuronal cortical cultures (Lovell et al., 1999). It has been proposed that zinc ions may protect against membrane permeability changes seen in AD. The zinc ions may provide competition for the copper ions for Aβ binding, thereby inhibiting the toxic copper mediated Aβ redox chemistry (Cuajungco et al., 2000; Smith et al., 2007a).

7.1.6. Aims

Earlier work had identified that Aβ generated H_2O_2 without the addition of metal ions to aggregating solutions. It has also been observed that Aβ not only generates but also degrades H_2O_2 in different proportions when prevented from aggregating at different time points during its aggregation, implicating the involvement of specific Aβ species in each of these processes. Both of these processes are likely to be reliant on the

presence of trace levels of metal ions in solution. Although the effects of metal ions on Aβ aggregation have been investigated previously, this study set out to complete a systematic investigation, not only looking at the aggregation of Aβ over time, but also at how this effects H_2O_2 generation by Aβ over this period. As the binding of metal ions may induce multiple effects, altering the aggregation of Aβ but also mediating its redox capabilities, the addition of metal ions may have complex effects on the resultant generation of H_2O_2 over the course of its aggregation.

7.2. Results

Although the effects of metal ions on Aβ aggregation have been studied, here metal ions have been tested to enable observation of their effects on H_2O_2 generation throughout the aggregation process. This may be mediated by complex metal-Aβ interactions altering aggregation kinetics and also facilitating redox reactions. A limited study has been performed on the effect of iron and zinc ions on aggregation and H_2O_2 generation. Nonetheless copper is considered to be principal metal ion involved in Aβ-mediated toxicity (Hung et al., 2010). For this reason most of the work presented here is focused on copper-mediated effects.

7.2.1. Copper and Aβ

7.2.1.1. Primary effects of copper on Aβ40 and Aβ42 aggregation state

The relatively high affinity of copper for Aβ has the potential to induce rapid changes in the aggregation state of the peptide. This can be seen in figure 7.2 where a range of copper concentrations have been added to Aβ40 and Aβ42. Over the range of copper to Aβ ratios tested (1:100000 to 10:1) Aβ40 exhibited a uniform increase in thioflavin

T signal at T=0. The increase in thioflavin T fluorescence was concurrent to increases in immunoassay fluorescence. However, the immunoassay suggests that there are differences in the level of oligomer content over the concentration range tested, with the lower concentrations exhibiting slightly larger fluorescence increases. When tested with Aβ42, the effect on thioflavin T and immunoassay fluorescence was not constant across the concentrations tested nor is there a clear concentration dependent effect, with significant increases in fluorescence seen at copper to Aβ ratios of 10:1 and 1:1000, and at 1:100000 in the immunoassay only (Tukey HSD, $p \leq 0.000$).

7.2.1.2. Aggregation and H_2O_2 generation of Aβ40 with copper

Aβ40 was aggregated over 72 hrs with this range of copper concentrations to observe their effects on aggregation and H_2O_2 generation. With no copper added H_2O_2 was made during the first 6 hrs, corresponding with small rises in both thioflavin T and immunoassay fluorescence (see figure 7.3). In fact, the immunoassay showed a 10 fold increase in fluorescence from the monomeric starting fluorescence. This was followed by a decrease in Amplex red fluorescence, actually below control levels which corresponded to increases in thioflavin T and immunoassay fluorescence. All the samples with copper added to them at 1:1000 copper to Aβ40 and below exhibited very similar H_2O_2 generation within the first 6 hrs. However, subsequent H_2O_2 generation/quenching differed between these samples. The aggregation and H_2O_2 generation from Aβ40 with the lowest copper concentration was similar to that with no copper added (see figure 7.3B). Despite the initial increase in thioflavin T and immunoassay fluorescence from this sample, aggregation actually proceeded marginally, slower than with no copper. Concurrently, the H_2O_2 generated by this sample appeared to decrease less-so than the sample with no added copper.

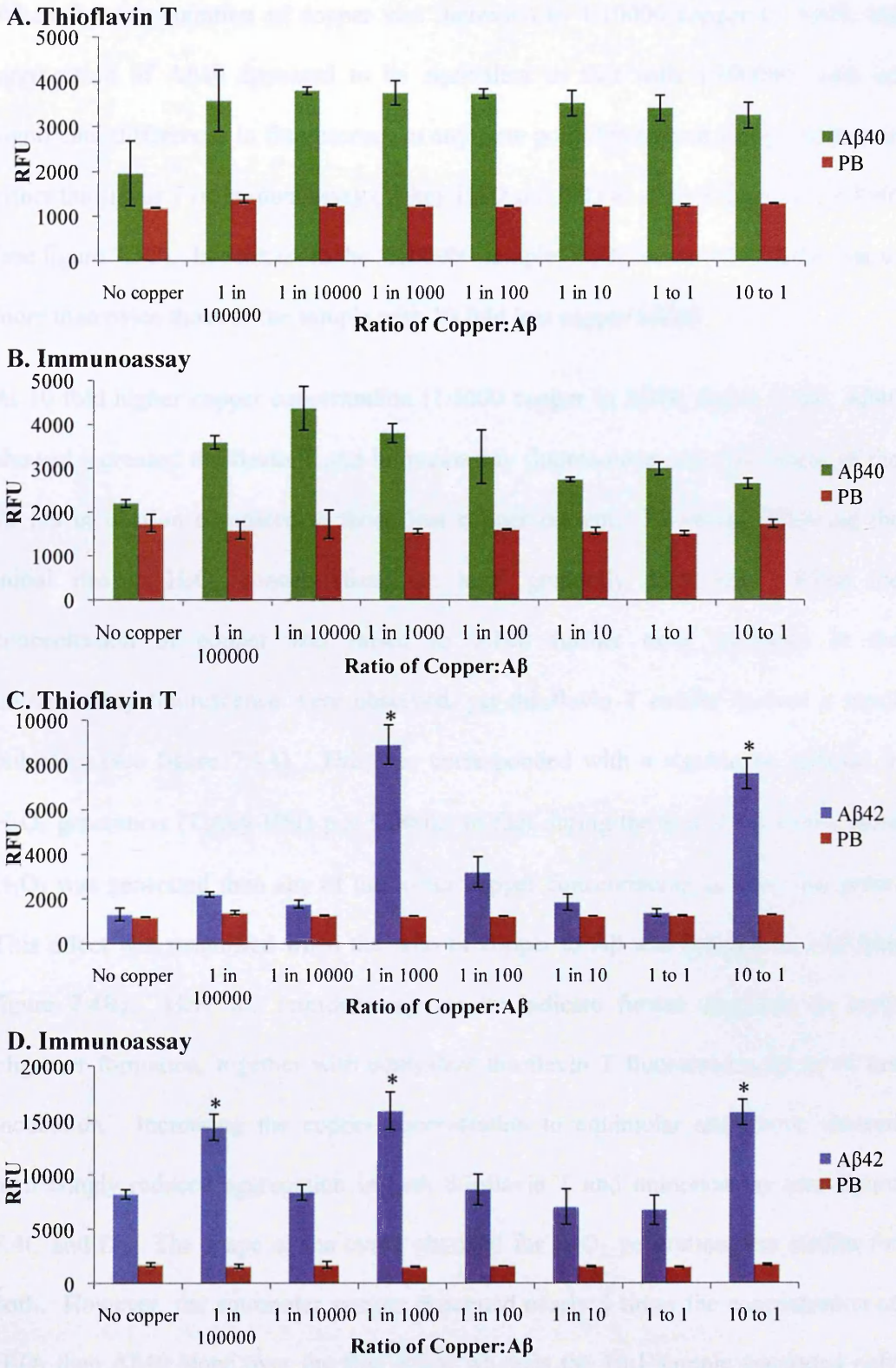

Figure 7.2. The effect of copper on initial aggregation state of Aβ40 and 42
TFA and HFIP treated Aβ40 and 42 were solubilised to 25 μM in 10 mM PB, pH 7.4 with and without the presence of copper (II) chloride. Copper concentrations used ranged from 250 pM to 250 μM and expressed as a ratio to Aβ concentration. Results are means ± S.D. (Thioflavin T: n=3, Immunoassay: n=4), * indicates Tukey HSD $p \leq 0.000$.

When the concentration of copper was increased to 1:10000 copper to Aβ40, the aggregation of Aβ40 appeared to be equivalent to that with 1:100000, with no significant differences in fluorescence at any time point throughout its aggregation in either thioflavin T or immunoassay (Tukey HSD $p > 0.05$ at all time points after T=0) (see figure 7.3C). In contrast to the 1:100000 sample, H_2O_2 levels continued to rise to more than twice those of the sample with 10 fold less copper added.

At 10 fold higher copper concentration (1:1000 copper to Aβ40, figure 7.4D), Aβ40 showed increased thioflavin T and immunoassay fluorescence over the course of the 72 hrs incubation compared to those less copper present. However, following the initial rise in H_2O_2 concentration, the level gradually decreased. When the concentration of copper was raised to 1:100 further early increases in the immunoassay fluorescence were observed, yet thioflavin T results showed a small reduction (see figure 7.4A). This was corresponded with a significant increase in H_2O_2 generation (Tukey HSD $p \leq 0.000$). In fact during the first 6 hrs >50% more H_2O_2 was generated than any of the lower copper concentrations at this time point. This effect was magnified when the ratio of copper to Aβ was brought to 1:10 (see figure 7.4B). Here the immunoassay results indicate further increases in early oligomer formation, together with equivalent thioflavin T fluorescence up to 48 hrs incubation. Increasing the copper concentration to equimolar and above showed increasingly reduced aggregation in both thioflavin T and immunoassay (see figure 7.4C and D). The shape of the curve obtained for H_2O_2 generation was similar for both. However, the equimolar sample generated nearly 3 times the concentration of H_2O_2 than Aβ40 alone over the first 6 hrs, whereas the 10:1 sample generated only slightly more than Aβ40 alone. Over the reminder of the incubation time the level of H_2O_2 in the solution gradually decreased in both samples.

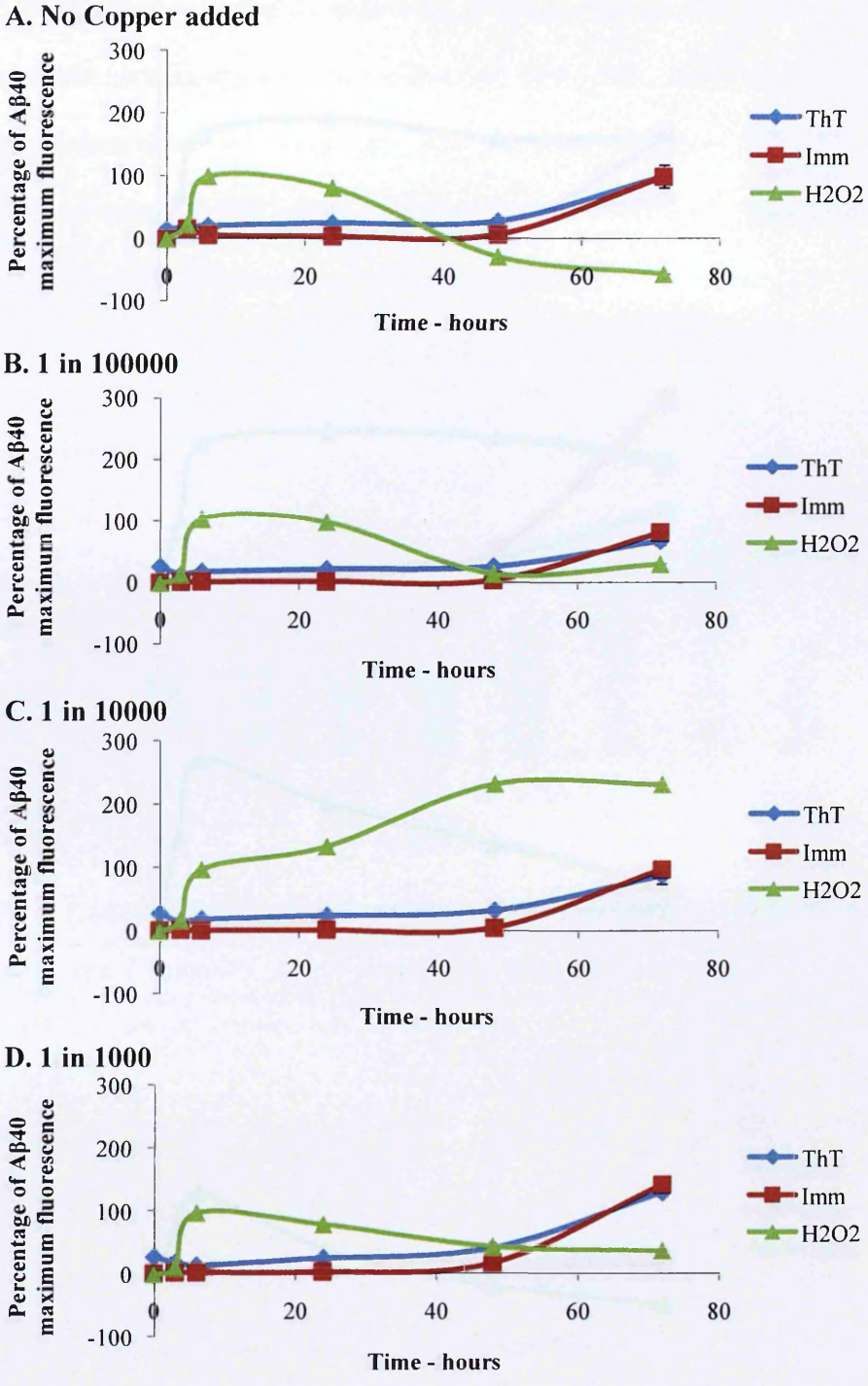

Figure 7.3. The effect of copper on aggregation and H_2O_2 generation by Aβ40
TFA and HFIP treated Aβ40 was solubilised to 25 μM in 10 mM PB, pH 7.4 with and without the presence of copper (II) chloride and incubated at 37°C for 72 hrs. Samples were taken for thioflavin T (ThT), Immunoassay (Imm) and Amplex red (H_2O_2) over 72 hrs. Copper concentrations used ranged from 250 pM to 250 μM and are expressed as a ratio to Aβ concentration. A = No copper added, B = 250 pM copper, C = 2.5 nM copper, D = 25 nM copper. Results are means ± S.D. (Thioflavin T and Amplex red: n=3, Immunoassay: n=4)

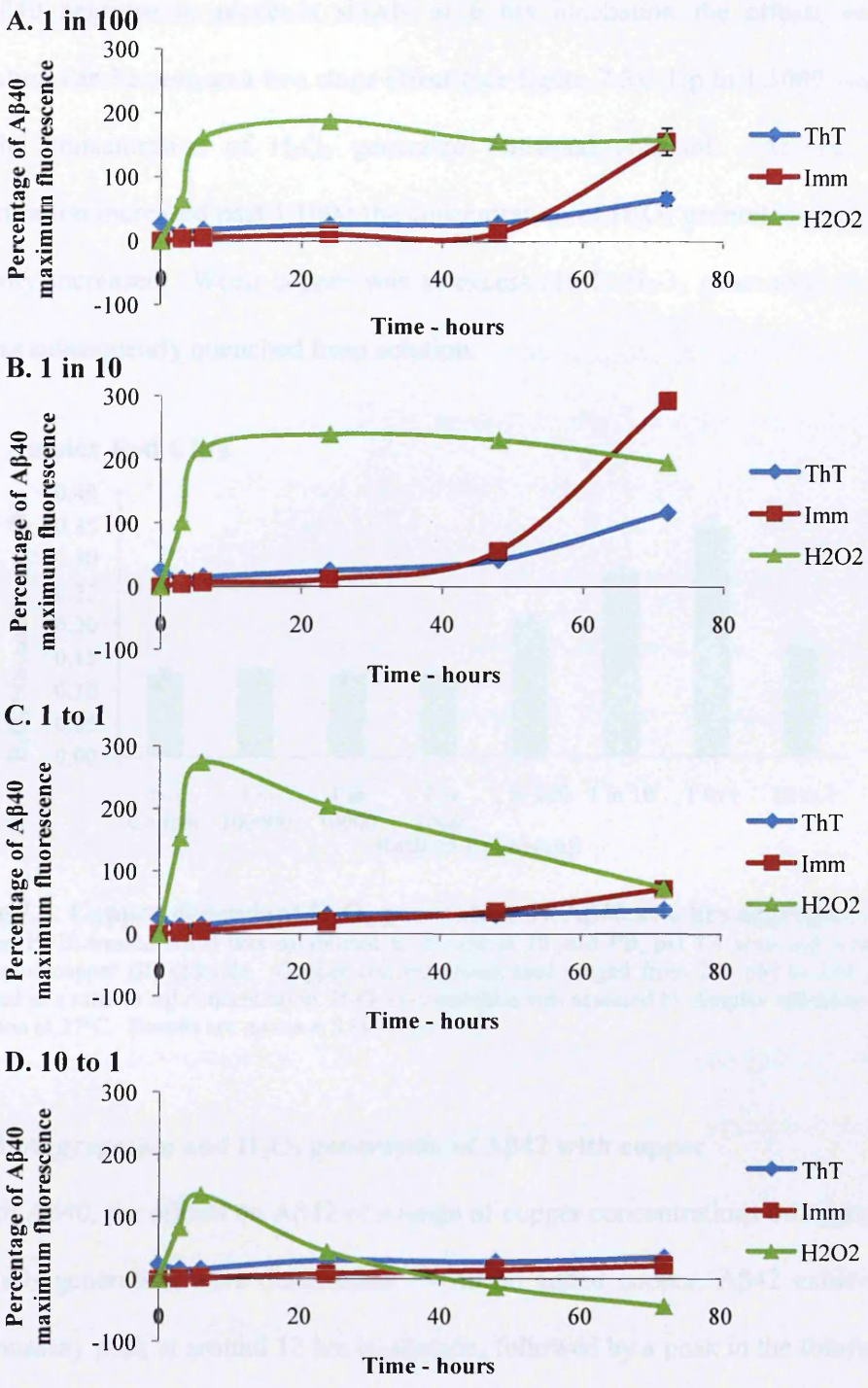

Figure 7.4. The effect of copper on aggregation and H_2O_2 generation by Aβ40, part 2

TFA and HFIP treated Aβ40 was solubilised to 25 μM in 10 mM PB, pH 7.4 with and without the presence of copper (II) chloride and incubated at 37°C for 72 hrs. Samples were taken for thioflavin T (ThT), Immunoassay (Imm) and Amplex red (H_2O_2) over 72 hrs. Copper concentrations used ranged from 250 pM to 250 μM and are expressed as a ratio to Aβ concentration. A = 250 nM copper, B = 2.5 μM copper, C = 25 μM copper, D = 250 μM copper. Results are means ± S.D. (Thioflavin T and Amplex red: n=3, Immunoassay: n=4)

As Aβ40 aggregation proceeds slowly at 6 hrs incubation the effects on H_2O_2 generation can be seen as a two stage effect (see figure 7.5). Up to 1:1000 copper to Aβ, the concentration of H_2O_2 generated remained constant. As the copper concentration increased past 1:1000 the concentration of H_2O_2 generated at this point gradually increased. When copper was in excess (10:1) H_2O_2 generation decreases and was subsequently quenched from solution.

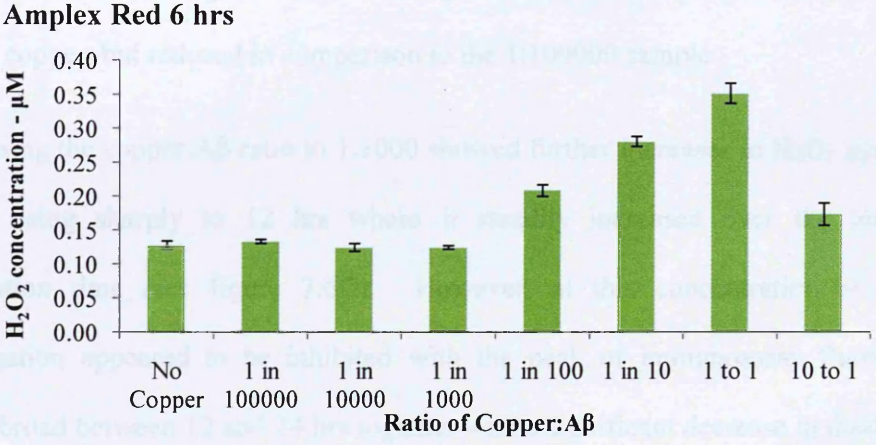

Figure 7.5. Copper dependant H_2O_2 generation by Aβ40 at 6 hrs aggregation
TFA and HFIP treated Aβ40 was solubilised to 25 µM in 10 mM PB, pH 7.4 with and without the presence of copper (II) chloride. Copper concentrations used ranged from 250 pM to 250 µM and expressed as a ratio to Aβ concentration. H_2O_2 concentration was assessed by Amplex red assay at 6 hrs incubation at 37°C. Results are means ± S.D. (n=3)

7.2.1.3. Aggregation and H_2O_2 generation of Aβ42 with copper

As with Aβ40, the effects on Aβ42 of a range of copper concentrations on aggregation and H_2O_2 generation were determined. With no added copper, Aβ42 exhibited an immunoassay peak at around 12 hrs incubation, followed by a peak in the thioflavin at 24 hrs (see figure 7.6A). In concordance with earlier experiments, H_2O_2 was generated to a peak at 12 hrs, where the curve plateaued. Addition of 1 in 100000 copper to Aβ42 showed no significant change in thioflavin T fluorescence throughout the incubation period compared to with no copper added, with later time points highly homogenous (Tukey HSD $p > 0.959$, T=12-48) (see figure 7.6B). The immunoassay

data was also very similar although an increase in fluorescence was observed at 12 hrs incubation. This corresponded to an increase in H_2O_2 generation, in particular, a slow steady rise from 12-48 hrs. When the copper concentration was increased to 1 in 10000, immunoassay fluorescence was again increased at 12 hrs compared to no added copper. However, this was less so than the 1:100000 copper to Aβ42 sample and concurrent with an increase in thioflavin T fluorescence throughout the course of the experiment (see figure 7.6C). H_2O_2 generation was increased compared to no added copper, but reduced in comparison to the 1:100000 sample.

Increasing the copper:Aβ ratio to 1:1000 showed further increases in H_2O_2 generation again rising sharply to 12 hrs where it steadily increased over the remaining incubation time (see figure 7.6D). However, at this concentration of copper, aggregation appeared to be inhibited with the peak of immunoassay fluorescence being broad between 12 and 24 hrs together with a significant decrease in thioflavin T fluorescence from T=6 onwards (Tukey HSD $p \leq 0.002$). Another 10 fold increase in copper showed further decreases in aggregation-associated fluorescence in both the thioflavin T and immunoassay. This was together with a significant increase in H_2O_2 generation by Aβ42 at 12 hrs incubation (Tukey HSD $p \leq 0.001$) which was sustained over the following 36 hrs (see figure 7.7A). This effect was supported by increasing the copper to Aβ to 1:10, which further increased early H_2O_2 generation, despite aggregation measured by thioflavin T fluorescence appearing to be promoted.

When copper was elevated to equimolar the immunoassay detected small increases in oligomeric content during the early incubation period, corresponding to a slight increase in H_2O_2 concentration during the first 6 hrs (see figure 7.7C). This peaked at 12 hrs but then decreased over the following 36 hrs, coinciding with a peak of immunoassay fluorescence at 24 hrs and greatly reduced thioflavin T fluorescence.

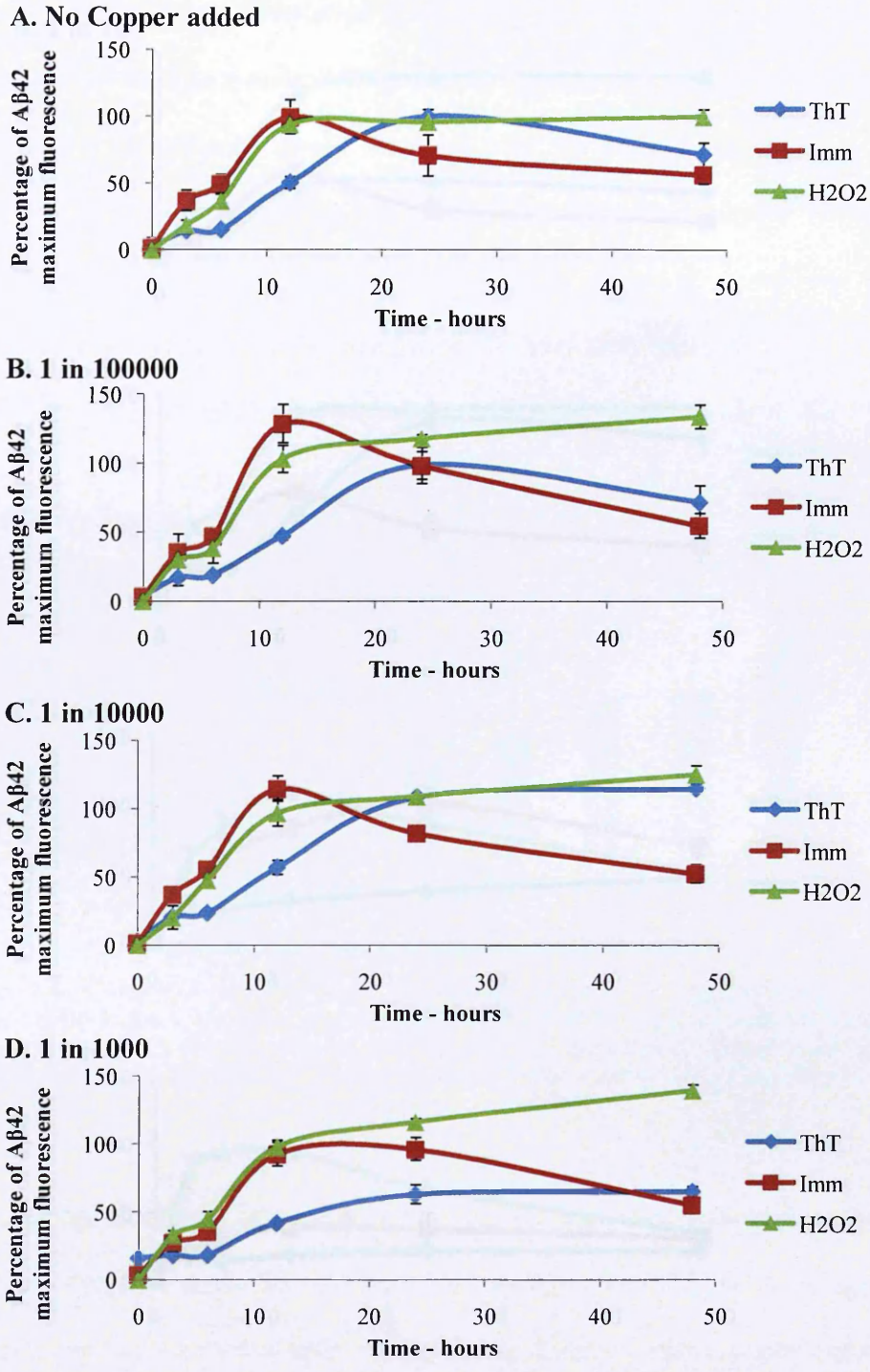

Figure 7.6. The effect of copper on aggregation and H_2O_2 generation by Aβ42
TFA and HFIP treated Aβ42 was solubilised to 25 μM in 10mM PB, pH 7.4 with and without the presence of copper (II) chloride and incubated at 37°C for 72 hrs. Samples were taken for thioflavin T (ThT), Immunoassay (Imm) and Amplex red (H_2O_2) over 72 hrs. Copper concentrations ranged from 250 pM to 250 μM and are expressed as a ratio to Aβ concentration. A = No copper added, B = 250 pM copper, C = 2.5 nM copper, D = 25 nM copper. Results are means ± S.D. (Thioflavin T and Amplex red: n=3, Immunoassay: n=4)

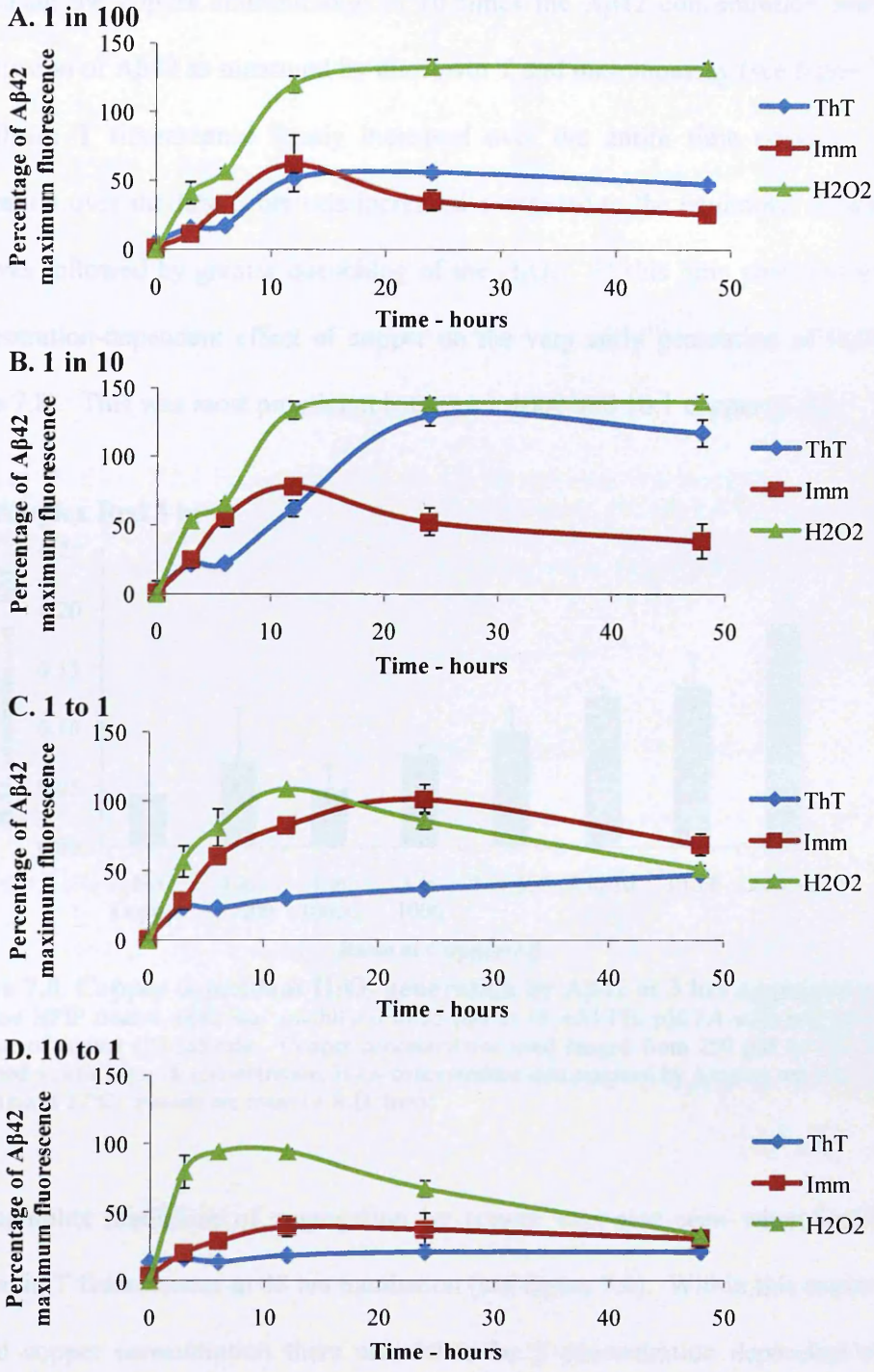

Figure 7.7. The effect of copper on aggregation and H_2O_2 generation by Aβ42, part 2

TFA and HFIP treated Aβ40 was solubilised to 25 μM in 10 mM PB, pH 7.4 with and without the presence of copper (II) chloride and incubated at 37°C for 72 hrs. Samples were taken for thioflavin T (ThT), Immunoassay (Imm) and Amplex red (H_2O_2) over 72 hrs. Copper concentrations used ranged from 250 pM to 250 μM and are expressed as a ratio to Aβ concentration. A = 250 nM copper, B = 2.5 μM copper, C = 25 μM copper, D = 250 μM copper. Results are means ± S.D. (Thioflavin T and Amplex red: n=3, Immunoassay: n=4)

Increasing the copper concentration to 10 times the Aβ42 concentration prevented aggregation of Aβ42 as measured by thioflavin T and immunoassay (see figure 7.8D). Thioflavin T fluorescence barely increased over the entire time course. H_2O_2 generation over the first 3 hrs was increased compared to the equimolar solution yet this was followed by greater quenching of the H_2O_2. At this time point there was a concentration-dependent effect of copper on the very early generation of H_2O_2 (see figure 7.8). This was most prominent between 1:1000 and 10:1 copper to Aβ.

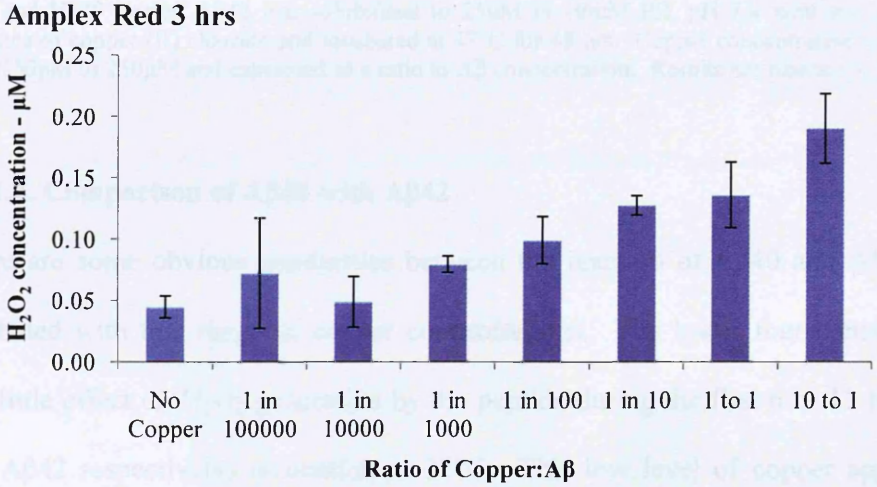

Figure 7.8. Copper dependant H_2O_2 generation by Aβ42 at 3 hrs aggregation
TFA and HFIP treated Aβ42 was solubilised to 25 µM in 10 mM PB, pH 7.4 with and without the presence of copper (II) chloride. Copper concentrations used ranged from 250 pM to 250 µM and expressed as a ratio to Aβ concentration. H_2O_2 concentration was assessed by Amplex red assay at 6 hrs incubation at 37°C. Results are means ± S.D. (n=3)

The complex mediation of aggregation by copper was also seen when looking at thioflavin T fluorescence at 48 hrs incubation (see figure 7.9). Within this exponential rise in copper concentration there seemed to be 2 concentration dependent effects where fibrillisation was promoted and then inhibited. The data in this figure also shows non-incubated controls for thioflavin T with the highest concentration of copper. This confirms that any observed deviation from the control fluorescence (no added copper) is due to the effect of copper on the aggregation state.

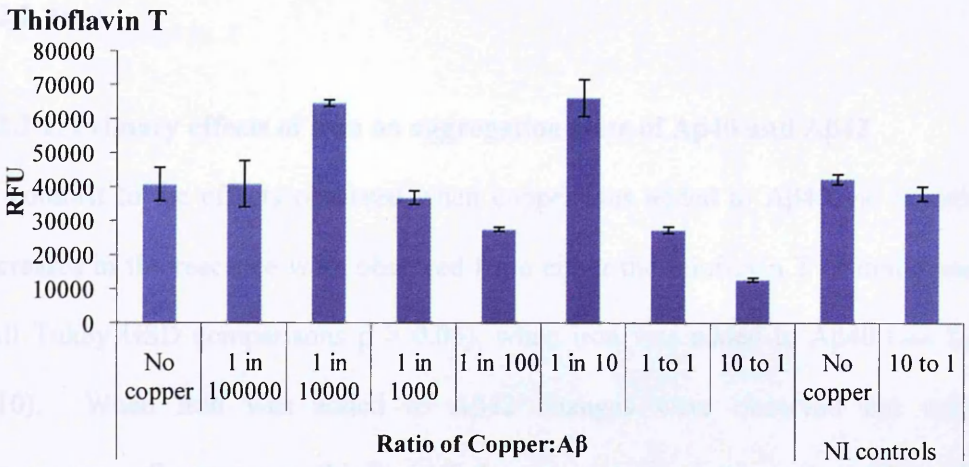

Figure 7.9. The effect of copper after 48 hrs on aggregation of Aβ42
TFA and HFIP treated Aβ42 was solubilised to 25μM in 10mM PB, pH 7.4 with and without the presence of copper (II) chloride and incubated at 37°C for 48 hrs. Copper concentrations used ranged from 250pM to 250μM and expressed as a ratio to Aβ concentration. Results are means ± S.D. (n=3)

7.2.1.4. Comparison of Aβ40 with Aβ42

There are some obvious similarities between the reaction of Aβ40 and Aβ42 when incubated with this range of copper concentrations. The lower four concentrations had little effect on H_2O_2 generation by the peptide during the first 6 or 12 hrs (Aβ40 and Aβ42 respectively) incubation at 37°C. This low level of copper appeared to exert its effects later in the aggregation time course. As copper concentration was increased to 1:100 and 1:10 both Aβ40 and Aβ42 show consecutive elevations in H_2O_2 generation. Further increases in copper concentration to 1:1 and 10:1 showed increasing prevention of aggregation along with concurrent decreases in H_2O_2 generation. These similarities, despite the different starting aggregation state and propensity for further aggregation, identify these effects as potentially being relevant to function of the Aβ species.

7.2.2. Iron

7.2.2.1. Primary effects of iron on aggregation state of Aβ40 and Aβ42

In contrast to the effects observed when copper was added to Aβ40, no significant increases in fluorescence were observed from either the thioflavin T or immunoassay (All Tukey HSD comparisons $p > 0.05$), when iron was added to Aβ40 (see figure 7.10). When iron was added to Aβ42 changes were observed but only in immunoassay fluorescence; thioflavin T fluorescence remained constant (Tukey HSD $p \geq 0.938$) whilst the addition of 1:100, 1:10 and 1:1 iron to Aβ42 all generated an increase in immunoassay fluorescence (Tukey HSD $p \leq 0.000$). This effect was not concentration dependant but rather constant across these concentrations.

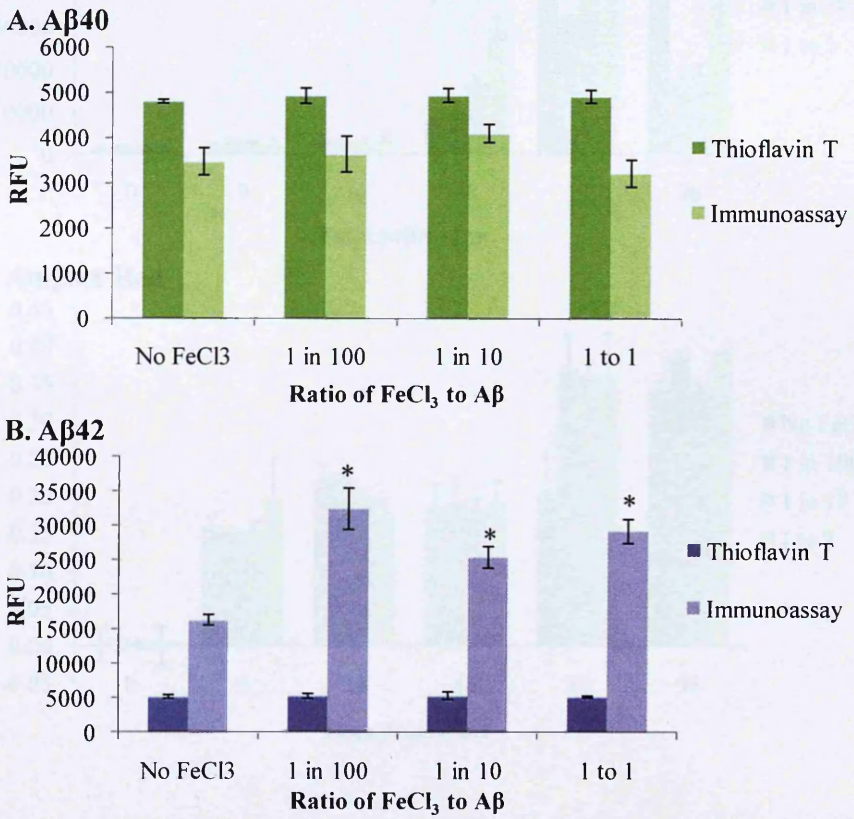

Figure 7.10. The effect of iron on the initial aggregation state of Aβ40 and Aβ42
TFA and HFIP treated Aβ40 and Aβ42 was solubilised to 25 μM in 10 mM PB, pH 7.4 with and without the presence of Iron (III) chloride. Iron concentrations used ranged from 250 nM to 250 μM and expressed as a ratio to Aβ concentration. Results are means ± S.D. (Thioflavin T: n=3, Immunoassay: n=4), * indicates Tukey HSD $p \leq 0.000$ compared to No $FeCl_3$.

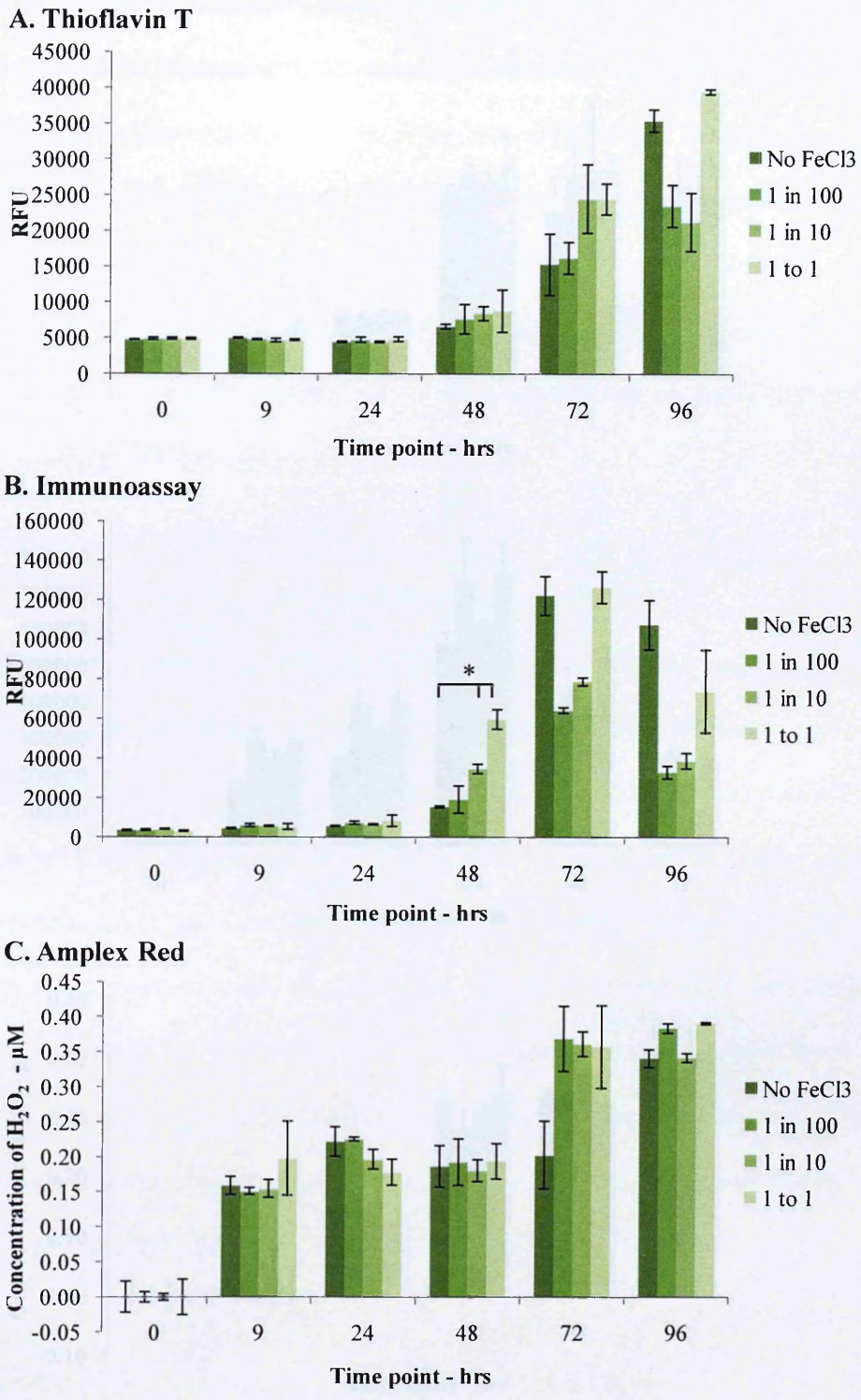

Figure 7.11. The effect of iron on aggregation and H_2O_2 generation by Aβ40
TFA and HFIP treated Aβ40 was solubilised to 25 µM in 10mM PB, pH 7.4 with and without the presence of iron (III) chloride and incubated at 37°C for 96 hrs. Samples were taken for thioflavin T, Immunoassay and Amplex red over 96 hrs. Iron concentrations ranged from 250 nM to 25 µM and are expressed as a ratio to Aβ concentration. Results are means ± S.D. (Thioflavin T and Amplex red: n=3, Immunoassay: n=4), * indicates Tukey HSD $p \leq 0.000$.

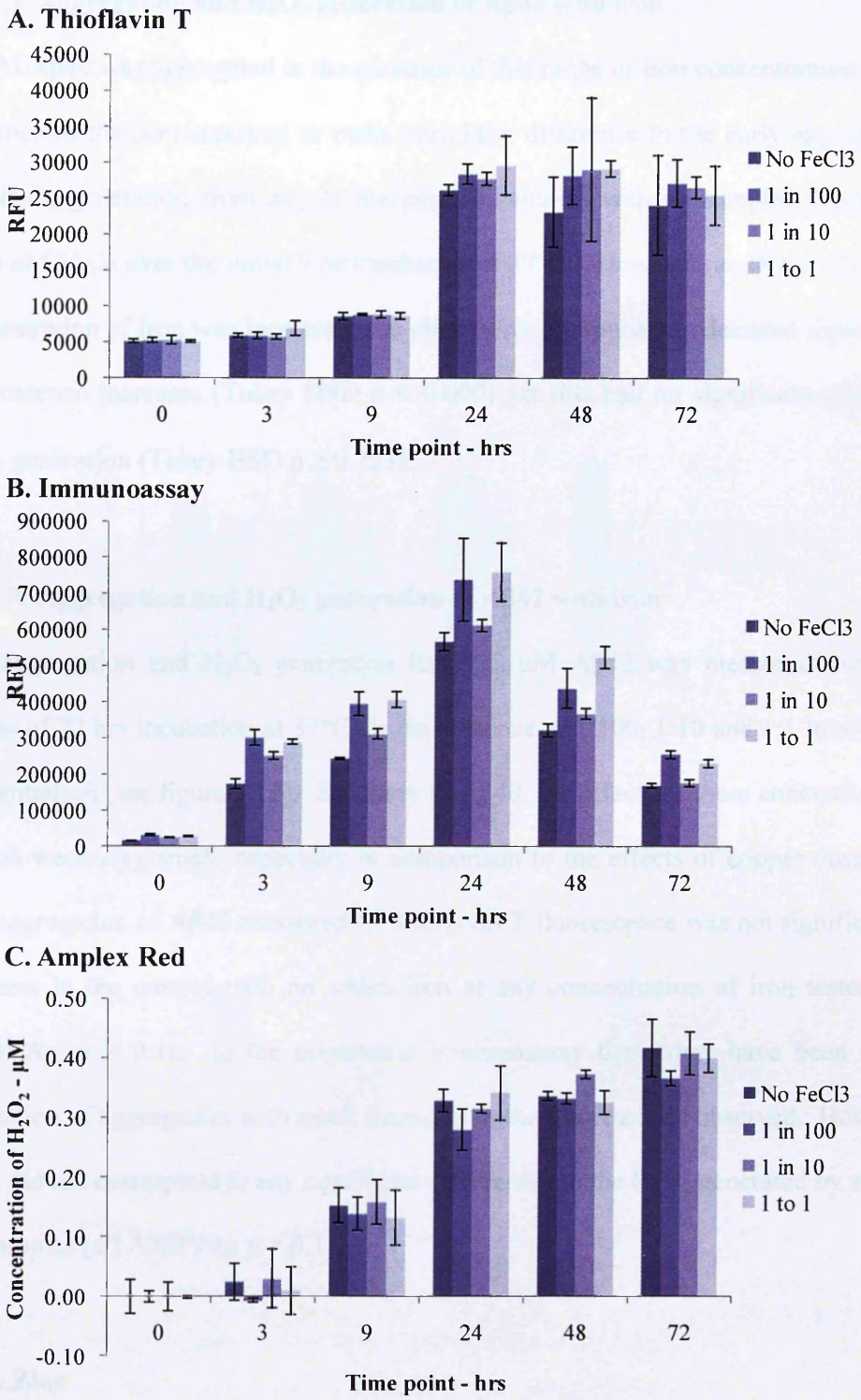

Figure 7.12. The effect of iron on aggregation and H_2O_2 generation by Aβ42
TFA and HFIP treated Aβ42 was solubilised to 25 µM in 10mM PB, pH 7.4 with and without the presence of iron (III) chloride and incubated at 37°C for 72 hrs. Samples were taken for thioflavin T, Immunoassay and Amplex red over 72 hrs. Iron concentrations ranged from 250 nM to 25 µM and are expressed as a ratio to Aβ concentration. Results are means ± S.D. (Thioflavin T and Amplex red: n=3, Immunoassay: n=4)

7.2.2.2. Aggregation and H_2O_2 generation of Aβ40 with iron

25 μM Aβ40 was aggregated in the presence of this range of iron concentrations. The presence of the iron appeared to make very little difference to the early aggregation and H_2O_2 generation from any of the peptide samples with all samples generating ~200 nM H_2O_2 over the initial 9 hr incubation at 37°C. However, at 48 hrs when the concentration of iron was increased, the oligomeric immunoassay detected significant fluorescence increases (Tukey HSD $p < 0.000$) yet this had no significant effect on H_2O_2 generation (Tukey HSD $p \geq 0.727$).

7.2.2.3. Aggregation and H_2O_2 generation of Aβ42 with iron

The aggregation and H_2O_2 generation from 25 μM Aβ42 was measured over the course of 72 hrs incubation at 37°C, in the presence of 1:100, 1:10 and 1:1 iron to Aβ concentration (see figure 7.12). Similarly to Aβ40, the effects of these concentrations of iron were very small, especially in comparison to the effects of copper observed. The aggregation of Aβ42 measured by thioflavin T fluorescence was not significantly different to the control with no added iron at any concentration of iron tested (all ANOVAs, $p > 0.1$). In the oligomeric immunoassay there may have been some promotion of aggregation with small increases in the fluorescence observed. However these did not correspond to any significant differences in the H_2O_2 generated by any of the samples (all ANOVAs $p > 0.1$).

7.2.3. Zinc

7.2.3.1. Primary effects of zinc on the aggregation state of Aβ40 and Aβ42

When zinc was tested for its effects on Aβ40 and Aβ42 there were changes observed in both the immunoassay and thioflavin T. Initially, with 1:100, 1:10 and 1:1 zinc to

Aβ40 no significant differences were observed in the thioflavin T (Tukey HSD, p = 0.148). However, there was a small reduction in immunoassay fluorescence at 1:1 zinc to Aβ40 (Tukey HSD, $p \leq 0.05$) (see figure 7.13). This was in contrast to the initial effects of zinc on Aβ42. Both thioflavin T and oligomeric immunoassay measured significant increases in fluorescence when zinc ions were added at 25 μM to Aβ42 (Tukey HSD: Immunoassay $p \leq 0.002$, thioflavin T $p \leq 0.000$).

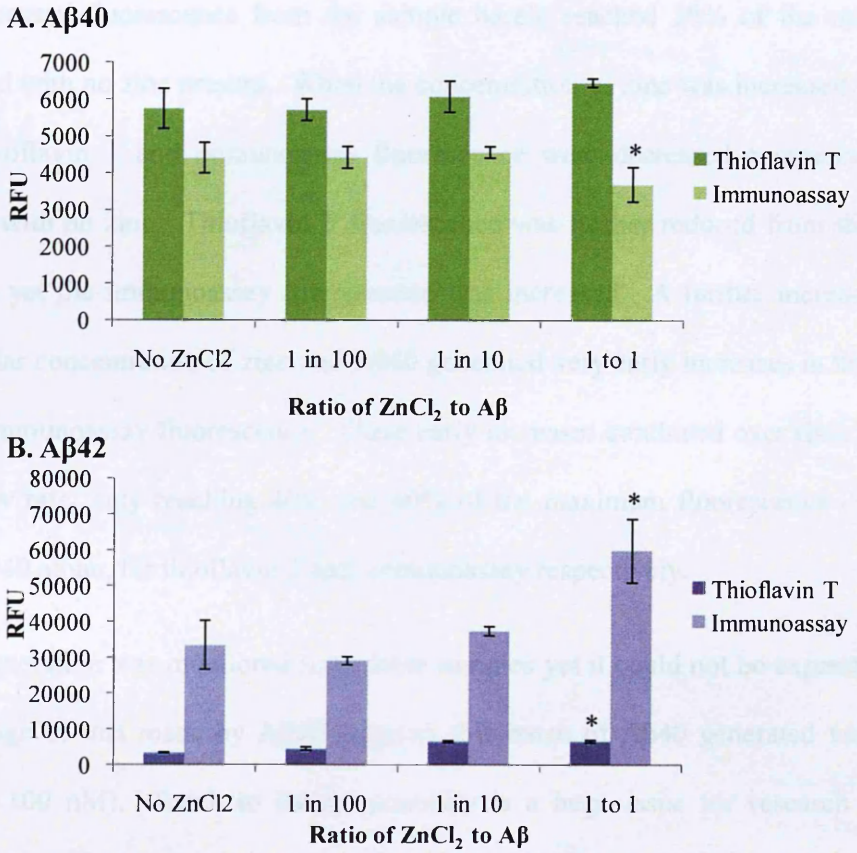

Figure 7.13. The effect of zinc on the initial aggregation state of Aβ40 and Aβ42
TFA and HFIP treated Aβ40 and Aβ42 was solubilised to 25 μM in 10 mM PB, pH 7.4 with and without the presence of Zinc (II) chloride. Zinc concentrations used ranged from 250 nM to 250 μM and expressed as a ratio to Aβ concentration. Results are means ± S.D. (Thioflavin T: n=3, Immunoassay: n=4), * indicates Tukey HSD $p \leq 0.05$ compared to No $ZnCl_2$

7.2.3.2. Aggregation and H_2O_2 generation of Aβ40 with zinc

The aggregation and H_2O_2 generation of 25 μM Aβ40 incubated over 96 hrs at 37°C was determined with the addition of zinc at 1:100 to 1:1 zinc to Aβ40. The addition

of the zinc induced visible effects at these different concentrations on the aggregation state of the peptide as measured by thioflavin T and immunoassay (see figure 7.14). Aβ40 with no added zinc aggregated slowly over the initial 48 hrs then both thioflavin T and immunoassay fluorescence increased significantly over the remaining 48 hrs (Tukey HSD $p \leq 0.000$). The addition of 1:100 zinc generated a small reduction in the thioflavin T fluorescence at 96 hrs. However, throughout the time course the immunoassay fluorescence from the sample barely reached 20% of the maximum achieved with no zinc present. When the concentration of zinc was increased 10 fold, both thioflavin T and immunoassay fluorescence were decreased compared to the control with no zinc. Thioflavin T fluorescence was further reduced from the 1:100 sample, yet the immunoassay fluorescence was increased. A further increase to an equimolar concentration of zinc and Aβ40 generated very early increases in thioflavin T and immunoassay fluorescence. These early increases continued over time but at a very low rate, only reaching 40% and 60% of the maximum fluorescence observed with Aβ40 alone, for thioflavin T and immunoassay respectively.

H_2O_2 generation was monitored from these samples yet it could not be expressed as a percentage of that made by Aβ40 alone as this batch of Aβ40 generated very little H_2O_2 (<100 nM). Batch to batch variability is a huge issue for research of Aβ. Deseeding massively reduced this variability, nevertheless it still occurs. It is for this reason that aggregation and H_2O_2 generation has not been directly compared where data was collected from different experiments, but especially where different batches were used. Only samples prepared from the same batch at the same time, with all the reagents made and used at the same time have been compared. Experimental repeats aim to reproduce and identify trends in the data, not the exact values.

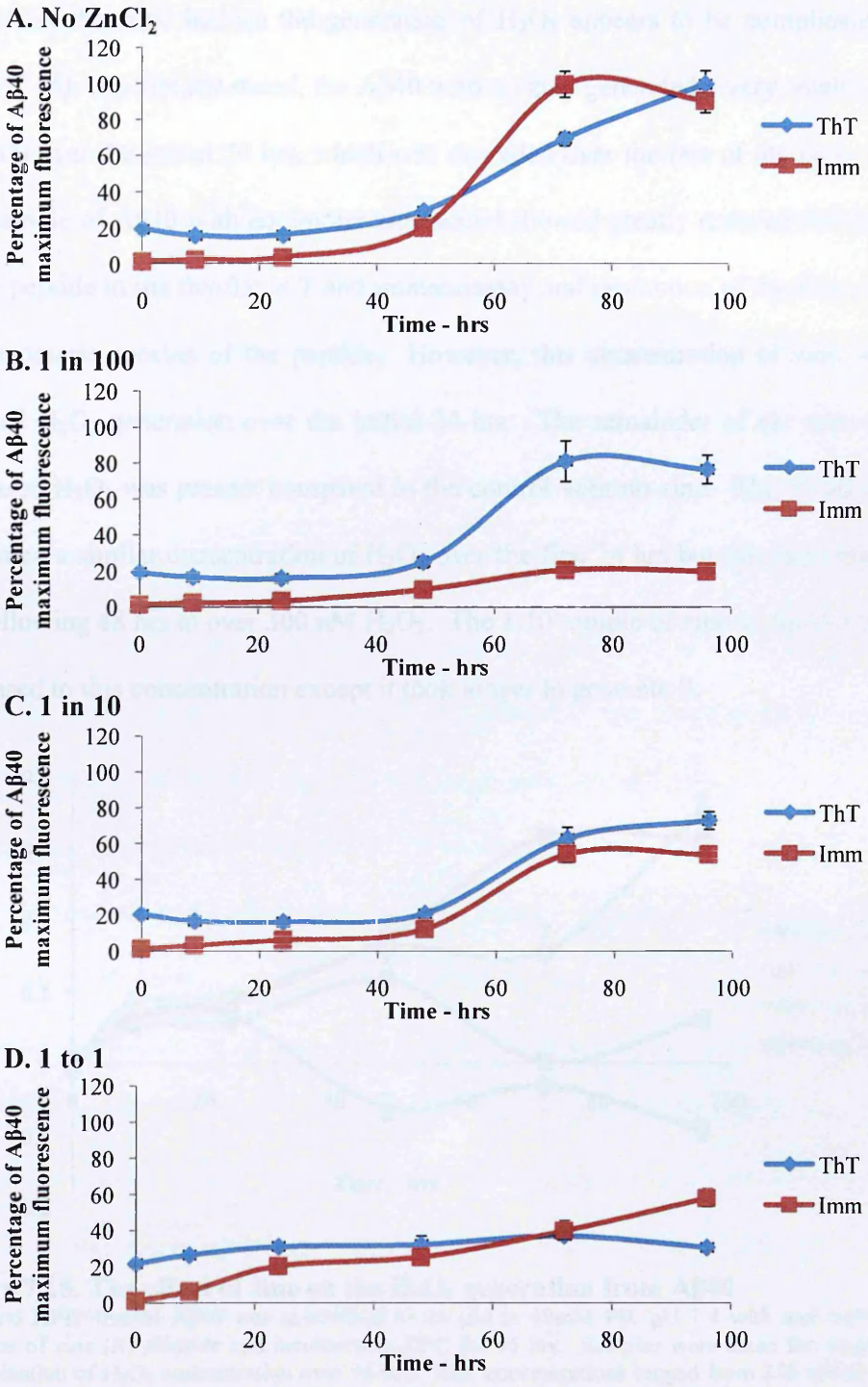

Figure 7.14. The effect of zinc on the aggregation Aβ40

TFA and HFIP treated Aβ40 was solubilised to 25 μM in 10mM PB, pH 7.4 with and without the presence of zinc (II) chloride and incubated at 37°C for 96 hrs. Samples were taken for thioflavin T (ThT) and Immunoassay (Imm) over 96 hrs. Iron concentrations ranged from 250 nM to 25 μM and are expressed as a ratio to Aβ concentration. A = No zinc, B = 250 nM, C = 2.5 μM and D = 25 μM zinc. Results are means ± S.D. (Thioflavin T: n=3, Immunoassay: n=4)

The effect that zinc had on the generation of H_2O_2 appears to be complicated (see figure 7.15). As already stated, the Aβ40 with no zinc generated a very small amount of H_2O_2 over the initial 24 hrs, which was degraded over the rest of the time course. The sample of Aβ40 with equimolar zinc added showed greatly reduced fibrillisation of the peptide in the thioflavin T and immunoassay and promotion of the formation of an oligomeric species of the peptide. However, this concentration of zinc showed reduced H_2O_2 generation over the initial 24 hrs. The remainder of the time course increased H_2O_2 was present compared to the control with no zinc. The 1:100 sample generated a similar concentration of H_2O_2 over the first 24 hrs but this increased over the following 48 hrs to over 300 nM H_2O_2. The 1:10 sample of zinc to Aβ40 similarly increased to this concentration except it took longer to generate it.

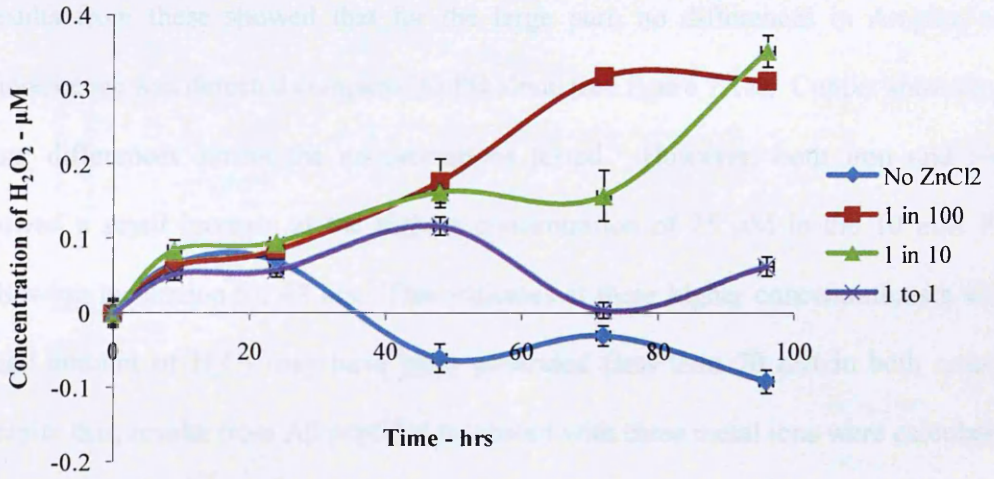

Figure 7.15. The effect of zinc on the H_2O_2 generation from Aβ40
TFA and HFIP treated Aβ40 was solubilised to 25 µM in 10mM PB, pH 7.4 with and without the presence of zinc (II) chloride and incubated at 37°C for 96 hrs. Samples were taken for Amplex red determination of H_2O_2 concentration over 96 hrs. Zinc concentrations ranged from 250 nM to 25 µM and are expressed as a ratio to Aβ concentration. Results are means ± S.D. (n=3)

7.2.3.3. Aggregation and H_2O_2 generation of Aβ42 with zinc

Several of the trends observed with Aβ40 were repeated when testing Aβ42. There was a clear, concentration dependant reduction in thioflavin T fluorescence compared

to the control with no zinc added, indicating a reduction in the fibrillisation of the peptide (see figure 7.16). In addition, when the concentration of zinc was increased to equimolar, the thioflavin T curve loses its sigmoidal shape, becoming shallow in its fluorescence increases in a similar manner to that seen with Aβ40. Immunoassay fluorescence showed small decreases in fluorescence at 1:100 and 1:10 zinc to Aβ42. However, at equimolar zinc to Aβ42, oligomeric immunoassay fluorescence was raised above control levels and was maintained at this level. H_2O_2 generation by these samples remained reasonably constant. Only at equimolar zinc was a small reduction in H_2O_2 generation detected (see figure 7.16 and 7.17).

For each of these experiments the controls were performed at every concentration tested and at every time point with no Aβ present in the metal containing buffer. Results from these showed that for the large part, no differences in Amplex red fluorescence was detected compared to PB alone (see figure 7.18). Copper showed no clear differences across the concentrations tested. However, both iron and zinc showed a small increase at the highest concentration of 25 μM in the 10 mM PB following incubation for 48 hrs. This indicates at these higher concentrations a very small amount of H_2O_2 may have been generated (less than 70 nM in both cases). Despite this, results from Aβ peptides incubated with these metal ions were calculated from the subtraction of the appropriate control reading at each time point; H_2O_2 concentrations calculated are for the contribution of Aβ to the generation of H_2O_2. It is acknowledged that the zinc controls all showed small fluorescence increases at 48 hrs compared to T=0. However, this was likely due to the light sensitivity of the Amplex red working solution. Precautions were taken to try to prevent light exposure, yet sometimes small increases in fluorescence were observed across all samples tested at the same time.

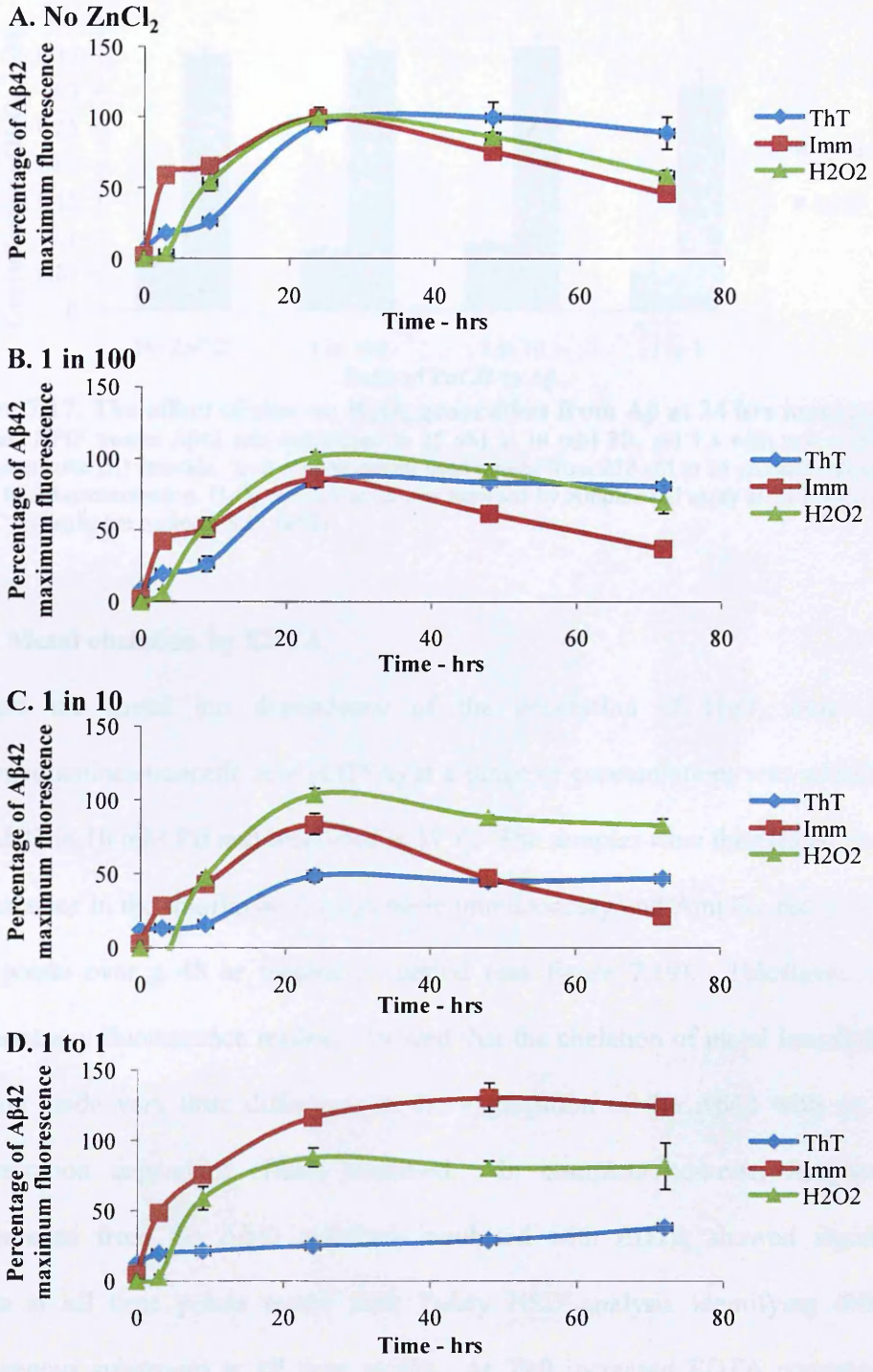

Figure 7.16. The effect of zinc on aggregation and H_2O_2 generation by Aβ42
TFA and HFIP treated Aβ42 was solubilised to 25 μM in 10mM PB, pH 7.4 with and without the presence of zinc (II) chloride and incubated at 37°C for 96 hrs. Samples were taken for thioflavin T (ThT), Immunoassay (Imm) and Amplex red (H_2O_2) over 72 hrs. Zinc concentrations ranged from 250 nM to 25 μM and expressed as a ratio to Aβ concentration. A = No zinc, B = 250 nM, C = 2.5 μM and D = 25 μM zinc. Results are means ± S.D. (Thioflavin T and Amplex red: n=3, Immunoassay: n=4)

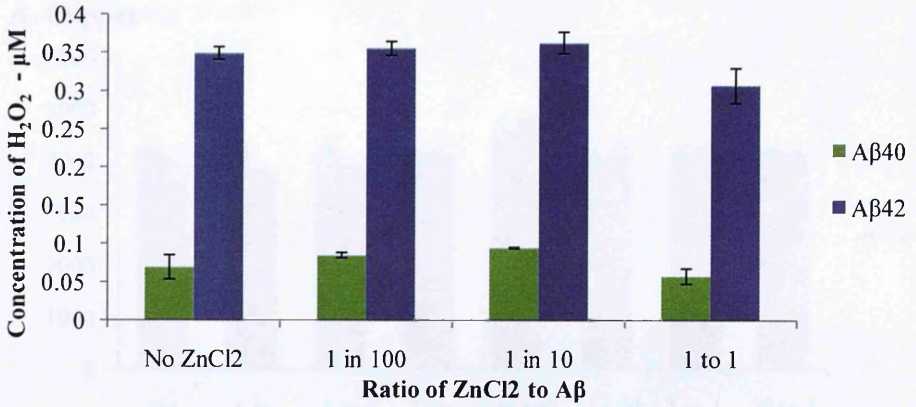

Figure 7.17. The effect of zinc on H_2O_2 generation from Aβ at 24 hrs incubation
TFA and HFIP treated Aβ42 was solubilised to 25 μM in 10 mM PB, pH 7.4 with and without the presence of zinc (II) chloride. Iron concentrations used ranged from 250 nM to 25 μM and expressed as a ratio to Aβ concentration. H_2O_2 concentration was assessed by Amplex red assay at 24 hrs incubation at 37°C. Results are means ± S.D. (n=3)

7.2.3. Metal chelation by EDTA

To test the metal ion dependency of the generation of H_2O_2 from Aβ42, ethylenediaminetetraacetic acid (EDTA) at a range of concentrations was added to 25 μM Aβ42 in 10 mM PB and incubated at 37°C. The samples were then tested for their fluorescence in the thioflavin T, oligomeric immunoassay and Amplex red at various time points over a 48 hr incubation period (see figure 7.19). Thioflavin T and immunoassay fluorescence readings showed that the chelation of metal ions from the solution made very little difference to the aggregation of the Aβ42 with no clear concentration dependant effects observed. In complete contrast, Amplex red fluorescence from the Aβ42 solutions incubated with EDTA showed significant effects at all time points tested with Tukey HSD analysis identifying different homogenous subgroups at all time points. At T=0 increased EDTA concentration caused increased Amplex red fluorescence indicative of up to 250 nM H_2O_2 being made. However, as aggregation proceeded, increasing the concentration of EDTA caused a decrease in the concentration of H_2O_2 generated with T=24 becoming significantly negatively correlated ($r = -0.529$, $p = 0.024$).

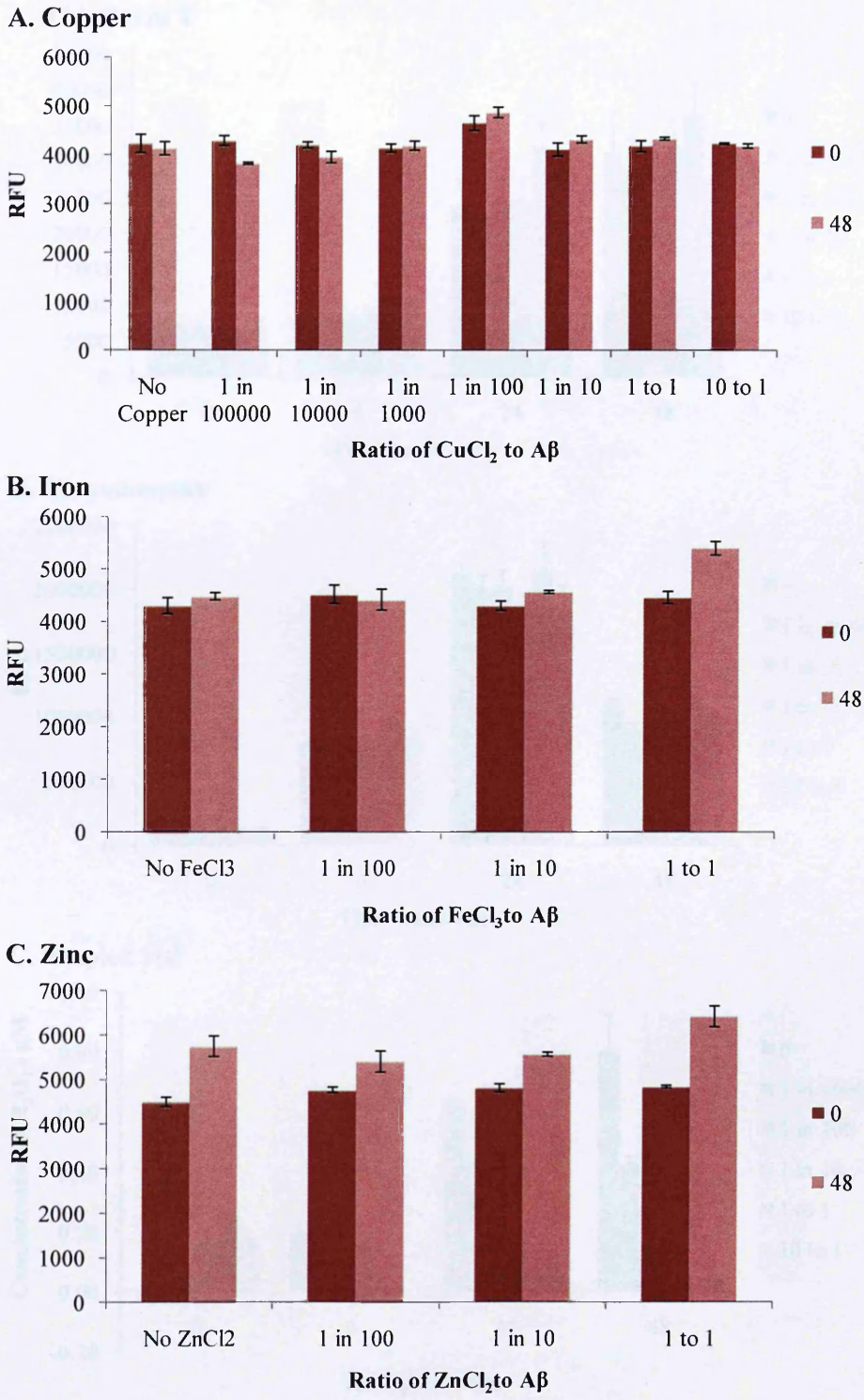

Figure 7.18. The effect of copper, iron and zinc on fluorescence of PB in the Amplex red assay

Every concentration of metal ion tested was also monitored by Amplex red assay throughout the time course of the aggregation experiments. Shown are the fluorescence readings obtained from the solutions at 0 and 48 hrs. A = copper, B = iron and C = zinc. Results are means ± S.D. (n=3)

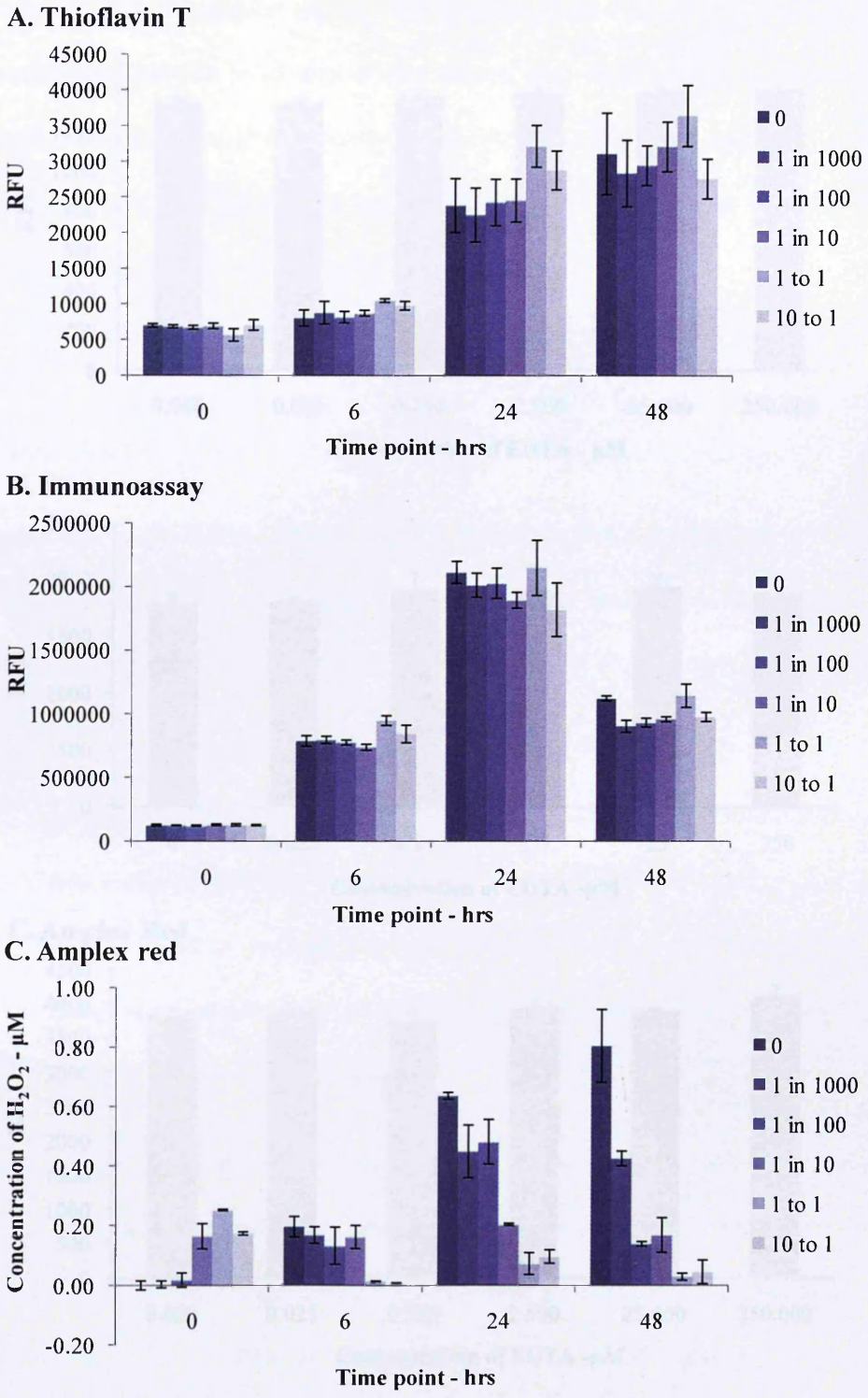

Figure 7.19. The effect of EDTA on aggregation and H_2O_2 generation by Aβ42
TFA and HFIP treated Aβ42 was solubilised to 25 µM in 10mM PB, pH 7.4 with and without the presence of EDTA and incubated at 37°C for 96 hrs. Samples were taken for thioflavin T, Immunoassay and Amplex red over 48 hrs. EDTA concentrations ranged from 25 nM to 250 µM and expressed as a ratio to Aβ concentration. A = thioflavin T, B = oligomeric immunoassay and C = Amplex red. Results are means ± S.D. (Thioflavin T and Amplex red: n=3, Immunoassay: n=4)

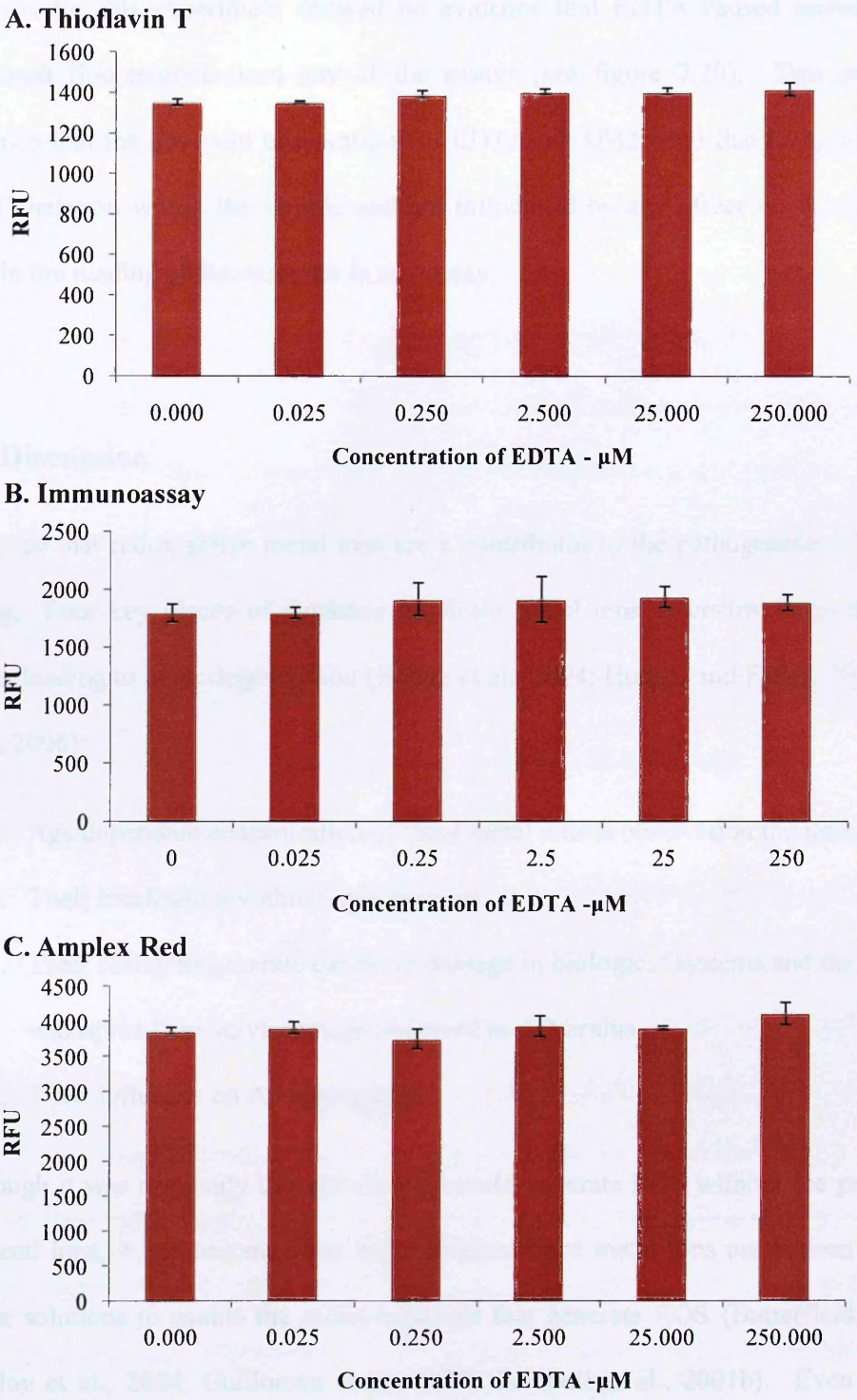

Figure 7.20. The effect of EDTA on fluorescence in the thioflavin T, oligomeric immunoassay and Amplex red assay

A range of EDTA concentrations were made in 10mM PB, pH 7.4. Samples were taken for thioflavin T, Immunoassay and Amplex Red. EDTA concentrations ranged from 25 nM to 250 µM. A = thioflavin T, B = oligomeric immunoassay and C = Amplex red. Results are means ± S.D. (Thioflavin T and Amplex red: n=3, Immunoassay: n=4)

Controls for this experiment showed no evidence that EDTA caused increased or decreased fluorescence from any of the assays (see figure 7.20). This provides evidence that the observed observations of EDTA on Aβ42 were due to its action in metal chelation within the sample and not influenced by any effect on the reagents used in the reading of fluorescence in any assay.

7.3. Discussion

Evidence that redox active metal ions are a contributor to the pathogenesis of AD is strong. Four key pieces of evidence implicate metal ions as central to pathogenic events leading to neurodegeneration (Huang et al., 2004; Hureau and Faller, 2009; Liu et al., 2006):

1. Age dependant concentration of these metal ions is observed in the neocortex
2. Their localisation within senile plaques
3. Their ability to generate oxidative damage in biological systems and the widespread oxidative damage observed in AD brains
4. Their influence on Aβ aggregation

Although it was originally thought that Aβ could generate ROS without the presence of metal ions, it has become clear that sufficient trace metal ions are present within buffer solutions to enable the redox reactions that generate ROS (Butterfield, 2002; Dikalov et al., 2004; Guilloreau et al., 2007; Turnbull et al., 2001b). Even before solubilisation synthetically made Aβ contains significant concentrations of copper and iron (Turnbull et al., 2001b). This chapter investigated the effects that the addition of copper, iron and zinc, the 3 key metal ions implicated in AD pathogenesis, had on both the aggregation and H_2O_2 generation of Aβ40 and Aβ42.

7.3.1. Copper

Aβ has been found to have an unusually strong affinity for binding copper, suggesting a potential functional role for this binding *in vivo* (Atwood et al., 2000b). This was firstly investigated by looking at the changes in thioflavin T and immunoassay fluorescence at T=0, the samples taken immediately following the wetting and sonication of the samples. Despite the strength of copper binding its coordination by Aβ is suggested to be dynamic, with several binding modes rapidly exchanging at room temperature (Hureau and Faller, 2009). For this reason a wide range of copper concentrations was tested from 1:100000 to 10:1 copper to Aβ to help elucidate binding effects at different concentrations.

When Aβ40 was tested increases in both thioflavin T and immunoassay fluorescence were observed at all copper concentrations compared to the sample with no copper added. This suggested that even significantly sub-molar concentrations of copper could induce early self-interactions in this largely monomeric solution of Aβ40. The increase in fluorescence was uniform in the thioflavin T. However in the immunoassay the lower concentrations showed slightly more oligomeric content than the higher concentrations. This may indicate that copper binding Aβ40 promotes different self interactions at different concentrations as the effect is not wholly concentration dependent. This data also reflects the increased sensitivity that the immunoassay has for early oligomeric interactions compared to thioflavin T. Evidence that copper (promoted by the presence of H_2O_2) forms dityrosine cross-links (Atwood et al., 2004) was investigated in chapter 5. During those experiments it was found Aβ40 to require 24 hrs for SDS-stable cross-links to be detected using a range of copper and H_2O_2 concentrations. This suggests that the increased fluorescence observed here is not due to the formation of dityrosine dimers, or any other form of

SDS-stable oligomeric Aβ species. In which case, the presence of the copper may be promoting rapid structural changes, such as promoting the switch to β-sheet conformation, but also having an effect on the ability of the Aβ40 to self-interact and perhaps the stability of those interactions without forming covalently cross-linked Aβ.

With Aβ42 there was no concentration dependant effect of these levels of copper on the initial aggregation state of the peptide. At 1:1000 and 10:1 copper to Aβ42 rapid interactions were observed, significantly increasing thioflavin T and immunoassay fluorescence (Tukey HSD $p \leq 0.000$). With Aβ42 several different types of early species may be present at T=0. The different concentrations of copper may be encouraging changes in these Aβ42-Aβ42 interactions in different ways for different species of Aβ42. Another, not exclusive explanation is that different levels of metalation of Aβ42 may promote different forms of Aβ self-interacting species. It has been reported that Aβ42 could theoretically bind up to 2.5 Cu(II) ions per peptide unit (Atwood et al., 2000b). This may be the case where excess copper was added to the Aβ (10:1), yet it is unlikely that this is also the case at 1:1000 copper ions to Aβ42 subunits. Yet, both generated increases in fluorescence in both assays. This supports different binding interactions between the Aβ42 and copper possibly promote different aggregation pathways. Similarly to Aβ40 though, cross-linking experiments suggested these copper promoted increases in Aβ-Aβ interactions were not due to SDS-stable interactions such as the formation of dityrosine dimers.

Aβ40, being largely monomeric upon wetting, aggregated slowly with no copper added, generating H_2O_2 over the initial 6 hours followed by a decrease in Amplex red fluorescence indicating H_2O_2 degradation. This suggests that, if a specific early Aβ species is responsible for H_2O_2 generation, then it is formed early in Aβ40 aggregation, but does not persist in the solution. Aβ42 aggregated at an increased

rate, generated more H_2O_2 and did not show the sharp decreases in H_2O_2 concentration that were observed in Aβ40 solutions. This may be related to a greater biological function of Aβ40 as an antioxidant rather than pro-oxidant. Interpretation of Aβ42 results are complicated by its greater tendency for aggregation and the fact that even deseeded samples contain some proportion of aggregated Aβ42. Measurements should be to be considered the net effect of copper on a range of Aβ42 species present at any particular point in time.

All samples of Aβ40 with 1:1000 or less copper added to them showed similar aggregation and H_2O_2 generation over the initial 6 hrs aggregation. After 6 hrs however, the H_2O_2 measured from these samples differs between further generation and degradation. This shows that these low concentrations of copper have little effect on the formation of the H_2O_2 generating species of Aβ, but may affect its longevity in solution as degradation of H_2O_2 was not as pronounced with only 1:100000 copper added. The degradation of H_2O_2 observed with Aβ40 supports the idea that that Aβ aggregation consists of different stages that differentially generate and degrade H_2O_2 (as observed in chapter 4 and 6). It is possible that this is directly determined by the oxidation state of the peptide and mediated by H_2O_2 directed oxidation of susceptible Aβ residues. These processes may be proceeding concurrently in an aggregating solution, and may contribute to the aggregation process via moderation of Aβ self-oxidation, i.e. the stabilising effect of dityrosine dimers.

Like Aβ40, aggregation of Aβ42 at 1:100000 and 1:10000 copper to Aβ, can be considered very similar to the sample with no copper, except there is an increase in oligomeric immunoassay fluorescence. Concurrently, the generation of H_2O_2 remains reasonably equivalent up to 12 hrs incubation yet after this point there is an increase in H_2O_2 generation by these samples. This supports observations with Aβ40 that these

low copper concentrations may act to prolong oligomeric interactions conducive of H_2O_2 generation. Increasing the concentration a further tenfold, does not show further increases in immunoassay fluorescence. Instead a broader peak was observed together with decreased fibrillisation, indicated by thioflavin T fluorescence. Concurrently, H_2O_2 generation was increased again, possibly due to extending the lifespan of oligomeric Aβ and subsequently the period in which H_2O_2 was generated.

As copper concentration increases within the samples of Aβ, the generation of H_2O_2 during the time course appears to be the result of a trade-off between concurrent effects of copper on the Aβ: increasing copper concentration appears to increase the stability/longevity of the H_2O_2 generating species together with increasing their redox potential, yet also promotes further aggregation. When copper was raised to 1:100 and 1:10 molar ratio with Aβ40, aggregation, particularly in the immunoassay was increased, indicating promotion of the formation of oligomeric Aβ. This was concurrent to significantly more H_2O_2 being generated by these samples by 6 hrs, with 1:10 more so than 1:100 (Tukey HSD $p \leq 0.000$, Pearson's $r = 0.854$, $p = 0.000$) supporting evidence that a key oligomeric species is responsible for H_2O_2 generation. A similar concentration dependent effect of copper on increasing H_2O_2 generation was also observed with Aβ42. This suggests that these copper concentrations may be playing a role in the formation of the H_2O_2 generating oligomeric species in addition to preserving its existence in solution and increasing facilitation of redox reactions.

Further increases in copper concentration to 1:1 and 10:1 appeared to prevent fibrillisation of Aβ40 and Aβ42. Both peptides showed early H_2O_2 generation to be promoted at 1:1 copper to Aβ but this rapidly declined. This effect was emphasized at 10:1 copper to Aβ as aggregation was further inhibited and degradation of the H_2O_2 generated promoted. High copper concentrations promote H_2O_2 generation

presumably due to its coordination within a greater number of Aβ molecules promoting the redox abilities of both peptides, yet, maybe this promotes the formation of non-H_2O_2 generating Aβ species rather than fibrils. High levels of copper may bind in such a way as to prevent the proliferation of β-sheet structure via Aβ fibrillisation. This is supported by evidence by Smith and colleagues that supra-molar concentrations of copper do not form fibrils but form spherical and amorphous Aβ aggregates (Smith et al., 2007b). It may be that these high copper concentrations result in prolific Aβ oxidation, cross-linking the peptide into these aggregates possibly halting generation of H_2O_2 by the Aβ. Following the research of copper/H_2O_2 cross-linking (chapter 5) it would be my hypothesis that the spherical oligomers observed by Dr. D.P. Smith may be composed of the Aβ42 tetramers observed by SDS-PAGE.

The concentration dependant effects of copper on H_2O_2 generation could be seen at 6 hrs and 3 hrs incubation for Aβ40 and Aβ42 respectively. Aβ42 showed early H_2O_2 generation to be concentration dependent implicating copper binding as key in Aβ mediated formation of H_2O_2. With Aβ40, sufficiently low concentrations of copper had very little effect on early aggregation nor were the redox capabilities of the peptide increased due to copper binding: the concentration of H_2O_2 generated remained reasonably constant. As the copper concentration increases past 1:1000 early aggregation intermediates were promoted over fibrils, concurrent to increased levels of copper binding to the peptide, thus the concentration of H_2O_2 generated gradually increases. When copper was in excess (10:1) Aβ becomes maximally copper bound and oxidised rapidly, driving it through its H_2O_2 generating phase quickly, degrading that which is made.

A point to remember is that in the brain the subject of oxidation events is likely not to be primarily Aβ itself but other biological targets such as membrane lipids especially

if Aβ is membrane associated. At low copper concentrations Aβ40, despite generating some H_2O_2 initially, may actually have greater antioxidant properties *in vivo*. As copper increases though it loses its antioxidant properties and becomes a pro-oxidant, due to increased Aβ/copper mediated redox reactions. With a reduction in subsequent self-oxidations the lifespan of early oligomers may be extended greatly. Aβ42 generates more H_2O_2, probably due to an increased interaction with copper and tendency for aggregation forming H_2O_2 generating oligomers. With increased copper binding again the copper promotes structural changes increasing H_2O_2 generation further which, *in vivo*, may continue to be generated if other targets are the subject of oxidation reactions rather than Aβ. It may be that these interactions are actually relevant to the yet to determined biological function of Aβ.

The reactions that generate H_2O_2 from redox cycling of copper require Cu(II) to be reduced to Cu(I). As discussed in chapter 4, without the addition of an external reductant, Met35 is the most likely candidate for this electron donation. Research performed with the addition of a reductant has found Aβ/copper complexes to generate more H_2O_2 than copper and reductant alone (Hureau and Faller, 2009). This seems quite reasonable to expect as a potent reductant would be expected to be more efficient at reducing Cu(II) than Met35. However, this seems an irrelevant comparison to make as free copper is kept to an absolute minimum in the body to ensure its damaging redox activities are kept to an absolute minimum. Instead copper is kept bound to copper binding proteins. A more relevant comparison observed by Hureau and Faller is that Aβ/copper complexes generate more ROS than other copper complexes (Guilloreau et al., 2007; Hureau and Faller, 2009). This shows that it is more oxidative than other complexes, in a biologically relevant manner.

Work by Nadal and colleagues that initially appeared to contradict our findings with Aβ/copper complexes actually supported our observations. They found that monomeric and fibrillar Aβ/copper not to generate H_2O_2 (again in comparison to copper plus reductant – a biologically irrelevant sample), but did not test any intermediate Aβ species (Nadal et al., 2008). In agreement, my research has found no evidence that either monomers or fibrils were capable of H_2O_2 generation. Unfortunately, if they had been able to test oligomeric Aβ they would have probably come to the same conclusion as they only allowed 1 hr for the generation of H_2O_2, and their assay was not sensitive enough to measure the levels of H_2O_2 that we have determined to be made from Aβ. The fact remains that testing oligomeric Aβ is fraught with issues due to the heterogeneous and ever-changing composition of a solution of Aβ. Hopefully further development of the immobilisation technique (described in chapter 6) may help in this respect. They suggest that monomeric Aβ may act as an antioxidant in so far as it binds free copper, removing its free copper redox potential from solution. The fact is that if this binding then promotes H_2O_2 generation in oligomeric forms of Aβ it becomes a pro-oxidant. Although this may not be more so than Cu(II) alone, it may be biologically relevant and directed at susceptible cellular features such as the PM.

The fact that copper does not exist freely in the brain poses another line of investigation: using the addition of chelated copper to solutions of Aβ. This would enable determination of how increasing copper concentrations effects H_2O_2 generation, in what may be considered a more biologically relevant manner.

7.3.2. Iron

Despite iron being found localised in senile plaques, Aβ is not believed to bind to iron as it does with copper although it has been reported to promote Aβ aggregation (Smith et al., 2007a). The effect of iron on aggregation of Aβ40 and Aβ42 was tested, alongside its effects on the generation of H_2O_2. Data certainly indicated iron to have a much reduced effect on the aggregation state of the peptides. With Aβ40 neither thioflavin T nor immunoassay fluorescence showed any difference to the sample with no iron added at T=0. Compared to copper, this indicates any interaction the Aβ40 may have with iron does not have a rapid effect on the aggregation state of the peptide. When tested on Aβ42, iron showed some increases in immunoassay fluorescence at T=0 compared to the sample with no iron. However, these increases were not paralleled by changes in thioflavin T fluorescence suggesting that Aβ-Aβ interactions may have been increased somewhat yet are not associated with structural changes promoting β-sheet.

Aggregation of Aβ40 with iron showed some concentration dependent increases in aggregation, notably at 48 hrs incubation when the Aβ40 initially starts to aggregate. However, these differences in aggregation did not correspond to any changes in Amplex red fluorescence that might implicate iron partaking in redox cycling with Aβ40. If Aβ40 was able to reduce Fe(III) to Fe(II) then we would expect to see variation in the H_2O_2 generated. These results were emulated by incubation of Aβ42 with iron; the addition of iron somewhat promoting aggregation associated increases, yet no significant differences in H_2O_2 generation was observed (All Tukey HSD comparisons $p > 0.1$). This suggests that although weak interactions may occur between Aβ and iron that may promote early aggregation to some extent, these interactions are not facilitative of redox reactions and H_2O_2 generation. This suggests

that the copper binding site may not the same as the site of iron interaction as displacement of copper ions would presumably reduce H_2O_2 generation. An interesting control experiment to test this would be to try cross-linking Aβ with iron and H_2O_2 to see if iron is also unable to oxidatively modify Aβ, reactions that copper readily partakes in. This supports evidence from others that Aβ does not directly bind iron and that altered iron homeostasis and sequestration into senile plaques may be due to secondary effects (Smith et al., 2007a).

7.3.3. Zinc

Existing evidence of the role played by zinc in the aggregation of Aβ and its connections to the pathogenesis of AD is unclear and sometimes conflicting. Unlike iron, evidence does suggest Aβ-zinc interactions to be physiologically relevant (Bush et al., 1994). However, whether this interaction is neurotoxic, neuroprotective or even relevant to AD is up for debate. Upon wetting of the peptides both Aβ40 and Aβ42 were found to have rapid changes in their aggregation associated fluorescence, although in different respects. Aβ40 despite being largely monomeric following deseeding showed a small decrease in immunoassay fluorescence when at 1:1 Aβ to zinc. On the other hand, Aβ42 showed concentration dependent increases in both thioflavin T and immunoassay fluorescence at T=0. This indicates that zinc binds rapidly to Aβ to induce these changes. In Aβ40 the binding of zinc promotes a conformation facilitating monomeric Aβ40. However, in Aβ42 its binding promotes β-sheet formation and self-interactions indicative of promotion of aggregation.

When Aβ40 was aggregated with these levels of zinc, complex concentration dependent binding effects were observed. At 1:100 zinc to Aβ40 immunoassay fluorescence was reduced yet thioflavin T fluorescence shows only a small reduction.

Interpretation of this isn't straightforward. Both low-order oligomers and fibrils generate low immunoassay fluorescence perhaps aiding its explanation. If zinc binds Aβ40 with a strong affinity it is possible that one effect is produced from those molecules bound by the zinc and another by those not zinc-bound: a proportion of the sample may aggregate to fibrils, but the low level of zinc ions binding to Aβ40 was able to prevent aggregation of a proportion of oligomers. Increasing zinc to Aβ40 to 1:10 and further to 1:1 supports this idea, generating separate zinc-bound and non zinc-bound effects. The increased proportion of Aβ40 that was zinc-bound was increasingly prevented from fibrillisation (reducing thioflavin T fluorescence) and preferentially forms zinc bound oligomers (increasing early immunoassay fluorescence).

The effect that zinc had on H_2O_2 generation by Aβ40 was complex but may be attributed to a combination of effects: the decreased fibrillisation rate prolonging the longevity of oligomeric species, the proportion of oligomers zinc bound and the reduced capacity for H_2O_2 generation by zinc-bound oligomers. The reduced fibrillisation exerted by the presence of zinc appeared to also reduce the degradation of H_2O_2 implying zinc binding may protect Aβ against oxidative events. In this respect it may also be of interest to test the effects of zinc on the copper/H_2O_2 dependent cross-linking performed in chapter 5. Would cross-linking be prevented, or may be it that different Aβ cross-linked species may be formed?

Results with Aβ42 support the deductions from Aβ40; the binding of zinc to Aβ42 appeared to inhibit fibrillisation yet promote the formation/longevity of certain oligomeric species of Aβ. The main difference was the increased speed at which Aβ42 aggregation proceeds. H_2O_2 generation from these samples was consistent, except for a small decrease in its generation when at 1:1 zinc to Aβ42 supporting

observations with Aβ40: zinc appears not to facilitate redox reactions by the peptide and its binding to Aβ42 promotes formation of oligomers have a reduced capacity for H_2O_2 generation compared to non-zinc bound species.

It has been determined that copper and zinc ions would be coordinated by the same 3 histidine residues. Therefore, in theory, zinc would have to displace copper to cause a reduction in its H_2O_2 generation. The quantities of zinc tested here were equimolar with Aβ and lower, but the endogenous copper present in the solution would be far reduced in comparison. In these samples a concentration dependent proportion of the Aβ present would be either zinc or copper bound. However, as soon as Aβ-Aβ interactions occur, an oligomeric Aβ species may be bound by zinc, copper or both metal ions increasing the potential for a range of effects to be elicited dependant on the levels of these metal ions. This implicates zinc in playing a regulatory role in binding Aβ, perhaps by providing competition for copper binding. This may go some way to explaining the contradictory effects observed when testing the effects of zinc with Aβ as they are highly concentration and time dependant. The observation that the generation of H_2O_2 by Aβ was augmented greater by zinc with Aβ40 than Aβ42, suggests that Aβ40 may have a greater inclination than Aβ42 to bind zinc over copper. This may be directly linked to the enhanced toxicity of Aβ42 over Aβ40 or possibly the actual biological function of Aβ.

There is evidence that Aβ, in AD, may be a corrupted antioxidant, with gain of toxicity being concentration, metalation and oxidation dependent (Smith et al., 2007a). This bares similarities to the hypothesised pathogenesis of Amyotrophic Lateral Sclerosis (ALS) where mutations in the gene for superoxide dismutase (SOD1) cause the familial disease (Bruijn et al., 1998). Presumably these mutations disable the antioxidant properties of the protein leading to increased oxidative stress. It has even

been postulated that Aβ may act as a SOD mimetic as it bears similar properties at low concentrations (Atwood et al., 2000b; Lynch et al., 2000). When bound to both copper and zinc simultaneously (like in SOD1) Aβ has been shown to have catalytic SOD-like activity with oxidative stress stimulating its production (Lynch et al., 2000). The supposition that Aβ may be an antioxidant when interacting with both copper and zinc, the zinc providing structural integrity (preventing fibrillisation) and regulating copper/Aβ redox activity is supported by the observations in this study (Lynch et al., 2000). In support of these interactions being related to neurodegeneration in AD, Aβ42 incubated with both copper and zinc has been found to have a lower toxicity than Aβ42 incubated with copper alone, reportedly due to zinc suppressing copper mediated production of H_2O_2 (Cuajungco et al., 2000). Testing of zinc and copper by the immobilisation technique described in chapter 6 may help clarify the roles of these metal ions.

7.3.4. H_2O_2 generation is metal dependent

The dependency of redox metal ions for the generation of H_2O_2 was tested by the addition of a range of EDTA concentrations. EDTA is a strong metal chelating agent for metal ions such as Cu(II) and Fe(III) due to its ability to act as a hexadentate ligand, coordinating the metal ion in a stable and soluble state. At no concentration did the presence of EDTA alter the aggregation of Aβ42. This was not wholly unexpected as it had been observed that the addition of very low concentrations of metals (below 1 in 10000 copper to Aβ) had only minor effects on the aggregation of Aβ; chelation of the trace metals in solution would also generate only slight differences. This implies that the residual metal ion concentration in the samples is low but also that metal interactions are not actually needed for aggregation of Aβ42.

On the other hand, the generation of H_2O_2 was severely reduced by the addition of EDTA, where clear concentration dependent decreases in the generation of H_2O_2 were observed. On a side note, at T=0 increasing the level of EDTA actually showed a small increase in H_2O_2 detected. This implies that loss of copper ions from Aβ42 to EDTA may have actually caused some redox cycling of the copper forming H_2O_2. This however, is rapidly quenched and overall the chelation of the residual metal ions in the samples prevented the interaction of Aβ with the ions, inhibiting Aβ mediated generation of H_2O_2. Considering the evidence presented, copper is presumably the principle ion involved in H_2O_2 generation. This supports evidence that the low level of residual copper in buffer solutions and even in the peptide at point of manufacture are sufficient to support H_2O_2 generation by Aβ.

It actually required a relatively high concentration of EDTA to remove H_2O_2 generation from the Aβ42. This would appear to suggest that either Aβ has a very high affinity for copper, or, there is more copper present in the samples than originally thought. However, trace levels of other metals such as iron would also be present, which would presumably be chelated preferentially to binding copper that is already Aβ-bound.

7.4. Conclusions

- Metal ions may have a central role in the pathogenesis of AD
- The experimental results support the generation of H_2O_2 as being a factor of the longevity and redox potential of Aβ aggregation intermediates
- Both Aβ40 and Aβ42 showed rapid increases in aggregation associated Aβ-Aβ interactions when incubated with copper, even at very low concentrations

- The effects of copper on Aβ aggregation and its generation of H_2O_2 are complex and highly interconnected
- Low sub-molar copper concentrations appear to increase the stability and longevity of the Aβ species generating H_2O_2
- Increasing copper towards equimolar and above appears to promote the formation of Aβ-Aβ interactions that facilitate H_2O_2 generation
- Increasing copper concentration increases the redox potential of the Aβ solution. However, the increased generation of H_2O_2 has the potential for oxidizing Aβ at susceptible residues, which appears to halt its ability to generate H_2O_2
- Any interaction of iron with Aβ appears to be weak with very little effect on aggregation but also iron does not appear to take part in Aβ-mediated redox reactions generating H_2O_2
- The effects of zinc were complex but the ion appeared to bind Aβ preventing fibrillisation and promoting the formation/stabilization of a pre-fibrillar form of Aβ that appeared to have a reduced capacity for H_2O_2 generation
- Zinc did not appear to facilitate Aβ-mediated redox reactions but instead appeared to have a regulatory role
- The chelation of metal ions had no effect on the aggregation of Aβ42 yet metal chelation eliminated H_2O_2 generation from Aβ42 showing the interaction of metal ions, most likely copper, with Aβ42 is critical for the redox reactions generating H_2O_2
- These experiments clearly show that Aβ requires the binding of copper to be able to generate H_2O_2 from redox reactions initiated by the Aβ mediated reduction of Cu(II) to Cu(I).

Chapter 8
The effect of short peptide aggregation inhibitors on H_2O_2 generation by β-amyloid

8.1. Introduction

The development of drugs which could alter the course of the disease is focused largely on reducing Aβ load. There are several different approaches being investigated which can be largely grouped into either trying to reduce Aβ production and aggregation or increase the clearance of Aβ (Blennow et al., 2006). Strategies include modulation of secretase action, immunotherapy, inhibition of aggregation and antioxidant therapy. In this chapter, a group of short peptide inhibitors have been investigated to assess their ability to inhibit the very early stages of aggregation, oligomer formation and H_2O_2 generation.

8.1.1. Secretase modulation

The two enzymes responsible for the production of Aβ are β-secretase (BACE1) and γ-secretase. Inhibiting the action of BACE1 is a highly attractive therapeutic strategy considering BACE1 knockout mice have no Aβ production together with no clinical phenotype (Luo et al., 2001). However, extrapolating these observations to humans requires consideration of the differences between the species; murine Aβ is different to human Aβ, Aβ production may be essential in humans or APP may not be BACE's physiological substrate. Inhibitors have been developed and have been found to lower the concentration of Aβ in the brain of AD transgenic mice (Chang et al., 2004). γ-secretase also cleaves other biological substrates (such as notch) and is consequently far less attractive as a therapeutic strategy. However, some γ-secretase inhibitors have

been developed that are not thought to affect the notch signalling pathways and these show good tolerability in phase I studies (Petit et al., 2001; Siemers et al., 2005). α-secretase stimulation is another strategy which would theoretically shift processing of APP towards the non-amyloidogenic pathway. An anticancer treatment in clinical trials called Bryostatin has been found to stimulate α-secretase, reducing Aβ production in AD transgenic mice (Etcheberrigaray et al., 2004).

8.1.2. Aβ immunotherapy

Research using AD transgenic mice found active immunisation with fibrillar Aβ raises antibodies against Aβ that attenuates deposition of Aβ into plaques (Schenk et al., 1999). Passive immunisation using anti-Aβ antibodies has also been found to halt plaque formation (Bard et al., 2000). The effect of anti-Aβ antibodies has been attributed to either binding Aβ in plaques, activating microglia to clear the peptide, or, binding soluble Aβ in the periphery, hence driving the efflux of Aβ from the brain. Following successful animal testing, a pre-aggregated Aβ42 vaccine called AN1792 went into clinical trials (Schenk et al., 2004). Disappointingly 6% of cases developed encephalitis, thus phase IIa trials had to be interrupted (Orgogozo et al., 2003). This was thought to be due to the mid- and C-terminal parts of Aβ inducing a T-cell response. Long term follow up examination determined that plaques were cleared in patients with AD yet this did not prevent progressive neurodegeneration (Holmes et al., 2008). This has led to the development of Aβ immunoconjugates to deliver active immunisation. These should avoid the adverse immune system activation as just the N-terminal fragment of Aβ is used, attached to either a carrier protein of a virus-like particle. These went into phase II trials along with passive immunisation with humanised anti-Aβ monoclonal antibodies (Schenk et al., 2004).

8.1.3. Aβ fibrillisation inhibition

This approach relies on inhibiting the interaction of pro-fibrillisation agents with Aβ. In theory, if the conformation of Aβ can be prevented from becoming β-sheet rich subsequent fibrillisation would be prevented. One tactic aims to disrupt interactions between Aβ and ApoE and with other Aβ-interacting molecules, obstructing potential interactions that augment formation of β-folded Aβ. Two small peptides have been developed that have been shown to interact in this fashion, reducing Aβ fibrillisation and Aβ load *in vitro* and in AD transgenic mice. These peptides have so far been found to act with no activated immune response (Permanne et al., 2002; Sadowski et al., 2004b). Colostrinin (CLN) is a proline rich polypeptide derived from colostrums which is thought to reduce Aβ fibril content, protecting cultured cells from its toxic effects (Schuster et al., 2005). Another tactic has been to prevent the interaction of glycosaminoglycans with Aβ which reportedly binds Aβ promoting its aggregation. A mimetic glycosaminoglycan which can interfere with this interaction has entered phase III trials (Blennow et al., 2006; van Horssen et al., 2003).

8.1.4. Antioxidants

Oxidative stress may be the primary cause of neurodegeneration in AD and other forms of dementia, with the senile plaque formation and NFTs being downstream events. This makes it an attractive target for potential therapeutics as it has the potential to be able to alter the course of the disease. Antioxidants are thought to slow the symptoms of AD and other dementias. However due to CNS being non-regenerative, and the widespread neurodegeneration upon diagnosis of AD, their use may be best reserved as a prophylactic throughout aging (Moreira et al., 2006; Sano, 2003). The protective value of taking antioxidants throughout life seems logical as

free radicals and oxidative stress have long been thought to be the source of aging. However, they do not tackle the source of the generation of ROS. It is suggested that it is unlikely that a high enough concentration could be administered to detoxify the cascade of ROS produced once the disease has taken hold (Smith et al., 2007a).

Several studies have found direct links between antioxidant intake in the elderly and a decreased incidence of dementia. Dietary antioxidants, such as Vitamin C and E, ubiquinone, lipoic acid, β-carotene, melatonin, ginkgo biloba and curcumin, are able to scavenge free radicals, detoxifying them. Vitamins C and E have been reported to inhibit Aβ-mediated production of nitric oxide (NO), a type of ROS (Chauhan and Chauhan, 2006). Some reports suggest AD risk may be reduced by these vitamins. It's reported that moderate to severe AD patients taking vitamin E (α-tocopherol) for 2 yrs showed a slight improvement in neurological decline. Other trials have had similar results but some have shown no benefit (Petersen et al., 2005; Sano et al., 1997). The contrary results may reflect the neuronal loss upon diagnosis and that by this point antioxidant treatment may only have marginal effects. In several animal models Ginkgo biloba extract EGb 761 is described as having neuroprotective effects attributed to its antioxidant activities. Aβ-induced free radical production and apoptosis were found to be prevented by its addition to cell cultures. It is also reported to improve or at least maintain AD cognitive function, nevertheless a recent double blind trial showed no significant benefit (Schneider et al., 2005; Yao et al., 2001). A yellow phenolic pigment found in turmeric called curcumin has also been associated with neuroprotective properties (Smith et al., 2007a). This spice is used in Indian cooking and, perhaps coincidentally, prevalence of AD in India is around 4.4 fold less than in the USA (Ganguli et al., 2000). It has been found to protect against Aβ-mediated toxicity, is anti-amyloidogenic and has anti-oxidant properties.

Curcumin binds redox active metals copper and iron effectively acting as a chelator of these ions, perhaps preventing their disease associated interactions with Aβ (Cole et al., 2005; Yang et al., 2005). This is being investigated as a potential therapy for AD. Other sources of antioxidants have been suggested as having neuroprotective properties, such as walnuts which are high in antioxidants and inhibit Aβ fibrillisation (Chauhan et al., 2004; Chauhan and Chauhan, 2006).

Metal chelators have been of interest as metals can promote Aβ aggregation and also permit oxidative reactions. Clioquinol (PBT-1) is one such metal chelator being investigated that has been found to decrease Aβ aggregates in AD transgenic mice but phase II trials had to be discontinued as a toxic impurity was formed (Ritchie et al., 2003). Further trials are now underway on an adapted chelator (PBT-2) which should avoid this toxicity. Clioquinol has been found to inhibit H_2O_2 production by Aβ-metal complexes, possibly a key pathogenic event leading to neurodegeneration (Barnham et al., 2004). The BBB is an obstacle for treatment. In nature metal chelators are largely hydrophilic and so cannot cross the BBB. However clioquinol is hydrophobic and reportedly can pass through the BBB (Smith et al., 2007a).

In addition, present therapeutic Galantamine, has been found to somewhat inhibit Aβ aggregation and protect against Aβ mediated cell death in SH-SY5Y human neuroblastoma cells and oxidative stress induced by Aβ in cortical neurons (Matharu et al., 2009; Melo et al., 2009).

8.1.5. Short peptide inhibitors

Strengthening evidence suggests that Aβ-mediated toxicity is due to early soluble oligomers and may be directly responsible for neurodegeneration in AD (Cleary et al., 2005; Haass and Selkoe, 2007; Kim et al., 2003; Lambert et al., 1998; Lashuel et al.,

2002; Walsh et al., 2002; Walsh and Selkoe, 2007). Consequently, one key strategy for preventing Aβ toxicity is to inhibit the very early stages of aggregation. An inhibitor that is limited to reducing the elongation rate of fibrillar material may prolong the longevity of earlier Aβ species, including the implicated toxic species. Inhibiting oligomer formation may target the underlying cause of AD making it a significant potential therapeutic strategy (De Felice et al., 2004) .

Several peptide-based approaches have evolved to prevent Aβ aggregation (Sciarretta et al., 2006). Central to their development is consideration of the region of Aβ thought to be responsible for the self-association reactions that initiate Aβ oligomerisation. This has been identified as being via residues 16-22 (KLVFFAE) (Tjernberg et al., 1999; Tjernberg et al., 1996). However, for propagation of aggregation, other residues of Aβ around this sequence are required (Tjernberg et al., 1999). A short peptide based on this sequence can theoretically bind to this region of an Aβ molecule thus preventing Aβ-Aβ interaction. One approach incorporates proline residues to form "β-sheet breaker" peptides that bind to Aβ but the proline residues prevent β-sheet formation, potentially a prerequisite for oligomer formation (Soto et al., 1996). A different strategy uses N-methylation of the inhibitor sequence. This modification allows hydrogen bonding to Aβ, but the replacement of a backbone NH group with N-methylation prevents further hydrogen bonding of the β-sheet formation (Kokkoni et al., 2006).

Here, the inhibitors OR1 and OR2 have been investigated. These peptides contain the sequence KLVFF, residues 16-20 of Aβ. To aid solubility and to prevent its own self-association (which may actually seed Aβ aggregation) a cationic arginine has been added at both the N- and C-terminus of the peptide, together with a Glycine spacer. This spacer residue is designed to improve binding of the KLVFF sequence to the

corresponding Aβ sequence (shown in figure 8.1) (Austen et al., 2008). Both OR1 and OR2 have been found to inhibit fibrillogenesis but only OR2 (with an amidated C-terminus) is thought to prevent oligomer formation. This peptide also prevented Aβ mediated toxicity to SH-SY5Y neuroblastoma cells (Austen et al., 2008).

OR1 $H_2N-R\rightarrow G\rightarrow K\rightarrow L\rightarrow V\rightarrow F\rightarrow F\rightarrow G\rightarrow R-COOH$

OR2 $H_2N-R\rightarrow G\rightarrow K\rightarrow L\rightarrow V\rightarrow F\rightarrow F\rightarrow G\rightarrow R-NH_2$

RI-OR2 $H_2N-r\leftarrow G\leftarrow k\leftarrow l\leftarrow v\leftarrow f\leftarrow f\leftarrow G\leftarrow r-Ac$

Figure 8.1. Structures of OR1, OR2 and RI-OR2
L-amino acids are in uppercase and D-amino acids in lowercase, with the direction of the peptide bonds indicated by arrows (Glycine has no separate enantiomers).

OR2 may prevent oligomer formation but its susceptibility to proteolytic attack means that it is not viable as a drug candidate. The peptide has been subsequently developed to retain the inhibitory properties yet avoid *in vivo* proteolysis. For this a "retro-inverso" version of OR2 has been made, named RI-OR2. In retro-inverso peptides all of the natural L-amino acids are replaced by the D-entantiomer, along with reversal of the peptide bonds (Chorev and Goodman, 1995). This approach should maintain a similar 3-dimensional shape to OR2 and retain its inhibition of oligomerisation, whilst preventing its proteolytic degradation.

Here, these peptides have been tested to evaluate their ability to prevent aggregation but also their effects on H_2O_2 generation by Aβ. Much of the evidence reported in this thesis implicates early oligomers to have this property which may be directly linked to the toxicity of Aβ. If these inhibitors prevent toxic oligomer formation, maybe H_2O_2 generation is also prevented.

8.2. Results

8.2.1. Aβ42 with OR1 and OR2

Upon initial investigation of these inhibitors OR1 and OR2 were tested for their effects on aggregation of Aβ42 as measured by thioflavin T and oligomeric immunoassay. Concurrently the H_2O_2 concentration of these aggregating solutions was assessed to look for any relationship between aggregation inhibition and H_2O_2 generation. Initial experiments were performed with Aβ42 at 50 μM and inhibitor at 100 μM (see figure 8.2). By 4 hrs Aβ42 alone had largely aggregated, with a large increase in thioflavin T fluorescence and oligomeric content (immunoassay). This can also be observed in the AFM images (see figure 8.3) where not only fibrillar but also very small pre-fibrillar material can be distinguished. Measurements indicate these oligomers to be less than 1 nm in height.

With the presence of OR1, thioflavin T fluorescence was approximately half that of Aβ42 alone. Conversely, immunoassay fluorescence with OR1 was increased compared to Aβ42 alone. AFM images show the inhibitor has caused the formation of a largely homogeneous solution of spherical oligomers, measuring 40-60 nm in diameter and 4-5 nm in height (see figure 8.4). Even accounting for tip-associated widening of features, these can be considered large. However, by 24 hrs the solution contains twice the β-sheet content of Aβ42 alone from the thioflavin T fluorescence accompanied by a sharp reduction in immunoassay fluorescence. AFM images showed irregular clumps of aggregated material to be made rather than fibrils (similar can be seen in figure 8.7E and F).

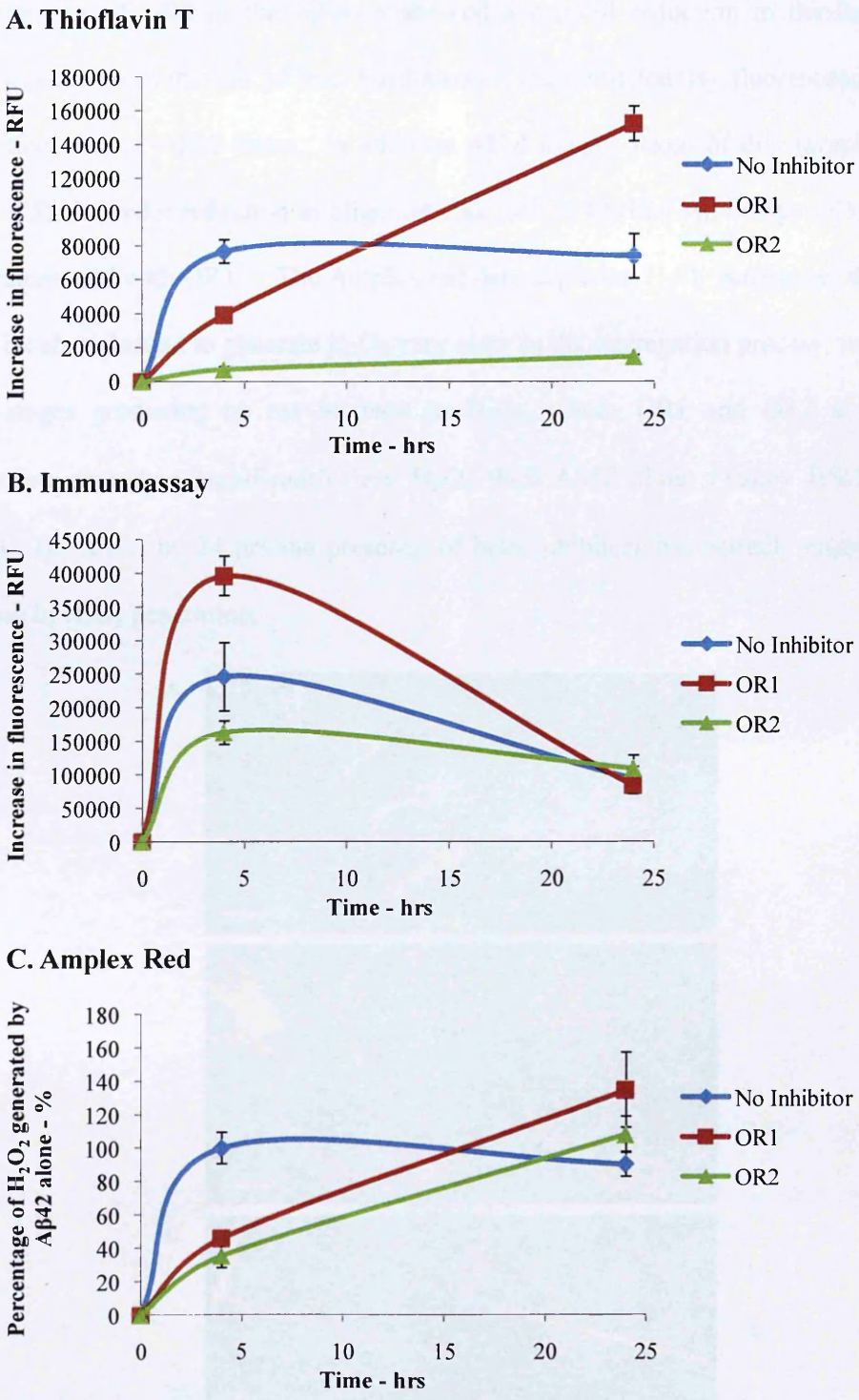

Figure 8.2. The effects of OR1 and OR2 on aggregation and H_2O_2 generation by Aβ42

HFIP treated Aβ42 was solubilised at 50 μM in 10 mM PB, with and without the presence of 100 μM OR1 or OR2. Aggregation was monitored over 24 hrs by thioflavin T fluorescence (A), Oligomeric immunoassay (B) and H_2O_2 generation measured by Amplex red fluorescence (C). Results are means ± S.D. (Thioflavin T and Amplex red: n=3, Immunoassay: n=4)

The presence of OR2 in the solution showed a marked reduction in thioflavin T fluorescence across the full 24 hrs. Furthermore, the immunoassay fluorescence was lower than that of Aβ42 alone. In addition AFM images taken of this sample (see figure 8.5) showed a reduction in oligomeric as well as fibrillar Aβ compared to both Aβ42 alone and with OR1. The Amplex red data depicting H_2O_2 generation showed Aβ42 incubated alone to generate H_2O_2 very early in the aggregation process, with the latter stages producing no net increase in H_2O_2. Both OR1 and OR2 at 4 hrs incubation generated significantly less H_2O_2 than Aβ42 alone (Tukey HSD, $p \leq 0.000$). However, by 24 hrs the presence of both inhibitors has actually enabled an increase in H_2O_2 generation.

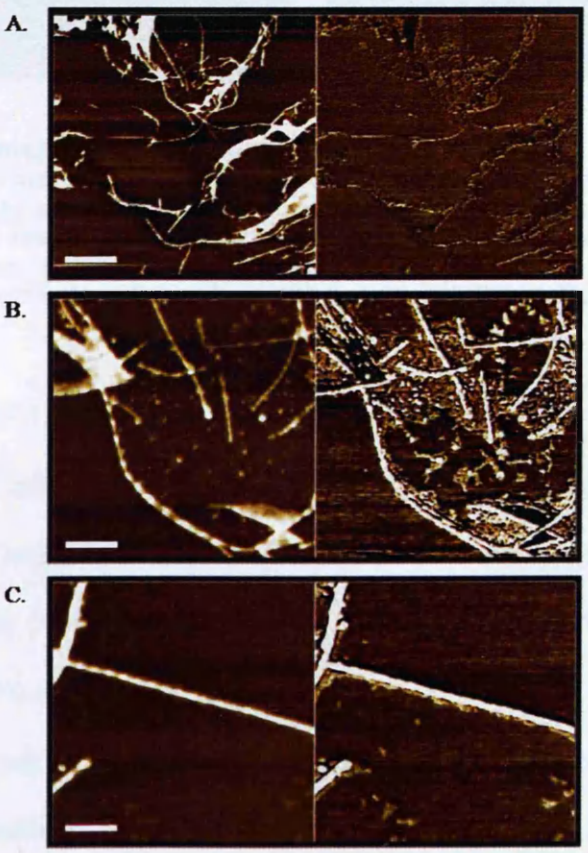

Figure 8.3. AFM images of Aβ42 with no OR at 4 hrs
50 μM Aβ42 incubated with no added OR in 10 mM PB, pH 7.4 for 4 hrs at 37°C was diluted 10 fold into MilliQ water and 2 μl spotted into the centre of a piece of cleaved mica. This was then imaged using a Digital Instruments SPM using tapping mode. Left hand image shows the height of objects, right hand image is phase contrast. Bar represents 2 μm in A, 400 nm in B and 200 nm in C.

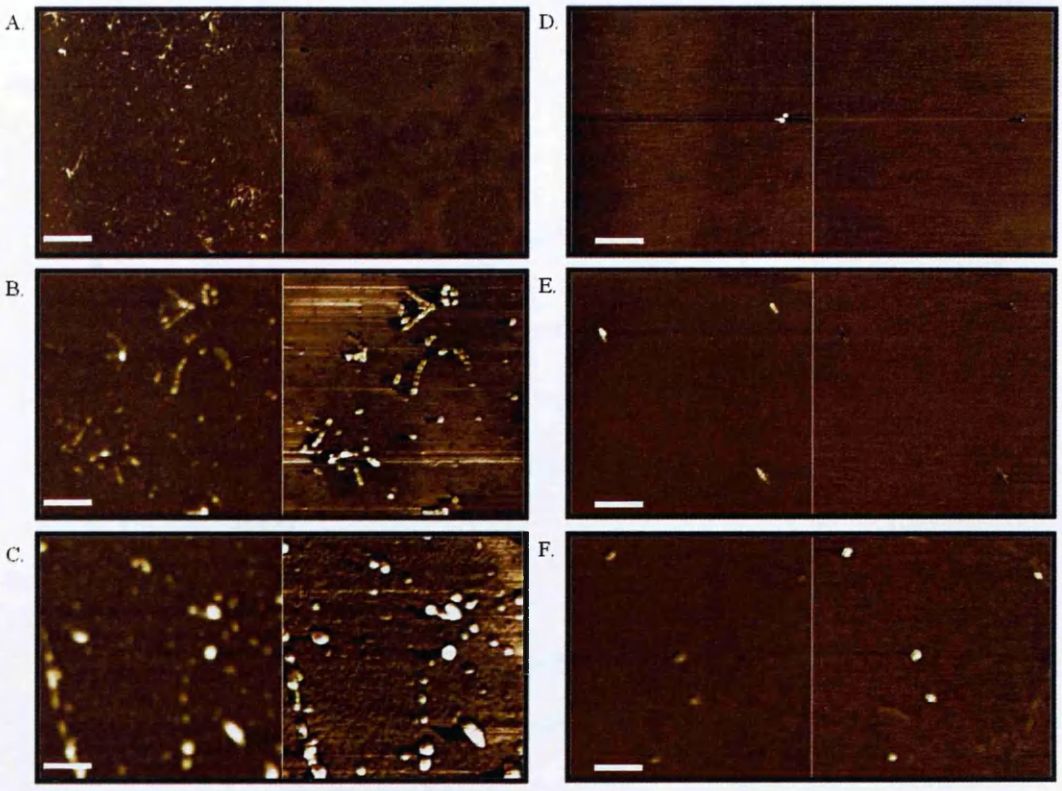

Figure 8.4. AFM images of Aβ42 with OR1 and OR2 at 4 hrs
50 μM Aβ42 incubated with 100μM OR1 or OR2 in 10 mM PB, pH 7.4 for 4 hrs at 37°C was diluted 10 fold into MilliQ water and 2 μl spotted into the centre of a piece of cleaved mica. This was then imaged using a Digital Instruments SPM using tapping mode. Left hand image shows the height of objects, right hand image is phase contrast. Images A, B and C are with OR1, D, E and F are with OR2. Bar represents 2 μm in A and D, 1 μM in E, 400 nm in B and 200 nm in C and F.

8.2.2. Aβ40 with OR1 and OR2

The effect of these inhibitors was also investigated on the less amyloidogenic Aβ40 (see figure 8.5). Over this 24 hr time period Aβ40 alone exhibits greatly reduced fluorescence in both thioflavin T and immunoassay compared to Aβ42; thioflavin T fluorescence is ~30% that of Aβ42 and immunoassay <10%. This suggests that over this period Aβ40 has undergone very little aggregation. Despite this at 4 hrs incubation both inhibitors appear to be exerting an effect on its aggregation. The presence of OR2 prevents any increase in thioflavin T fluorescence over the first 4 hrs and the increase in immunoassay fluorescence is less than one third of Aβ40 alone.

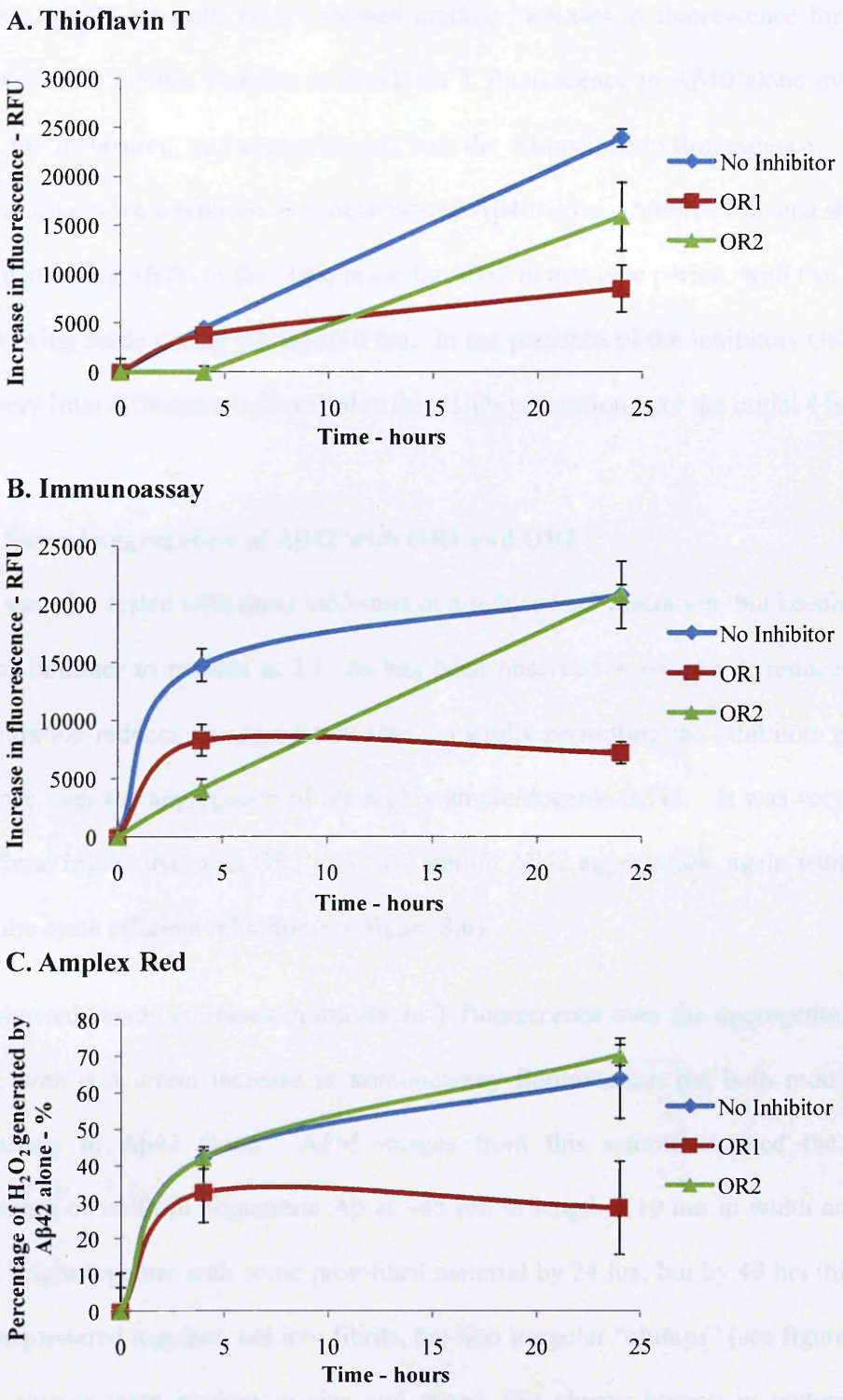

Figure 8.5. The effect of OR1 and OR2 on aggregation and H_2O_2 generation by Aβ40

HFIP treated Aβ40 was solubilised at 50 μM in 10 mM PB, with and without the presence of 100 μM OR1 or OR2. Aggregation was monitored over 24 hrs by thioflavin T fluorescence (A), Oligomeric immunoassay (B) and H_2O_2 generation measured by Amplex red fluorescence (C). Results are means ± S.D. (Thioflavin T and Amplex red: n=3, Immunoassay: n=4)

However, by 24 hrs both assays showed marked increases in fluorescence for OR2. OR1 showed a similar increase in thioflavin T fluorescence to Aβ40 alone over the first 4 hrs incubation, and approximately half the immunoassay fluorescence. By 24 hrs both assays were reduced in comparison to Aβ40 alone. Amplex red data showed Aβ40 generating ~60% of the H_2O_2 made by Aβ42 in this time period, with two thirds of this being made during the initial 4 hrs. In the presence of the inhibitors OR1 and OR2 very little difference is observed in this H_2O_2 generation over the initial 4 hrs.

8.2.3. Slowed aggregation of Aβ42 with OR1 and OR2

Aβ42 was also tested with these inhibitors at a reduced concentration, but keeping the ratio of inhibitor to peptide at 2:1. As has been observed in chapter 4, reducing Aβ concentration reduces its aggregation rate, hopefully permitting the inhibitors greater influence over the aggregation of the highly amyloidogenic Aβ42. It was very clear from these results that both OR1 and OR2 inhibit Aβ42 aggregation, again with OR2 being the more efficient inhibitor (see figure 8.6).

OR1 showed steady increases in thioflavin T fluorescence over the aggregation time course with concurrent increase in immunoassay fluorescence, but both reduced in comparison to Aβ42 alone. AFM images from this sample showed the clear appearance of uniform oligomeric Aβ at ~45 nm in length, ~10 nm in width and 0.8 nm in height together with some protofibril material by 24 hrs, but by 48 hrs this had been sequestered together, not into fibrils, but into irregular "clumps" (see figure 8.7). These clumps were random in size and shape, but always bumpy in texture. In conjunction with this, the presence of the inhibitor reduced the concentration of H_2O_2 generated by Aβ42 by ~50% at 24 hrs. However, whereas Aβ42 generation of H_2O_2 plateaued, the presence of OR1 permitted it to continue to rise steadily.

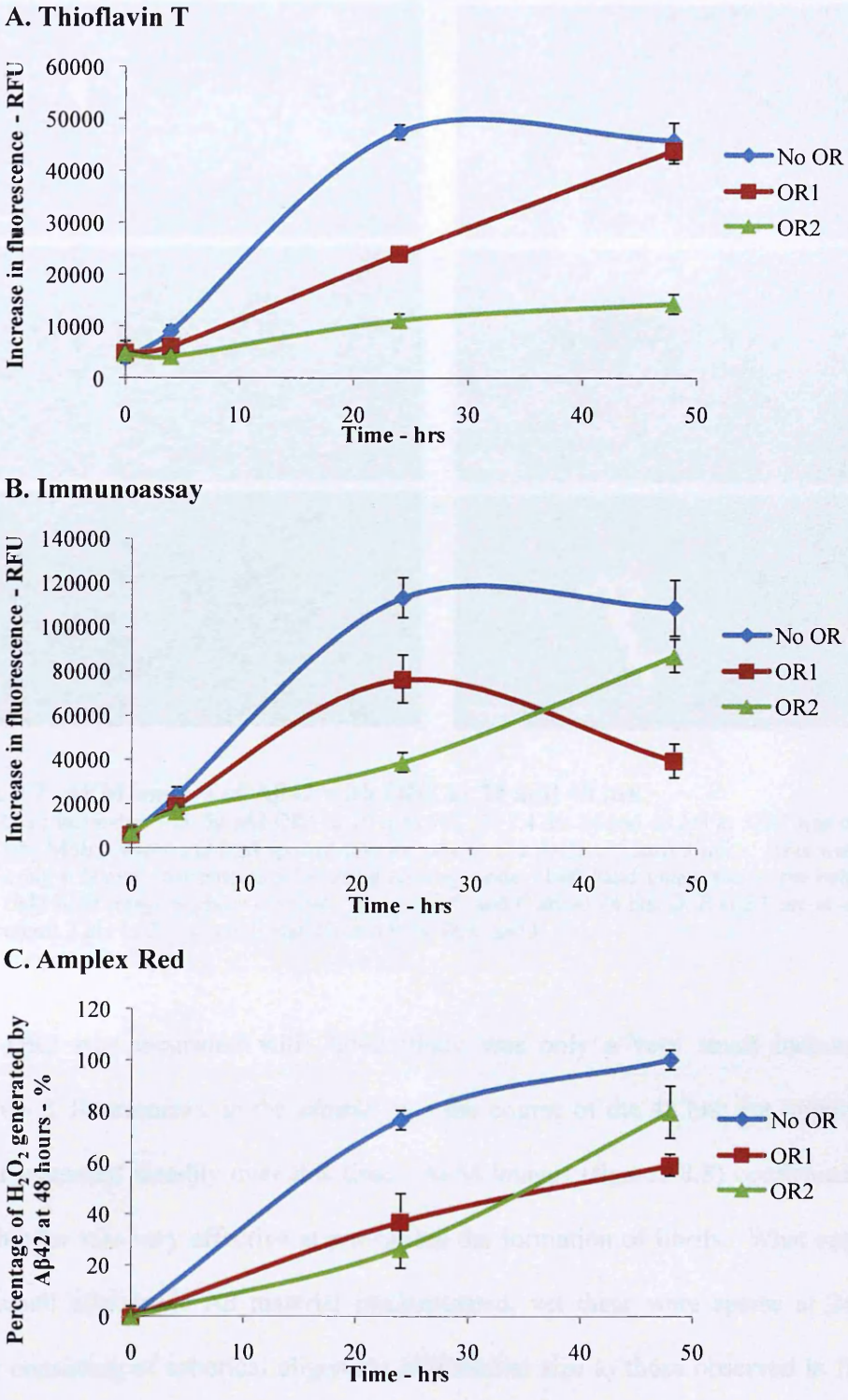

Figure 8.6. The effect of OR1 and OR2 on aggregation and H_2O_2 generation by Aβ42

HFIP treated Aβ42 was solubilised at 25 μM in 10 mM PB, with and without the presence of 50 μM OR1 or OR2. Aggregation was monitored over 24 hrs by thioflavin T fluorescence (A), Oligomeric immunoassay (B) and H_2O_2 generation measured by Amplex red fluorescence (C). Results are means ± S.D. (Thioflavin T and Amplex red: n=3, Immunoassay: n=4)

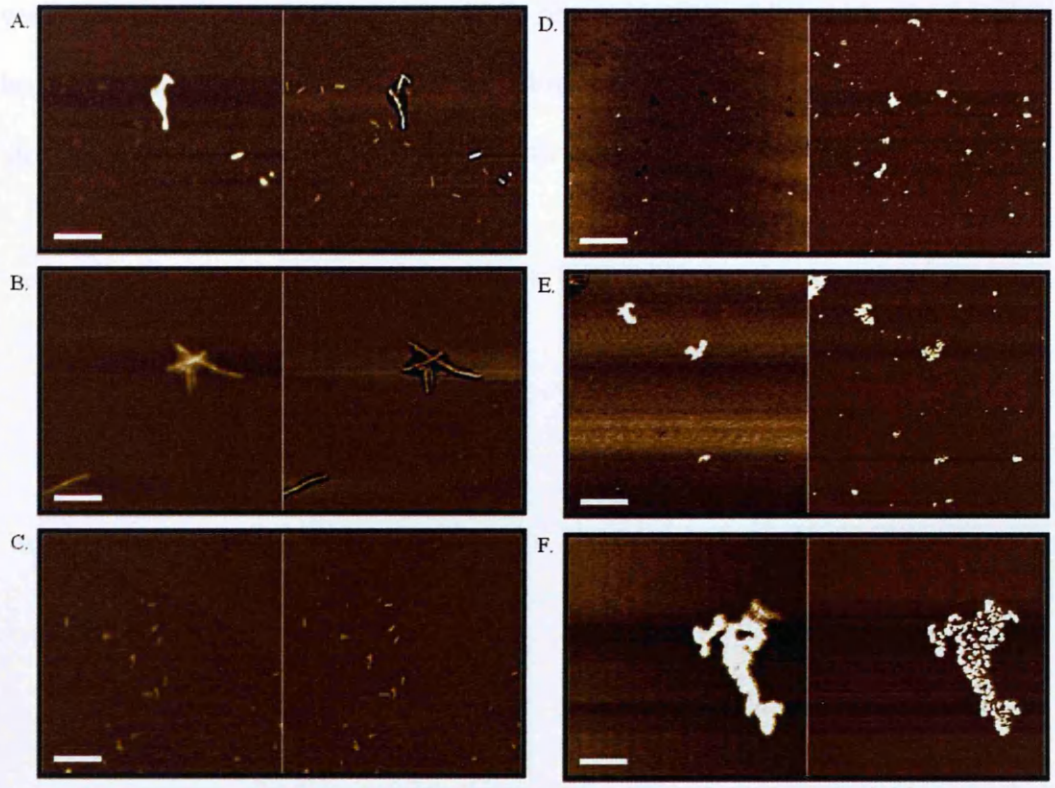

Figure 8.7. AFM images of Aβ42 with OR1 at 24 and 48 hrs
25 μM Aβ42 incubated with 50 μM OR1 in 10 mM PB, pH 7.4 for 24 and 48 hrs at 37°C was diluted 10 fold into MilliQ water and 2 μl spotted into the centre of a piece of cleaved mica. This was then imaged using a Digital Instruments SPM using tapping mode. Left hand image shows the height of objects, right hand image is phase contrast. Images A, B and C are at 24 hrs, D, E and F are at 48 hrs. Bar represents 2 μm in D, 1 μm in E and 200 nm in A, B, C and F.

When OR2 was incubated with Aβ42, there was only a very small increase in thioflavin T fluorescence in the sample over the course of the 48 hrs, yet oligomeric content increased steadily over this time. AFM images (figures 8.8) confirmed that this inhibitor was very effective at preventing the formation of fibrils. What appears to be small oligomeric Aβ material predominated, yet these were sparse at 24 hrs largely consisting of spherical oligomers of a similar size to those observed in figure 8.4 (Aβ42 with OR2 at 4 hrs) but also containing the occasional aggregate resembling a short chain of beads on a string (figure 8.8C). At 48 hrs, the aggregates do not appear to have increased in size yet there appears to be an increased abundance of

very small oligomeric material. The H_2O_2 generation from this sample was found to be reduced compared to Aβ42 over the initial 24 hrs of incubation (<50% of Aβ42 alone), yet this increased to nearly 80% by 48 hrs.

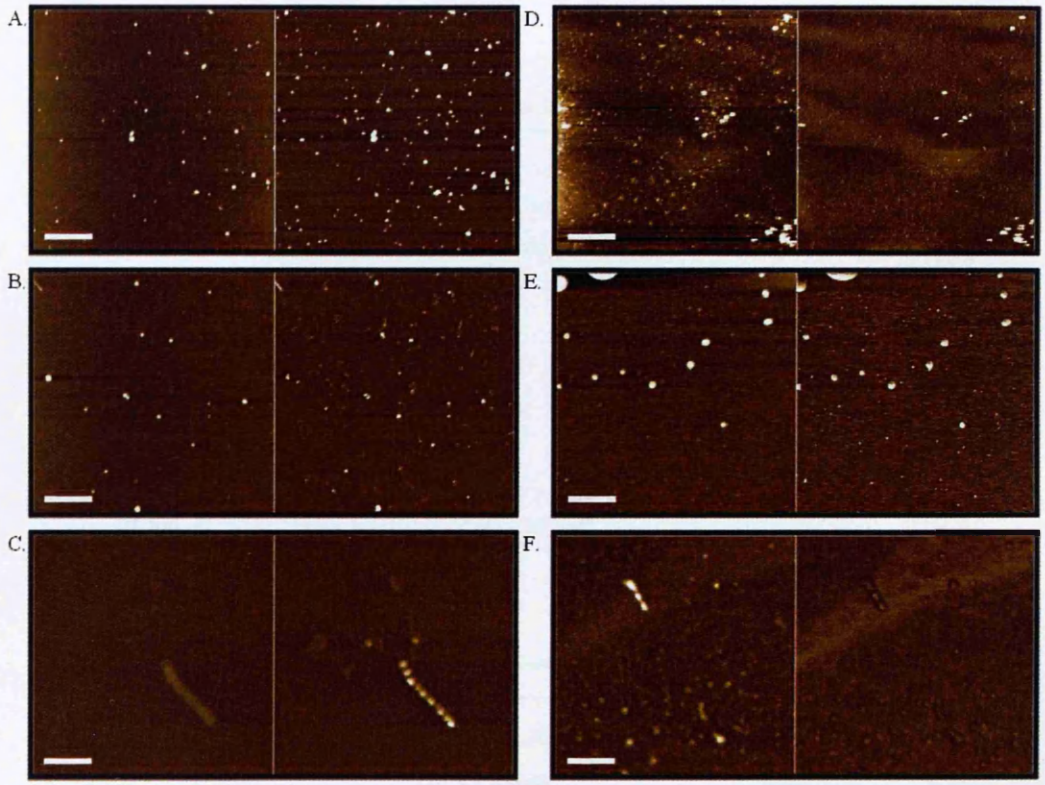

Figure 8.8. AFM images of Aβ42 with OR2 at 24 and 48 hrs
25 μM Aβ42 incubated with 50 μM OR2 in 10 mM PB, pH 7.4 for 24 and 48 hrs at 37°C was diluted 10 fold into MilliQ water and 2 μl spotted into the centre of a piece of cleaved mica. This was then imaged using a Digital Instruments SPM using tapping mode. Left hand image shows the height of objects, right hand image is phase contrast. Images A, B and C are at 24 hrs, D E and F are at 48 hrs. Bar represents 2 μm in A and D, 1μm in B, 400 nm in E and 200 nm in C and F.

8.2.4. Aβ with RI-OR2

The development of RI-OR2 was hoped to provide a means of retaining the inhibitory properties of the peptide yet be resistant to proteolysis. In fact, this alteration appears to improve upon the inhibition of the parent peptide (see figure 8.9). Thioflavin T results showed no increase in β-sheet over the course of 48 hrs when RI-OR2 was incubated with either Aβ40 or Aβ42.

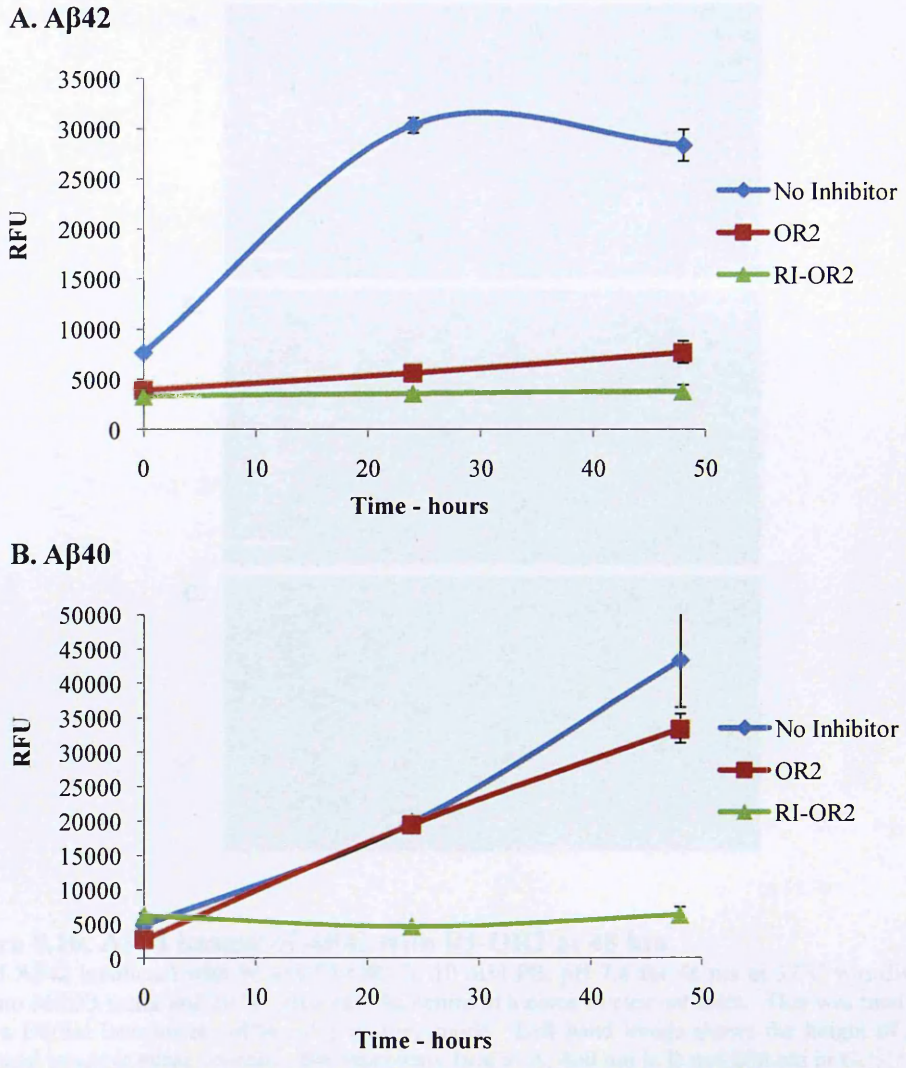

Figure 8.9. The effect of OR2 and RI-OR2 on aggregation of Aβ
HFIP treated Aβ40 and 42 were solubilised at 25 μM in 10 mM PB, with and without the presence of 50 μM OR2 or RI-OR2. Aggregation was monitored over 48 hrs by thioflavin T fluorescence for Aβ42 (A) and Aβ40 (B). Results are means ± S.D. (n=3)

AFM images taken support this with no fibrillar material detected, but also no small oligomers. The larger spherical oligomeric species are again present, yet even these appear to be sparse (see figure 8.10). In addition, at T=0 a clear reduction in thioflavin T fluorescence was observed upon wetting the peptide (the reduction in immunoassay fluorescence was less so) (figure 8.11). Non-incubated controls have shown that this effect was not due to the presence of the inhibitor reducing thioflavin T fluorescence by an alternative mechanism.

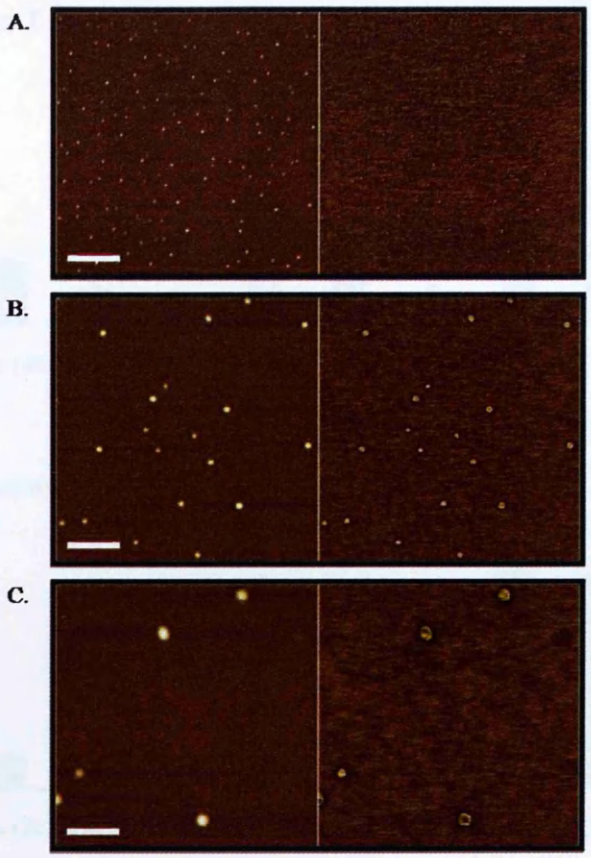

Figure 8.10. AFM images of Aβ42 with RI-OR2 at 48 hrs
25 μM Aβ42 incubated with 50 μM RI-OR1 in 10 mM PB, pH 7.4 for 48 hrs at 37°C was diluted 10 fold into MilliQ water and 2μl spotted into the centre of a piece of cleaved mica. This was then imaged using a Digital Instruments SPM using tapping mode. Left hand image shows the height of objects, right hand image is phase contrast. Bar represents 1μm in A, 400 nm in B and 200 nm in C.

The immunoassay results also showed the presence of RI-OR2 had reduced fluorescence at 48 hrs to approximately one third of the initial fluorescence of the peptide. Again non-incubated controls confirmed that any changes in fluorescence compared to the peptide alone were due to the action of the inhibitor on Aβ aggregation. Concurrently, the generation of H_2O_2 from the Aβ42 incubated with RI-OR2 showed a significant increase in its formation compared to Aβ42 alone (T=6, 24 and 48 Tukey HSD, $p \leq 0.004$) (see figure 8.12).

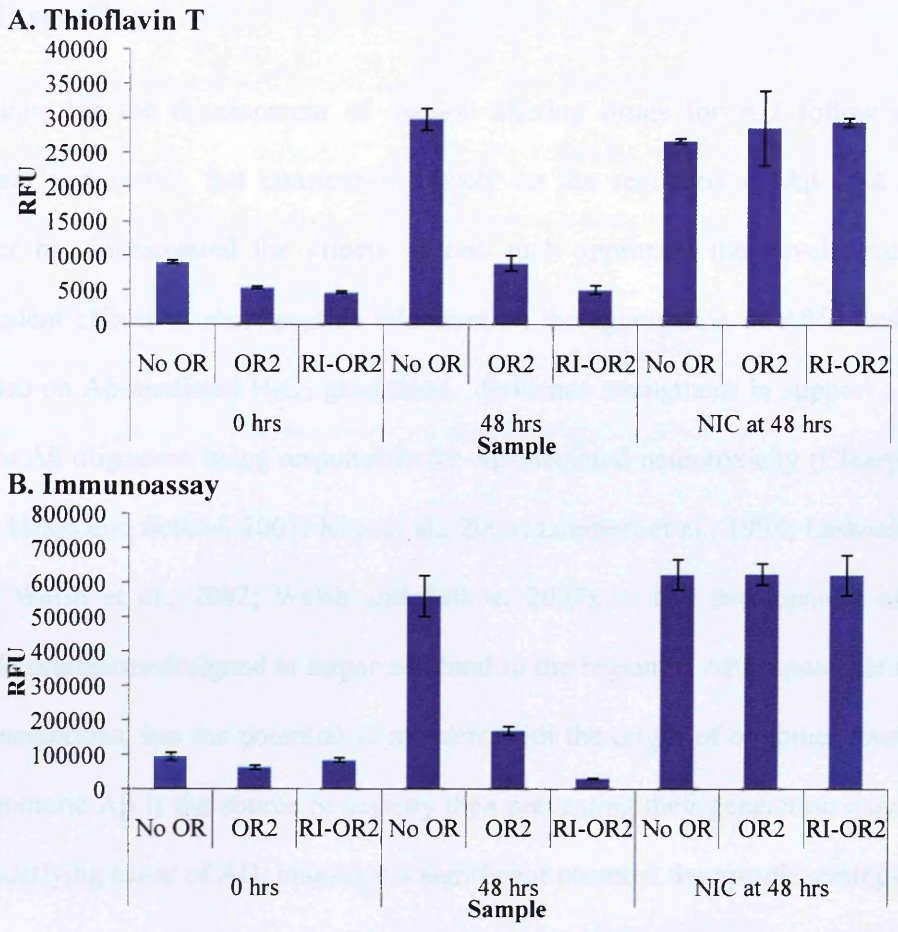

Figure 8.11. The effect of OR2 and RI-OR2 on aggregation of Aβ
HFIP treated Aβ42 was solubilised at 25 μM in 10 mM PB, with and without the presence of 50 μM OR2 or RI-OR2. Aggregation was monitored over 48 hrs by thioflavin T fluorescence (A) and oligomeric immunoassay (B). Non-incubated controls were taken at 48 hrs. Results are means ± S.D. (Thioflavin T: n=3, Immunoassay: n=4)

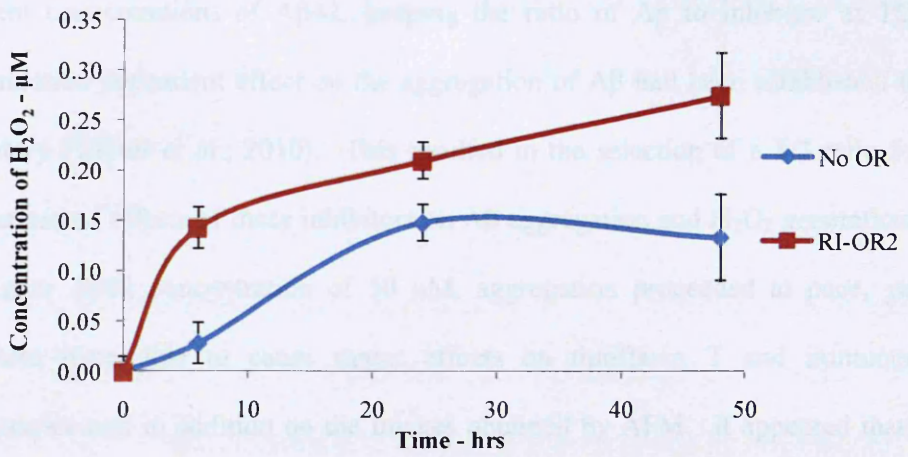

Figure 8.12. The effect of RI-OR2 on the H_2O_2 generation of Aβ42
25 μM Aβ42 was solubilised in 10 mM PB with and without the presence of 50 μM RI-OR2. H_2O_2 generation was monitored over 48 hrs by Amplex red fluorescence. Results are means ± S.D. (n=3)

8.3. Discussion

Strategies for the development of disease altering drugs for AD follow several different approaches, but concentrate largely on the reduction of Aβ load. This chapter has investigated the effects of one such approach: the development and subsequent effects of short peptide inhibitors on the aggregation of Aβ40 and Aβ42 and also on Aβ-mediated H_2O_2 generation. Evidence strengthens in support of early soluble Aβ oligomers being responsible for Aβ-mediated neurotoxicity (Cleary et al., 2005; Haass and Selkoe, 2007; Kim et al., 2003; Lambert et al., 1998; Lashuel et al., 2002; Walsh et al., 2002; Walsh and Selkoe, 2007). The development of short peptide sequences designed to target and bind to the region of Aβ responsible for Aβ self interactions, has the potential to interfere with the origin of oligomer formation. If oligomeric Aβ is the source of toxicity then preventing their generation may target the underlying cause of AD, making it a significant potential therapeutic strategy.

8.3.1. The effects of OR1 and OR2 with Aβ42

Aβ42 aggregation was monitored with and without the presence of OR1 and OR2 at 2 different concentrations of Aβ42, keeping the ratio of Aβ to inhibitor at 1:2. A concentration dependent effect on the aggregation of Aβ had been established in our laboratory (Taylor et al., 2010). This resulted in the selection of a 1:2 ratio for the comparison of effects of these inhibitors on Aβ aggregation and H_2O_2 generation. At the higher Aβ42 concentration of 50 μM, aggregation proceeded at pace, yet the inhibitors were able to cause major effects on thioflavin T and immunoassay fluorescence and in addition on the images obtained by AFM. It appeared that both OR1 and OR2 prevented aggregation of Aβ42 however OR2 appeared to be much more effective in this respect. In fact at 4 hrs incubation the formation of fibrils could

be seen in AFM pictures of Aβ42 with no inhibitor added yet both samples with OR1 and OR2 added showed no fibrillar material. Concurrently thioflavin T fluorescence was reduced at 4 hrs for both OR1 and OR2 containing samples. However, in the immunoassay, only OR2 generated reduced fluorescence, whereas OR1 immunoassay fluorescence was actually raised compared to that with no inhibitor. This is indicative of a rise in oligomer formation when incubated with OR1 and is supported by the observation of spherical Aβ species rather than fibrillar by AFM.

These results support observations by Austen and colleagues that OR1 inhibits fibril formation but not the generation of oligomers (Austen et al., 2008). They claimed that OR2 also prevents oligomer formation. However, the results I obtained clearly show increases in fluorescence with both thioflavin T and immunoassay indicative of aggregation associated events. These changes are greater in the immunoassay (albeit reduced compared to Aβ42 alone or with OR1), which implies that oligomeric Aβ is made and is only somewhat reduced compared to Aβ42 alone. This was confirmed by AFM which identified similar small Aβ species that appear far fewer in number than those observed with Aβ42 alone or with OR1. This shows that the modification of OR1 to have 2 amino termini (rather than normal N- and C-termini) improves the binding affinity of the OR sequence to the hydrophobic region of Aβ thus preventing Aβ self interactions that promote aggregation.

The generation of H_2O_2 by these solutions suggests that a particular oligomeric form of Aβ that is responsible. Aggregation is slowed by the presence of both inhibitors due to Aβ binding the inhibitor rather than other Aβ subunits. H_2O_2 generating Aβ is formed albeit at a reduced rate due to the competition provided by the inhibitor. Thus at 4 hrs aggregation, H_2O_2 generation from the Aβ42 samples with OR1 and OR2 added is reduced compared to the Aβ42 with no inhibitor added. This effect is greater

for OR2 correlating with the reduced oligomer formation observed by this sample. However, where the Aβ42 H_2O_2 concentration plateaus from the sequestration of H_2O_2 generating Aβ species into fibrils, the generation from the samples with OR1 and OR2 continues to rise. This supports earlier evidence that slowing aggregation may have the consequence of generating more H_2O_2 ultimately; H_2O_2 generation is slower yet sustained. There is a reduced rate of formation of H_2O_2 generating Aβ, together with a decrease in the rate of sequestration into fibrils, having the net effect of prolonging the longevity of the H_2O_2 generating oligomers.

To slow Aβ42 aggregation further the concentrations of Aβ and inhibitor were reduced to provide the inhibitors greater opportunity to augment Aβ aggregation. With aggregation proceeding at a reduced speed, despite all interactions remaining dynamic with a variety of Aβ species in existence, the homogeny of the solution would be somewhat improved. This was hoped to aid interpretation of the effects of the inhibitors, particularly on oligomer and H_2O_2 generation. These results backed up the earlier observations with both OR1 and OR2 able to prevent aggregation associated increases in fluorescence, OR2 being more efficient in this respect. This correlated with a reduction in H_2O_2 generation by these samples in comparison to Aβ42 with no inhibitor added, suggesting a reduction in the formation of H_2O_2 generating Aβ. The observation that an inhibitor designed to prevent Aβ self interactions reduces H_2O_2 generation supports the notion that these interactions are needed for Aβ to be capable of generating H_2O_2, and monomeric Aβ is not responsible. AFM images lend further insight into these results. At 24 hrs, the Aβ42 sample with OR1 added has many more, small, oligomeric Aβ than that of the OR2 sample (together with some small protofibrillar Aβ). This corresponds to greater H_2O_2 generation in the OR1/Aβ42 sample. The H_2O_2 generation from the sample

with OR1 has begun to plateau at 48 hrs. AFM images show these small oligomers and protofibrils to "clump" together, presumably limiting their capacity for H_2O_2 generation (as well as their antibody binding in the immunoassay). This is compared to OR2/Aβ42 which continues to generate H_2O_2 as it retains smaller oligomeric Aβ42 preventing its fibrillisation or "clumping". This provides strong support that an early species of Aβ is responsible for H_2O_2 generation. However, the solutions do still contain a mixture of aggregating Aβ species making any further stipulations on the identity of the H_2O_2 generating species highly tenuous. Yet, this investigation demonstrated the importance of considering both assays and AFM images when considering the effects of inhibitors.

8.3.2. The effect of Aβ40 with OR1 and OR2

Testing the inhibitors on Aβ40 was hoped to help identify the effects OR1 and OR2 have on early Aβ self interactions, due to the largely monomeric nature of Aβ40 upon wetting. Observation that OR2 but not OR1 prevented any thioflavin T fluorescence increase at 4 hrs (with concurrent reduced immunoassay fluorescence) indicated OR2 to interact with Aβ40 rapidly inhibiting aggregation associated changes in the Aβ40 solution. This suggests OR2 was able to prevent early β-folding events and oligomer formation but furthermore, that oligomers exist that contain very little/no β-folding. However, OR2 fluorescence in both assays then rises above that seen for OR1. This suggests that OR1 is less able to inhibit initial Aβ self-interactions, yet it is capable of reducing later aggregation. This may be due to OR2 having a greater affinity for monomeric or low β-sheet content Aβ40, whereas OR1 has a greater affinity for Aβ40 that has initiated the shift to β-sheet and/or self-interacting. This is different to results seen with Aβ42, where OR2 appears to have greater affinity than OR1 throughout the

aggregation of Aβ42. This may be solely due to the greater heterogeneity of Aβ42 compared to Aβ40 upon wetting which consequently complicates interpretation of results. However, it may also be due to different affinities that the 2 similar inhibitors have for these 2 similar Aβ peptides. Aβ40 has a reduced propensity for aggregation compared to Aβ42 due to the omission of the final 2 residues. This reduces the overall hydrophobicity of the molecule, and its tendency for propagating self interactions. It seems reasonable to suggest that the OR inhibitors may not bind Aβ40 with as strong affinity of Aβ42 as the OR inhibitors are actually designed to imitate the KLVFF sequence at residues 16-20 that is thought to be responsible for the self interactions of Aβ. It would also be reasonable to suspect that OR1 and OR2 may bind with different affinities during the aggregation process as the Aβ changes in respect of its structure and conformation over time. With OR2 appearing to act so early in binding Aβ40, it may be expected that it would reduce H_2O_2 generation, yet this was not observed, implicating the H_2O_2 generating Aβ to be formed very early in the aggregation process. This would support evidence that electron abstraction from Met35 is enabled by the α-helical structure (Kanski et al., 2002b).

As fibrillisation of Aβ40 has not truly begun by 24 hrs (even at this concentration) no conclusions can be made on the capability of each of these inhibitors on preventing fibrillisation from this data. Aβ40 and Aβ42 have many similar qualities but also many differences. As Aβ40 is less toxic than Aβ42, inhibiting Aβ42 oligomerisation is the primary objective. However, results observed with Aβ42 are complicated by the aggregation state of the peptide upon wetting, which inevitably incurs greater heterogeneity on the subsequent aggregation of the solution. The measured effect of an inhibitor on aggregation and H_2O_2 generation for Aβ42 is the net result for possibly several different effects on a wide range of different Aβ species present. For this

reason, consideration of results obtained with Aβ40 over this early aggregation phase may be useful for the interpretation of observations with Aβ42. With this in mind, H_2O_2 generation was observed to be formed very early in the aggregation process. In addition, the generation of H_2O_2 by Aβ40 with OR2 present is almost identical to Aβ40 alone. As no increase in thioflavin T fluorescence was observed with OR2 present during this 4 hr incubation the implication arises that this oligomer with little/no β-folding is responsible for H_2O_2 generation and it is also invisible in the thioflavin T assay. However, it is possible that different Aβ species are responsible for H_2O_2 generation by Aβ40 and Aβ42.

8.3.3. The effects of RI-OR2 on aggregation and H_2O_2 generation from Aβ40 and Aβ42

The success of OR2 at preventing Aβ-Aβ interactions and reducing early H_2O_2 generation lead to testing of the retro-inverso version of OR2. This should maintain the inhibitor qualities of OR2 but be resistant to proteolysis. This proved more successful than anticipated as aggregation was inhibited more so than that observed with OR2. Not only did it inhibit aggregation but it appeared to promote disaggregation of Aβ42, particularly so in the thioflavin T assay. The fact that this effect was not seen as strongly at T=0 in the immunoassay as in the thioflavin T may allude to the mode of action of this inhibitor; RI-OR2 binding Aβ rapidly encourages loss of β-sheet content which slowly permits the disaggregation of any pre-aggregated material. Interestingly, RI-OR2 was far less effective at inhibiting Aβ40 aggregation than Aβ42. It does show greater inhibition than OR2, yet there was a small but significant increase in thioflavin T fluorescence at T=0 compared to the Aβ40 alone (Tukey HSD, $p = 0.008$). The fact that the Aβ40 starting material is largely

monomeric obviously means that the inhibitor cannot act to disaggregate as it does with Aβ42. There was also no increase in thioflavin T fluorescence over the 48 hrs whereas the sample with no inhibitor and with OR2 both showed thioflavin T fluorescence increases. The inhibitor appears to be promoting an oligomeric species in both Aβ peptides that is low in β-sheet content indicated by the thioflavin T fluorescence. Perhaps the aggregation state of both peptides converges on this alternative oligomerisation pathway/species when incubated with RI-OR2 that binding the inhibitor provides.

AFM images of Aβ42 at 48 hrs aggregation clearly show the lack of fibrillar material, but also show a relatively low number spherical oligomeric Aβ, very similar to those observed with OR2 and Aβ42. This leads to speculations that the mode of action of these OR inhibitors may promote the formation of these oligomeric species as an alternative to fibrillisation. In our laboratory RI-OR2 has also been found to prevent Aβ-mediated toxicity to SH-SY5Y neuroblastoma cells (Taylor et al., 2010). This suggests that the action of the RI-OR2 in inhibiting normal oligomerisation and aggregation of Aβ is successful in removing its toxicity; the toxic oligomer is not formed. However, unlike OR1 and OR2 which showed reduced H_2O_2 generation compared to Aβ42 alone, RI-OR2 appears to increase the H_2O_2 measured from an aggregating sample of Aβ42 (see figure 8.12). This does not necessarily negate H_2O_2 generation by the peptide as playing a role in augmenting Aβ toxicity in AD. It may be that not only does it prevent Aβ42 aggregation but also inhibit access to the site of action for toxicity. If for example, membrane insertion is a pre-requisite for Aβ toxicity, or indeed Aβ-generated H_2O_2 mediated toxicity (discussed in 4.3.5), and RI-OR2 binds in such a way as to prevent this insertion, then toxicity would be prevented. It does confirm that a very early oligomeric species must be responsible

for the generation of H_2O_2 as RI-OR2 appears to be extremely effective at inhibiting aggregation. Maybe the spherical oligomers observed by AFM, are, or are composed of H_2O_2 generating species of Aβ. However, it is also possible that the H_2O_2 generating species is too small to be identified by AFM and that the spherical oligomers observed are an alternative sequestration event to fibrils. This seems perhaps more likely due to their increased occurrence with OR2 and the increased aggregation with OR2 showing reduced generation of H_2O_2.

It would be of interest to test these inhibitors for their effects using the immobilisation technique to assess the Aβ species generated by the action of the OR inhibitors. This may help identify the H_2O_2 generating species of Aβ, but also, if the generation of H_2O_2 is linked to Aβ neurotoxicity, then identifying inhibitors that also act to reduce its existence may prove useful in disease course altering therapeutic development.

The generation of H_2O_2 from solutions of Aβ42 that are inhibited from aggregating data lends strong support to the hypothesis that a specific early oligomer is responsible. However, the heterogeneous nature of aggregating solutions is a resilient issue when interpreting data. The AFM images obtained whist studying these inhibitors combined with the data from the aggregation assays appears to suggest that fibrillisation and oligomerisation should be considered as 2 separate pathways, both proceeding throughout Aβ aggregation. Some oligomers may be part of the fibrillisation process ("On" the fibrillisation pathway) but there does seem to be a subset that can be considered "Off" the fibrillisation pathway (see figure 8.13). The relationships between monomeric Aβ and the 2 populations of oligomers are unclear (dashed lines). Both OR1 and OR2 can be considered to inhibit the fibrillisation pathway, but also, to varying degrees early oligomeric interactions.

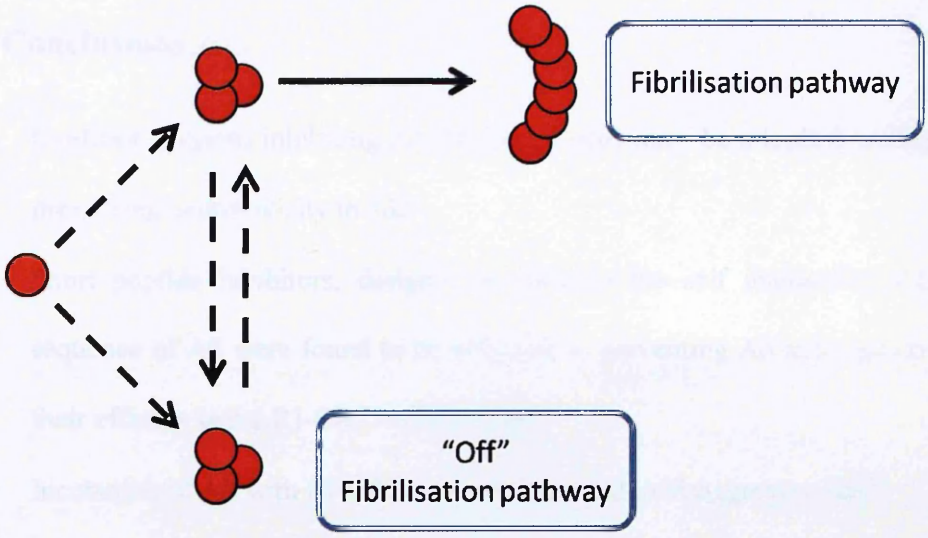

Figure 8.13. Diagram of the "on" and "off" fibrillisation pathways
Monomeric Aβ oligomerises during aggregation to fibrils. Some oligomers may be considered "on" (grow into or directly sequestered into fibrils) or "off" (cannot directly grow into or be sequestered in fibrils) the fibrillisation pathway. Whether monomeric can assemble directly into both on and off oligomers, and the interaction between on and off oligomers is unclear.

The evidence gathered cannot at present identify if the oligomer responsible for H_2O_2 generation is on or off the fibrillisation pathway. Without elucidation of the relationships that control the early evolution of oligomers both possibilities can be explained by the data. However, considering Aβ accumulates and aggregates on a vastly increased time scale (many years compared to 48 hrs) in the AD brain an inhibitor based on OR2 may prove a useful therapeutic. The short burst of H_2O_2 generated would be prolonged and sustained in the brain with biological targets. Although H_2O_2 generation with the inhibitors present prolongs its generation, an inhibitor that reduces oligomer formation and H_2O_2 generation in this accelerated system, may actually be effective *in vivo* at successfully preventing "toxic" oligomer formation.

8.4. Conclusions

- Evidence suggests inhibiting Aβ-Aβ interactions may be a logical strategy for preventing neurotoxicity in AD
- Short peptide inhibitors, designed to bind to the self interaction, KLVFF sequence of Aβ were found to be effective at preventing Aβ aggregation with their efficacy being RI-OR2 > OR2 > OR1
- Incubation of Aβ with RI-OR2 actually appeared to disaggregate Aβ42
- Inhibition of Aβ aggregation was more effective when the inhibitors were tested on Aβ42 compared to Aβ40
- The inhibitors may provide an alternative aggregation pathway into spherical oligomers and amorphous aggregates rather than fibrils
- With the less effective OR1 and OR2, H_2O_2 generation from Aβ42 was decreased yet prolonged, suggesting they acted to decrease the formation of Aβ species able to generate H_2O_2 yet increased its longevity in solution
- With RI-OR2, the generation of H_2O_2 from Aβ42 was increased compared to Aβ42 alone suggesting it acted to promote the formation, longevity or capability of H_2O_2 generating Aβ42
- Evidence from these studies suggests H_2O_2 generation is from a very early species of Aβ, appearing to be of low β-sheet content.
- RI-OR2 may prevent Aβ-mediated cell death yet this appears not be due to loss of the generation of H_2O_2 by Aβ.
- If the generation of H_2O_2 by Aβ is linked to its toxicity then it would appear that the binding of RI-OR2 prevented Aβ toxicity via an additional mechanism such as inhibiting membrane insertion

Chapter 9
Final Discussion

9.1. Discussion

Strong evidence now implicates soluble early oligomeric Aβ as being responsible for neurotoxicity in AD (Cleary et al., 2005; Haass and Selkoe, 2007; Kim et al., 2003; Lambert et al., 1998; Lashuel et al., 2002; Walsh et al., 2002; Walsh and Selkoe, 2007). To investigate these early Aβ species, rigorous deseeding protocols were tested. They identified TFA treatment (which promotes α-helix) in the presence of 4.5% thioanisol (which protects from Met35 oxidation) as able to provide the optimal Aβ, containing the fewest seeds. Efficient and reproducible deseeding of Aβ was critical because the generation of H_2O_2 is believed to be an early event in Aβ aggregation (Tabner et al., 2005). This implicates H_2O_2 formation as a potential property of these early oligomeric Aβ species and is possibly linked to Aβ-mediated cellular toxicity.

Aβ42 has been found to generate more H_2O_2 than Aβ40, corresponding to the increased aggregation and toxicity attributed to Aβ42. This also correlated with increased covalent cross-linking of Aβ42 when subjected to oxidative insults, with the copper/H_2O_2 system generating tetramers preferentially and HRP/H_2O_2 generating larger multimers of ~45 and 56 kDa from Aβ42. Aβ not only generates H_2O_2 but can be the subject of oxidative attack. This may be directly linked to the formation or stabilisation of toxic Aβ oligomers, but could also feed into the aggregation of the peptide. Bearing in mind the membrane association of Aβ, the generation of H_2O_2 is likely to be directed *in vivo* at lipid membranes rather than Aβ self-oxidation (Murray

et al., 2005). Therefore, once formed, these Aβ species may be capable of continuing to generate H_2O_2 rather than their rapid sequestration into fibrils, so extensively oxidatively modifying the membrane and altering its permeability.

Attempts to immobilise Aβ at different stages of aggregation to study its capacity for H_2O_2 generation have had limited success thus far. However, the technique shows promise, and the data do suggest that earlier aggregation species generate increased H_2O_2 compared to later aggregation species. In fact, mature fibrils appear to be a sink for oxidative stress, with the ability to degrade H_2O_2 added externally, perhaps indicating an anti-oxidative neuroprotective mechanism. The 'dual nature' of Aβ (both anti-oxidant and pro-oxidant) has been noted by other investigators (Fang, 2010).

Using the HRP/H_2O_2 system, Tyr10 has been identified as being critical for the formation of covalently cross-linked Aβ, as detected by SDS-PAGE. However, it is not essential for the formation of fibrillar Aβ. This may indicate that some oligomer formation is not on the fibrillisation pathway. The dityrosine dimers are a potential source of H_2O_2 as they can bring 2 copper ions within close vicinity of each other. However H_2O_2 generation from Aβ42-Y10A indicates that dityrosine dimers are not the source, or at least not the sole source, of H_2O_2 generation. This tyrosine residue does appear to be the prime target for oxidative modification of Aβ42 and may be key for the stabilisation of early oligomeric Aβ *in vivo*. The stabilisation of oligomeric Aβ may be directly linked to prolonging its mode of toxicity, potentially via the generation of H_2O_2.

The binding of copper ions to Aβ appears to be critical for H_2O_2 generation, supporting evidence that copper modulates Aβ toxicity (Smith et al., 2006), yet trace levels are sufficient for this. Aβ42 substituted peptides that would be hypothesised to

have reduced copper binding capabilities indeed show a marked reduction in H_2O_2 generation. The binding of copper appears to have complex effects on Aβ aggregation and its generation of H_2O_2 which are highly interconnected. Increasing copper concentration provides the means for greater generation of H_2O_2 via its reduction to Cu(I) and subsequent redox reactions. However, copper ion binding may also promote the stability and longevity of oligomeric Aβ, and as copper concentration increases, Aβ-Aβ interactions may be promoted, facilitating H_2O_2 generation. Copper concentration increases to equimolar and above further increase early H_2O_2 generation and potentially cause the aberrant oxidation of Aβ, halting its generation of H_2O_2. This observation may bear lesser relevance *in vivo* as Aβ is unlikely to be the prime target for oxidation. Fully metalated Aβ may generate large quantities of H_2O_2 directed at lipid membranes with reduced potential for self-oxidation compared to these aggregation studies. Met35, implicated in the reduction of the copper ion, was not critical for H_2O_2 generation implying that another residue, possibly Tyr10, can also reduce the copper ion, albeit at a reduced rate. The substituted peptides thought to have decreased copper reduction capabilities, due to a loss of Met35 or a histidine for copper coordination, all show reduced cross-linking compared to wt Aβ42 perhaps indicating the importance of copper in early Aβ-Aβ interactions.

The other metal ions tested did not facilitate Aβ generation of H_2O_2. Iron appeared to have very little effect on Aβ aggregation whereas the effects of zinc were complex and possibly regulatory of copper binding. Binding of zinc appeared to prevent Aβ fibrillisation, instead promoting a pre-fibrillar form of Aβ with reduced generation of H_2O_2. This evidence suggests that the binding of copper and zinc to various forms of Aβ may play an important role in the regulation of Aβ aggregation and its redox

properties *in vivo,* supporting evidence from toxicity studies, that zinc may protect against Aβ-copper mediated cell death (Lovell et al., 1999).

It may be that H_2O_2 generation by oligomeric Aβ is not determined by a specific oligomeric form but many different forms. Early Aβ-Aβ interactions may just facilitate the bringing together of 2 (or more) copper ions primed for redox reactions. Other factors, such as metal binding and Aβ oxidation play a role in promoting or preserving the formation of early Aβ-Aβ interactions and thus the activity of the subsequent redox reactions. Certain oligomeric Aβ species may be superior to others in H_2O_2 generation yet other factors such as its ability to direct H_2O_2 at biological targets i.e. lipid membranes may influence their toxicity.

This study, including the investigation of peptide-based inhibitors that can prevent Aβ-Aβ interactions, supports the generation of H_2O_2 as being the result of the longevity and redox potential of Aβ aggregation intermediates. Preventing these interactions largely reduced the levels of H_2O_2 detected during early aggregation and yet prolonged its generation, presumably due to increasing the longevity of intermediates capable of producing H_2O_2. However observation that the most efficient version of this inhibitor promoted disaggregation of Aβ42, yet actually increased the levels of H_2O_2 produced indicates that a very early species of Aβ oligomer is capable of H_2O_2 generation. Despite this, the inhibitor appeared to prevent Aβ-mediated cell death (Taylor et al., 2010), implying that the generation of H_2O_2 may not be pertinent to Aβ-mediated toxicity. However, this effect on Aβ mediated toxixity may be due to other reasons. In support of this, OR2 has also been found to prevent Aβ-mediated toxicity (Austen et al., 2008) yet this inhibitor was found to reduce Aβ generated H_2O_2. It is possible these inhibitors may block the site responsible for the insertion of Aβ into lipid membranes, preventing the Aβ from

causing toxicity despite altered redox capacity. In addition, this work has highlighted the metal ion, concentration and time dependency of H_2O_2 generation by Aβ which may not directly correspond to toxicity measurements. These experiments measuring H_2O_2 generation from Aβ need to be conducted in unison with cell toxicity studies to investigate these effects further.

9.2. Future work and Conclusions

The idea that the generation of H_2O_2 is an important aspect of the pathophysiology of Aβ requires continuing investigation, not only for research into AD, but also because of the similarities that exist between this disease and other neurodegenerative amyloidopathies. The oxidative stress that is observed in the AD brain, combined with age-related metal accumulation, and the central role that Aβ appears to play in AD pathogenesis, makes the generation of H_2O_2 by early oligomeric Aβ an attractive hypothesis for explaining its neurotoxicity. Identification of the source of oligomer toxicity in AD may lead to the development of disease course altering drugs.

The development of the immobilisation technique is one method that may be beneficial for identification of the species responsible for Aβ-mediated H_2O_2 generation. Improvement of the capture and recovery of Aβ present may enable the HRP/H_2O_2 cross-linked Aβ to be properly tested for their ability to generate H_2O_2. It may also be interesting to test the substituted Aβ peptides in the copper/H_2O_2 system especially considering the effects that copper alone had on Aβ aggregation and H_2O_2 generation. Without the presence of HRP, cross-linked Aβ made via this method may be easier to test for its ability to generate H_2O_2. It may also be useful to test the effects of copper on H_2O_2 generation from pre-immobilized Aβ. This way the effects

of copper concentration on Aβ-mediated H_2O_2 generation could be observed without its effects on aggregation altering the Aβ species present.

Research into the properties of the potentially toxic oligomeric species of Aβ is severely hampered by their transient nature and irreversible sequestration into mature fibrils. Manipulating cross-linking and immobilisation reactions may provide a means of studying low-order soluble oligomeric Aβ not only in respect of generation of H_2O_2 but also in combination may prove valuable to both potential diagnostic marker and drug development for AD.

Publications

Submitted – Allsop, D., Mayes, J., and Tabner, B.J. Hypothesis: soluble Aβ oligomers in association with redox-active metal ions are a potential source of reactive oxygen species in Alzheimer's disease. International Journal of Alzheimer's Disease.

Submitted – Crawford, T. J., Parker E., Solis-Trapala, I., Mayes, J. Is the Reaction Time of a Prosaccade a Better Predictor of Antisaccade Errors than Working Memory? Experimental Brain Research

Taylor, M., Moore, S., Mayes, J., Parkin, E., Beeg, M., Canovi, M., Gobbi, M., Mann, D.M., and Allsop, D. (2010). Development of a proteolytically stable retro-inverso peptide inhibitor of beta-amyloid oligomerization as a potential novel treatment for Alzheimer's disease. Biochemistry *49*, 3261-3272.

Allsop, D., Mayes, J., Moore, S., Masad, A., and Tabner, B.J. (2008). Metal-dependent generation of reactive oxygen species from amyloid proteins implicated in neurodegenerative disease. Biochem Soc Trans *36*, 1293-1298.

Presentations and Conferences

Presentation at Mental health and neural systems (MHNS) meeting, Lancaster University (2009). Investigations of hydrogen peroxide generation by β-amyloid and its role in Alzheimer's disease. Mayes, J. and Allsop, D.

Presentation for School of Health and Medicine, Lancaster University (2009) Hydrogen peroxide generation from β-amyloid: its toxicity and role in Alzheimer's disease. Mayes, J., Moore, S., Tabner, B.J. and Allsop, D.

Poster presented at 9th International Conference AD/PD 2009, Prague. Hydrogen peroxide production from oligomeric forms of β-amyloid. Mayes, J., Moore, S., Tabner, B.J. and Allsop, D.

Poster presented at Metals and disease conference, London. (2008) Studies into the production of hydrogen peroxide during the aggregation of β-amyloid using Amplex red. Mayes, J., Moore, S., Tabner, B.J. and Allsop, D.

Posters presented at School of Health and Medicine, Lancaster University (2007, 2008 and 2009)

Presentations for Alzheimer's Society lay panel (2007, 2008 and 2009)

Alzheimer's Society Branch meeting, Barrow-in-Furness (2007)

References

Abramov, A.Y., Canevari, L., and Duchen, M.R. (2004). Calcium signals induced by amyloid beta peptide and their consequences in neurons and astrocytes in culture. Biochim Biophys Acta *1742*, 81-87.

Aksenova, M.V., Aksenov, M.Y., Payne, R.M., Trojanowski, J.Q., Schmidt, M.L., Carney, J.M., Butterfield, D.A., and Markesbery, W.R. (1999). Oxidation of cytosolic proteins and expression of creatine kinase BB in frontal lobe in different neurodegenerative disorders. Dement Geriatr Cogn Disord *10*, 158-165.

Ali, F.E., Barnham, K.J., Barrow, C.J., and Separovic, F. (2004). Metal catalyzed oxidation of tyrosine residues by different oxidation systems of copper/hydrogen peroxide. J Inorg Biochem *98*, 173-184.

Allinson, T.M., Parkin, E.T., Turner, A.J., and Hooper, N.M. (2003). ADAMs family members as amyloid precursor protein alpha-secretases. J Neurosci Res *74*, 342-352.

Allsop, D., Landon, M., and Kidd, M. (1983). The isolation and amino acid composition of senile plaque core protein. Brain Res *259*, 348-352.

Allsop, D., Mayes, J., Moore, S., Masad, A., and Tabner, B.J. (2008). Metal-dependent generation of reactive oxygen species from amyloid proteins implicated in neurodegenerative disease. Biochem Soc Trans *36*, 1293-1298.

Arimon, M., Diez-Perez, I., Kogan, M.J., Durany, N., Giralt, E., Sanz, F., and Fernandez-Busquets, X. (2005). Fine structure study of Abeta1-42 fibrillogenesis with atomic force microscopy. FASEB J *19*, 1344-1346.

Arispe, N., Rojas, E., and Pollard, H.B. (1993). Alzheimer disease amyloid beta protein forms calcium channels in bilayer membranes: blockade by tromethamine and aluminum. Proc Natl Acad Sci U S A *90*, 567-571.

Assaf, S.Y., and Chung, S.H. (1984). Release of endogenous Zn2+ from brain tissue during activity. Nature *308*, 734-736.

Atwood, C.S., Huang, X., Khatri, A., Scarpa, R.C., Kim, Y.S., Moir, R.D., Tanzi, R.E., Roher, A.E., and Bush, A.I. (2000a). Copper catalyzed oxidation of Alzheimer Abeta. Cell Mol Biol (Noisy-le-grand) *46*, 777-783.

Atwood, C.S., Moir, R.D., Huang, X., Scarpa, R.C., Bacarra, N.M., Romano, D.M., Hartshorn, M.A., Tanzi, R.E., and Bush, A.I. (1998). Dramatic aggregation of Alzheimer abeta by Cu(II) is induced by conditions representing physiological acidosis. J Biol Chem *273*, 12817-12826.

Atwood, C.S., Obrenovich, M.E., Liu, T., Chan, H., Perry, G., Smith, M.A., and Martins, R.N. (2003). Amyloid-beta: a chameleon walking in two worlds: a review of the trophic and toxic properties of amyloid-beta. Brain Res Brain Res Rev *43*, 1-16.

Atwood, C.S., Perry, G., Zeng, H., Kato, Y., Jones, W.D., Ling, K.Q., Huang, X., Moir, R.D., Wang, D., Sayre, L.M., *et al.* (2004). Copper mediates dityrosine cross-linking of Alzheimer's amyloid-beta. Biochemistry *43*, 560-568.

Atwood, C.S., Scarpa, R.C., Huang, X., Moir, R.D., Jones, W.D., Fairlie, D.P., Tanzi, R.E., and Bush, A.I. (2000b). Characterization of copper interactions with alzheimer amyloid beta peptides: identification of an attomolar-affinity copper binding site on amyloid beta1-42. J Neurochem *75*, 1219-1233.

Austen, B.M., Paleologou, K.E., Ali, S.A., Qureshi, M.M., Allsop, D., and El-Agnaf, O.M. (2008). Designing peptide inhibitors for oligomerization and toxicity of Alzheimer's beta-amyloid peptide. Biochemistry *47*, 1984-1992.

Balbach, J.J., Petkova, A.T., Oyler, N.A., Antzutkin, O.N., Gordon, D.J., Meredith, S.C., and Tycko, R. (2002). Supramolecular structure in full-length Alzheimer's beta-amyloid fibrils: evidence for a parallel beta-sheet organization from solid-state nuclear magnetic resonance. Biophys J *83*, 1205-1216.

Balcells, M., Wallins, J.S., and Edelman, E.R. (2008). Amyloid beta toxicity dependent upon endothelial cell state. Neurosci Lett *441*, 319-322.

Bard, F., Cannon, C., Barbour, R., Burke, R.L., Games, D., Grajeda, H., Guido, T., Hu, K., Huang, J., Johnson-Wood, K., *et al.* (2000). Peripherally administered antibodies against amyloid beta-peptide enter the central nervous system and reduce pathology in a mouse model of Alzheimer disease. Nat Med *6*, 916-919.

Barnham, K.J., Haeffner, F., Ciccotosto, G.D., Curtain, C.C., Tew, D., Mavros, C., Beyreuther, K., Carrington, D., Masters, C.L., Cherny, R.A., *et al.* (2004). Tyrosine gated electron transfer is key to the toxic mechanism of Alzheimer's disease beta-amyloid. Faseb J *18*, 1427-1429.

Barnham, K.J., McKinstry, W.J., Multhaup, G., Galatis, D., Morton, C.J., Curtain, C.C., Williamson, N.A., White, A.R., Hinds, M.G., Norton, R.S., *et al.* (2003). Structure of the Alzheimer's disease amyloid precursor protein copper binding domain. A regulator of neuronal copper homeostasis. J Biol Chem *278*, 17401-17407.

Barrow, C.J., and Zagorski, M.G. (1991). Solution structures of beta peptide and its constituent fragments: relation to amyloid deposition. Science *253*, 179-182.

Behl, C., Davis, J.B., Lesley, R., and Schubert, D. (1994). Hydrogen peroxide mediates amyloid beta protein toxicity. Cell *77*, 817-827.

Benedek, S., and McGovern, V. (1949). A case of Alzheimer's disease with amyloidosis of the vessels of the cerebral cortex. Med J Aust *2*, 429, pl.

Bharadwaj, P.R., Dubey, A.K., Masters, C.L., Martins, R.N., and Macreadie, I.G. (2009). Abeta aggregation and possible implications in Alzheimer's disease pathogenesis. J Cell Mol Med *13*, 412-421.

Bitan, G., Kirkitadze, M.D., Lomakin, A., Vollers, S.S., Benedek, G.B., and Teplow, D.B. (2003a). Amyloid beta -protein (Abeta) assembly: Abeta 40 and Abeta 42 oligomerize through distinct pathways. Proc Natl Acad Sci U S A *100*, 330-335.

Bitan, G., Lomakin, A., and Teplow, D.B. (2001). Amyloid beta-protein oligomerization: prenucleation interactions revealed by photo-induced cross-linking of unmodified proteins. J Biol Chem *276*, 35176-35184.

Bitan, G., Tarus, B., Vollers, S.S., Lashuel, H.A., Condron, M.M., Straub, J.E., and Teplow, D.B. (2003b). A molecular switch in amyloid assembly: Met35 and amyloid beta-protein oligomerization. J Am Chem Soc *125*, 15359-15365.

Blennow, K., de Leon, M., and Zetterberg, H. (2006). Alzheimer's Disease. Lancet *368*, 387-403.

Brown, J. (1991). Mutations in amyloid precursor protein gene and disease. Lancet *337*, 923-924.

Bruijn, L.I., Houseweart, M.K., Kato, S., Anderson, K.L., Anderson, S.D., Ohama, E., Reaume, A.G., Scott, R.W., and Cleveland, D.W. (1998). Aggregation and motor neuron toxicity of an ALS-linked SOD1 mutant independent from wild-type SOD1. Science *281*, 1851-1854.

Burdick, D., Soreghan, B., Kwon, M., Kosmoski, J., Knauer, M., Henschen, A., Yates, J., Cotman, C., and Glabe, C. (1992). Assembly and aggregation properties of synthetic Alzheimer's A4/beta amyloid peptide analogs. J Biol Chem *267*, 546-554.

Bush, A.I., Pettingell, W.H., Multhaup, G., d Paradis, M., Vonsattel, J.P., Gusella, J.F., Beyreuther, K., Masters, C.L., and Tanzi, R.E. (1994). Rapid induction of Alzheimer A beta amyloid formation by zinc. Science *265*, 1464-1467.

Butterfield, D.A. (2002). Amyloid beta-peptide (1-42)-induced oxidative stress and neurotoxicity: implications for neurodegeneration in Alzheimer's disease brain. A review. Free Radic Res *36*, 1307-1313.

Butterfield, D.A., and Bush, A.I. (2004). Alzheimer's amyloid beta-peptide (1-42): involvement of methionine residue 35 in the oxidative stress and neurotoxicity properties of this peptide. Neurobiol Aging *25*, 563-568.

Butterfield, D.A., Drake, J., Pocernich, C., and Castegna, A. (2001). Evidence of oxidative damage in Alzheimer's disease brain: central role for amyloid beta-peptide. Trends Mol Med *7*, 548-554.

Butterfield, D.A., Hensley, K., Harris, M., Mattson, M., and Carney, J. (1994). beta-Amyloid peptide free radical fragments initiate synaptosomal lipoperoxidation in a sequence-specific fashion: implications to Alzheimer's disease. Biochem Biophys Res Commun *200*, 710-715.

Carson, J.A., and Turner, A.J. (2002). Beta-amyloid catabolism: roles for neprilysin (NEP) and other metallopeptidases? J Neurochem *81*, 1-8.

Chang, W.P., Koelsch, G., Wong, S., Downs, D., Da, H., Weerasena, V., Gordon, B., Devasamudram, T., Bilcer, G., Ghosh, A.K., and Tang, J. (2004). In vivo inhibition of Abeta production by memapsin 2 (beta-secretase) inhibitors. J Neurochem *89*, 1409-1416.

Chauhan, N., Wang, K.C., Wegiel, J., and Malik, M.N. (2004). Walnut extract inhibits the fibrillization of amyloid beta-protein, and also defibrillizes its preformed fibrils. Curr Alzheimer Res *1*, 183-188.

Chauhan, V., and Chauhan, A. (2006). Oxidative stress in Alzheimer's disease. Pathophysiology *13*, 195-208.

Chen, J., Anderson, J.B., DeWeese-Scott, C., Fedorova, N.D., Geer, L.Y., He, S., Hurwitz, D.I., Jackson, J.D., Jacobs, A.R., Lanczycki, C.J., *et al.* (2003). MMDB: Entrez's 3D-structure database. Nucleic Acids Res *31*, 474-477.

Chen, Y.R., and Glabe, C.G. (2006). Distinct early folding and aggregation properties of Alzheimer amyloid-beta peptides Abeta40 and Abeta42: stable trimer or tetramer formation by Abeta42. J Biol Chem *281*, 24414-24422.

Chorev, M., and Goodman, M. (1995). Recent developments in retro peptides and proteins--an ongoing topochemical exploration. Trends Biotechnol *13*, 438-445.

Chromy, B.A., Nowak, R.J., Lambert, M.P., Viola, K.L., Chang, L., Velasco, P.T., Jones, B.W., Fernandez, S.J., Lacor, P.N., Horowitz, P., *et al.* (2003). Self-assembly of Abeta(1-42) into globular neurotoxins. Biochemistry *42*, 12749-12760.

Cleary, J.P., Walsh, D.M., Hofmeister, J.J., Shankar, G.M., Kuskowski, M.A., Selkoe, D.J., and Ashe, K.H. (2005). Natural oligomers of the amyloid-beta protein specifically disrupt cognitive function. Nat Neurosci *8*, 79-84.

Clements, A., Allsop, D., Walsh, D.M., and Williams, C.H. (1996). Aggregation and metal-binding properties of mutant forms of the amyloid A beta peptide of Alzheimer's disease. J Neurochem *66*, 740-747.

Colangelo, V., Schurr, J., Ball, M.J., Pelaez, R.P., Bazan, N.G., and Lukiw, W.J. (2002). Gene expression profiling of 12633 genes in Alzheimer hippocampal CA1: transcription and neurotrophic factor down-regulation and up-regulation of apoptotic and pro-inflammatory signaling. J Neurosci Res *70*, 462-473.

Cole, G.M., Lim, G.P., Yang, F., Teter, B., Begum, A., Ma, Q., Harris-White, M.E., and Frautschy, S.A. (2005). Prevention of Alzheimer's disease: Omega-3 fatty acid and phenolic anti-oxidant interventions. Neurobiol Aging *26 Suppl 1*, 133-136.

Coles, M., Bicknell, W., Watson, A.A., Fairlie, D.P., and Craik, D.J. (1998). Solution structure of amyloid beta-peptide(1-40) in a water-micelle environment. Is the membrane-spanning domain where we think it is? Biochemistry *37*, 11064-11077.

Corder, E.H., Saunders, A.M., Strittmatter, W.J., Schmechel, D.E., Gaskell, P.C., Small, G.W., Roses, A.D., Haines, J.L., and Pericak-Vance, M.A. (1993). Gene dose of apolipoprotein E type 4 allele and the risk of Alzheimer's disease in late onset families. Science *261*, 921-923.

Crescenzi, O., Tomaselli, S., Guerrini, R., Salvadori, S., D'Ursi, A.M., Temussi, P.A., and Picone, D. (2002). Solution structure of the Alzheimer amyloid beta-peptide (1-42) in an apolar microenvironment. Similarity with a virus fusion domain. Eur J Biochem *269*, 5642-5648.

Crews, L., Rockenstein, E., and Masliah, E. (2010). APP transgenic modeling of Alzheimer's disease: mechanisms of neurodegeneration and aberrant neurogenesis. Brain Struct Funct *214*, 111-126.

Cuajungco, M.P., Goldstein, L.E., Nunomura, A., Smith, M.A., Lim, J.T., Atwood, C.S., Huang, X., Farrag, Y.W., Perry, G., and Bush, A.I. (2000). Evidence that the beta-amyloid plaques of Alzheimer's disease represent the redox-silencing and entombment of abeta by zinc. J Biol Chem *275*, 19439-19442.

Cummings, J.L., Vinters, H.V., Cole, G.M., and Khachaturian, Z.S. (1998). Alzheimer's disease: etiologies, pathophysiology, cognitive reserve, and treatment opportunities. Neurology *51*, S2-17; discussion S65-17.

Dahlgren, K.N., Manelli, A.M., Stine, W.B., Jr., Baker, L.K., Krafft, G.A., and LaDu, M.J. (2002). Oligomeric and fibrillar species of amyloid-beta peptides differentially affect neuronal viability. J Biol Chem *277*, 32046-32053.

De Felice, F.G., Vieira, M.N., Saraiva, L.M., Figueroa-Villar, J.D., Garcia-Abreu, J., Liu, R., Chang, L., Klein, W.L., and Ferreira, S.T. (2004). Targeting the neurotoxic species in Alzheimer's disease: inhibitors of Abeta oligomerization. FASEB J *18*, 1366-1372.

De Jonghe, C., Esselens, C., Kumar-Singh, S., Craessaerts, K., Serneels, S., Checler, F., Annaert, W., Van Broeckhoven, C., and De Strooper, B. (2001). Pathogenic APP mutations near the gamma-secretase cleavage site differentially affect Abeta secretion and APP C-terminal fragment stability. Hum Mol Genet *10*, 1665-1671.

Demuro, A., Mina, E., Kayed, R., Milton, S.C., Parker, I., and Glabe, C.G. (2005). Calcium dysregulation and membrane disruption as a ubiquitous neurotoxic mechanism of soluble amyloid oligomers. J Biol Chem *280*, 17294-17300.

Deraeve, C., Pitie, M., and Meunier, B. (2006). Influence of chelators and iron ions on the production and degradation of H2O2 by beta-amyloid-copper complexes. J Inorg Biochem *100*, 2117-2126.

Dikalov, S.I., Vitek, M.P., and Mason, R.P. (2004). Cupric-amyloid beta peptide complex stimulates oxidation of ascorbate and generation of hydroxyl radical. Free Radic Biol Med *36*, 340-347.

Etcheberrigaray, R., Tan, M., Dewachter, I., Kuiperi, C., Van der Auwera, I., Wera, S., Qiao, L., Bank, B., Nelson, T.J., Kozikowski, A.P., *et al.* (2004). Therapeutic effects of PKC activators in Alzheimer's disease transgenic mice. Proc Natl Acad Sci U S A *101*, 11141-11146.

Evans, K.C., Berger, E.P., Cho, C.G., Weisgraber, K.H., and Lansbury, P.T., Jr. (1995). Apolipoprotein E is a kinetic but not a thermodynamic inhibitor of amyloid formation: implications for the pathogenesis and treatment of Alzheimer disease. Proc Natl Acad Sci U S A *92*, 763-767.

Fancy, D.A., and Kodadek, T. (1999). Chemistry for the analysis of protein-protein interactions: rapid and efficient cross-linking triggered by long wavelength light. Proc Natl Acad Sci U S A *96*, 6020-6024.

Fang, C., Wu, W., Liu, Q., Sun, X., Ma, Y., Zhao, Y., Li, Y. (2010). Dual functions of β-amyloid oligomer and fibril in Cu(II)-induced H2O2 production. Regulatory Peptides, 1-6.

Farkas, E., and Luiten, P.G. (2001). Cerebral microvascular pathology in aging and Alzheimer's disease. Prog Neurobiol *64*, 575-611.

Farrer, L.A., Cupples, L.A., Haines, J.L., Hyman, B., Kukull, W.A., Mayeux, R., Myers, R.H., Pericak-Vance, M.A., Risch, N., and van Duijn, C.M. (1997). Effects of age, sex, and ethnicity on the association between apolipoprotein E genotype and Alzheimer disease. A meta-analysis. APOE and Alzheimer Disease Meta Analysis Consortium. Jama *278*, 1349-1356.

Ferri, C.P., Prince, M., Brayne, C., Brodaty, H., Fratiglioni, L., Ganguli, M., Hall, K., Hasegawa, K., Hendrie, H., Huang, Y., *et al.* (2005). Global prevalence of dementia: a Delphi consensus study. Lancet *366*, 2112-2117.

Fezoui, Y., Hartley, D.M., Harper, J.D., Khurana, R., Walsh, D.M., Condron, M.M., Selkoe, D.J., Lansbury, P.T., Jr., Fink, A.L., and Teplow, D.B. (2000). An improved method of preparing the amyloid beta-protein for fibrillogenesis and neurotoxicity experiments. Amyloid *7*, 166-178.

Fraser, P.E., Nguyen, J.T., Surewicz, W.K., and Kirschner, D.A. (1991). pH-dependent structural transitions of Alzheimer amyloid peptides. Biophys J *60*, 1190-1201.

Frautschy, S.A., Cole, G.M., and Baird, A. (1992). Phagocytosis and deposition of vascular beta-amyloid in rat brains injected with Alzheimer beta-amyloid. Am J Pathol *140*, 1389-1399.

Fukumoto, H., Tokuda, T., Kasai, T., Ishigami, N., Hidaka, H., Kondo, M., Allsop, D., and Nakagawa, M. (2010). High-molecular-weight {beta}-amyloid oligomers are elevated in cerebrospinal fluid of Alzheimer patients. FASEB J.

Gaeta, A., and Hider, R.C. (2005). The crucial role of metal ions in neurodegeneration: the basis for a promising therapeutic strategy. Br J Pharmacol *146*, 1041-1059.

Galeazzi, L., Ronchi, P., Franceschi, C., and Giunta, S. (1999). In vitro peroxidase oxidation induces stable dimers of beta-amyloid (1-42) through dityrosine bridge formation. Amyloid *6*, 7-13.

Ganguli, M., Chandra, V., Kamboh, M.I., Johnston, J.M., Dodge, H.H., Thelma, B.K., Juyal, R.C., Pandav, R., Belle, S.H., and DeKosky, S.T. (2000). Apolipoprotein E polymorphism and Alzheimer disease: The Indo-US Cross-National Dementia Study. Arch Neurol *57*, 824-830.

Gatz, M., Reynolds, C.A., Fratiglioni, L., Johansson, B., Mortimer, J.A., Berg, S., Fiske, A., and Pedersen, N.L. (2006). Role of genes and environments for explaining Alzheimer disease. Arch Gen Psychiatry *63*, 168-174.

Glenner, G.G., and Wong, C.W. (1984). Alzheimer's disease: initial report of the purification and characterization of a novel cerebrovascular amyloid protein. Biochem Biophys Res Commun *120*, 885-890.

Goate, A., Chartier-Harlin, M.C., Mullan, M., Brown, J., Crawford, F., Fidani, L., Giuffra, L., Haynes, A., Irving, N., James, L., and et al. (1991). Segregation of a missense mutation in the amyloid precursor protein gene with familial Alzheimer's disease. Nature *349*, 704-706.

Grundke-Iqbal, I., Iqbal, K., Tung, Y.C., Quinlan, M., Wisniewski, H.M., and Binder, L.I. (1986). Abnormal phosphorylation of the microtubule-associated protein tau (tau) in Alzheimer cytoskeletal pathology. Proc Natl Acad Sci U S A *83*, 4913-4917.

Guilloreau, L., Combalbert, S., Sournia-Saquet, A., Mazarguil, H., and Faller, P. (2007). Redox chemistry of copper-amyloid-beta: the generation of hydroxyl radical in the presence of ascorbate is linked to redox-potentials and aggregation state. Chembiochem *8*, 1317-1325.

Gunawardena, S., and Goldstein, L.S. (2001). Disruption of axonal transport and neuronal viability by amyloid precursor protein mutations in Drosophila. Neuron *32*, 389-401.

Haass, C., and Selkoe, D.J. (2007). Soluble protein oligomers in neurodegeneration: lessons from the Alzheimer's amyloid beta-peptide. Nat Rev Mol Cell Biol *8*, 101-112.

Hansen, L.A., DeTeresa, R., Davies, P., and Terry, R.D. (1988). Neocortical morphometry, lesion counts, and choline acetyltransferase levels in the age spectrum of Alzheimer's disease. Neurology *38*, 48-54.

Hardy, J., and Allsop, D. (1991). Amyloid deposition as the central event in the aetiology of Alzheimer's disease. Trends Pharmacol Sci *12*, 383-388.

Hardy, J., and Selkoe, D.J. (2002). The amyloid hypothesis of Alzheimer's disease: progress and problems on the road to therapuetics. Science *297*, 353-356.

Harman, D. (1956). Aging: a theory based on free radical and radiation chemistry. J Gerontol *11*, 298-300.

Hartley, D.M., Walsh, D.M., Ye, C.P., Diehl, T., Vasquez, S., Vassilev, P.M., Teplow, D.B., and Selkoe, D.J. (1999). Protofibrillar intermediates of amyloid beta-protein induce acute electrophysiological changes and progressive neurotoxicity in cortical neurons. J Neurosci *19*, 8876-8884.

Hendriks, L., van Duijn, C.M., Cras, P., Cruts, M., Van Hul, W., van Harskamp, F., Warren, A., McInnis, M.G., Antonarakis, S.E., Martin, J.J., and et al. (1992). Presenile dementia and cerebral haemorrhage linked to a mutation at codon 692 of the beta-amyloid precursor protein gene. Nat Genet *1*, 218-221.

Hershey, C.O., Hershey, L.A., Varnes, A., Vibhakar, S.D., Lavin, P., and Strain, W.H. (1983). Cerebrospinal fluid trace element content in dementia: clinical, radiologic, and pathologic correlations. Neurology *33*, 1350-1353.

Himes, R.A., Park, G.Y., Siluvai, G.S., Blackburn, N.J., and Karlin, K.D. (2008). Structural studies of copper(I) complexes of amyloid-beta peptide fragments: formation of two-coordinate bis(histidine) complexes. Angew Chem Int Ed Engl *47*, 9084-9087.

Hirakura, Y., Azimov, R., Azimova, R., and Kagan, B.L. (2000). Polyglutamine-induced ion channels: a possible mechanism for the neurotoxicity of Huntington and other CAG repeat diseases. J Neurosci Res *60*, 490-494.

Holmes, C., Boche, D., Wilkinson, D., Yadegarfar, G., Hopkins, V., Bayer, A., Jones, R.W., Bullock, R., Love, S., Neal, J.W., *et al.* (2008). Long-term effects of Abeta42 immunisation in Alzheimer's disease: follow-up of a randomised, placebo-controlled phase I trial. Lancet *372*, 216-223.

Holtzman, D.M., Bales, K.R., Tenkova, T., Fagan, A.M., Parsadanian, M., Sartorius, L.J., Mackey, B., Olney, J., McKeel, D., Wozniak, D., and Paul, S.M. (2000). Apolipoprotein E isoform-dependent amyloid deposition and neuritic degeneration in a mouse model of Alzheimer's disease. Proc Natl Acad Sci U S A *97*, 2892-2897.

Hou, L., and Zagorski, M.G. (2004). Sorting out the driving forces for parallel and antiparallel alignment in the abeta peptide fibril structure. Biophys J *86*, 1-2.

Huang, X., Atwood, C.S., Hartshorn, M.A., Multhaup, G., Goldstein, L.E., Scarpa, R.C., Cuajungco, M.P., Gray, D.N., Lim, J., Moir, R.D., *et al.* (1999a). The A beta peptide of Alzheimer's disease directly produces hydrogen peroxide through metal ion reduction. Biochemistry *38*, 7609-7616.

Huang, X., Atwood, C.S., Moir, R.D., Hartshorn, M.A., Vonsattel, J.P., Tanzi, R.E., and Bush, A.I. (1997). Zinc-induced Alzheimer's Abeta1-40 aggregation is mediated by conformational factors. J Biol Chem *272*, 26464-26470.

Huang, X., Cuajungco, M.P., Atwood, C.S., Hartshorn, M.A., Tyndall, J.D., Hanson, G.R., Stokes, K.C., Leopold, M., Multhaup, G., Goldstein, L.E., *et al.* (1999b). Cu(II) potentiation of alzheimer abeta neurotoxicity. Correlation with cell-free hydrogen peroxide production and metal reduction. J Biol Chem *274*, 37111-37116.

Huang, X., Moir, R.D., Tanzi, R.E., Bush, A.I., and Rogers, J.T. (2004). Redox-active metals, oxidative stress, and Alzheimer's disease pathology. Ann N Y Acad Sci *1012*, 153-163.

Hung, Y.H., Bush, A.I., and Cherny, R.A. (2010). Copper in the brain and Alzheimer's disease. J Biol Inorg Chem *15*, 61-76.

Hureau, C., and Faller, P. (2009). Abeta-mediated ROS production by Cu ions: structural insights, mechanisms and relevance to Alzheimer's disease. Biochimie *91*, 1212-1217.

Hutton, M., and Hardy, J. (1997). The presenilins and Alzheimer's disease. Hum Mol Genet *6*, 1639-1646.

Iqbal, K., Alonso Adel, C., Chen, S., Chohan, M.O., El-Akkad, E., Gong, C.X., Khatoon, S., Li, B., Liu, F., Rahman, A., *et al.* (2005). Tau pathology in Alzheimer disease and other tauopathies. Biochim Biophys Acta *1739*, 198-210.

Iwata, N., Tsubuki, S., Takaki, Y., Watanabe, K., Sekiguchi, M., Hosoki, E., Kawashima-Morishima, M., Lee, H.J., Hama, E., Sekine-Aizawa, Y., and Saido, T.C. (2000). Identification of the major Abeta1-42-degrading catabolic pathway in brain parenchyma: suppression leads to biochemical and pathological deposition. Nat Med *6*, 143-150.

Jao, S., Ma, K., Talafous, J., Orlando, R., and Zagorski, M.G. (1997). Trifluoroacetic acid pretreatment reproducibly disaggregates the amyloid beta peptide. Amyloid: Int. J. Exp. Clin. Invest., 240-252.

Jarrett, J.T., Berger, E.P., and Lansbury, P.T., Jr. (1993). The carboxy terminus of the beta amyloid protein is critical for the seeding of amyloid formation: implications for the pathogenesis of Alzheimer's disease. Biochemistry *32*, 4693-4697.

Jellinger, K.A. (2004). Head injury and dementia. Curr Opin Neurol *17*, 719-723.

Kagan, B.L., Azimov, R., and Azimova, R. (2004). Amyloid peptide channels. J Membr Biol *202*, 1-10.

Kanski, J., Aksenova, M., and Butterfield, D.A. (2002a). The hydrophobic environment of Met35 of Alzheimer's Abeta(1-42) is important for the neurotoxic and oxidative properties of the peptide. Neurotox Res *4*, 219-223.

Kanski, J., Aksenova, M., Schoneich, C., and Butterfield, D.A. (2002b). Substitution of isoleucine-31 by helical-breaking proline abolishes oxidative stress and neurotoxic properties of Alzheimer's amyloid beta-peptide. Free Radic Biol Med *32*, 1205-1211.

Karr, J.W., Akintoye, H., Kaupp, L.J., and Szalai, V.A. (2005). N-Terminal deletions modify the Cu2+ binding site in amyloid-beta. Biochemistry *44*, 5478-5487.

Kayed, R., Head, E., Thompson, J.L., McIntire, T.M., Milton, S.C., Cotman, C.W., and Glabe, C.G. (2003). Common structure of soluble amyloid oligomers implies common mechanism of pathogenesis. Science *300*, 486-489.

Kayed, R., Sokolov, Y., Edmonds, B., McIntire, T.M., Milton, S.C., Hall, J.E., and Glabe, C.G. (2004). Permeabilization of lipid bilayers is a common conformation-dependent activity of soluble amyloid oligomers in protein misfolding diseases. J Biol Chem *279*, 46363-46366.

Kidd, M. (1963). Paired helical filaments in electron microscopy of Alzheimer's disease. Nature *197*, 192-193.

Kim, H.J., Chae, S.C., Lee, D.K., Chromy, B., Lee, S.C., Park, Y.C., Klein, W.L., Krafft, G.A., and Hong, S.T. (2003). Selective neuronal degeneration induced by soluble oligomeric amyloid beta protein. FASEB J *17*, 118-120.

Klein, W.L., Krafft, G.A., and Finch, C.E. (2001). Targeting small Abeta oligomers: the solution to an Alzheimer's disease conundrum? Trends Neurosci *24*, 219-224.

Klug, G.M., Losic, D., Subasinghe, S.S., Aguilar, M.I., Martin, L.L., and Small, D.H. (2003). Beta-amyloid protein oligomers induced by metal ions and acid pH are distinct from those generated by slow spontaneous ageing at neutral pH. Eur J Biochem *270*, 4282-4293.

Knapp, M., and Prince, M. (2007). Dementia UK. (London, London School of Economics and the Institute of Psychiatry, King's College London), p. 189.

Kokkoni, N., Stott, K., Amijee, H., Mason, J.M., and Doig, A.J. (2006). N-Methylated peptide inhibitors of beta-amyloid aggregation and toxicity. Optimization of the inhibitor structure. Biochemistry *45*, 9906-9918.

Kong, G.K., Adams, J.J., Harris, H.H., Boas, J.F., Curtain, C.C., Galatis, D., Masters, C.L., Barnham, K.J., McKinstry, W.J., Cappai, R., and Parker, M.W. (2007). Structural studies of the Alzheimer's amyloid precursor protein copper-binding domain reveal how it binds copper ions. J Mol Biol *367*, 148-161.

Kopke, E., Tung, Y.C., Shaikh, S., Alonso, A.C., Iqbal, K., and Grundke-Iqbal, I. (1993). Microtubule-associated protein tau. Abnormal phosphorylation of a non-paired helical filament pool in Alzheimer disease. J Biol Chem *268*, 24374-24384.

Lambert, J.C., and Amouyel, P. (2007). Genetic heterogeneity of Alzheimer's disease: complexity and advances. Psychoneuroendocrinology *32 Suppl 1*, S62-70.

Lambert, M.P., Barlow, A.K., Chromy, B.A., Edwards, C., Freed, R., Liosatos, M., Morgan, T.E., Rozovsky, I., Trommer, B., Viola, K.L., *et al.* (1998). Diffusible, nonfibrillar ligands derived from Abeta1-42 are potent central nervous system neurotoxins. Proc Natl Acad Sci U S A *95*, 6448-6453.

Lashuel, H.A., Hartley, D., Petre, B.M., Walz, T., and Lansbury, P.T., Jr. (2002). Neurodegenerative disease: amyloid pores from pathogenic mutations. Nature *418*, 291.

Lauderback, C.M., Kanski, J., Hackett, J.M., Maeda, N., Kindy, M.S., and Butterfield, D.A. (2002). Apolipoprotein E modulates Alzheimer's Abeta(1-42)-induced oxidative damage to synaptosomes in an allele-specific manner. Brain Res *924*, 90-97.

Lee, J.Y., Mook-Jung, I., and Koh, J.Y. (1999). Histochemically reactive zinc in plaques of the Swedish mutant beta-amyloid precursor protein transgenic mice. J Neurosci *19*, RC10.

Lesne, S., Koh, M.T., Kotilinek, L., Kayed, R., Glabe, C.G., Yang, A., Gallagher, M., and Ashe, K.H. (2006). A specific amyloid-beta protein assembly in the brain impairs memory. Nature *440*, 352-357.

LeVine, H. (1993). Thioflavine T interaction with synthetic Alzheimer's disease beta-amyloid peptides: detection of amyloid aggregation in solution. Protein Sci *2*, 404-410.

LeVine, H., 3rd (1999). Quantification of beta-sheet amyloid fibril structures with thioflavin T. Methods Enzymol *309*, 274-284.

Levy-Lahad, E., Wasco, W., Poorkaj, P., Romano, D.M., Oshima, J., Pettingell, W.H., Yu, C.E., Jondro, P.D., Schmidt, S.D., Wang, K., and et al. (1995). Candidate gene for the chromosome 1 familial Alzheimer's disease locus. Science *269*, 973-977.

Lim, A., Tsuang, D., Kukull, W., Nochlin, D., Leverenz, J., McCormick, W., Bowen, J., Teri, L., Thompson, J., Peskind, E.R., *et al.* (1999). Clinico-neuropathological correlation of Alzheimer's disease in a community-based case series. J Am Geriatr Soc *47*, 564-569.

Liu, G., Huang, W., Moir, R.D., Vanderburg, C.R., Lai, B., Peng, Z., Tanzi, R.E., Rogers, J.T., and Huang, X. (2006). Metal exposure and Alzheimer's pathogenesis. J Struct Biol *155*, 45-51.

Losic, D., Martin, L.L., Mechler, A., Aguilar, M.I., and Small, D.H. (2006). High resolution scanning tunnelling microscopy of the beta-amyloid protein (Abeta1-40) of Alzheimer's disease suggests a novel mechanism of oligomer assembly. J Struct Biol *155*, 104-110.

Lovell, M.A., Robertson, J.D., Teesdale, W.J., Campbell, J.L., and Markesbery, W.R. (1998). Copper, iron and zinc in Alzheimer's disease senile plaques. J Neurol Sci *158*, 47-52.

Lovell, M.A., Xie, C., and Markesbery, W.R. (1999). Protection against amyloid beta peptide toxicity by zinc. Brain Res *823*, 88-95.

Luchsinger, J.A., and Mayeux, R. (2004). Dietary factors and Alzheimer's disease. Lancet Neurol *3*, 579-587.

Lue, L.F., Kuo, Y.M., Roher, A.E., Brachova, L., Shen, Y., Sue, L., Beach, T., Kurth, J.H., Rydel, R.E., and Rogers, J. (1999). Soluble amyloid beta peptide concentration as a predictor of synaptic change in Alzheimer's disease. Am J Pathol *155*, 853-862.

Luengo-Fernandez, R., Leal, J., Gray, A (2010). Dementia 2010. (Cambridge, Health Economics Research Centre, University of Oxford), p. 38.

Luhrs, T., Ritter, C., Adrian, M., Riek-Loher, D., Bohrmann, B., Dobeli, H., Schubert, D., and Riek, R. (2005). 3D structure of Alzheimer's amyloid-beta(1-42) fibrils. Proc Natl Acad Sci U S A *102*, 17342-17347.

Luo, Y., Bolon, B., Kahn, S., Bennett, B.D., Babu-Khan, S., Denis, P., Fan, W., Kha, H., Zhang, J., Gong, Y., *et al.* (2001). Mice deficient in BACE1, the Alzheimer's beta-secretase, have normal phenotype and abolished beta-amyloid generation. Nat Neurosci *4*, 231-232.

Lynch, T., Cherny, R.A., and Bush, A.I. (2000). Oxidative processes in Alzheimer's disease: the role of abeta-metal interactions. Exp Gerontol *35*, 445-451.

Malinchik, S.B., Inouye, H., Szumowski, K.E., and Kirschner, D.A. (1998). Structural analysis of Alzheimer's beta(1-40) amyloid: protofilament assembly of tubular fibrils. Biophys J *74*, 537-545.

Mann, D.M., Yates, P.O., and Marcyniuk, B. (1984). Alzheimer's presenile dementia, senile dementia of Alzheimer type and Down's syndrome in middle age form an age related continuum of pathological changes. Neuropathol Appl Neurobiol *10*, 185-207.

Manzoni, C., Colombo, L., Messa, M., Cagnotto, A., Cantu, L., Del Favero, E., and Salmona, M. (2009). Overcoming synthetic Abeta peptide aging: a new approach to an age-old problem

Masad, A., Hayes, L., Tabner, B.J., Turnbull, S., Cooper, L.J., Fullwood, N.J., German, M.J., Kametani, F., El-Agnaf, O.M., and Allsop, D. (2007). Copper-mediated formation of hydrogen peroxide from the amylin peptide: a novel mechanism for degeneration of islet cells in type-2 diabetes mellitus? FEBS Lett *581*, 3489-3493.

Masters, C.L., Simms, G., Weinman, N.A., Multhaup, G., McDonald, B.L., and Beyreuther, K. (1985). Amyloid plaque core protein in Alzheimer disease and Down syndrome. Proc Natl Acad Sci U S A *82*, 4245-4249.

Matharu, B., Gibson, G., Parsons, R., Huckerby, T.N., Moore, S.A., Cooper, L.J., Millichamp, R., Allsop, D., and Austen, B. (2009). Galantamine inhibits beta-amyloid aggregation and cytotoxicity. J Neurol Sci *280*, 49-58.

Matsui, T., Ingelsson, M., Fukumoto, H., Ramasamy, K., Kowa, H., Frosch, M.P., Irizarry, M.C., and Hyman, B.T. (2007). Expression of APP pathway mRNAs and proteins in Alzheimer's disease. Brain Res *1161*, 116-123.

Mattson, M.P., Cheng, B., Culwell, A.R., Esch, F.S., Lieberburg, I., and Rydel, R.E. (1993). Evidence for excitoprotective and intraneuronal calcium-regulating roles for secreted forms of the beta-amyloid precursor protein. Neuron *10*, 243-254.

May, P.C., Gitter, B.D., Waters, D.C., Simmons, L.K., Becker, G.W., Small, J.S., and Robison, P.M. (1992). beta-Amyloid peptide in vitro toxicity: lot-to-lot variability. Neurobiol Aging *13*, 605-607.

Mayeux, R. (2003). Epidemiology of neurodegeneration. Annu Rev Neurosci *26*, 81-104.

Maynard, C.J., Cappai, R., Volitakis, I., Cherny, R.A., White, A.R., Beyreuther, K., Masters, C.L., Bush, A.I., and Li, Q.X. (2002). Overexpression of Alzheimer's disease amyloid-beta opposes the age-dependent elevations of brain copper and iron. J Biol Chem *277*, 44670-44676.

McLean, C.A., Cherny, R.A., Fraser, F.W., Fuller, S.J., Smith, M.J., Beyreuther, K., Bush, A.I., and Masters, C.L. (1999). Soluble pool of Abeta amyloid as a determinant of severity of neurodegeneration in Alzheimer's disease. Ann Neurol *46*, 860-866.

Melo, J.B., Sousa, C., Garcao, P., Oliveira, C.R., and Agostinho, P. (2009). Galantamine protects against oxidative stress induced by amyloid-beta peptide in cortical neurons. Eur J Neurosci *29*, 455-464.

Meyer, M.R., Tschanz, J.T., Norton, M.C., Welsh-Bohmer, K.A., Steffens, D.C., Wyse, B.W., and Breitner, J.C. (1998). APOE genotype predicts when--not whether--one is predisposed to develop Alzheimer disease. Nat Genet *19*, 321-322.

Miller, B.C., Eckman, E.A., Sambamurti, K., Dobbs, N., Chow, K.M., Eckman, C.B., Hersh, L.B., and Thiele, D.L. (2003). Amyloid-beta peptide levels in brain are inversely correlated with insulysin activity levels in vivo. Proc Natl Acad Sci U S A *100*, 6221-6226.

Miners, J.S., Baig, S., Palmer, J., Palmer, L.E., Kehoe, P.G., and Love, S. (2008). Abeta-degrading enzymes in Alzheimer's disease. Brain Pathol *18*, 240-252.

Mirzabekov, T.A., Lin, M.C., and Kagan, B.L. (1996). Pore formation by the cytotoxic islet amyloid peptide amylin. J Biol Chem *271*, 1988-1992.

Moir, R.D., Atwood, C.S., Romano, D.M., Laurans, M.H., Huang, X., Bush, A.I., Smith, J.D., and Tanzi, R.E. (1999). Differential effects of apolipoprotein E isoforms on metal-induced aggregation of A beta using physiological concentrations. Biochemistry *38*, 4595-4603.

Moreira, P.I., Zhu, X., Liu, Q., Honda, K., Siedlak, S.L., Harris, P.L., Smith, M.A., and Perry, G. (2006). Compensatory responses induced by oxidative stress in Alzheimer disease. Biol Res *39*, 7-13.

Mortimer, J.A., Snowdon, D.A., and Markesbery, W.R. (2003). Head circumference, education and risk of dementia: findings from the Nun Study. J Clin Exp Neuropsychol *25*, 671-679.

MRCCFAS (2001). Pathological correlates of late-onset dementia in a multicentre, community-based population in England and Wales. Neuropathology Group of the Medical Research Council Cognitive Function and Ageing Study. Lancet *357*, 169-175.

Murray, I.V., Sindoni, M.E., and Axelsen, P.H. (2005). Promotion of oxidative lipid membrane damage by amyloid beta proteins. Biochemistry *44*, 12606-12613.

Nadal, R.C., Rigby, S.E., and Viles, J.H. (2008). Amyloid beta-Cu2+ complexes in both monomeric and fibrillar forms do not generate H2O2 catalytically but quench hydroxyl radicals. Biochemistry *47*, 11653-11664.

Naylor, R., Hill, A.F., and Barnham, K.J. (2008). Is covalently crosslinked Abeta responsible for synaptotoxicity in Alzheimer's disease? Curr Alzheimer Res *5*, 533-539.

Nunomura, A., Tamaoki, T., Tanaka, K., Motohashi, N., Nakamura, M., Hayashi, T., Yamaguchi, H., Shimohama, S., Lee, H.G., Zhu, X., *et al.* (2010). Intraneuronal amyloid beta accumulation and oxidative damage to nucleic acids in Alzheimer disease. Neurobiol Dis *37*, 731-737.

Oddo, S., Caccamo, A., Tran, L., Lambert, M.P., Glabe, C.G., Klein, W.L., and LaFerla, F.M. (2006). Temporal profile of amyloid-beta (Abeta) oligomerization in an in vivo model of Alzheimer disease. A link between Abeta and tau pathology. J Biol Chem *281*, 1599-1604.

Odetti, P., Angelini, G., Dapino, D., Zaccheo, D., Garibaldi, S., Dagna-Bricarelli, F., Piombo, G., Perry, G., Smith, M., Traverso, N., and Tabaton, M. (1998). Early

glycoxidation damage in brains from Down's syndrome. Biochem Biophys Res Commun *243*, 849-851.

Ono, K., Condron, M.M., and Teplow, D.B. (2009). Structure-neurotoxicity relationships of amyloid beta-protein oligomers. Proc Natl Acad Sci U S A *106*, 14745-14750.

Orgogozo, J.M., Gilman, S., Dartigues, J.F., Laurent, B., Puel, M., Kirby, L.C., Jouanny, P., Dubois, B., Eisner, L., Flitman, S., *et al.* (2003). Subacute meningoencephalitis in a subset of patients with AD after Abeta42 immunization. Neurology *61*, 46-54.

Page, C.C., Moser, C.C., Chen, X., and Dutton, P.L. (1999). Natural engineering principles of electron tunnelling in biological oxidation-reduction. Nature *402*, 47-52.

Paola, D., Domenicotti, C., Nitti, M., Vitali, A., Borghi, R., Cottalasso, D., Zaccheo, D., Odetti, P., Strocchi, P., Marinari, U.M., *et al.* (2000). Oxidative stress induces increase in intracellular amyloid beta-protein production and selective activation of betaI and betaII PKCs in NT2 cells. Biochem Biophys Res Commun *268*, 642-646.

Permanne, B., Adessi, C., Saborio, G.P., Fraga, S., Frossard, M.J., Van Dorpe, J., Dewachter, I., Banks, W.A., Van Leuven, F., and Soto, C. (2002). Reduction of amyloid load and cerebral damage in a transgenic mouse model of Alzheimer's disease by treatment with a beta-sheet breaker peptide. Faseb J *16*, 860-862.

Perry, G., Nunomura, A., Hirai, K., Zhu, X., Perez, M., Avila, J., Castellani, R.J., Atwood, C.S., Aliev, G., Sayre, L.M., *et al.* (2002). Is oxidative damage the fundamental pathogenic mechanism of Alzheimer's and other neurodegenerative diseases? Free Radic Biol Med *33*, 1475-1479.

Petersen, R.C. (2004). Mild cognitive impairment as a diagnostic entity. J Intern Med *256*, 183-194.

Petersen, R.C., Thomas, R.G., Grundman, M., Bennett, D., Doody, R., Ferris, S., Galasko, D., Jin, S., Kaye, J., Levey, A., *et al.* (2005). Vitamin E and donepezil for the treatment of mild cognitive impairment. N Engl J Med *352*, 2379-2388.

Petit, A., Bihel, F., Alves da Costa, C., Pourquie, O., Checler, F., and Kraus, J.L. (2001). New protease inhibitors prevent gamma-secretase-mediated production of Abeta40/42 without affecting Notch cleavage. Nat Cell Biol *3*, 507-511.

Poirier, J. (1994). Apolipoprotein E in animal models of CNS injury and in Alzheimer's disease. Trends Neurosci *17*, 525-530.

Poirier, J., Davignon, J., Bouthillier, D., Kogan, S., Bertrand, P., and Gauthier, S. (1993). Apolipoprotein E polymorphism and Alzheimer's disease. Lancet *342*, 697-699.

Praticò, D. (2008). Evidence of oxidative stress in Alzheimer's disease brain and antioxidant therapy: lights and shadows. Ann N Y Acad Sci., 70-78.

Raber, J., Huang, Y., and Ashford, J.W. (2004). ApoE genotype accounts for the vast majority of AD risk and AD pathology. Neurobiol Aging *25*, 641-650.

Ramassamy, C., Averill, D., Beffert, U., Bastianetto, S., Theroux, L., Lussier-Cacan, S., Cohn, J.S., Christen, Y., Davignon, J., Quirion, R., and Poirier, J. (1999). Oxidative damage and protection by antioxidants in the frontal cortex of Alzheimer's disease is related to the apolipoprotein E genotype. Free Radic Biol Med *27*, 544-553.

Rauk, A., Armstrong, D., and Fairlie, D. (2000). Is oxidative damage mediated by amyoid beta and prion peptide mediated by hydrogen atom transfer from glycine alpha-carbon to methionine sulfur within beta-sheets? J. Am. Chem. Soc. *122*, 9761-9767.

Rice, M.E. (2000). Ascorbate regulation and its neuroprotective role in the brain. Trends Neurosci *23*, 209-216.

Ritchie, C.W., Bush, A.I., Mackinnon, A., Macfarlane, S., Mastwyk, M., MacGregor, L., Kiers, L., Cherny, R., Li, Q.X., Tammer, A., *et al.* (2003). Metal-protein attenuation with iodochlorhydroxyquin (clioquinol) targeting Abeta amyloid deposition and toxicity in Alzheimer disease: a pilot phase 2 clinical trial. Arch Neurol *60*, 1685-1691.

Rogers, J.T., Randall, J.D., Cahill, C.M., Eder, P.S., Huang, X., Gunshin, H., Leiter, L., McPhee, J., Sarang, S.S., Utsuki, T., *et al.* (2002). An iron-responsive element type II in the 5'-untranslated region of the Alzheimer's amyloid precursor protein transcript. J Biol Chem *277*, 45518-45528.

Roghani, M., Becherer, J.D., Moss, M.L., Atherton, R.E., Erdjument-Bromage, H., Arribas, J., Blackburn, R.K., Weskamp, G., Tempst, P., and Blobel, C.P. (1999). Metalloprotease-disintegrin MDC9: intracellular maturation and catalytic activity. J Biol Chem *274*, 3531-3540.

Rovelet-Lecrux, A., Hannequin, D., Raux, G., Le Meur, N., Laquerriere, A., Vital, A., Dumanchin, C., Feuillette, S., Brice, A., Vercelletto, M., *et al.* (2006). APP locus duplication causes autosomal dominant early-onset Alzheimer disease with cerebral amyloid angiopathy. Nat Genet *38*, 24-26.

Sadowski, M., Pankiewicz, J., Scholtzova, H., Li, Y.S., Quartermain, D., Duff, K., and Wisniewski, T. (2004a). Links between the pathology of Alzheimer's disease and vascular dementia. Neurochem Res *29*, 1257-1266.

Sadowski, M., Pankiewicz, J., Scholtzova, H., Ripellino, J.A., Li, Y., Schmidt, S.D., Mathews, P.M., Fryer, J.D., Holtzman, D.M., Sigurdsson, E.M., and Wisniewski, T. (2004b). A synthetic peptide blocking the apolipoprotein E/beta-amyloid binding mitigates beta-amyloid toxicity and fibril formation in vitro and reduces beta-amyloid plaques in transgenic mice. Am J Pathol *165*, 937-948.

Sano, M. (2003). Do dietary antioxidants prevent Alzheimer's Disease? Lancet Neurol *1*, 342.

Sano, M., Ernesto, C., Thomas, R.G., Klauber, M.R., Schafer, K., Grundman, M., Woodbury, P., Growdon, J., Cotman, C.W., Pfeiffer, E., *et al.* (1997). A controlled

trial of selegiline, alpha-tocopherol, or both as treatment for Alzheimer's disease. The Alzheimer's Disease Cooperative Study. N Engl J Med *336*, 1216-1222.

Schenk, D., Barbour, R., Dunn, W., Gordon, G., Grajeda, H., Guido, T., Hu, K., Huang, J., Johnson-Wood, K., Khan, K., *et al.* (1999). Immunization with amyloid-beta attenuates Alzheimer-disease-like pathology in the PDAPP mouse. Nature *400*, 173-177.

Schenk, D., Hagen, M., and Seubert, P. (2004). Current progress in beta-amyloid immunotherapy. Curr Opin Immunol *16*, 599-606.

Schneider, L.S., DeKosky, S.T., Farlow, M.R., Tariot, P.N., Hoerr, R., and Kieser, M. (2005). A randomized, double-blind, placebo-controlled trial of two doses of Ginkgo biloba extract in dementia of the Alzheimer's type. Curr Alzheimer Res *2*, 541-551.

Schuster, D., Rajendran, A., Hui, S.W., Nicotera, T., Srikrishnan, T., and Kruzel, M.L. (2005). Protective effect of colostrinin on neuroblastoma cell survival is due to reduced aggregation of beta-amyloid. Neuropeptides *39*, 419-426.

Sciarretta, K.L., Gordon, D.J., and Meredith, S.C. (2006). Peptide-based inhibitors of amyloid assembly. Methods Enzymol *413*, 273-312.

Seitz, J., Keppler, C., Fahimi, H.D., and Volkl, A. (1991). A new staining method for the detection of activities of H2O2-producing oxidases on gels and blots using cerium and 3,3'-diaminobenzidine. Electrophoresis *12*, 1051-1055.

Selkoe, D.J. (1991). The molecular pathology of Alzheimer's disease. Neuron *6*, 487-498.

Selkoe, D.J. (2001). Alzheimer's disease: genes, proteins, and therapy. Physiol Rev *81*, 741-766.

Selkoe, D.J. (2002). Alzheimer's disease is a synaptic failure. Science *298*, 789-791.

Shao, H., Jao, S., Ma, K., and Zagorski, M.G. (1999). Solution structures of micelle-bound amyloid beta-(1-40) and beta-(1-42) peptides of Alzheimer's disease. J Mol Biol *285*, 755-773.

Shearer, J., and Szalai, V.A. (2008). The amyloid-beta peptide of Alzheimer's disease binds Cu(I) in a linear bis-his coordination environment: insight into a possible neuroprotective mechanism for the amyloid-beta peptide. J Am Chem Soc *130*, 17826-17835.

Shelat, P.B., Chalimoniuk, M., Wang, J.H., Strosznajder, J.B., Lee, J.C., Sun, A.Y., Simonyi, A., and Sun, G.Y. (2008). Amyloid beta peptide and NMDA induce ROS from NADPH oxidase and AA release from cytosolic phospholipase A2 in cortical neurons. J Neurochem *106*, 45-55.

Shen, C.L., Fitzgerald, M.C., and Murphy, R.M. (1994). Effect of acid predissolution on fibril size and fibril flexibility of synthetic beta-amyloid peptide. Biophys J *67*, 1238-1246.

Sherrington, R., Rogaev, E.I., Liang, Y., Rogaeva, E.A., Levesque, G., Ikeda, M., Chi, H., Lin, C., Li, G., Holman, K., and et al. (1995). Cloning of a gene bearing missense mutations in early-onset familial Alzheimer's disease. Nature *375*, 754-760.

Siemers, E., Skinner, M., Dean, R.A., Gonzales, C., Satterwhite, J., Farlow, M., Ness, D., and May, P.C. (2005). Safety, tolerability, and changes in amyloid beta concentrations after administration of a gamma-secretase inhibitor in volunteers. Clin Neuropharmacol *28*, 126-132.

Small, D.H., Nurcombe, V., Reed, G., Clarris, H., Moir, R., Beyreuther, K., and Masters, C.L. (1994). A heparin-binding domain in the amyloid protein precursor of Alzheimer's disease is involved in the regulation of neurite outgrowth. J Neurosci *14*, 2117-2127.

Smith, D.G., Cappai, R., and Barnham, K.J. (2007a). The redox chemistry of the Alzheimer's disease amyloid beta peptide. Biochim Biophys Acta *1768*, 1976-1990.

Smith, D.G., Ciccotosto, G.D., Tew, D.J., Perez, K., Curtain, C.C., Boas, J.F., Masters, C.L., Cappai, R., and Barnham, K.J. (2010). Histidine 14 modulates membrane binding and neurotoxicity of the Alzheimer's disease amyloid-beta peptide. J Alzheimers Dis *19*, 1387-1400.

Smith, D.P., Ciccotosto, G.D., Tew, D.J., Fodero-Tavoletti, M.T., Johanssen, T., Masters, C.L., Barnham, K.J., and Cappai, R. (2007b). Concentration dependent Cu2+ induced aggregation and dityrosine formation of the Alzheimer's disease amyloid-beta peptide. Biochemistry *46*, 2881-2891.

Smith, D.P., Smith, D.G., Curtain, C.C., Boas, J.F., Pilbrow, J.R., Ciccotosto, G.D., Lau, T.L., Tew, D.J., Perez, K., Wade, J.D., *et al.* (2006). Copper-mediated amyloid-beta toxicity is associated with an intermolecular histidine bridge. J Biol Chem *281*, 15145-15154.

Smith, M.A., Perry, G., Richey, P.L., Sayre, L.M., Anderson, V.E., Beal, M.F., and Kowall, N. (1996). Oxidative damage in Alzheimer's. Nature *382*, 120-121.

Soto, C., Kindy, M.S., Baumann, M., and Frangione, B. (1996). Inhibition of Alzheimer's amyloidosis by peptides that prevent beta-sheet conformation. Biochem Biophys Res Commun *226*, 672-680.

Storey, E., Beyreuther, K., and Masters, C.L. (1996). Alzheimer's disease amyloid precursor protein on the surface of cortical neurons in primary culture co-localizes with adhesion patch components. Brain Res *735*, 217-231.

Streltsov, V.A., Titmuss, S.J., Epa, V.C., Barnham, K.J., Masters, C.L., and Varghese, J.N. (2008). The structure of the amyloid-beta peptide high-affinity copper II binding site in Alzheimer disease. Biophys J *95*, 3447-3456.

Tabner, B.J., El-Agnaf, O.M., Turnbull, S., German, M.J., Paleologou, K.E., Hayashi, Y., Cooper, L.J., Fullwood, N.J., and Allsop, D. (2005). Hydrogen peroxide is generated during the very early stages of aggregation of the amyloid peptides implicated in Alzheimer disease and familial British dementia. J Biol Chem *280*, 35789-35792.

Tabner, B.J., Turnbull, S., El-Agnaf, O., and Allsop, D. (2001). Production of reactive oxygen species from aggregating proteins implicated in Alzheimer's disease, Parkinson's disease and other neurodegenerative diseases. Curr Top Med Chem *1*, 507-517.

Tabner, B.J., Turnbull, S., El-Agnaf, O.M., and Allsop, D. (2002). Formation of hydrogen peroxide and hydroxyl radicals from A(beta) and alpha-synuclein as a possible mechanism of cell death in Alzheimer's disease and Parkinson's disease. Free Radic Biol Med *32*, 1076-1083.

Tamagno, E., Bardini, P., Guglielmotto, M., Danni, O., and Tabaton, M. (2006). The various aggregation states of beta-amyloid 1-42 mediate different effects on oxidative stress, neurodegeneration, and BACE-1 expression. Free Radic Biol Med *41*, 202-212.

Tamagno, E., Parola, M., Bardini, P., Piccini, A., Borghi, R., Guglielmotto, M., Santoro, G., Davit, A., Danni, O., Smith, M.A., *et al.* (2005). Beta-site APP cleaving enzyme up-regulation induced by 4-hydroxynonenal is mediated by stress-activated protein kinases pathways. J Neurochem *92*, 628-636.

Tanzi, R.E., Moir, R.D., and Wagner, S.L. (2004). Clearance of Alzheimer's Abeta peptide: the many roads to perdition. Neuron *43*, 605-608.

Taylor, B.M., Sarver, R.W., Fici, G., Poorman, R.A., Lutzke, B.S., Molinari, A., Kawabe, T., Kappenman, K., Buhl, A.E., and Epps, D.E. (2003). Spontaneous aggregation and cytotoxicity of the beta-amyloid Abeta1-40: a kinetic model. J Protein Chem *22*, 31-40.

Taylor, M., Moore, S., Mayes, J., Parkin, E., Beeg, M., Canovi, M., Gobbi, M., Mann, D.M., and Allsop, D. (2010). Development of a proteolytically stable retro-inverso peptide inhibitor of beta-amyloid oligomerization as a potential novel treatment for Alzheimer's disease. Biochemistry *49*, 3261-3272.

Teplow, D.B. (1998). Structural and kinetic features of amyloid beta-protein fibrillogenesis. Amyloid *5*, 121-142.

Thinakaran, G., and Koo, E.H. (2008). Amyloid precursor protein trafficking, processing, and function. J Biol Chem *283*, 29615-29619.

Tjernberg, L.O., Callaway, D.J., Tjernberg, A., Hahne, S., Lilliehook, C., Terenius, L., Thyberg, J., and Nordstedt, C. (1999). A molecular model of Alzheimer amyloid beta-peptide fibril formation. J Biol Chem *274*, 12619-12625.

Tjernberg, L.O., Naslund, J., Lindqvist, F., Johansson, J., Karlstrom, A.R., Thyberg, J., Terenius, L., and Nordstedt, C. (1996). Arrest of beta-amyloid fibril formation by a pentapeptide ligand. J Biol Chem *271*, 8545-8548.

Turnbull, S., Tabner, B.J., Brown, D.R., and Allsop, D. (2003a). Copper-dependent generation of hydrogen peroxide from the toxic prion protein fragment PrP106-126. Neurosci Lett *336*, 159-162.

Turnbull, S., Tabner, B.J., Brown, D.R., and Allsop, D. (2003b). Generation of hydrogen peroxide from mutant forms of the prion protein fragment PrP121-231. Biochemistry *42*, 7675-7681.

Turnbull, S., Tabner, B.J., El-Agnaf, O.M., Moore, S., Davies, Y., and Allsop, D. (2001a). alpha-Synuclein implicated in Parkinson's disease catalyses the formation of hydrogen peroxide in vitro. Free Radic Biol Med *30*, 1163-1170.

Turnbull, S., Tabner, B.J., El-Agnaf, O.M., Twyman, L.J., and Allsop, D. (2001b). New evidence that the Alzheimer beta-amyloid peptide does not spontaneously form free radicals: an ESR study using a series of spin-traps. Free Radic Biol Med *30*, 1154-1162.

van Horssen, J., Wesseling, P., van den Heuvel, L.P., de Waal, R.M., and Verbeek, M.M. (2003). Heparan sulphate proteoglycans in Alzheimer's disease and amyloid-related disorders. Lancet Neurol *2*, 482-492.

Varadarajan, S., Kanski, J., Aksenova, M., Lauderback, C., and Butterfield, D.A. (2001). Different mechanisms of oxidative stress and neurotoxicity for Alzheimer's A beta(1--42) and A beta(25--35). J Am Chem Soc *123*, 5625-5631.

Varadarajan, S., Yatin, S., Kanski, J., Jahanshahi, F., and Butterfield, D.A. (1999). Methionine residue 35 is important in amyloid beta-peptide-associated free radical oxidative stress. Brain Res Bull *50*, 133-141.

Vassar, R., Bennett, B.D., Babu-Khan, S., Kahn, S., Mendiaz, E.A., Denis, P., Teplow, D.B., Ross, S., Amarante, P., Loeloff, R., *et al.* (1999). Beta-secretase cleavage of Alzheimer's amyloid precursor protein by the transmembrane aspartic protease BACE. Science *286*, 735-741.

Vigo-Pelfrey, C., Lee, D., Keim, P., Lieberburg, I., and Schenk, D.B. (1993). Characterization of beta-amyloid peptide from human cerebrospinal fluid. J Neurochem *61*, 1965-1968.

Vogt, W. (1995). Oxidation of methionyl residues in proteins: tools, targets, and reversal. Free Radic Biol Med *18*, 93-105.

Walsh, D.M., Hartley, D.M., Kusumoto, Y., Fezoui, Y., Condron, M.M., Lomakin, A., Benedek, G.B., Selkoe, D.J., and Teplow, D.B. (1999). Amyloid beta-protein fibrillogenesis. Structure and biological activity of protofibrillar intermediates. J Biol Chem *274*, 25945-25952.

Walsh, D.M., Klyubin, I., Fadeeva, J.V., Cullen, W.K., Anwyl, R., Wolfe, M.S., Rowan, M.J., and Selkoe, D.J. (2002). Naturally secreted oligomers of amyloid beta protein potently inhibit hippocampal long-term potentiation in vivo. Nature *416*, 535-539.

Walsh, D.M., Lomakin, A., Benedek, G.B., Condron, M.M., and Teplow, D.B. (1997). Amyloid beta-protein fibrillogenesis. Detection of a protofibrillar intermediate. J Biol Chem *272*, 22364-22372.

Walsh, D.M., and Selkoe, D.J. (2007). A beta oligomers - a decade of discovery. J Neurochem *101*, 1172-1184.

Wang, Y., Addess, K.J., Chen, J., Geer, L.Y., He, J., He, S., Lu, S., Madej, T., Marchler-Bauer, A., Thiessen, P.A., *et al.* (2007). MMDB: annotating protein sequences with Entrez's 3D-structure database. Nucleic Acids Res *35*, D298-300.

Wataya, T., Nunomura, A., Smith, M.A., Siedlak, S.L., Harris, P.L., Shimohama, S., Szweda, L.I., Kaminski, M.A., Avila, J., Price, D.L., *et al.* (2002). High molecular weight neurofilament proteins are physiological substrates of adduction by the lipid peroxidation product hydroxynonenal. J Biol Chem *277*, 4644-4648.

Weller, R.O., Massey, A., Newman, T.A., Hutchings, M., Kuo, Y.M., and Roher, A.E. (1998). Cerebral amyloid angiopathy: amyloid beta accumulates in putative interstitial fluid drainage pathways in Alzheimer's disease. Am J Pathol *153*, 725-733.

White, A.R., Reyes, R., Mercer, J.F., Camakaris, J., Zheng, H., Bush, A.I., Multhaup, G., Beyreuther, K., Masters, C.L., and Cappai, R. (1999). Copper levels are increased in the cerebral cortex and liver of APP and APLP2 knockout mice. Brain Res *842*, 439-444.

Wilcock, G.K., and Esiri, M.M. (1982). Plaques, tangles and dementia. A quantitative study. J Neurol Sci *56*, 343-356.

Wong, C.W., Quaranta, V., and Glenner, G.G. (1985). Neuritic plaques and cerebrovascular amyloid in Alzheimer disease are antigenically related. Proc Natl Acad Sci U S A *82*, 8729-8732.

Wu, Z., Guo, H., Chow, N., Sallstrom, J., Bell, R.D., Deane, R., Brooks, A.I., Kanagala, S., Rubio, A., Sagare, A., *et al.* (2005). Role of the MEOX2 homeobox gene in neurovascular dysfunction in Alzheimer disease. Nat Med *11*, 959-965.

Yang, F., Lim, G.P., Begum, A.N., Ubeda, O.J., Simmons, M.R., Ambegaokar, S.S., Chen, P.P., Kayed, R., Glabe, C.G., Frautschy, S.A., and Cole, G.M. (2005). Curcumin inhibits formation of amyloid beta oligomers and fibrils, binds plaques, and reduces amyloid in vivo. J Biol Chem *280*, 5892-5901.

Yao, Z., Drieu, K., and Papadopoulos, V. (2001). The Ginkgo biloba extract EGb 761 rescues the PC12 neuronal cells from beta-amyloid-induced cell death by inhibiting the formation of beta-amyloid-derived diffusible neurotoxic ligands. Brain Res *889*, 181-190.

Zagorski, M.G., Yang, J., Shao, H., Ma, K., Zeng, H., and Hong, A. (1999). Methodological and chemical factors affecting amyloid beta peptide amyloidogenicity. Methods Enzymol *309*, 189-204.

Zhou, M., Diwu, Z., Panchuk-Voloshina, N., and Haugland, R.P. (1997). A stable nonfluorescent derivative of resorufin for the fluorometric determination of trace hydrogen peroxide: applications in detecting the activity of phagocyte NADPH oxidase and other oxidases. Anal Biochem *253*, 162-168.

Zou, K., and Michikawa, M. (2008). Angiotensin-converting enzyme as a potential target for treatment of Alzheimer's disease: inhibition or activation? Rev Neurosci *19*, 203-212.